Pulmonary Lymphoproliferative Disorders

15

Sergio Pina-Oviedo, Girish S. Shroff, Chad D. Strange, Jitesh Ahuja, Bradley S. Sabloff, Labib Gilles Debiane, Angel Rolando Peralta, Avi Cohen, Michael J. Simoff, Vishisht Mehta, Javier Diaz-Mendoza, William P. Brasher, Saadia A. Faiz, Patricia M. de Groot, and Mylene T. Truong

Benign Lymphoproliferative Lesions of the Lung

Introduction

The specialized lymphoid tissue found around the respiratory mucosa of small bronchi and bronchioles constitutes the bronchial-associated lymphoid tissue (BALT) [1–3]. The BALT is not conspicuous in normal conditions (Figs. 15.1and 15.2), but it can become hyperplastic after chronic antigenic stimulation, chronic infections, immune dysregulation, or autoimmune disorders. Reactive pulmonary lymphoid processes occur more commonly as interstitial infiltrates but may occasionally form a mass [4]. Reactive pulmonary lymphoid proliferations discussed in this chapter include nodular lymphoid hyperplasia, follicular bronchiolitis, diffuse lymphoid hyperplasia/lymphoid interstitial pneumonia (LIP), and IgG4-related lung disease. Some authors hypothesize that LIP is the precursor lesion to pulmonary marginal zone lymphoma of the mucosa-associated lymphoid tissue (pulmonary MALT lymphoma; discussed in the second part of this chapter).

Even though the diagnosis of most of these lesions can be accomplished without difficulty in a wedge resection or a partial pneumonectomy, this may not be the case in a core needle biopsy, a transbronchial biopsy, or in speci-

S. Pina-Oviedo (✉)
Department of Pathology, Duke University Medical Center, Durham, NC, USA
e-mail: Sergio.pinaoviedo@duke.edu

G. S. Shroff · C. D. Strange · J. Ahuja · B. S. Sabloff
P. M. de Groot · M. T. Truong
Department of Thoracic Imaging, The University of Texas MD Anderson Cancer Center, Houston, TX, USA

L. G. Debiane
Interventional Pulmonology, Pleural Disease Program, Division of Pulmonary and Critical Care Medicine, Henry Ford Hospital, Detroit, MI, USA

Wayne State University School of Medicine, Detroit, MI, USA
e-mail: ldebian1@hfhs.org

A. R. Peralta
Interventional Pulmonology, Bronchoscopy Services, Lung Cancer Screening, Division of Pulmonary and Critical Care Medicine, Henry Ford Hospital, Detroit, MI, USA
e-mail: aperalt2@hfhs.org

A. Cohen
Interventional Pulmonology, Advanced Therapeutic Bronchoscopy, Division of Pulmonary and Critical Care Medicine, Henry Ford Hospital, Detroit, MI, USA
e-mail: acohen4@hfhs.org

M. J. Simoff
Wayne State University School of Medicine, Detroit, MI, USA

Bronchoscopy and Interventional Pulmonology, Lung Cancer Screening Program, Pulmonary and Critical Care Medicine, Henry Ford Hospital, Detroit, MI, USA
e-mail: MSimoff1@hfhs.org

V. Mehta
Interventional Pulmonology, Henry Ford Hospital, Detroit, MI, USA
e-mail: vmehta1@hfhs.org

J. Diaz-Mendoza
Interventional Pulmonology, Bronchoscopy Education Associate Program, Pulmonary and Critical Care Fellowship, Henry Ford Hospital, Detroit, MI, USA

Wayne State University, Detroit, MI, USA
e-mail: Jdiaz1@hfhs.org

W. P. Brasher
Section of Pulmonary, Critical Care and Sleep Medicine, Department of Medicine, Baylor College of Medicine, Houston, TX, USA

S. A. Faiz
Department of Pulmonary Medicine, The University of Texas MD Anderson Cancer Center, Houston, TX, USA

C. A. Moran et al. (eds.), *The Thorax*, https://doi.org/10.1007/978-3-031-21040-2_15

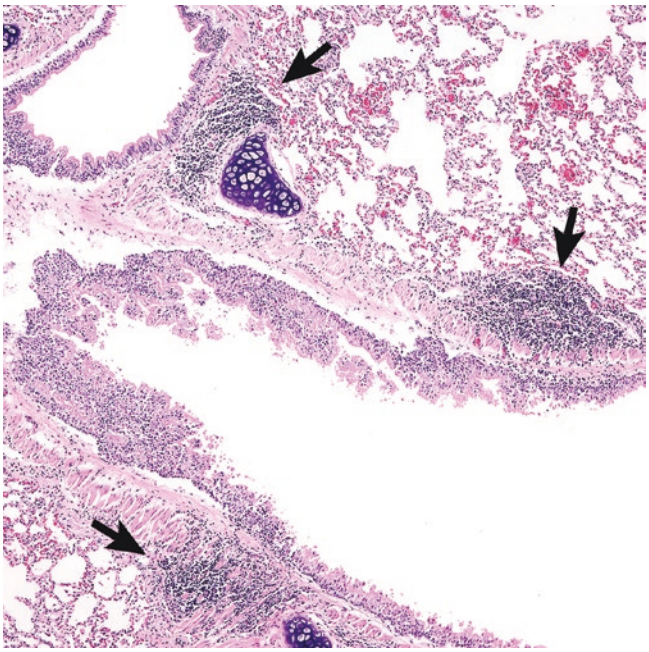

Fig. 15.1 Bronchial-associated lymphoid tissue. The arrows point to aggregates of small lymphocytes around a bronchus and at a bronchial bifurcation

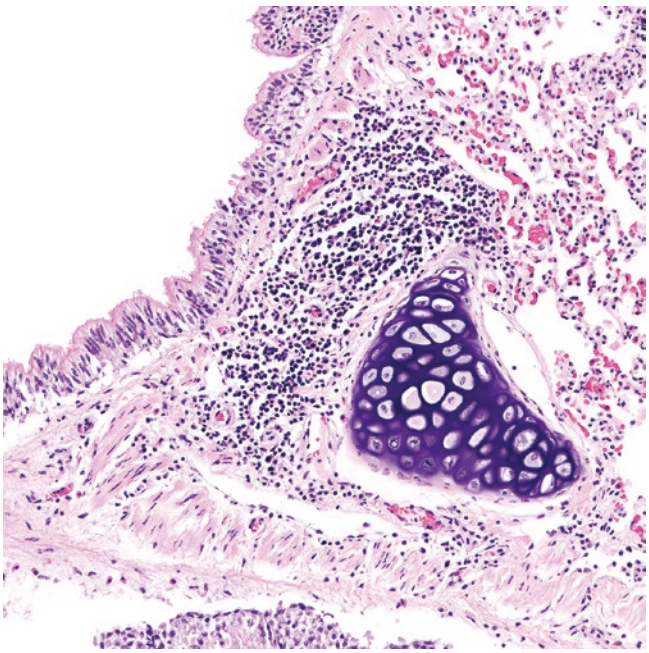

Fig. 15.2 Bronchial-associated lymphoid tissue (BALT). Small collections of lymphocytes in so-called "resting" BALT

mens with significant cellular artifact. Therefore, in these instances, the diagnosis of reactive pulmonary lymphoid lesions benefits substantially from additional ancillary tests, namely immunohistochemistry, flow cytometry immunophenotyping, and cytogenetic and/or molecular analysis.

Pulmonary Nodular Lymphoid Hyperplasia (PNLH)

Introduction

Once designated as "pseudolymphoma" by Saltzstein in 1963 [5], pulmonary nodular lymphoid hyperplasia (PNLH) is a lesion composed of hyperplastic lymphoid tissue that forms ≥1 localized lung nodules [6]. The term PNLH was first suggested by Kradin and Mark in 1983 [7]. PNLH is rare and most likely develops secondary to local lung trauma. There is no association between this lesion and autoimmune diseases and/or congenital or acquired immunodeficiency disorders. Likewise, there is no association between PNLH and smoking.

Clinical Features

The median age of presentation is 65 years, with only rare cases reported in children. The male-to-female ratio is approximately 1:1 [8]. Patients may be asymptomatic, and PNLH is discovered incidentally on imaging performed for other reasons. In a recent case series, four pediatric patients with classic Hodgkin lymphoma developed PNLH [9]**.** In contrast, symptomatic patients can present with nonproductive cough, dyspnea, or pleuritic chest pain. Surgical resection is curative.

Pathology

Grossly, PNLH consists of a firm, tan-white nodule (usually around 2–4 cm) with more or less distinct borders with the adjacent lung (Fig. 15.3). Cases with subpleural localization may abut but do not extend beyond the visceral pleura. On microscopic examination, PNLH consists of a nodule or

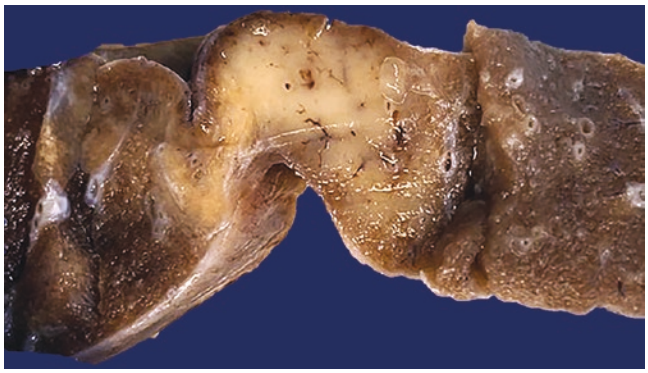

Fig. 15.3 Pulmonary nodular lymphoid hyperplasia (PNLH). This relatively well-circumscribed 2-cm tan-white soft lesion was identified in a lobectomy performed for adenocarcinoma located elsewhere in the lung. On imaging, this lesion was suspicious for a separate tumor nodule but microscopically was confirmed to be PNLH. (*Courtesy of Dr. Susanne Jeffus and Dr. Miki Lindsey*)

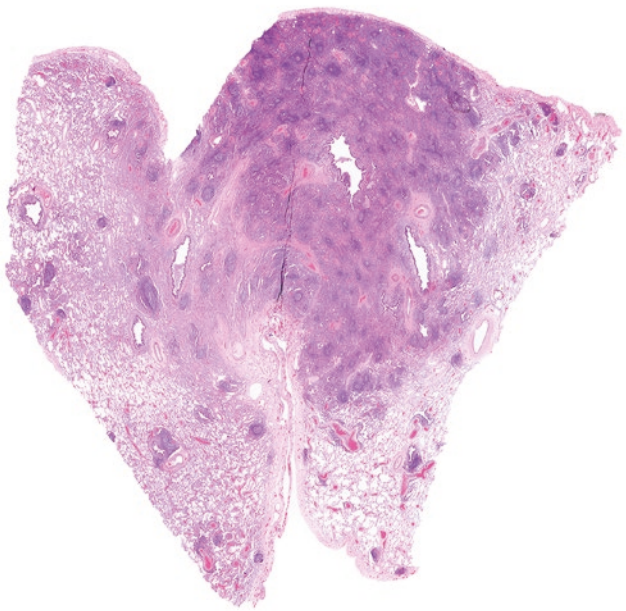

Fig. 15.4 Slide digital scan in a case of pulmonary nodular lymphoid hyperplasia. The lesion is relatively well-delimited, does not invade the pleura, and is centered around a bronchovascular bundle. This lesion is composed of numerous lymphoid follicles and eosinophilic interfollicular areas containing plasma cells. (*Courtesy of Dr. Susanne Jeffus and Dr. Miki Lindsey*)

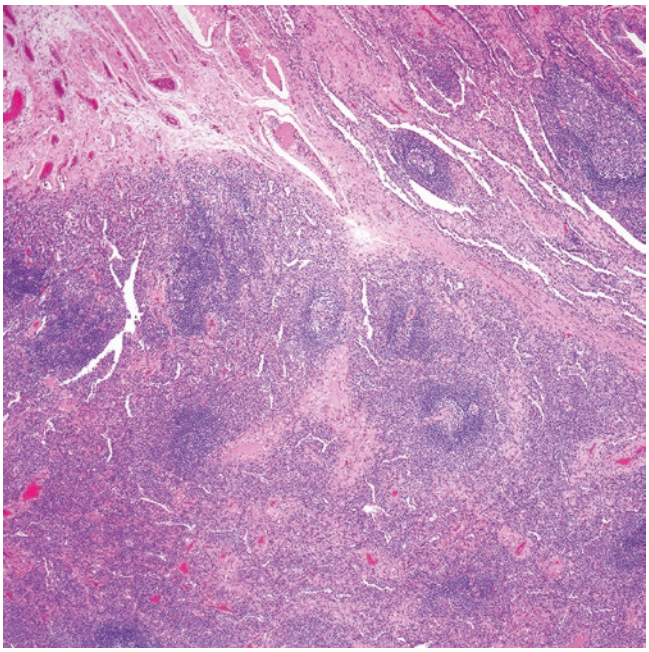

Fig. 15.5 Pulmonary nodular lymphoid hyperplasia (bottom) is well demarcated from the adjacent lung that shows chronic inflammation (top)

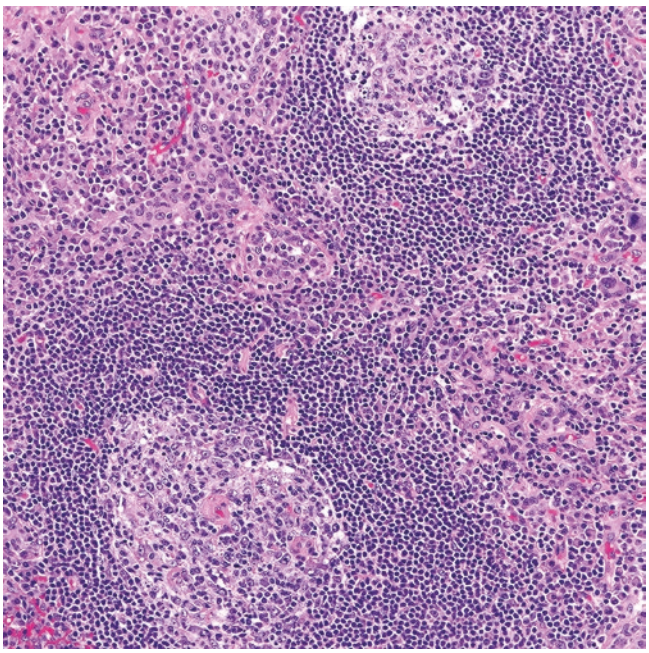

Fig. 15.6 Pulmonary nodular lymphoid hyperplasia is composed of reactive lymphoid follicles and interfollicular plasma cells and histiocytes

mass-forming lesion with well-defined borders comprised of reactive lymphoid follicles along a bronchovascular bundle (Figs. 15.4 and 15.5). The amount and size of follicles are variable, and they all contain germinal centers with polarization, tingible-body macrophages, and a mantle zone. The interfollicular areas may or may not contain abundant plasma cells and lymphocytes, or may show fibrosis with scant lymphoid cells (Fig. 15.6). Scattered histiocytes and/or multinucleated giant cells may or may not be present. Effacement of the adjacent lung parenchyma or lymphoepithelial lesions are not seen. Subpleural lesions do not infiltrate the visceral pleura.

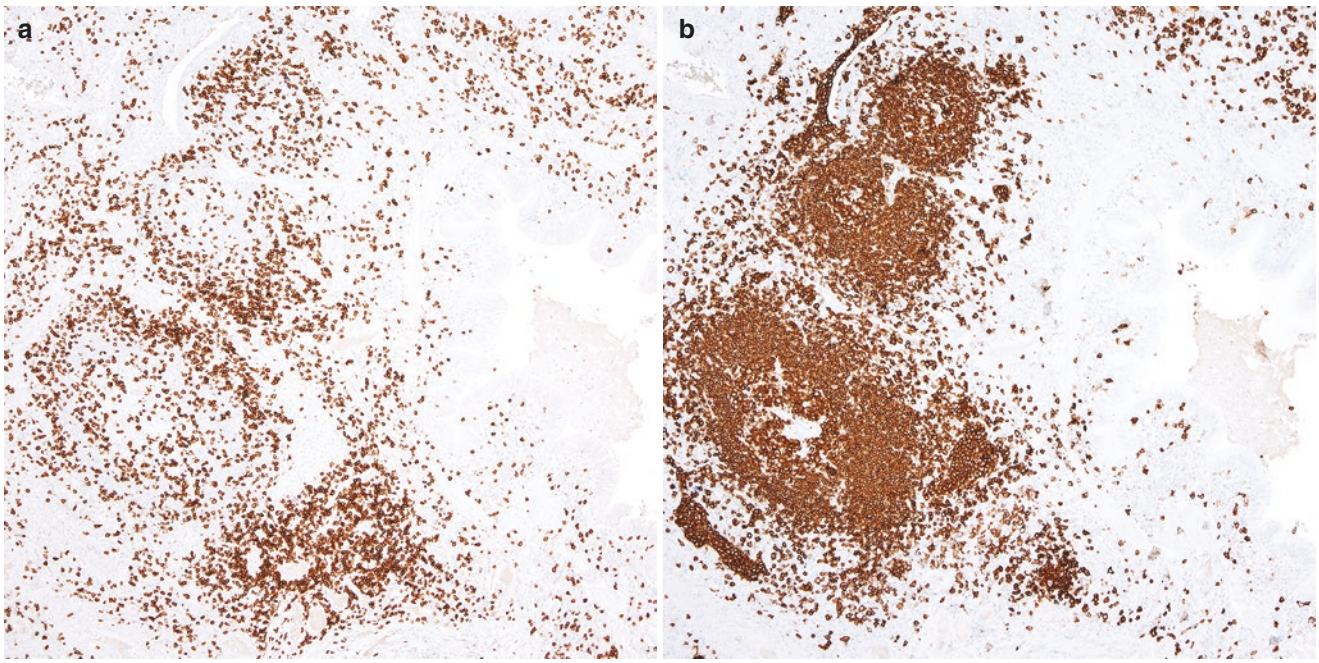

Fig. 15.7 Pulmonary nodular lymphoid hyperplasia. Immunohistochemistry for (**a**) CD3 and (**b**) CD20 shows adequate compartmentalization of T-cells and B-cells, respectively

Immunohistochemistry and Other Ancillary Studies

Immunohistochemical stains are not usually required for diagnosis. However, core needle biopsies may benefit from CD3 and CD20 immunostains to determine the amount and distribution of T- and B-cells, respectively. Reactive follicles are positive for CD20, whereas the interfollicular areas and a few scattered cells within follicles are positive for CD3 [8] (Fig. 15.7). As in any other site, the reactive germinal centers in PNLH are positive for CD10 and bcl-6 and are negative for bcl-2, CD5, and cyclin D1. bcl-2 and CD5 show a similar pattern of distribution as CD3 with the difference that bcl-2 also labels mantle zone B-cells. CD21, CD23, or CD35 highlight preserved follicular dendritic cell (FDC) meshworks. The Ki-67 proliferation index is high in reactive germinal centers and low in interfollicular areas. The plasma cells in the interfollicular areas are polytypic by immunohistochemistry or by in situ hybridization (ISH) (Fig. 15.8). By flow cytometry immunophenotyping, B-cells are polytypic without co-expression of CD5 or CD10, plasma cells are also polytypic, and T-cells show normal antigen expression and a normal CD4:CD8 ratio of 3–4:1. One study has suggested that PNLH could represent a lesion within the spectrum of IgG4-related disease [10].

If *IGH* gene rearrangement is tested in a small lesion or a core biopsy, this study usually shows a polyclonal pattern. However, pathologists should be aware that the detection of a clone by this method does not necessarily translate into lymphoma since tissues with large reactive germinal centers, including PNLH, may occasionally show an oligoclonal or clonal pattern. Therefore, the interpretation of *IGH* gene rearrangement studies should always be done in correlation with the clinical presentation and the morphologic findings.

Differential Diagnosis

PNLH should be distinguished from malignant lymphoid lesions forming a mass, particularly pulmonary MALT lymphoma and follicular lymphoma [8, 11–13] and from a nodule of IgG4-related lung disease and as well as an intrapulmonary lymph node (see Table 15.1).

Pulmonary MALT lymphoma is a CD5-/CD10- B-cell lymphoma that forms a mass composed of reactive lymphoid follicles and abundant plasma cells, but in contrast to PNLH, MALT lymphoma effaces the lung architecture and shows ill-defined borders with the extension of lymphoma cells into adjacent alveolar interstitial spaces. Lymphoepithelial lesions, monocytoid cells, and "colonized" follicles are common. By immunohistochemistry, the normal expected distribution of CD3 and CD20 is lost, and most of the lymphoid infiltrate consists of B-cells. A useful tool to recognize "colonized" follicles is the evaluation of CD21, CD23, and CD35 to highlight disrupted FDC meshworks in pulmonary MALT lymphoma. FDC meshworks are typically preserved in PNLH. If flow cytometry immunophenotyping is performed, detection of monotypic CD5-/CD10- B-cells confirms lym-

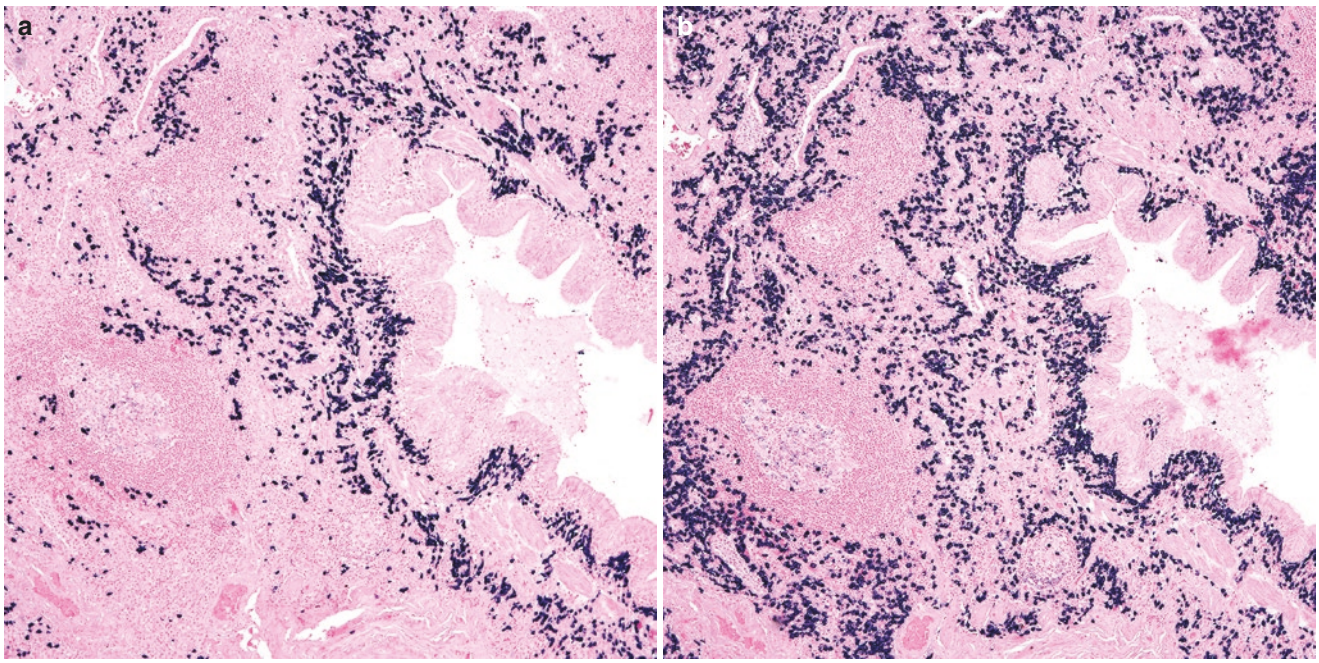

Fig. 15.8 Pulmonary nodular lymphoid hyperplasia, in situ hybridization for (**a**) kappa and (**b**) lambda light chains show polytypic plasma cells, with focal areas showing either a predominance for kappa or for lambda

Table 15.1 Differential diagnosis of pulmonary nodular lymphoid hyperplasia

Pulmonary marginal zone lymphoma of the mucosa-associated lymphoid tissue
Pulmonary follicular lymphoma
IgG4-related lung disease, solid nodular growth
Intrapulmonary lymph node

phoma and rules out a reactive process. If abundant plasma cells are present, immunohistochemistry, ISH, and/or flow cytometry immunophenotyping can be used to confirm or not the presence of monotypic plasma cells. However, plasma cells are not always monotypic in MALT lymphoma.

Follicular lymphoma is exceedingly rare in the lung, and it does not typically present as a mass. However, if this is the case, follicular lymphoma can be distinguished from PNLH because the follicles in this lymphoma are back-to-back, lack polarization, and have attenuated mantle zones. In addition, the germinal centers are positive for bcl-2 that excludes a reactive process. If flow cytometry is performed, the detection of CD10+ monotypic B-cells supports follicular lymphoma and rules out PNLH.

The solid nodular pattern seen in some cases of IgG4-related lung disease may superficially resemble PNLH. However, careful morphologic evaluation of lung lesions in IgG4-related disease usually shows absent or scant reactive follicles, and there is storiform fibrosis, increased plasma cells, and a variable number of eosinophils. Obliterative phlebitis or vasculitis may not be present. In addition, there is a lymphoplasmacytic infiltrate with fibrosis that involves interlobular septa, bronchovascular bundles, and the visceral pleura; these are not features of PNLH. However, as mentioned above, a subset of cases of PNLH may be part of the spectrum of IgG4-related lung disease, and thus, immunohistochemistry for IgG and IgG4 may be required in PNLH with abundant plasma cells.

PNLH may resemble an intraparenchymal lymph node; however, a lymph node has a capsule, a subcapsular sinus, and readily recognizable cortex, paracortex, and medullary regions. In addition, it is common to identify large collections of histiocytes laden with anthracotic pigment.

Follicular Bronchiolitis

Introduction

This is a reactive process with follicular hyperplasia of the BALT preferentially located around bronchioles and bronchial bifurcations. The pathogenesis of follicular bronchiolitis appears to be associated with persistent antigen stimulation and expansion of the BALT due to multiple underlying factors, including chronic inflammatory processes, autoimmune disorders, and congenital or acquired immunodeficiencies. There is no apparent association between follicular bronchiolitis and smoking.

Clinical Features

Follicular bronchiolitis is a disease that affects adults, usually men rather than women [14]. This disorder is extremely uncommon in children unless it develops in the setting of a congenital immunodeficiency. A large subset of patients has an underlying autoimmune disorder (rheumatoid arthritis, lupus erythematosus, Sjögren syndrome) or a congenital or acquired immunodeficiency.

Congenital disorders that have been associated with follicular bronchiolitis include Wiskott–Aldrich syndrome, IgA deficiency, and common variable immunodeficiency (CVID), whereas acquired conditions include acquired immunodeficiency syndrome (AIDS), other immunocompromised states, and connective tissue diseases [15]. Patients may present with dyspnea, nonproductive cough, and/or weight loss. Follicular bronchiolitis has a good to intermediate prognosis, but its progression to more severe disease depends on adequate control with steroids or immunomodulatory medications of the underlying immunologic disorder or autoimmune disease.

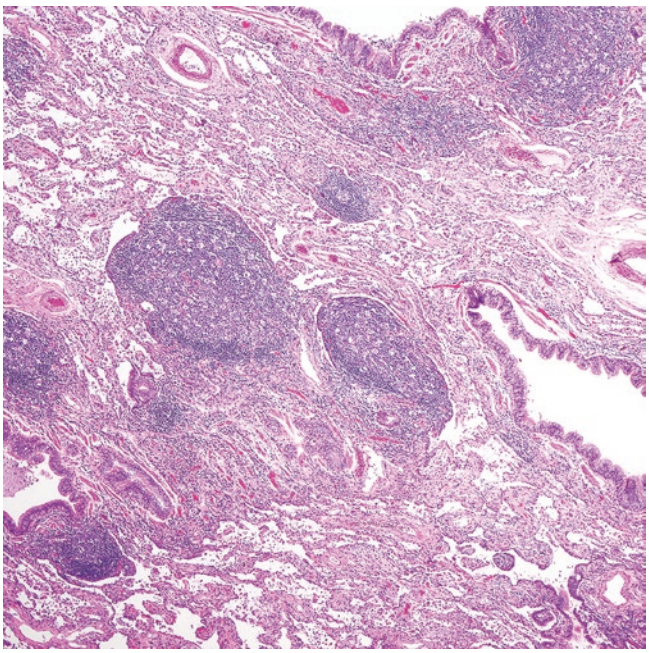

Fig. 15.9 Follicular bronchiolitis. Multiple reactive lymphoid follicles with a peribronchiolar distribution

Pathology

Lung specimens usually do not show significant gross findings, as most lesions in follicular bronchiolitis are microscopic, but occasionally small tan-white pin-point nodules may be recognized by a meticulous pathologist. Microscopically, this disease consists of multiple primary and secondary reactive lymphoid follicles eccentrically located around bronchioles and/or at bronchial bifurcations, as the name implies (Fig. 15.9). The amount of involvement is variable from case to case but can usually seen throughout the lung parenchyma. The germinal centers of secondary follicles are polarized and contain tingible-body macrophages and a mantle zone. A few small lymphocytes can percolate into the immediate alveolar septa, but they do not extend beyond a few alveoli or become a diffuse infiltrate (Fig. 15.10). Bronchioles adjacent to a reactive follicle may show narrowing or distortion of the lumen, but they are not effaced. A few intraepithelial lymphocytes may be seen, but lymphoepithelial lesions are not identified. The histopathology of follicular bronchiolitis is always similar regardless of the etiology.

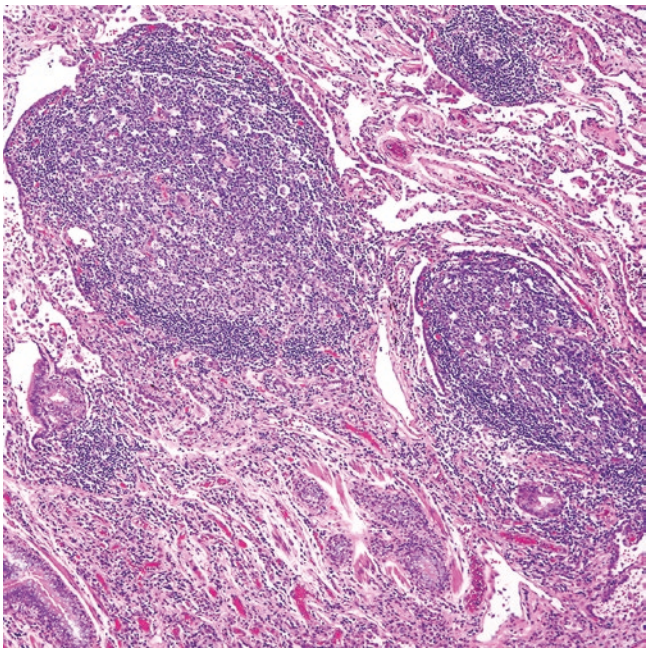

Fig. 15.10 The reactive lymphoid follicles distort and extrinsically compress—but do not replace—the bronchiolar respiratory epithelium

Immunohistochemistry and Other Ancillary Studies

Immunohistochemical stains are not usually required for diagnosis. When the process is conspicuous and raises concern for a neoplastic process, immunostains for CD3 and CD20 are useful to determine the amount and distribution of T- and B-cells, respectively. Reactive follicles are positive for CD20 with only a few scattered intrafollicular T-cells (Fig. 15.11). As in any other site, the reactive germinal centers in follicular bronchiolitis are positive for CD10 and bcl-6 and are negative for bcl-2, CD5, and cyclin D1. bcl-2 and CD5 show a similar pattern of distribution as CD3 with the difference that bcl-2 is positive in mantle zone B-cells. CD21, CD23, or CD35 highlight preserved FDC mesh-

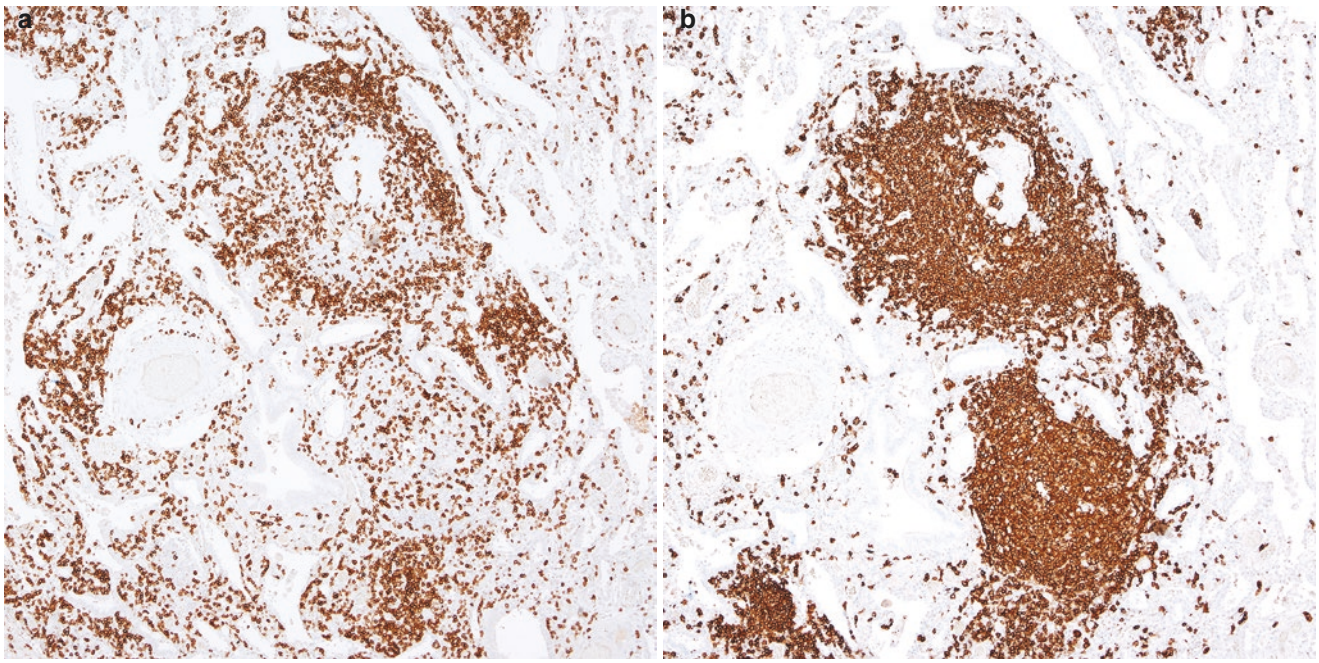

Fig. 15.11 Follicular bronchiolitis. Immunohistochemistry for (**a**) CD3 and (**b**) CD20 shows adequate compartmentalization of T-cells and B-cells, respectively

works. The Ki-67 proliferation index is high in the reactive germinal centers. T-cells show a normal expression of T-cell markers with no aberrant loss of antigens. Flow cytometry is not typically performed in these cases as the lesions are microscopic.

Differential Diagnosis

Because reactive lymphoid follicles with the same pattern of distribution as seen in follicular bronchiolitis can be observed in subacute pneumonia, organizing pneumonia, abscess, granulomas, cavitation, primary or metastatic lung tumors, etc., this diagnosis should be made with caution and only suspected when areas distant from the pathologic process retain the presence of reactive lymphoid follicles around bronchioles. Clinical history and laboratory analysis are crucial to exclude an underlying immunologic cause (congenital immunodeficiency, AIDS, positive rheumatoid factor, autoantibodies) as the potential reason for the development of follicular bronchiolitis.

Another differential diagnosis that may be considered is LIP. This disorder is characterized by the presence of diffuse interstitial infiltrates and not reactive lymphoid follicles located around bronchioles. Occasional lymphoid aggregates -but not well-formed secondary follicles- may be seen associated with cystic spaces, which is not a feature of follicular bronchiolitis. Given the characteristic morphologic distinction between LIP and follicular bronchiolitis, immunohistochemistry is usually not required. If immunohistochemistry is performed, LIP typically contains abundant B-cells that also extend into adjacent alveolar septa and there is no compartmentalization of CD3 and CD20 as seen in reactive lymphoid follicles.

Hypersensitivity pneumonitis (extrinsic allergic alveolitis) usually presents as a patchy interstitial infiltrate with bronchiolocentric distribution that may resemble follicular bronchiolitis. However, hypersensitivity pneumonitis is typically accompanied by loose granulomas that may or may not contain polarizable material as well as collections of alveolar macrophages. The clinical history in these cases is that of a prior exposure to a foreign antigen with secondary development of pulmonary histopathologic findings, which would not be expected in follicular bronchiolitis.

In rare instances, chronic lymphocytic leukemia/small lymphocytic lymphoma (CLL/SLL)—and even more rarely, other small B-cell lymphomas—may involve the lung and exhibit a bronchiolocentric pattern that may vaguely resemble follicular bronchiolitis. However, the infiltrates in CLL/SLL are made of monotonous lymphocytes with variable destruction of the bronchioles, there is a significant extension of the process into adjacent alveolar septa, and there are no reactive follicles. By immunohistochemistry, the lymphoma cells show aberrant expression of CD5, CD23, and bcl-2 and are negative for cyclin D1, and in the case that flow cytometry is performed, the B-cells are monotypic and co-express CD5, CD23, and CD200. A summary of the differential diagnosis of follicular bronchiolitis is listed in Table 15.2.

Table 15.2 Differential diagnosis of follicular bronchiolitis

Any chronic inflammatory response in the lung parenchyma adjacent to: • Subacute/organizing pneumonia, abscess, aspiration • Granulomas, cavitation • Primary or metastatic lung tumor
Lymphoid interstitial pneumonia
Hypersensitivity pneumonitis (extrinsic allergic alveolitis)
Any low-grade B-cell lymphoma with bronchiolocentric pattern • Chronic lymphocytic leukemia/small lymphocytic lymphoma • Follicular lymphoma • Others (rare)

Lymphoid Interstitial Pneumonia (LIP)/ Diffuse Lymphoid Hyperplasia

Introduction

This rare disease was designated "diffuse pulmonary lymphoreticular infiltration associated with dysproteinemia" by Liebow and Carrington in 1973 [16]. LIP, as the disorder is still known today, consists of diffuse lymphoid infiltrates along the alveolar interstitial compartment of the lung. The pathogenesis of LIP appears to be related to alterations in processes of cellular-induced autoimmunity or perhaps to an underlying infection, likely a virus [17], and there is no association between LIP and smoking. Up to date, a definitive etiology of this disease remains unknown. There is significant morphologic overlap between LIP and pulmonary MALT lymphoma, and sometimes the distinction of both is difficult and hinges on clinic-radiologic correlation and the results of ancillary studies.

Clinical Features

Most affected individuals are adults around 40 to 60 years of age, and the disease appears to be more common in women. Children affected by LIP are usually HIV-positive or have an underlying immunodeficiency, namely CVID [18, 19]. The presence of an underlying autoimmune disorder or disorders that produce alterations in immune regulation has been described in association with LIP, with some of the most characteristic being Sjögren syndrome and Castleman disease [18, 20]. It is estimated that about 1% of patients with Sjögren syndrome have LIP and that 25% of adults with LIP have Sjögren syndrome [6]. Infections associated with LIP include Epstein–Barr virus (EBV), human herpesvirus-8 (HHV-8), and *Mycoplasma pneumoniae* [21, 22]. LIP may also develop as a complication of graft-versus-host disease in patients who have received a bone marrow transplant. LIP is considered an AIDS-defining disease in children under 13 years with AIDS [23]. About 60% of patients with LIP present with nonproductive cough and dyspnea, and some other patients may develop fever and weight loss. Similarly, about 60% of patients present with polyclonal hypergammaglobulinemia and dysproteinemia and only a small subset develops hypoglobulinemia [6].

The prognosis of LIP varies from case to case. Some patients show complete resolution of symptoms after steroid treatment, while some others eventually die from complications of the underlying immunologic disease. A subset of patients can progress to end-stage lung disease, and these individuals have a poor outcome. Close to 5% of patients with LIP can develop pulmonary MALT lymphoma and less commonly pulmonary large B-cell lymphoma [23].

Pathology

LIP is not usually recognized grossly, but in some cases a lobar ill-defined consolidation may be observed. When LIP progresses to end-stage lung disease, the gross features are similar to those seen in cases with pulmonary fibrosis (cobblestone pleura, subpleural cysts, honeycomb fibrosis). Microscopically, LIP consists of a diffuse lymphoid infiltrate within and expanding the alveolar interstitial compartment (Fig. 15.12). The majority of lymphocytes are mature and small with a variable number of plasma cells and histiocytes (Fig. 15.13). The infiltrate may be more prominent along bronchovascular bundles and lobular septa. Some cases may feature few lymphoepithelial lesions and/or perivascular lymphoid aggregates, but no replacement of airways or angiodestruction is identified. Reactive lymphoid follicles and ill-defined granulomas with multinucleated giant cells and cholesterol clefts may or may not be present. Type 2 pneumocyte hyperplasia is commonly seen. The alveolar spaces can contain macrophages with foamy cytoplasm, multinucleated giant cells, and intraalveolar proteinaceous material (Fig. 15.14). Acute inflammation, increased eosinophils, or necrosis is not identified. Cases that have progressed to end-stage disease show interstitial fibrosis, cyst formation with variable amounts of lymphoid aggregates in the cysts walls, and honeycombing with varying numbers of background lymphocytes.

Immunohistochemistry and Other Ancillary Studies

The lymphoid infiltrate in LIP is composed of a mixture of CD3+ T-cells and CD20+ B-cells, with predominance of the T-cells [17] (Fig. 15.15). If reactive lymphoid follicles are present, they have normal expression of CD20, CD10, bcl-6 and a negative bcl-2 in the germinal centers. In HIV-positive individuals, the CD4:CD8 ratio is inverted, and B-cells are increased, whereas cases of LIP from patients

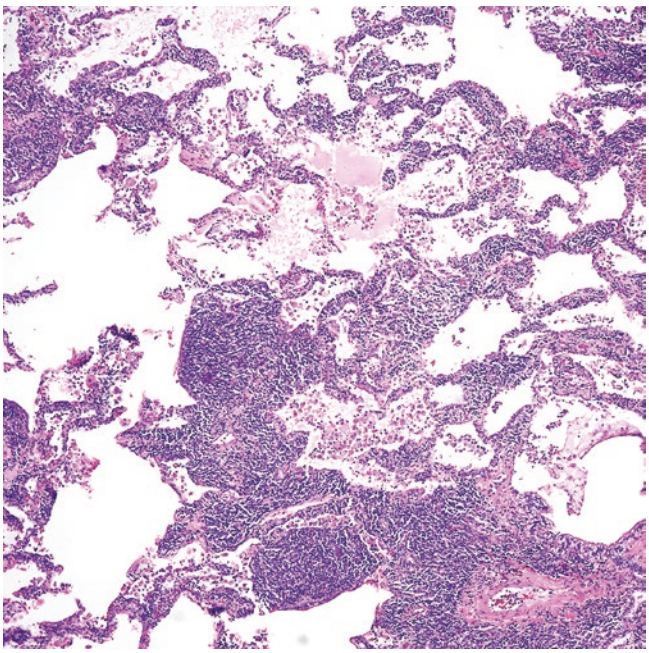

Fig. 15.12 Lymphoid interstitial pneumonia. Numerous small lymphocytes expand the alveolar interstitium

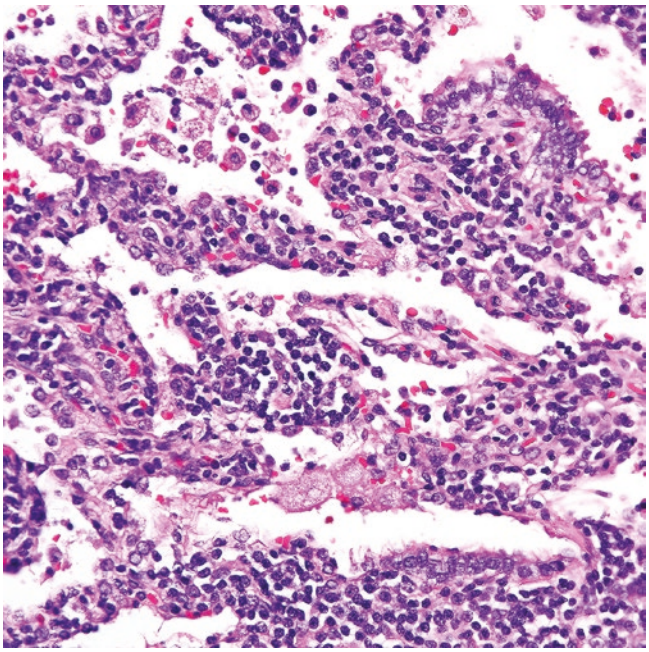

Fig. 15.14 Small lymphocytes and occasional plasma cells expand the alveolar interstitium in lymphoid interstitial pneumonia

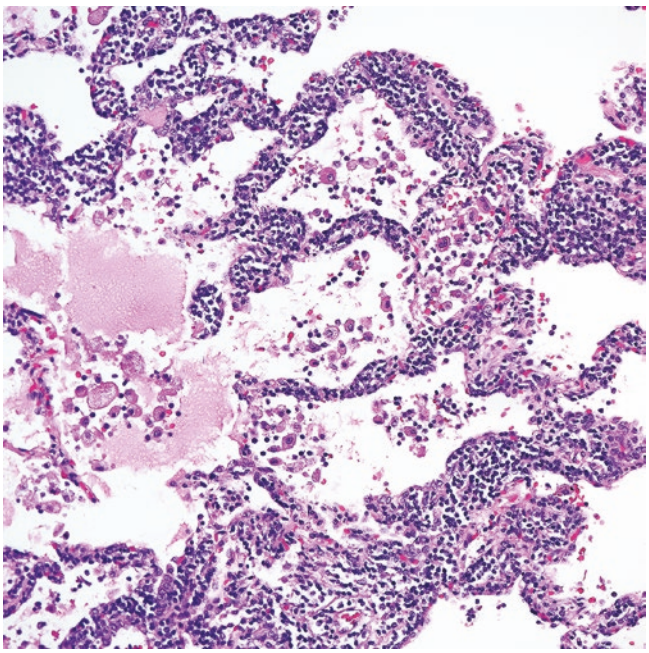

Fig. 15.13 Lymphoid interstitial pneumonia. The alveolar space contains a few foamy macrophages and proteinaceous eosinophilic material

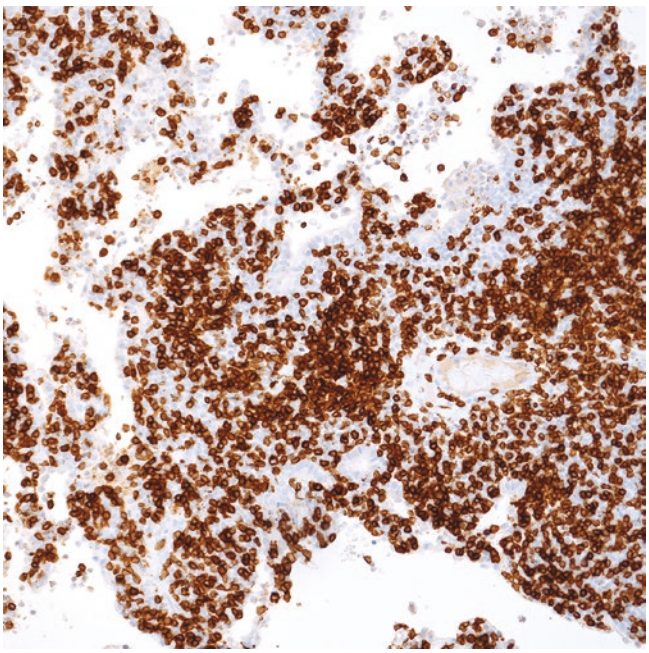

Fig. 15.15 Most lymphocytes in lymphoid interstitial pneumonia are T-cells, as shown with the CD3 immunostain

with other underlying conditions or with hypogammaglobulinemia have a normal to increased CD4:CD8 ratio and a variable number of B-cells [6]. Plasma cells are polytypic by immunohistochemistry and/or ISH. Some cases may be positive for HHV-8 or may show scattered small lymphocytes positive for EBER by ISH. By flow cytometry immunophenotyping, B-cells are polytypic without co-expression of CD5 or CD10, plasma cells are also polytypic, and T-cells show normal antigen expression.

If *IGH* gene rearrangement is tested, this study usually demonstrates a polyclonal pattern. However, pathologists should be aware that detection of a clone by this method does not necessarily translate into lymphoma since reactive pro-

cesses may show an oligoclonal or clonal pattern. Therefore, interpretation of *IGH* gene rearrangement studies should be always done in correlation with the clinical presentation and the morphologic findings.

Differential Diagnosis

LIP should be distinguished from follicular bronchiolitis, hypersensitivity pneumonitis, pulmonary lymphoid processes occurring in the setting of EBV infection, pulmonary MALT lymphoma, and pulmonary CLL/SLL. If LIP has progressed to interstitial fibrosis, the differential diagnosis includes an interstitial lung disease and distinction from a specific etiology may be extremely difficult unless a prior history of LIP is documented.

As mentioned in the corresponding section, follicular bronchiolitis consists of multiple primary and secondary reactive lymphoid follicles eccentrically located around bronchioles and/or at bronchial bifurcations, and although few small lymphocytes percolate into the immediate alveolar septa, these cells do not extend beyond few alveoli or become a diffuse interstitial infiltrate.

Hypersensitivity pneumonitis (extrinsic allergic alveolitis) usually presents as a patchy interstitial infiltrate with bronchiolocentric distribution rather than a diffuse lymphoid interstitial infiltrate as seen in LIP. In addition, hypersensitivity pneumonitis is typically accompanied by loose granulomas that may or may not contain polarizable material as well as collections of alveolar macrophages. Although loose granulomas may be seen in LIP, they do not typically contain foreign material. The clinical history in cases of hypersensitivity pneumonitis is exposure to a foreign antigen with secondary development of the lung histopathologic findings, whereas in LIP there is usually a history of immunosuppression or an autoimmune disorder.

Although not typically biopsied unless the process is severe or shows significant findings on imaging, the pulmonary involvement by infectious mononucleosis may resemble LIP with a diffuse interstitial distribution. Nevertheless, the infiltrate in this EBV-related process is more polymorphic (small lymphocytes, immunoblasts, Reed–Sternberg-like cells, plasma cells, occasional eosinophils) rather than the one seen in LIP (mostly small lymphocytes, variable amount of plasma cells and macrophages). EBER ISH is positive in both conditions. A recent clinical history more characteristic of infectious mononucleosis (pharyngitis, organomegalies, lymphadenopathy) may aid in this scenario.

Some authors consider that LIP is the precursor lesion of pulmonary MALT lymphoma [24, 25], and it is well described that a small subset of patients with LIP (~5%) can progress to pulmonary MALT lymphoma. Both lesions can show significant overlap. However, features that favor pulmonary MALT lymphoma over LIP include effacement of the architecture, nodules or sheets of lymphocytes and monocytoid lymphocytes, abundant lymphoepithelial lesions, increased mitoses, destruction of bronchial cartilage and invasion into visceral pleura. Regional lymph node involvement is practically diagnostic of lymphoma (see corresponding section). Although these previously described features are easily recognized in a lobectomy or wedge resection, this is not the case in a small biopsy where the distinction of these two lesions is more challenging. Imaging correlation is extremely useful to favor LIP over MALT lymphoma since the former presents as bilateral lower lobe reticulonodular infiltrates and not as a mass with ill-defined borders as seen in the latter. Ancillary studies are also helpful. By immunohistochemistry, MALT lymphoma is composed predominantly of B-cells whereas the infiltrate in LIP is T-cell predominant. If flow cytometry is available, it shows polytypic B-cells and polytypic plasma cells in LIP whereas the detection of a monotypic CD5-/CD10- B-cell population with/without monotypic plasma cells supports MALT lymphoma.

The pulmonary infiltrates in CLL/SLL may be sometimes indistinguishable from LIP, but they usually do not contain plasma cells. By immunohistochemistry, this B-cell lymphoma is positive for CD5 and CD23 and negative for cyclin D1, and in the case that flow cytometry is performed, B-cells are monotypic and co-express CD5, CD23, and CD200.

IGH gene rearrangement testing may be helpful to distinguish between LIP and B-cell lymphomas, but the presence of a polyclonal pattern does not exclude MALT lymphoma and detection of a small oligoclonal or monoclonal population may occasionally be seen in LIP. Therefore, the interpretation of *IGH* gene rearrangement should always be done in correlation with the clinico-radiologic presentation and the morphologic findings.

LIP that has progressed to interstitial fibrosis is extremely challenging and sometimes not possible to distinguish from other interstitial lung disorders, namely nonspecific interstitial pneumonia and usual interstitial pneumonia. Correlation with clinical history, laboratory, and imaging findings is mandatory to suggest the possibility of LIP (history of congenital/acquired immunodeficiency or an autoimmune disorder, hypergammaglobulinemia, prior diagnosis of LIP). The differential diagnosis of LIP is summarized in Table 15.3.

Table 15.3 Differential diagnosis of lymphoid interstitial pneumonia (LIP)

Follicular bronchiolitis
Hypersensitivity pneumonitis (extrinsic allergic alveolitis)
EBV pulmonary lymphoid infiltrates in infectious mononucleosis
Pulmonary marginal zone lymphoma of mucosa-associated lymphoid tissue • About 5% of cases of LIP can progress to marginal zone lymphoma
Chronic lymphocytic leukemia/small lymphocytic lymphoma with interstitial distribution
LIP with progression to interstitial fibrosis/end-stage lung disease • Nonspecific interstitial pneumonia • Usual interstitial pneumonia

IgG4-Related Lung Disease (IgG4-RLD)

Introduction

The first recognition of IgG4-related disease as a distinct entity occurred in the early 2000s by Hamano et al. [26] and Kamisawa et al. [27, 28] who reported cases of "autoimmune pancreatitis" with peculiar features and elevated IgG4 serum levels. Since then, the disease has been identified in virtually any organ, including the lung. IgG4-related disease is a systemic fibroinflammatory condition with characteristic mass-forming lesions that are rich in IgG4+ plasma cells and fibrosis [29]. Pulmonary involvement has been recognized as part of systemic IgG4-related disease, whereas isolated lung involvement is exceedingly rare [30]. In addition, lesions well-recognized for many years in lung pathology, such as plasma cell granuloma/inflammatory pseudotumor, have been recognized as part of the spectrum of IgG4-RLD. The incidence of IgG-RLD is unknown. Lung involvement in the setting of systemic IgG4-related disease varies from study to study with percentages ranging from around 15% to up to 50% [31].

Clinical Features

IgG4-RLD occurs in adults (50–60 years), and it is more common in men [32]. Patients can present with cough, dyspnea, or chest pain with or without systemic symptoms [33]. No definitive association between IgG4-RLD and underlying autoimmune disorders, immunodeficiency, or smoking has been demonstrated. Laboratory abnormalities include the detection of increased serum levels of IgG4 of >135 mg/dL and increased serum IgE. Patients with IgG4-RLD usually have involvement by IgG4-related disease at other sites, and mediastinal involvement may present in the form of sclerosing mediastinitis (see the corresponding section). IgG4-RLD responds well to steroid treatment. Surgical resection may be performed for localized lung lesions, and they are sometimes resected because they mimic lung cancer or a metastasis. The prognosis of IgG4-related disease depends on the recognition of this disorder in its early phase [32]. Without treatment, the disease can progress to full systemic disease with high co-morbidity or even death.

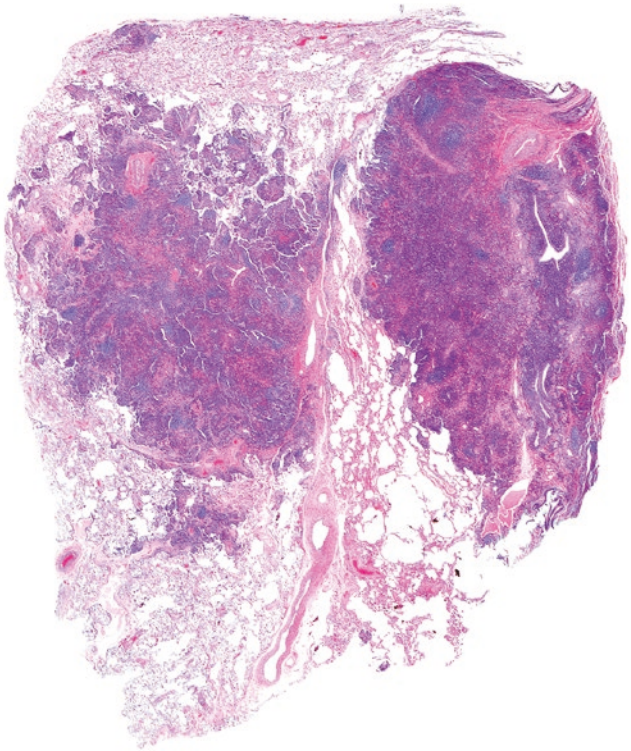

Fig. 15.16 Digital scan of IgG4-related lung disease (solid/nodular pattern). The nodules show bronchovascular and paraseptal distribution

Pathology

Lung involvement consists of a lymphoplasmacytic infiltrate with fibrosis that involves interlobular septa, bronchovascular bundles, and the visceral pleura [31, 33], and several patterns have been described, including solid nodular, bronchovascular, alveolar interstitial, pleural, and airway distributed patterns (Figs. 15.16, 15.17, 15.18 and 15.19). The morphologic triad of IgG4-related disease includes (1) fibrosis with storiform or concentric arrangement, (2) increased lymphoplasmacytic infiltrate, and (3) obliterative phlebitis [34]. Additional findings include the presence of eosinophils, necrotizing arteritis, and phlebitis without vascular obliteration (Fig. 15.20). A combination of these patterns may be seen in the same case. Although these findings are suggestive of IgG4-RLD, they are not entirely specific as they may be seen in other pulmonary inflammatory processes (see differential diagnosis). Some cases may

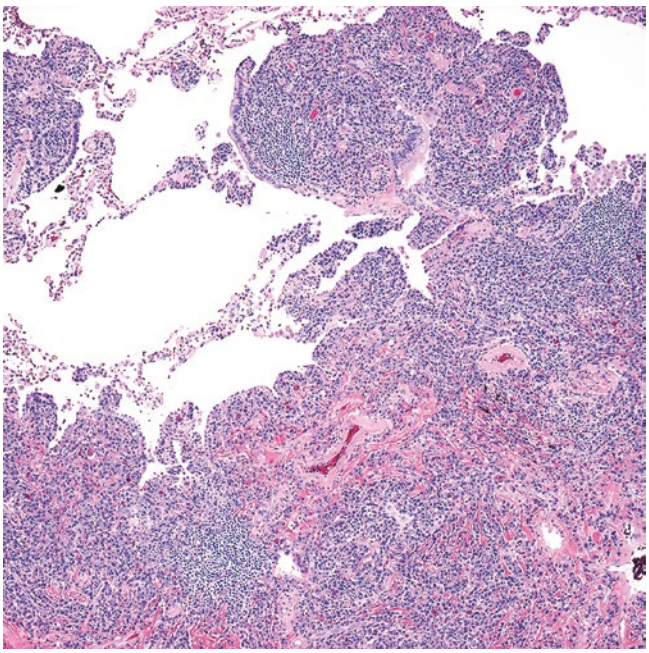

Fig. 15.17 Edge of a nodule of IgG4-related lung disease. There is a distortion of the lung architecture with numerous plasma cells and few lymphoid aggregates

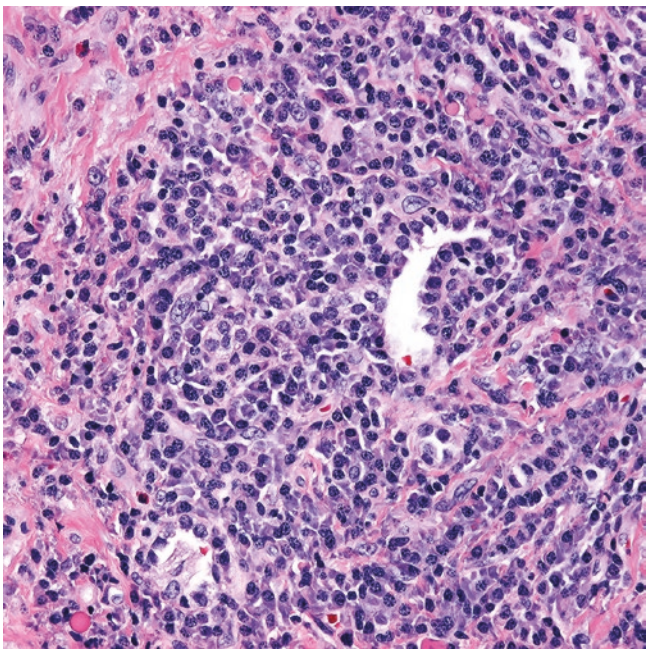

Fig. 15.19 IgG4-related lung disease. The lung parenchyma is replaced by aggregates of plasma cells, occasional eosinophils, and fibrosis. A few Russell bodies (top, right) and residual small airways are seen (center and bottom)

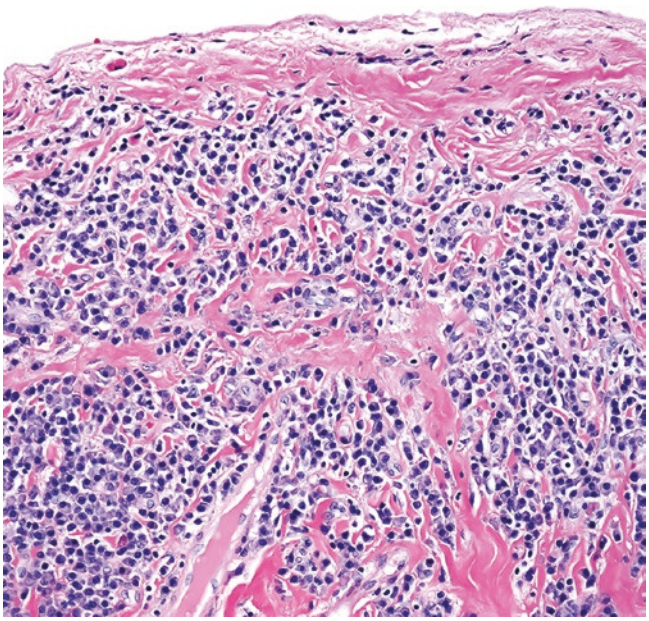

Fig. 15.18 Visceral pleura with aggregates of plasma cells and fibrosclerosis in IgG4-related lung disease

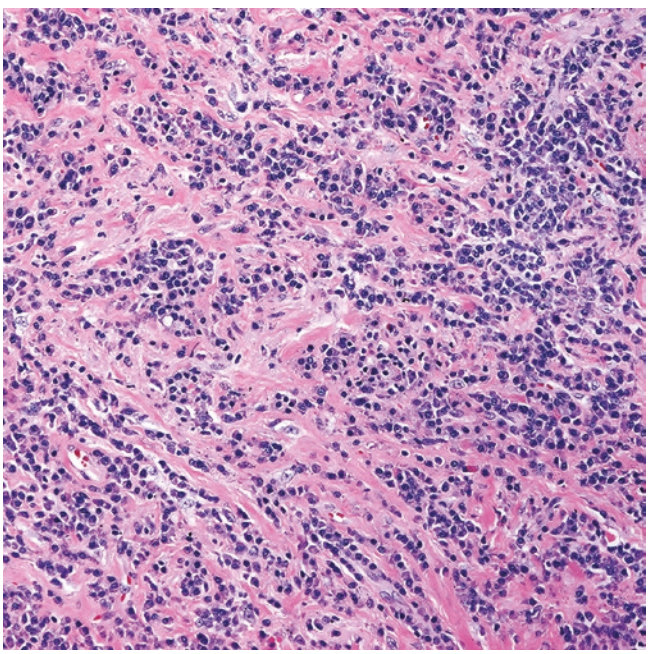

Fig. 15.20 Fibrosclerosis and numerous plasma cells in IgG4-related lung disease

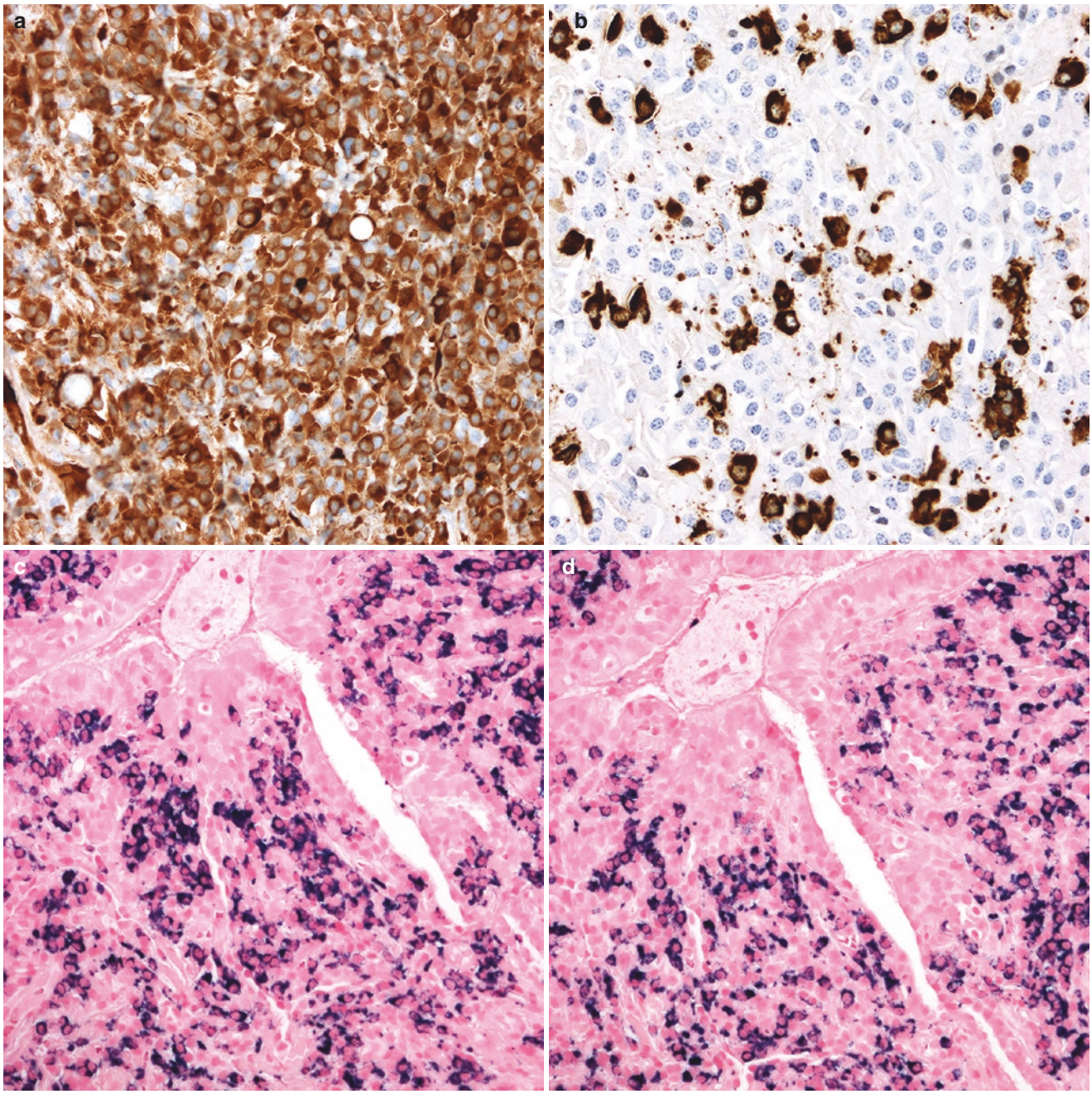

Fig. 15.21 IgG4-related lung disease. (**a**) IgG and (**b**) IgG4 immunohistochemistry. By in situ hybridization, the plasma cells are polytypic for (**c**) kappa and (**d**) lambda

exhibit areas resembling interstitial lung disease, namely cellular nonspecific interstitial pneumonia. One study suggests that transbronchial biopsies may be potentially diagnostic of IG4-RLD [35].

Immunohistochemistry and Other Ancillary Studies

Immunohistochemistry for IgG and IgG4 is mandatory to establish the diagnosis (Fig. 15.21). According to the 2012 consensus criteria for IgG-related disease, lung involvement should specifically show >50 IgG4+ plasma cells/high power field (HPF) in surgical specimens and >20 IgG4+ plasma cells/HPF in biopsies, and the IgG4/IgG ratio should always be >40% [34]. By definition, immunohistochemistry or ISH studies for kappa and lambda light chains always show polytypic plasma cells (Fig. 15.21). CD3 and CD20 immunostains highlight interspersed T-cells and B-cells, respectively, with a predominance of T-cells. B-cells are polytypic by flow cytometry immunophenotyping. The diagnostic criteria of IgG4-RLD are listed in Table 15.4.

Table 15.4 Diagnostic criteria of IgG4-related lung disease

Morphologic
(1) Fibrosis with storiform or concentric arrangement
(2) Increased lymphoplasmacytic infiltrate
(3) Obliterative phlebitis (not always)
• May be present but not required: eosinophils, necrotizing arteritis, phlebitis without obliteration
Immunohistochemistry
>50 IgG4+ plasma cells/high power field in a surgical resection
>20 IgG4+ plasma cells/high power field in a biopsy
IgG4/IgG ratio should always be >40%

Table 15.5 Differential diagnosis of IgG4-related lung disease

Lung conditions that may be accompanied by increased IgG4+ plasma cells
• Non-specific interstitial pneumonia, idiopathic
• Usual interstitial pneumonia
• Necrotizing granulomatous inflammation
• Collagen vascular diseases
• Inflammatory reaction around a lung mass (benign or malignant)
Pulmonary nodular lymphoid hyperplasia (although a subset of cases may form part of the spectrum of IgG4-related lung disease)
Pulmonary marginal zone lymphoma of the mucosa-associated lymphoid tissue with extensive plasmacytic differentiation
Idiopathic multicentric Castleman disease with lung involvement

Differential Diagnosis

A combined clinical, laboratory, morphologic, and immunohistochemical scoring is used to classify a case as "possible", "probable", and "definitive" IgG4-related disease and this applies to all organs involved [34]. Regardless of the location, the IgG4/IgG ratio should always be >40% [34].

IgG4-RLD can present with a wide variety of morphologic patterns and therefore a high level of suspicion for this disease is required to avoid missing the diagnosis [36]. Features that militate against IgG4-RLD include the presence of sarcoid-type granulomas and necrotizing vasculitis. The detection of increased IgG4+ plasma cells is mandatory, but pathologists should be aware that this feature is not specific to this disorder and many other entities may be accompanied by increased IgG4+ plasma cells, namely idiopathic nonspecific interstitial pneumonia, usual interstitial pneumonia, necrotizing granulomatous inflammation, and collagen vascular diseases [31, 37]. Clinical and laboratory correlation is required to determine the origin of a plasma cell-rich inflammatory lung lesion and rule in or rule out the diagnostic possibility of IgG4-RLD. Similarly, secondary vs. primary lung involvement by IgG4-related disease can only be established by clinical and radiologic correlation. Interestingly, one study has suggested that PNLH could represent a lesion within the spectrum of IgG4-related disease [10].

Increased IgG4+ plasma cells are not uncommonly seen around primary or metastatic tumors in any organ including the lung, and this should be taken in consideration when a biopsy of a mass suspicious for malignancy demonstrates increased IgG4+ plasma cells and fibrosis, which could well represent the capsule or the peripheral inflammatory reaction to a tumor. One of the authors (S.P.O) has seen core biopsies of lung masses that have been diagnosed as "probable" IgG4-RLD with hyalinized tissue and moderately increased IgG4+ plasma cells only to find out on a subsequent resection that the findings in the biopsy corresponded to the edge of a pulmonary hyalinizing granuloma.

Pulmonary MALT lymphoma with extensive plasmacytic differentiation is distinguished from IgG4-RLD with a solid/nodular pattern by the detection of IgG4+ polytypic plasma cells. However, not all cases of MALT lymphoma contain a monotypic plasma cell component. Features that favor pulmonary MALT lymphoma over tumefactive IgG4-RLD include effacement of the architecture, nodules or sheets of lymphocytes and monocytoid lymphocytes, abundant lymphoepithelial lesions, and invasion of bronchial cartilage and of the visceral pleura.

Idiopathic multicentric (plasma cell-rich) Castleman disease may occasionally involve the lung, and it significantly overlaps with IgG4-RLD by morphology and pattern of distribution. A recent study suggests that a low IgG4/IgG ratio, a decreased eosinophil count, an IgA-positive cell count, and increased expression of interleukin-6 support lung involvement by multicentric Castleman disease over IgG4-RLD [38]. The differential diagnosis of IgG4-RLD is summarized in Table 15.5.

The clinicopathologic features of the different types of pulmonary reactive lymphoid disorders and their comparison to pulmonary MALT lymphoma are summarized in Table 15.6.

Table 15.6 Differential diagnosis of reactive lymphoid lesions of the lung and pulmonary MALT lymphoma

	Follicular bronchiolitis	Pulmonary nodular lymphoid hyperplasia	Lymphoid interstitial pneumonia	IgG4-related lung disease (IgG4-RLD)	Pulmonary MALT lymphoma
Clinical features					
Age group	Adults > children	Adults > children	Adults = children	Adults > children	Adults > children
Gender	Slight male predominance	Slight male predominance	F > M	M > F	Slight female predominance
Associated autoimmune disorder, immunodeficiency, or HIV infection	Yes	No	Yes	No	Yes, ~30% of patients
Other infectious agents	No	No	EBV, HHV-8, *Mycoplasma*	No	Not clear; subset of cases might be associated with *Achromobacter xylosoxidans* infection
Extrapulmonary disease	No	No	No	Common	Sometimes, gastric or salivary gland MALT lymphoma
Progression to lymphoma	No	No	Yes, 5% to pulmonary MALT lymphoma	No	N/A
Imaging					
Localized mass	No	Yes	No	Uncommon	Yes
Ground-glass opacities	Yes	No	Yes	Yes, but more common as multiple nodules	Sometimes at the periphery of the tumor
Histopathology					
Localized mass	No	Yes	No	Uncommon	Yes
Diffuse/interstitial	No	No	Yes	Yes, along with multiple nodules	May be at the periphery or mass
Lymphoid follicles with reactive germinal centers	Yes, peribronchiolar distribution	Yes, forming a mass with/without interfollicular fibrosis	May be present, but not prominent	May be present, but not prominent	Yes, but may be absent
Follicular "colonization" (disrupted FDC meshworks)	No	No	No	No	Yes, highlighted by CD21, CD23, or CD35
Plasma cells	Not prominent	Yes, interfollicular areas	Variable, usually not prominent	Prominent	Variable, some cases with extensive plasmacytic differentiation
Increased IgG4+ plasma cells	No	Variable Positive cases may belong to Ig4-RLD	No	Yes	No Only rarely MALT lymphomas are IgG4+
Monocytoid B-cells and lymphoepithelial lesions	No	No	No Only rarely few lymphoepithelial lesions may be seen	No	Yes
Type of interstitial lymphoid infiltrate	N/A	N/A	T-cells Occasionally >B-cells (if HIV+)	T-cells	B-cells
Light chain restriction (IHC, ISH, FC)	No	No	No	No	Yes
Clonal *IGH* gene rearrangement	No	No	No	No	Yes, some cases may be negative

MALT mucosa-associated lymphoid tissue, *HIV* human immunodeficiency virus, *EBV* Epstein–Barr virus, *HHV-8* human herpesvirus-8, *FDC* follicular dendritic cell, *IHC* immunohistochemistry, *ISH* in situ hybridization, *FC* flow cytometry, *IGH* immunoglobulin heavy chain gene

Malignant Lymphoproliferative Disorders and Other Hematopoietic Disorders of the Lung

Introduction

Malignant hematolymphoid disorders of the lung are rare. They include cases of non-Hodgkin lymphoma (B and T), classic Hodgkin lymphoma, and myeloid sarcoma/acute myeloid leukemia [12]. Secondary involvement by systemic disease is much more common than primary lung disease. Therefore, the definition of a hematopoietic lung neoplasm as primary or secondary relies on a prior positive or negative history of lymphoma or leukemia. The radiologic findings in these disorders vary according to the subtype of hematopoietic neoplasm, and by imaging none of them can be distinguished from more common pulmonary diseases, namely lobar pneumonia, tuberculosis, primary lung carcinoma, or metastatic disease [39, 40]. Ultimately, the diagnosis requires histopathologic confirmation.

Primary lung lymphomas comprise <1% of all primary lung tumors and <5% of all extranodal lymphomas [41]. They are defined as lymphomatous involvement of the lung and/or hilar lymph nodes without evidence of systemic disease at the time of diagnosis or 3 months thereafter. In general, patients with primary lung lymphoma are adults (median age 60 years), although some cases may occur in younger individuals with an underlying immunodeficiency or autoimmune disorder [6]. Non-Hodgkin lymphomas of B-cell origin include pulmonary marginal zone lymphoma of the mucosa-associated lymphoid tissue (pulmonary MALT lymphoma), pulmonary diffuse large B-cell lymphoma (DLBCL), intravascular LBCL, lymphomatoid granulomatosis (LYG), pulmonary plasmacytoma, and other small B-cell lymphomas. MALT lymphoma and DLBCL alone comprise >95% of cases. Pulmonary T-cell lymphomas include anaplastic large cell lymphoma (ALCL) and peripheral T-cell lymphoma, not otherwise specified (PTCL, NOS). Pulmonary classic Hodgkin lymphoma (CHL) is very rare, and in most situations, lung involvement represents extension of mediastinal CHL to the lung. Acute myeloid leukemia may present as a mass (pulmonary myeloid sarcoma), as a multifocal process, or as diffuse reticulonodular infiltrates. Histiocytic disorders can also affect the lung with some of the most representative lesions described at the end of this section. Table 15.7 summarizes the malignant hematopoietic tumors of the lung.

Table 15.7 Malignant hematopoietic tumors of the lung

Lymphoid
Non-Hodgkin of B-cell origin
• Marginal zone lymphoma of the mucosa-associated lymphoid tissue
• Diffuse large B-cell lymphoma
• Intravascular large B-cell lymphoma
• Lymphomatoid granulomatosis
• Plasmacytoma
• Other small B-cell lymphomas: chronic lymphocytic leukemia/small lymphocytic lymphoma, mantle cell lymphoma, follicular lymphoma, lymphoplasmacytic lymphoma
Non-Hodgkin of T-cell origin
• Anaplastic large cell lymphoma
• Peripheral T-cell lymphoma, not otherwise specified
• Others: angioimmunoblastic T-cell lymphoma, extranodal NK/T-cell lymphoma, "visceral" mycoses fungoides
Classic Hodgkin lymphoma
• Most common subtypes: nodular sclerosis and mixed cellularity
Myeloid
• Acute myeloid leukemia/myeloid sarcoma
Histiocytic
• Langerhans cell histiocytosis
• Extranodal Rosai–Dorfman disease
• Erdheim–Chester disease

Common imaging patterns of pulmonary lymphomas include nodular (i.e., nodules and masses), pneumonic-alveolar (i.e., consolidative opacities, often with air bronchograms), and bronchovascular-lymphangitic (i.e., thickening of bronchovascular bundles and interlobular septa) [42–44]. Lymphomatous nodules can be single or multiple, tend to be round or oval with ill-defined margins, and more commonly involve the lower lobes [42] (Fig. 15.22). They may contain air bronchograms, cavitate, and traverse interlobar fissures. The pneumonic-alveolar pattern is indistinguishable from pneumonia and may be segmental, lobar, unilateral, or bilateral [42] (Fig. 15.23). The bronchovascular-lymphangitic pattern mimics lymphangitic carcinomatosis and, when extensive, can mimic bronchopneumonia [42] (Fig. 15.24).

Even though the diagnosis of most of these lesions can be accomplished without difficulty in a wedge resection or partial pneumonectomy, this may not be the case in a core needle biopsy or in specimens with a significant cellular artifact. Therefore, in these instances, the diagnosis of a malignant hematolymphoid disorder benefits substantially from additional ancillary tests, namely immunohistochemistry, flow cytometry immunophenotyping, and cytogenetic and/or molecular analysis.

Fig. 15.22 Lymphoma—nodular pattern. CT shows a right lower lobe mass (black arrow) and left lower lobe nodules (white arrows)

Fig. 15.23 Lymphoma—pneumonic-alveolar pattern. CT shows air-space consolidation (arrows) with air bronchograms in the right lung

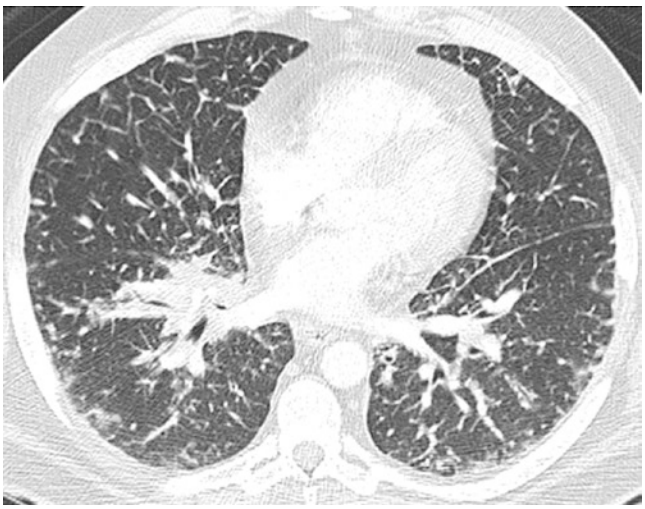

Fig. 15.24 Lymphoma—bronchovascular-lymphangitic pattern. CT shows diffuse bilateral interlobular septal thickening as well as peribronchovascular thickening in the right lower lobe

Pulmonary Non-Hodgkin Lymphomas of B-Cell Origin

Pulmonary Marginal Zone Lymphoma of the Mucosa-Associated Lymphoid Tissue (Pulmonary MALT Lymphoma)

Introduction

Extranodal marginal zone lymphoma/MALT lymphoma was originally described in 1983 by Isaacson and Wright as a low-grade lymphoma that involved the gastrointestinal tract [45]. The term MALT was coined due to its morphologic resemblance to "normal" MALT, namely Peyer patches and the Waldeyer ring. Since then, MALT lymphoma has been recognized in several other organs, including the lung. It is hypothesized that pulmonary MALT lymphoma develops from persistent antigenic exposure (inflammatory, infectious, autoimmune) resulting in a chronically stimulated BALT that eventually transforms into a clonal process [46] (Fig. 15.25).

MALT lymphoma is the most common primary pulmonary lymphoma (about 80% of cases) and about 8% of all extranodal MALT lymphomas [41, 47]. The association

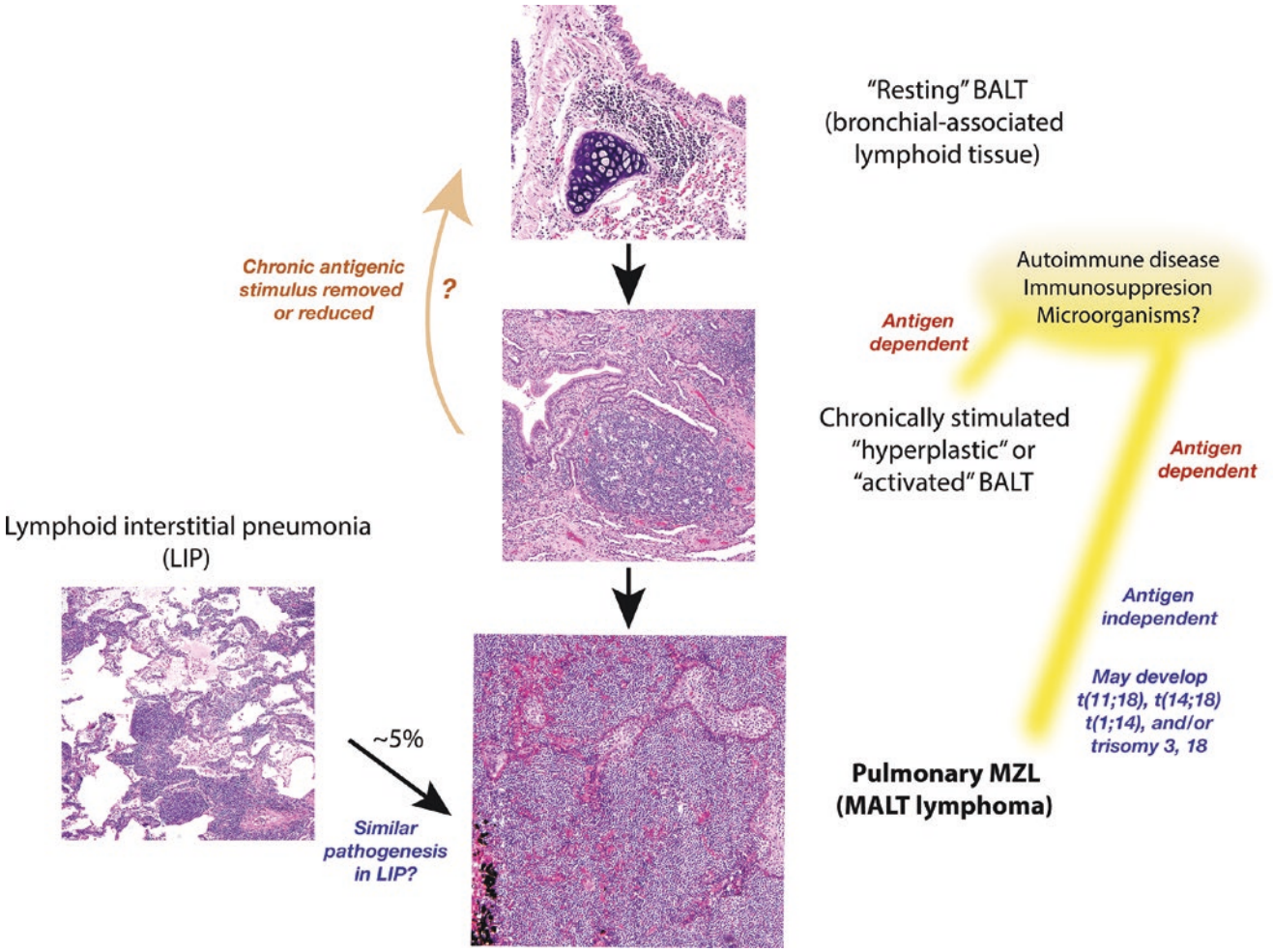

Fig. 15.25 Pathogenesis of pulmonary marginal zone lymphoma (MZL) of mucosa-associated lymphoid tissue (MALT lymphoma). In normal conditions, the bronchial-associated lymphoid tissue (BALT) is not conspicuous, also referred to as "resting" BALT. After chronic exposure to antigens or after a persistent chronic inflammatory response (highlighted in yellow), the BALT proliferates and expands in the form of secondary lymphoid follicles with germinal centers, plasma cells, and other inflammatory cells. If the antigenic stimulus is removed or reduced, the BALT may likely return to a "resting" state (light brown arrow). However, if the antigenic stimulus persists, the BALT can eventually proliferate independently from this stimulus and turn into a clonal process. Cytogenetic abnormalities may or may not develop at this point or perhaps at earlier stages. On the other hand, a small subset of cases of lymphoid interstitial pneumonia (LIP) can progress to pulmonary MALT lymphoma. It is possible that the same pathogenetic mechanisms mentioned above may play a role in the development of pulmonary lymphoma in the setting of LIP. (t(14;18)(q32;q21) refers to *IGH-MALT1* gene rearrangement, not *IGH-BCL2*)

between *Achromobacter xylosoxidans* chronic lung infection and pulmonary MALT lymphoma is controversial and requires further study.

Clinical Features

Pulmonary MALT lymphoma occurs primarily in adults (median age 68 years), and it is slightly more frequent in women than men [44]. Younger patients are usually immunosuppressed, likely due to HIV infection, post-allogeneic transplantation, or a congenital immunodeficiency. A third of patients have an underlying autoimmune disease, namely rheumatoid arthritis, systemic lupus erythematosus, or Sjögren syndrome. Up to 30% of patients are asymptomatic, whereas the remaining two-thirds may have nonspecific symptoms, such as fever and malaise, along with cough, dyspnea, chest pain, or hemoptysis [48–53]. The initial clinical presentation usually suggests a pneumonic process, but the clinical symptoms persist despite antibiotic treatment. Laboratory abnormalities are nonspecific, and up to 40% of patients may develop a serum M-protein. Concurrent involvement may be observed in mediastinal/hilar lymph nodes. Progression to large cell lymphoma occurs in about 10% of patients.

The prognosis of pulmonary MALT lymphoma is good, with survival rates of 90% and 70% at 5 years and 10 years, respectively [51, 52, 54, 55]. According to a recent study from China evaluating 90 cases of primary pulmonary lymphoma (56% of cases were MALT lymphoma), age above 60 years, elevated serum LDH and beta-2 microglobulin,

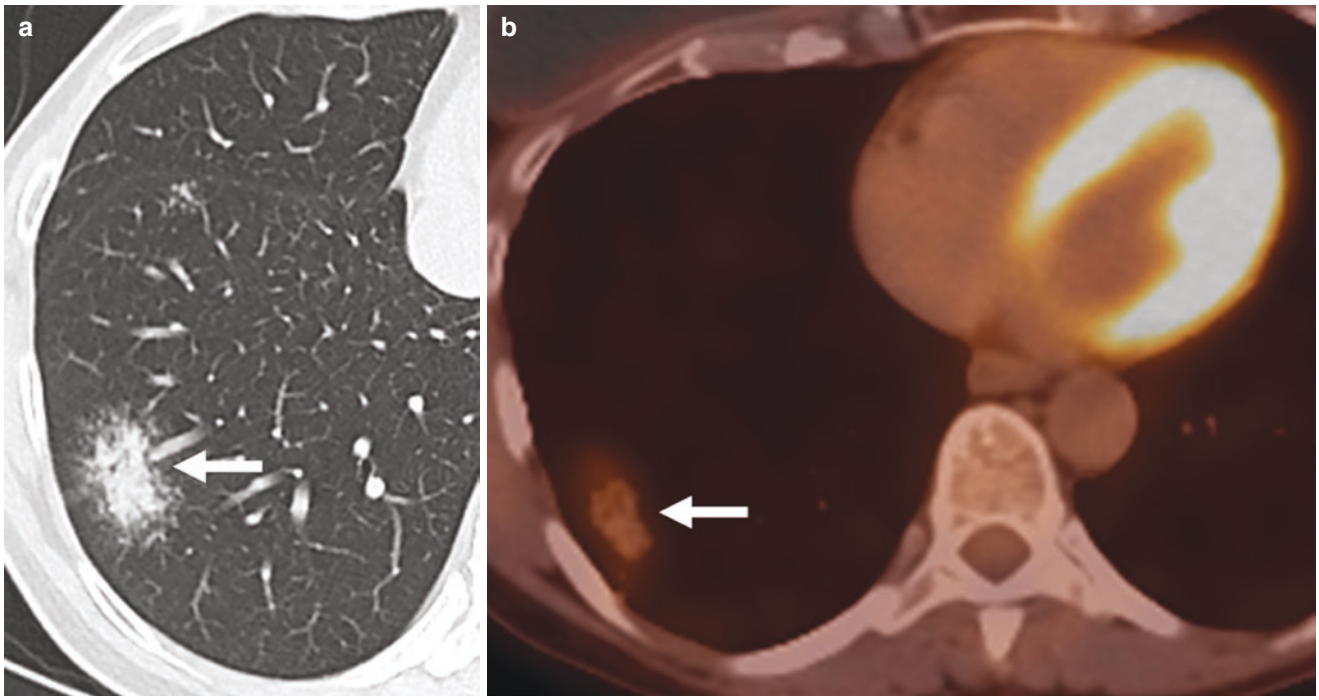

Fig. 15.26 MALT lymphoma. (**a**) CT shows a part-solid nodule (arrow) in the right lower lobe; (**b**) PET/CT shows the nodule (arrow) is not FDG-avid

clinical stage II2E or higher, and nonsurgical treatment were associated with poor prognosis [53]. Pulmonary MALT lymphoma may be followed by observation, but in some instances surgical excision or single agent/rituximab chemotherapy may be required depending on the extension of the disease, its location within the lung, and the presence/absence of regional lymphadenopathy [39, 50, 54, 55].

Diagnostic Imaging

MALT lymphoma in the lung has a wide variety of manifestations on CT [43, 56–58]. Bae and colleagues described the following four patterns on CT in their review of 21 patients with pulmonary MALT lymphoma: single nodular or consolidative; multinodular or consolidative (lesions distributed along bronchovascular bundles or subpleural regions); bronchiectasis and bronchiolitis (tree-in-bud pattern of abnormality with bronchiectasis); and diffuse interstitial lung disease (patchy areas of ground-glass opacity distributed in the subpleural lungs with lower lung zone predominance) [57]. Single or multiple nodules or consolidative opacities are the most common patterns (>70%), and lesions tend to be multiple and bilateral (>70%) and peribronchovascular [43]. Peribronchovascular opacities are commonly associated with bronchial dilatation [43]. Hilar and/or mediastinal lymphadenopathy is present in approximately 30% of cases [43]. MALT lymphoma lesions, because they are typically low-grade with mild metabolic activity, usually have only low-grade or no FDG uptake on PET/CT [59] (Fig. 15.26a, b).

Pathology

Sampling of a lung lesion is usually accomplished via an imaging-guided needle biopsy or a transbronchial biopsy, and the diagnosis is established either in a cytology specimen, a core-needle biopsy, or a transbronchial biopsy. If the diagnosis of pulmonary lymphoma is rendered in any of these specimens, then a wedge resection or a lobectomy is not performed. However, a resection may still be done when a biopsy is inconclusive for diagnosis.

Grossly, pulmonary MALT lymphoma is described as a tan-white mass with relatively well-delimited borders and peripheral consolidation. Residual entrapped airways within the mass correspond to the air bronchograms observed on imaging. Necrosis is uncommon. If the tumor involves the pleura, it occurs in the form of a tan-white thickened plaque or as multiple pleural nodules. On microscopic examination, pulmonary MALT lymphoma consists of sheets of small lymphocytes and monocytoid lymphocytes with diffuse effacement of the architecture (Fig. 15.27a, b). The center of the tumor tends to be sclerotic, and residual bronchial cartilage and "ghosts" of smaller airways are frequently seen (Fig. 15.28). The periphery of the tumor is relatively well-delimited with lymphomatous extension into the adjacent lung in a lymphangitic pattern or through alveolar interstitial spaces mimicking LIP (Fig. 15.29). Bronchi and bronchioles that are apart from the epicenter of the tumor may contain small collections of lymphocytes that resemble hyperplas-

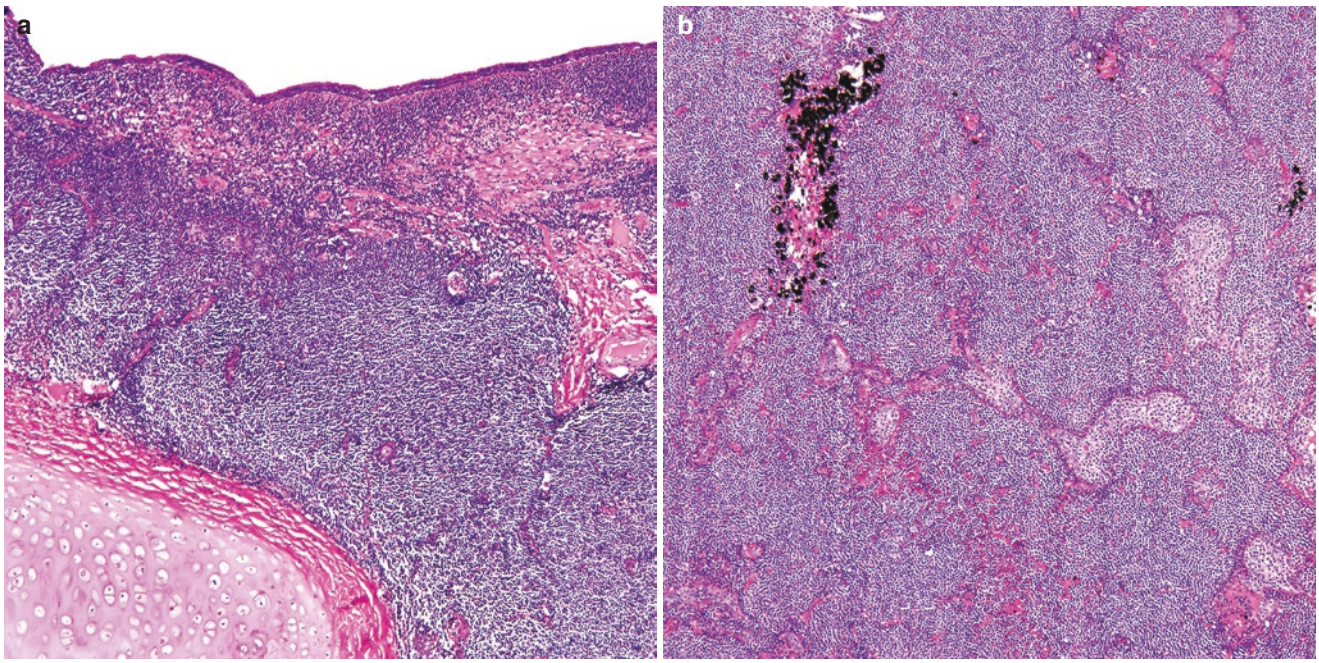

Fig. 15.27 (**a**) Pulmonary MALT lymphoma diffusely infiltrating bronchial submucosa, and (**b**) effacement of the lung architecture by MALT lymphoma. The elongated pale structures to the right are residual bronchioles distorted by numerous intraepithelial lymphocytes (lymphoepithelial lesions)

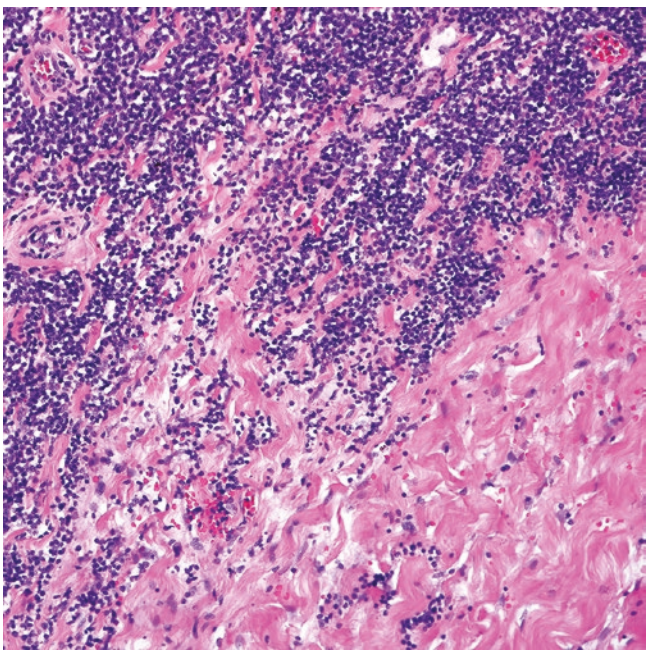

Fig. 15.28 Pulmonary MALT lymphoma with areas of sclerosis

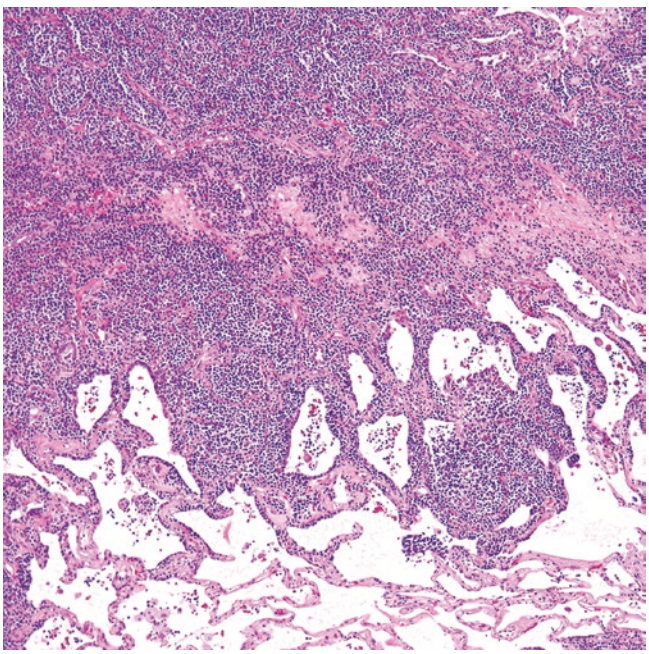

Fig. 15.29 The periphery of pulmonary MALT lymphoma can show interstitial expansion by numerous lymphoma cells, mimicking the pattern seen in lymphoid interstitial pneumonia

tic BALT (Fig. 15.30). Most lymphoma cells are small, and there is a variable proportion of monocytoid lymphocytes and centrocyte-like cells (cells with cleaved nucleus, moderately condensed chromatin and inconspicuous nucleolus) [60, 61]. A few scattered large immunoblast-like cells may or may not be present (Fig. 15.31a, b). Likewise, plasmacytoid lymphocytes and plasma cells are variably seen, with some cases showing extensive plasmacytic differentiation. Lymphoepithelial lesions are seen in the respiratory epithelium of bronchi or bronchioles as well as in alveoli (Fig. 15.32a, b). Reactive lymphoid follicles may or may not be present, and they may be colonized by lymphoma cells with distortion of the germinal center morphology (no polarization or tingible-body macrophages) (Fig. 15.33). Neither necrosis nor significant increase in large cells are seen. Additional findings that may be observed in pulmonary MALT lymphoma include epithelioid granulomas (sometimes prominent enough to obscure the lymphomatous component), multinucleated cells associated with cholesterol clefts, and amyloid deposition within or at the periphery the tumor. The adjacent uninvolved lung or partially replaced areas contain abundant alveolar macrophages with foamy cytoplasm, multinucleated giant cells, intraalveolar proteinaceous material (Fig. 15.34), and/or large lamellar bodies (rings of eosinophilic material made of surfactant protein) [6, 51, 60]. When the visceral pleura is involved, the lymphoma cells percolate into the mesothelium without breaking through the pleura and they tend to form polypoid structures [48] (Fig. 15.35). Rarely, pulmonary MALT lymphoma may be associated with crystal-storing histiocytosis [62] (Fig. 15.36).

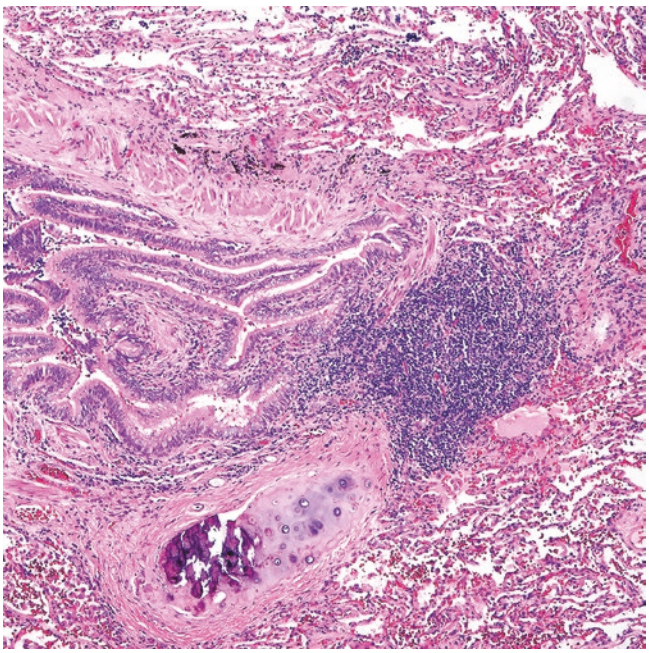

Fig. 15.30 The bronchus is apart from the areas of lymphoma but shows a neoplastic lymphoid aggregate mimicking bronchial-associated lymphoid tissue (BALT)

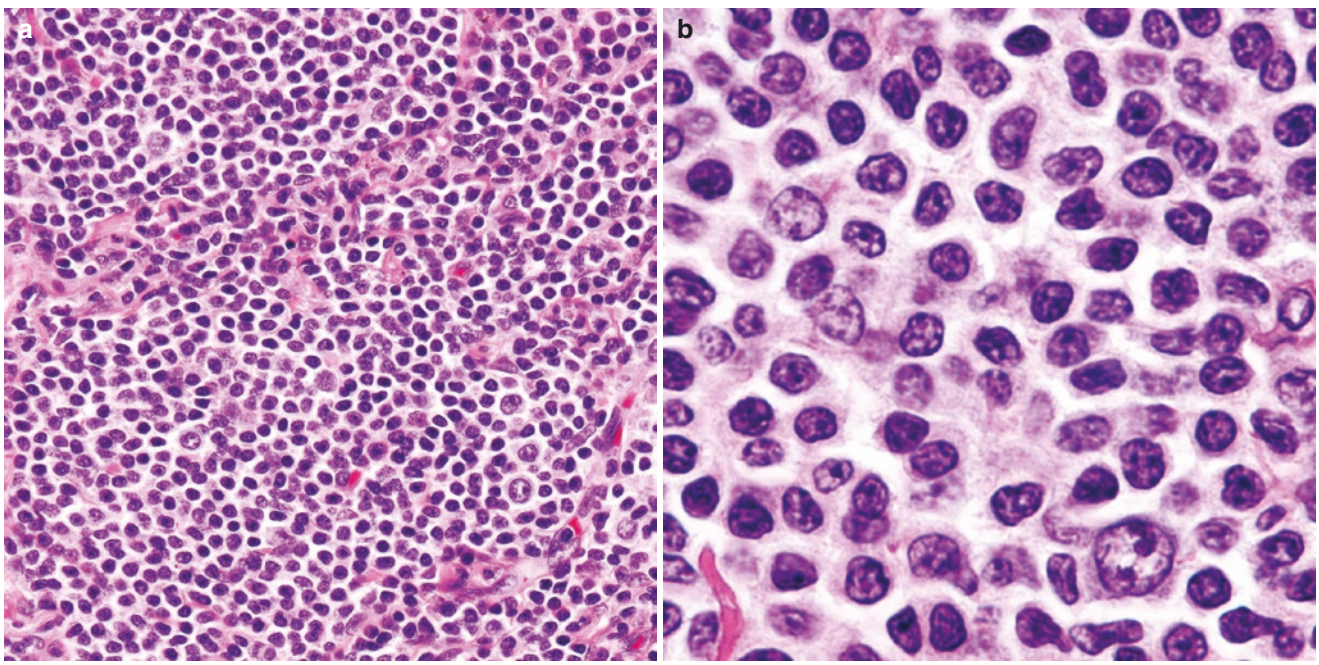

Fig. 15.31 (**a**–**b**) Pulmonary MALT lymphoma is composed of sheets of small lymphocytes, centrocyte-like cells, monocytoid cells, and scattered large immunoblast-like cells with prominent nucleolus (bottom, right; in both panels)

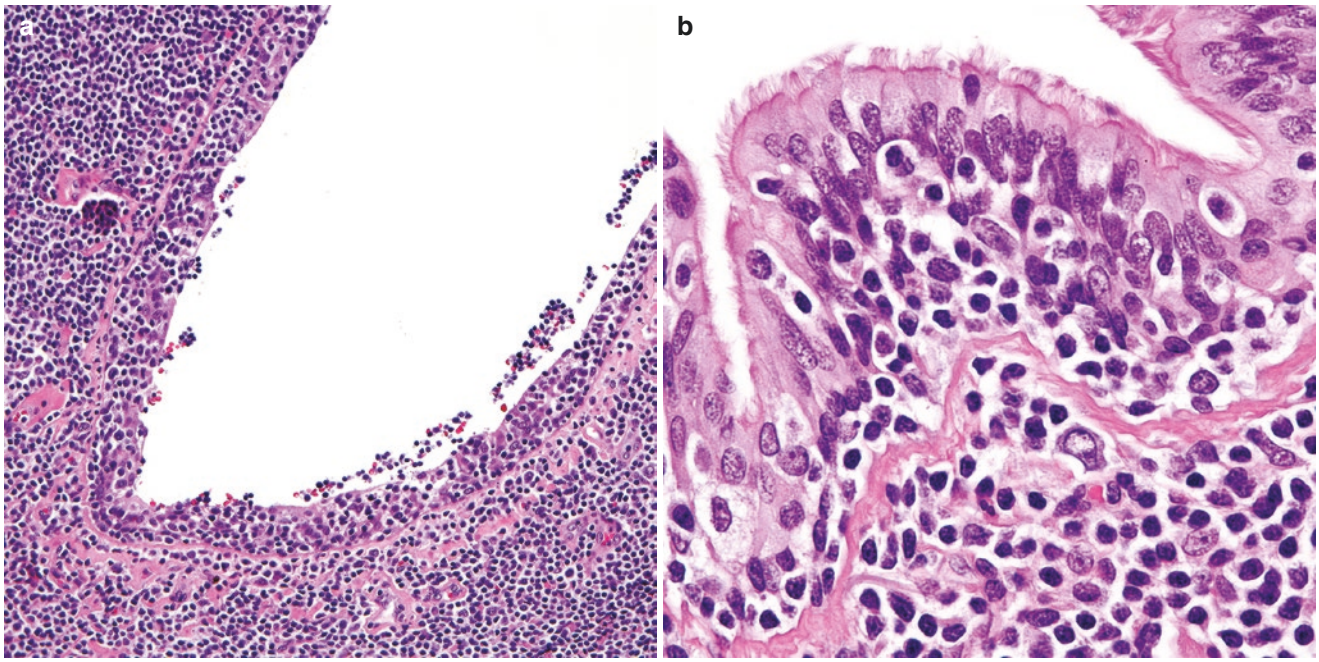

Fig. 15.32 (**a**) Lymphoepithelial lesion in a large bronchus with marked distortion of the epithelium, and (**b**) lymphoepithelial lesion with only partial distortion of the respiratory epithelium

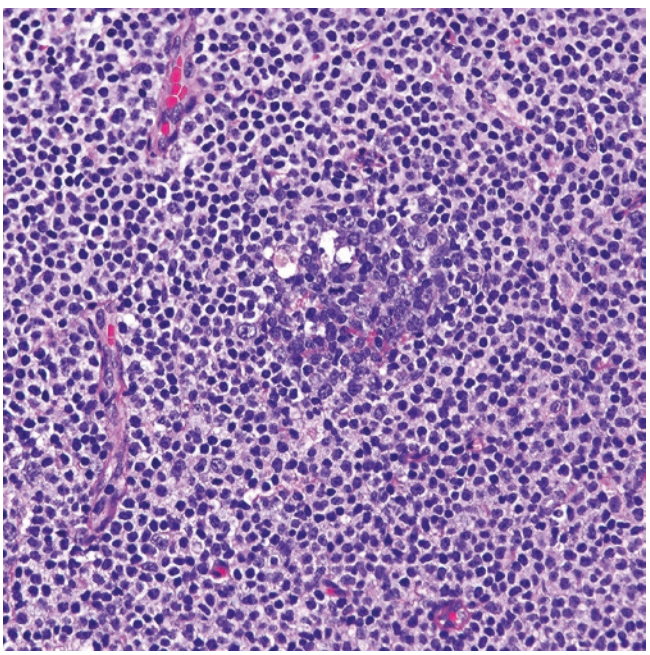

Fig. 15.33 Follicular colonization. The lymphoid follicle is almost entirely replaced by lymphoma cells with monocytoid morphology. The central darker area corresponds to the residual germinal center

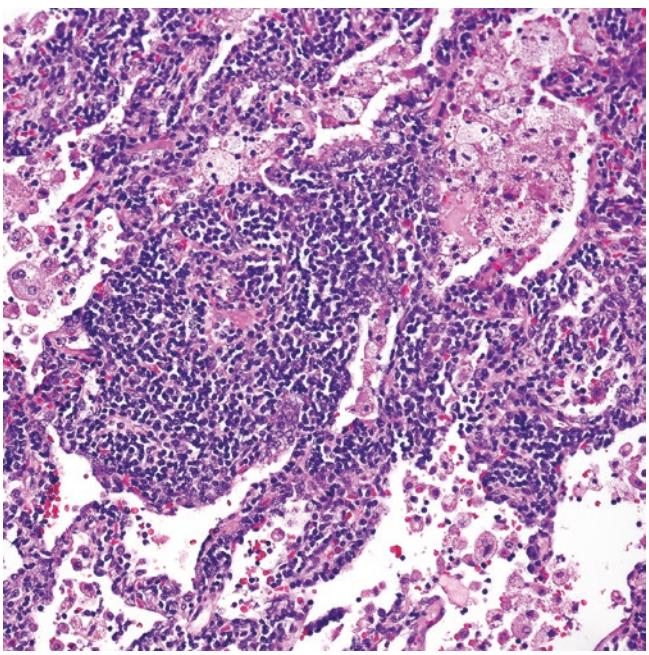

Fig. 15.34 Areas at the periphery of pulmonary MALT lymphoma may show a pattern identical to that of lymphoid interstitial pneumonia and may contain abundant intraalveolar macrophages with foamy cytoplasm and proteinaceous eosinophilic material

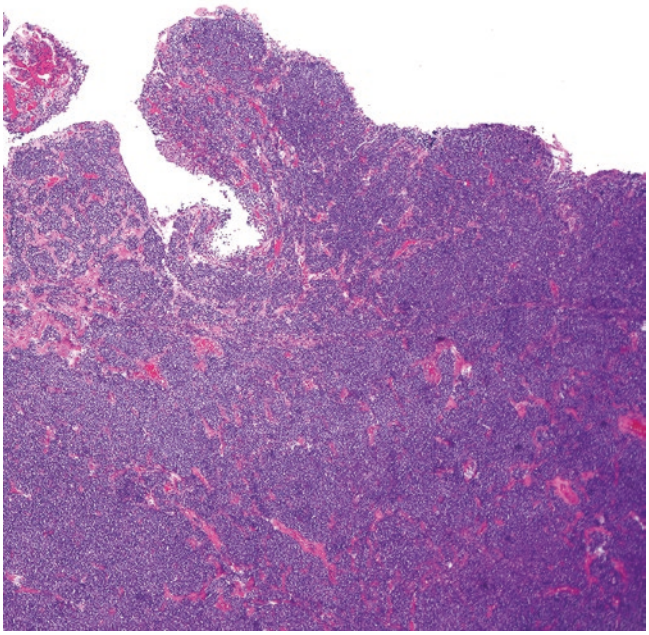

Fig. 15.35 Pulmonary MALT lymphoma involving visceral pleura as characteristic nodular structures grossly seen as tan-white pleural nodules

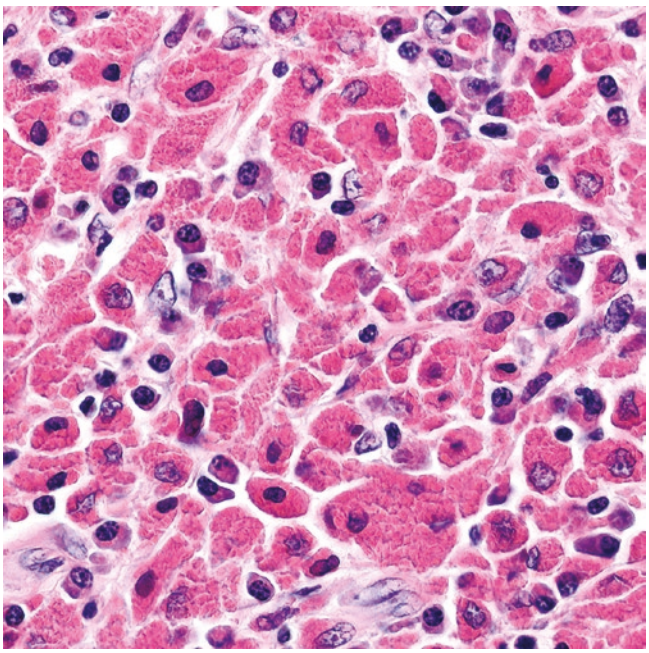

Fig. 15.36 Crystal-storing histiocytosis in a case of pulmonary MALT lymphoma with extensive plasmacytic differentiation. Only a few residual plasma cells are seen in this field

Immunohistochemistry and Other Ancillary Studies

MALT lymphoma is a CD5-/CD10- B-cell lymphoma (CD20+/PAX5+). The neoplastic B-cells co-express bcl-2 and in some cases also CD43. The lymphoma cells are negative for T-cell markers, CD23, bcl-6, LMO2, LEF1, and cyclin D1 (Fig. 15.37a–e). Extranodal MALT lymphomas are positive for MNDA (myeloid nuclear differentiation antigen) and IRTA-1 (immunoglobulin superfamily receptor translocation-associated 1), and these markers are usually positive in lymphoma cells in and around lymphoepithelial lesions [63, 64]. Plasma cells are positive for CD138 and MUM1, and light chain restriction may or may not be detected (usually seen in cases with extensive plasmacytic differentiation) (Fig. 15.38). Residual germinal centers are positive for CD10 and bcl-6, and the FDC markers CD21, CD23, and/or CD35 are useful to highlight disrupted FDC meshworks of colonized follicles (Fig. 15.39). CD20 highlights lymphoepithelial lesions while pan-cytokeratin decorates residual disrupted bronchial or alveolar epithelium (Fig. 15.40). MALT lymphoma has a low Ki-67 proliferation index (<30%). A high Ki-67 is only seen in residual reactive germinal centers. If flow cytometry is performed, there is a population of CD5-/CD10- monotypic B-cells, and a monotypic population of plasma cells (with identical light chain as that of the B-cells) may or may not be detected.

Differential Diagnosis

Pulmonary MALT lymphoma needs to be distinguished from reactive pulmonary lymphoid conditions, such as PNLH and LIP, as well as from other small B-cell lymphomas, namely CLL/SLL, mantle cell lymphoma, and follicular lymphoma involving the lung.

Although PNLH and LIP may not pose a significant challenge for diagnosis in a resection, their distinction from pulmonary MALT lymphoma may be difficult in a core needle biopsy. On imaging, both PNLH and pulmonary MALT lymphoma present as a mass. Histologically, PNLH consists of a nodule or mass-forming lesion made of reactive lymphoid follicles with well-defined borders. All follicles contain germinal centers with polarization, tingible-body macrophages, and mantle zones, and there is no follicular colonization. Sheets of monocytoid lymphocytes or centrocyte-like cells are not seen. The interfollicular areas may or may not contain plasma cells or may show fibrosis. Effacement of the adjacent lung parenchyma and lymphoepithelial lesions are not seen, and peripheral lesions do not infiltrate the visceral pleura. By immunohistochemistry, B-cells do not show co-expression of CD43 and bcl-2, and FDC markers highlight normal FDC meshworks. B-cells and plasma cells are always polytypic. If *IGH* gene rearrangement prophile is performed in a small lesion or a core biopsy, this study usually shows a polyclonal pattern. However, pathologists should be aware that the detection of a clone by this method does not necessarily translate into lymphoma since tissues with large reactive germinal centers, including PNLH, may occasionally show an oligoclonal or clonal pattern. Therefore, the interpretation of *IGH* gene rearrangement should always be done in correlation with the clinical presentation and the morpho-

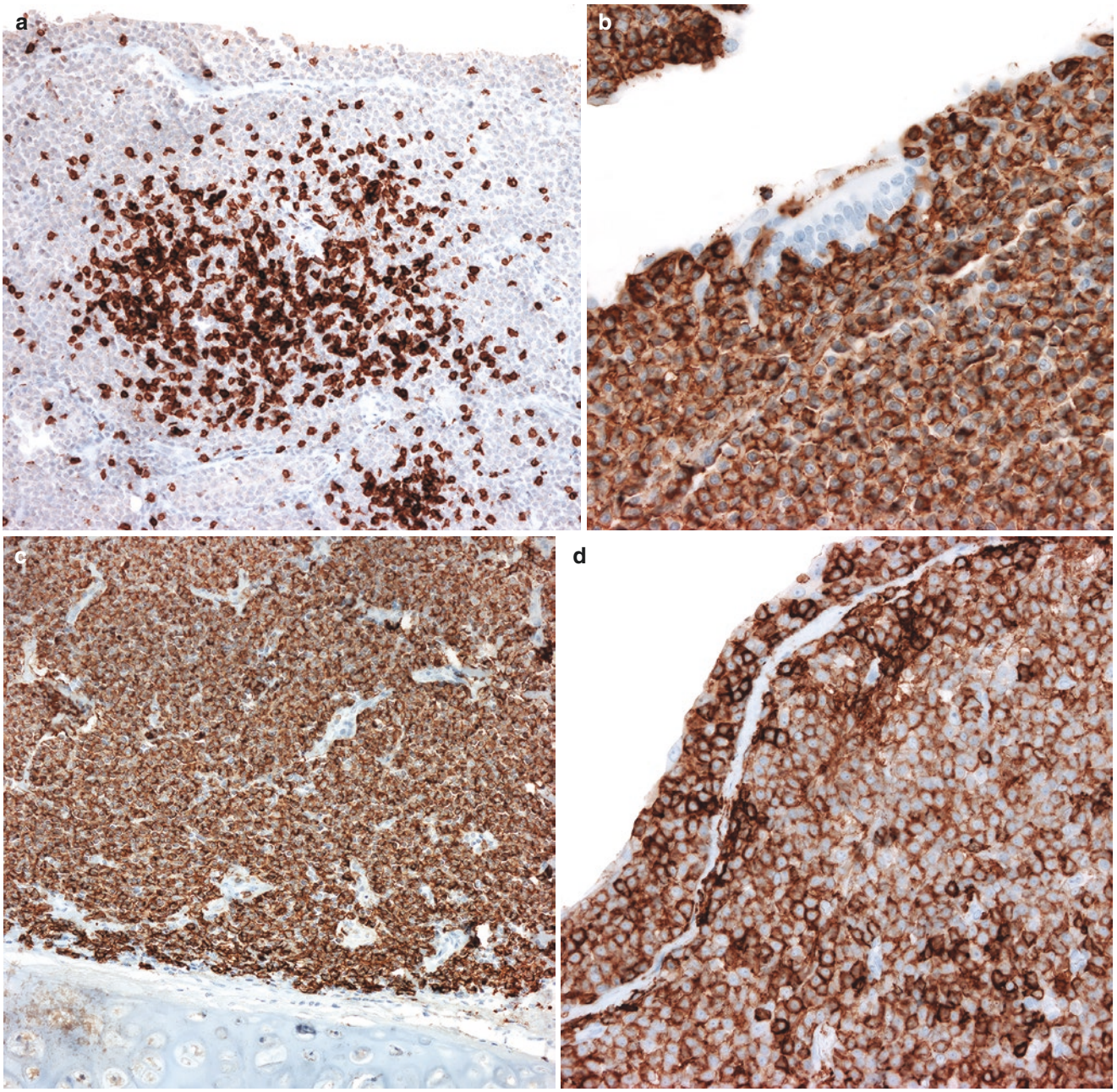

Fig. 15.37 (**a**) Pulmonary MALT lymphoma, CD3 immunostain, (**b**) pulmonary MALT lymphoma with numerous intraepithelial lymphocytes (lymphoepithelial lesion), CD20 immunostain, (**c**) pulmonary MALT lymphoma, CD20 immunostain, (**d**) pulmonary MALT lymphoma with numerous intraepithelial lymphocytes (lymphoepithelial lesion); immunohistochemistry for CD43. Co-expression of this T-cell marker is seen in 30–40% of cases of MALT lymphoma. (**e**) pulmonary MALT lymphoma with numerous intraepithelial lymphocytes (lymphoepithelial lesion). Immunostain for cyclin D1 is negative in the lymphoma cells and positive in residual entrapped epithelial cells and stromal cells

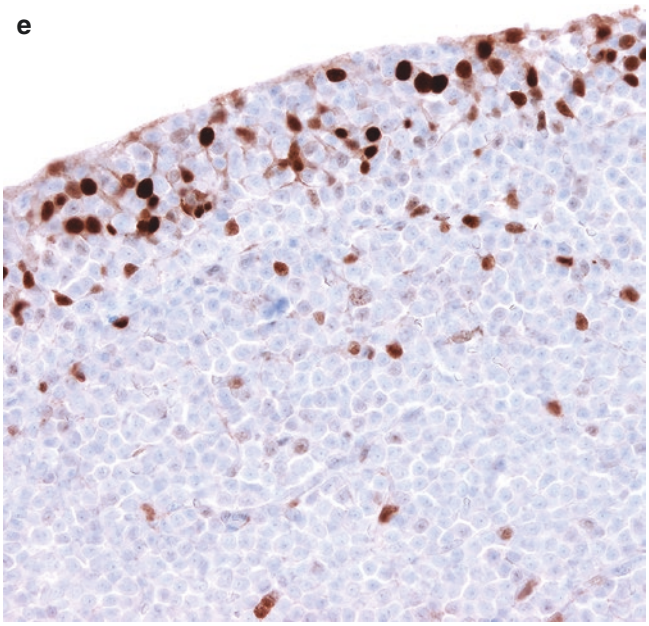

Fig. 15.37 (continued)

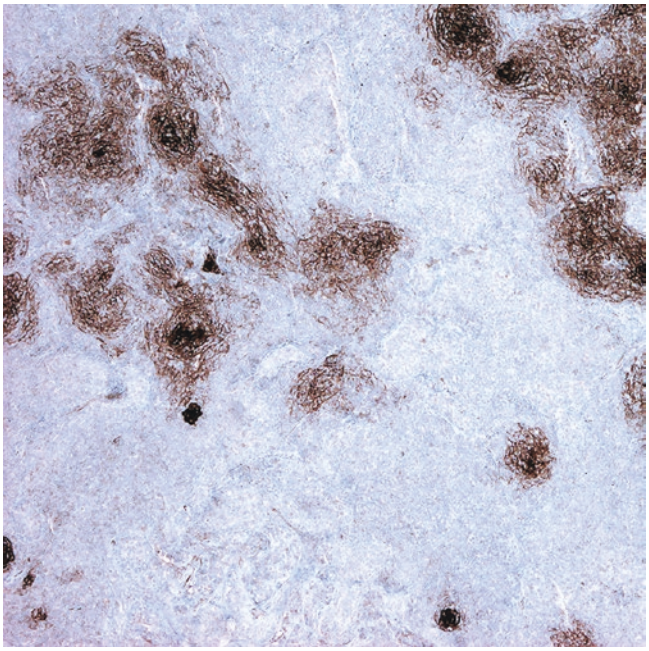

Fig. 15.39 The CD21 immunostain highlights residual/distorted follicular dendritic cell meshworks

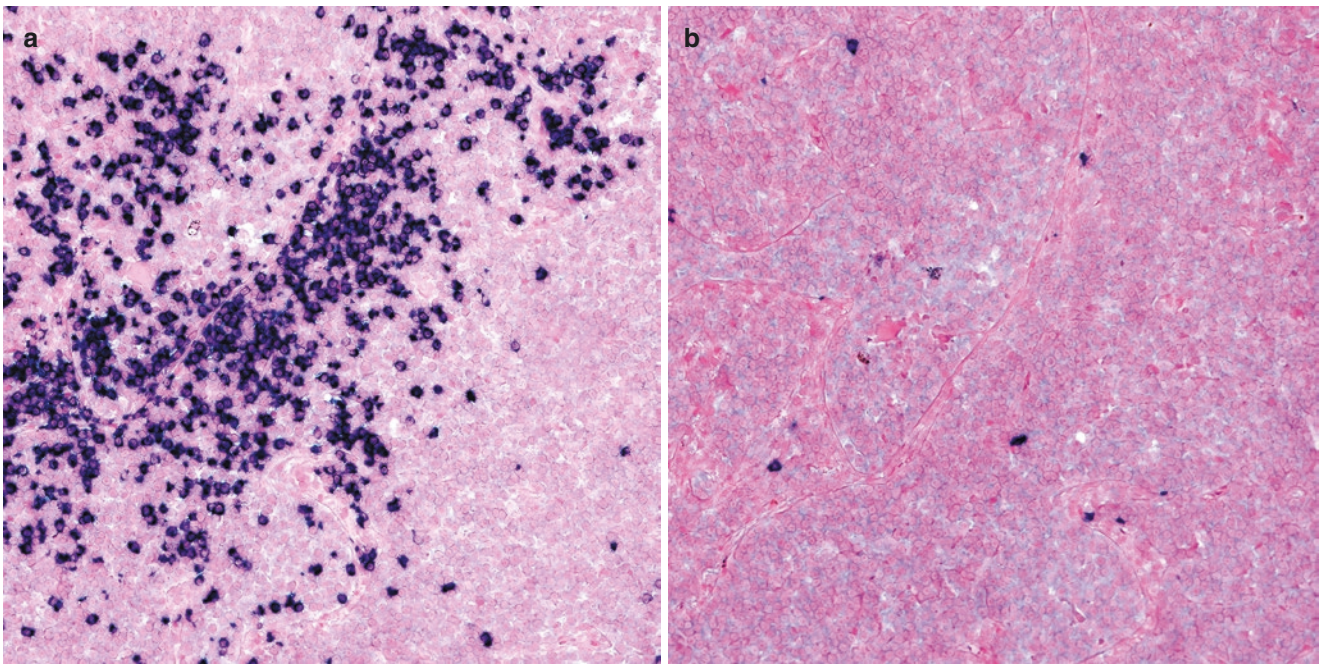

Fig. 15.38 Pulmonary MALT lymphoma. In situ hybridization shows areas with restricted plasma cells, positive for (**a**) kappa light chain and negative for (**b**) lambda light chain

logic findings. Fluorescence in situ hybridization (FISH) analysis is negative for t(11;18), which may be detected in about 30–40% of pulmonary MALT lymphomas.

Some authors consider that LIP is the precursor lesion of pulmonary MALT lymphoma [24, 25] and it is well described that a small subset of patients with LIP (~5%) can progress to pulmonary MALT lymphoma. On imaging, however, LIP presents as bilateral reticular infiltrates and not as a mass. Histologically, both lesions can show significant overlap and the edges of a pulmonary MALT lymphoma can have a pattern identical to LIP. Despite the presence of few lymphoepithelial lesions and/or perivascular lymphoid aggregates, in LIP there is no replacement of the architecture. In addition, the lymphoid infiltrate consists mostly of T-cells [17] rather than B-cells as seen in pulmonary MALT lymphoma. In a small biopsy, the diagnosis may be challeng-

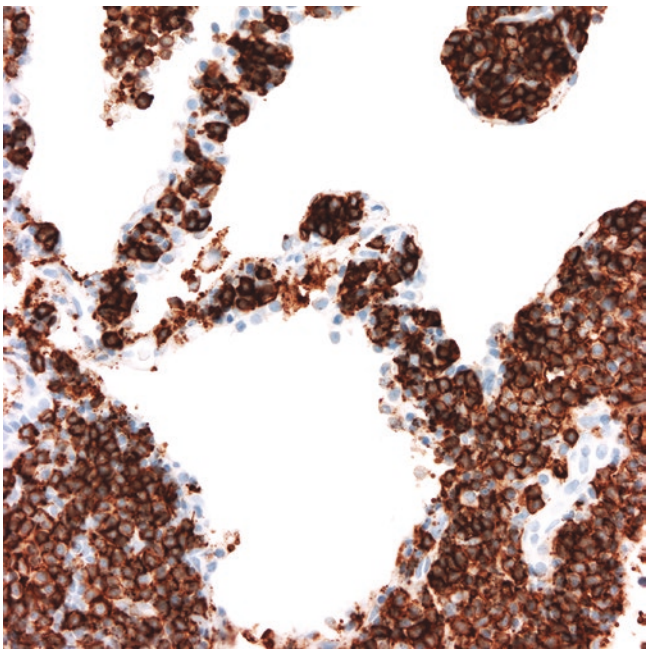

Fig. 15.40 Alveolar lymphoepithelial lesions, CD20 immunostain

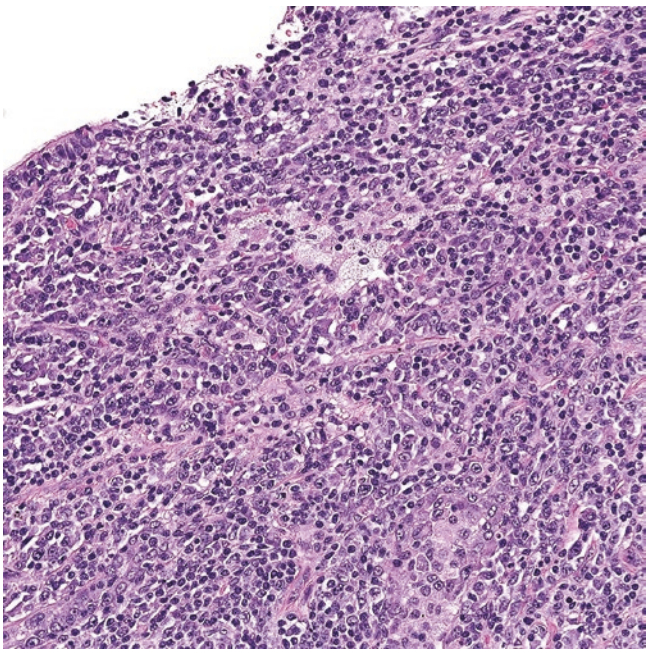

Fig. 15.41 Pulmonary MALT lymphoma with "increased large cells"

ing and determination of light chain restriction by flow cytometry and/or clonality by molecular studies may be the only source to favor one diagnosis over the other, but this is not always possible.

The distinction between pulmonary MALT lymphoma and other pulmonary small B-cell lymphomas is done by morphology and immunohistochemistry and/or flow cytometry. Importantly, other small B-cell lymphomas only occur exceedingly rare in the lung as a primary disease. CLL/SLL is composed of sheets of monotonous small lymphocytes with clumped chromatin and scattered pale areas known as proliferation centers containing prolymphocytes and paraimmunoblasts. CLL/SLL is positive for CD20, CD5, CD23, and LEF1 and negative for CD10, bcl-6, and cyclin D1. Mantle cell lymphoma is composed of monotonous small lymphocytes with a cleaved nucleus that resemble centrocyte-like cells. This lymphoma may show vague nodularity, and there are usually hyalinized vessels and interspersed epithelioid macrophages. By immunohistochemistry, mantle cell lymphoma is positive for CD20, CD5, and cyclin D1 and negative for CD10, CD23, and bcl-6. Follicular lymphoma may be confused with MALT lymphoma with numerous colonized follicles. Follicular lymphoma is positive for CD10 and bcl-6 and negative for CD5, CD23, CD43, and cyclin D1. In difficult cases, FISH may be useful to detect the translocation t(14;18)(*bcl2::IGH*) characteristic of follicular lymphoma and not seen in MALT lymphoma.

Pulmonary MALT lymphoma with extensive plasmacytic differentiation may be confused with pulmonary plasmacytoma. In the latter, however, the tumor is exclusively composed of plasma cells and no small lymphocytes, monocytoid cells, or reactive lymphoid follicles. Although abundant plasma cells are seen in MALT lymphoma with extensive plasmacytic differentiation, there are always areas with monocytoid cells, small lymphocytes, lymphoepithelial lesions, and/or reactive germinal centers. A prior history of lymphoplasmacytic lymphoma/Waldeström hypergammaglobulinemia and detection of an IgM paraprotein is helpful to support a diagnosis of lymphoplasmacytic lymphoma. Nevertheless, the distinction between lymphoplasmacytic lymphoma and MALT lymphoma may be extremely challenging in some cases since both tumors are negative for CD5 and CD10. In this situation, the clinical presentation and detection of *MYD88* (L265P) mutation are useful to discern between these two lymphomas. *MYD88* (L265P) mutation is common in lymphoplasmacytic lymphoma and infrequent in MALT lymphoma.

Last, pulmonary MALT lymphoma usually contains scattered large immunoblast-like cells, and when these cells form large aggregates, there should be a concern for transformation to large B-cell lymphoma [60]. However, the number of large cells may not be sufficient to make a diagnosis of large B-cell lymphoma, and some authors suggest referring to these cases as "MALT lymphoma with increased large cells" (Fig. 15.41). This finding is relevant since these cases an behave more aggressively than conventional MALT lymphoma and may progress to large cell transformation in a shorter period of time. Table 15.8 summarizes the differential diagnosis of pulmonary MALT lymphoma.

Molecular Findings

A clonal *IGH* gene rearrangement may only be detected in about 60% of cases of pulmonary MALT lymphoma. The most frequent translocation (30–40% of cases) in pulmonary MALT lymphoma is t(11;18)(q21;q21) with the generation of

Table 15.8 Differential diagnosis of pulmonary marginal zone lymphoma of mucosa-associated lymphoid tissue (CD5-/CD10-)

Reactive conditions
Pulmonary nodular lymphoid hyperplasia
Lymphoid interstitial pneumonia (5% of cases can progress to marginal zone lymphoma)
Neoplastic conditions (lung involvement extremely rare as primary disease)
Chronic lymphocytic leukemia/small lymphocytic lymphoma (CD5+, CD23+, cyclin D1-)
Mantle cell lymphoma (CD5+, CD23-/+, cyclin D1+)
Follicular lymphoma (CD10+, bcl6+)
Lymphoplasmacytic lymphoma (CD5-/CD10-, >90% of cases *MYD88* L265P)
Plasmacytoma (cases of MALT lymphoma with extensive plasmacytic differentiation)
If increased large cells: rule out transformation to diffuse large B-cell lymphoma

Table 15.9 Genetic alterations in pulmonary marginal zone lymphoma of mucosa-associated lymphoid tissue

Translocation/cytogenetic abnormality	Genes involved	Frequency in lung cases
t(11;18)(q21;q21)	*API2::MALT1*	30–40%
t(14;18)(q32;q21)	*IGH::MALT1*	5–10%
t(1;14)(p22;q32)	*IGH::bcl10*	~5%
Trisomy 3	N/A	20%
Trisomy 18	N/A	5–10%

an *API2::MALT1* fusion transcript that plays a role in NF-κB signaling activation [65–67]. However, this translocation is not specific to pulmonary MALT lymphoma and may be seen in those cases arising in the stomach. Additional genetic alterations include trisomy 3, t(14;18)(q32;q21)(*IGH::MALT1*) and t(1;14)(p22;q32)(*IgH::BCL10*) [58] (see Table 15.9). t(11;18)(q21;q21) can be detected by FISH with a break-apart probe for the *MALT1* gene located in 18q21 or by RT-PCR from paraffin-embedded tissue or fresh or frozen samples. By gene expression profiling, pulmonary MALT lymphoma demonstrates upregulation of marginal zone or memory B-cell-associated genes, and cases with extensive plasmacytic differentiation are usually negative for t(11;18)(q21;q21) [68].

Pulmonary Diffuse Large B-Cell Lymphoma (DLBCL)

Introduction

Pulmonary DLBCL is the second most common primary pulmonary lymphoma (10–20% of cases). It may occur de novo or may arise from pulmonary MALT lymphoma. The same diagnostic criteria defined for DLBCL at other sites apply to pulmonary DLBCL, namely classification as germinal center B-cell-like (GCB) or non-GCB/activated B-cell-like phenotype, or distinction according to the presence/absence of rearrangements of the *MYC*, *bcl2*, and/or *bcl6* genes. In general, extranodal DLBCL, including pulmonary DLBCL, features a non-GCB/activated B-cell-like phenotype.

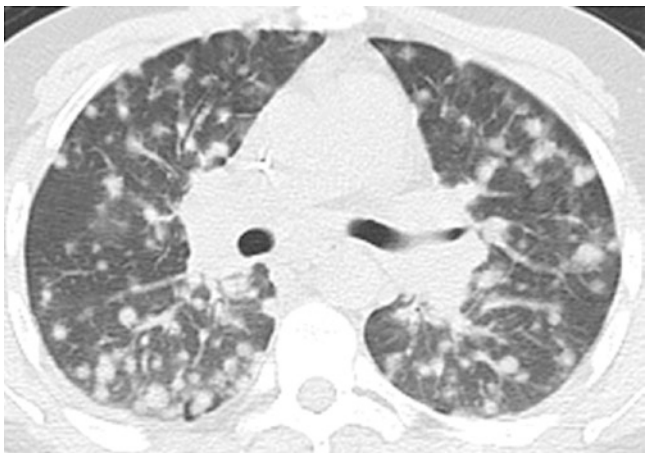

Fig. 15.42 Diffuse large B-cell lymphoma. CT shows numerous bilateral solid nodules

Clinical Features

De novo pulmonary DLBCL occurs in older individuals (mean age 60 years). Cases arising from pulmonary MALT lymphoma (large cell transformation) have similar demographics as described for this neoplasm (see prior section). Pediatric patients who develop de novo pulmonary DLBCL may have an underlying immunodeficiency [69]. In both de novo or secondary disease, pulmonary DLBCL presents with systemic B symptoms (fever, drenching night sweats, weight loss of at least 10% of body weight over 6 months), chest pain, respiratory distress (if the lesion obstructs an airway), dyspnea, cough, or hemoptysis. Regional/hilar lymphadenopathy occurs in about 50% of cases. According to a recent study from China evaluating 90 cases of primary pulmonary lymphoma (32% of cases were DLBCL), age above 60 years, elevated serum LDH and beta-2 microglobulin, clinical stage II2E or higher, and nonsurgical treatment were associated with poor prognosis [53]. Treatment includes the use of chemotherapy with rituximab, cyclophosphamide, Adriamycin, vincristine, and prednisone (R-CHOP) or other related regimens. The median survival is 3–5 years and less in relapsed/refractory disease. More recently, chimeric antigen receptor (CAR) T cell therapies targeting CD19 are being investigated [70, 71].

Diagnostic Imaging

Diffuse large B-cell lymphoma (DLBCL) in the lung manifests most commonly with single or multiple solid nodules or masses [43] (Fig. 15.42). Cavitation secondary to necrosis occurs in approximately 50% [43]. Rare instances of DLBCL presenting with only diffuse bilateral ground-glass opacities without nodules or masses have been reported [72, 73]. Untreated and still-viable treated DLBCL typically shows high FDG uptake on PET/CT [74].

Pathology

Today sampling of a lung lesion is usually accomplished via an imaging-guided needle biopsy or a transbronchial biopsy,

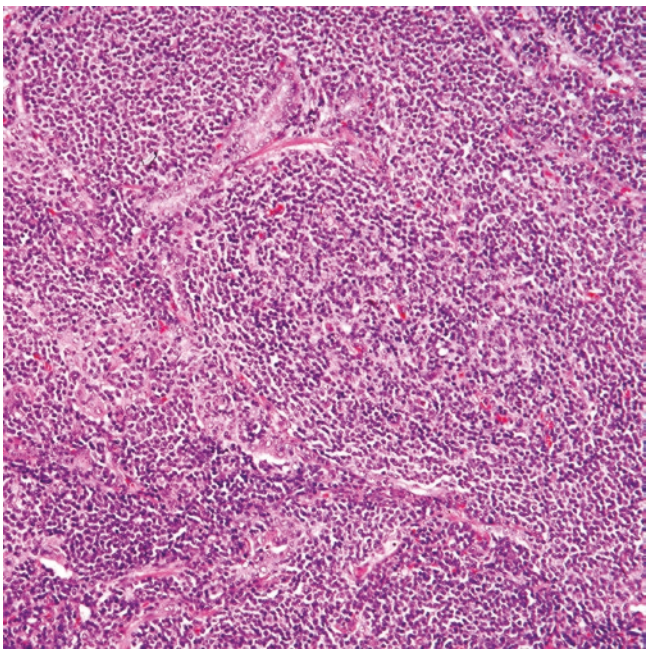

Fig. 15.43 Pulmonary diffuse large B-cell lymphoma. There is effacement of the lung parenchyma by sheets of intermediate to large lymphoma cells

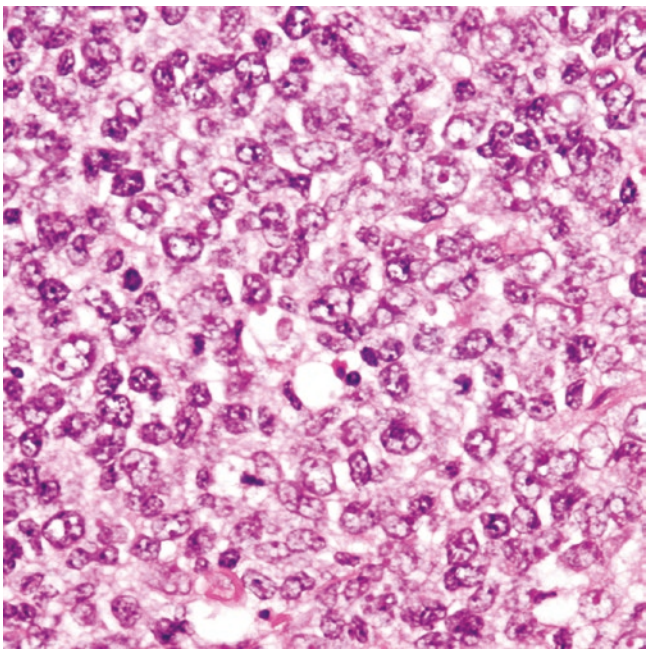

Fig. 15.44 Pulmonary diffuse large B-cell lymphoma. Sheets of large lymphoma cells with centroblastic morphology

and the diagnosis is established either in a cytology specimen, a core-needle biopsy, or a transbronchial biopsy. If the diagnosis of pulmonary lymphoma is rendered in any of these specimens, then a wedge resection or a lobectomy is not performed. However, a resection may still be done when a biopsy is inconclusive for diagnosis.

Grossly, pulmonary DLBCL has been described as a tan-white vaguely nodular mass with well-demarcated borders, common central necrosis with cavitation, and areas of hemorrhage. Peripheral tumors may extend and penetrate the visceral pleura, while centrally located lesions diffusely involve hilar structures. On microscopic examination, pulmonary DLBCL is identical to any large cell lymphoma at another site, composed of sheets of large lymphoid cells infiltrating the lung and adjacent structures (Fig. 15.43). The morphology of the lymphoma cells is predominantly centroblastic, with oval to round nucleus with fine chromatin, >2 juxtanuclear nucleoli, and scant to moderate amount of basophilic cytoplasm (Fig. 15.44). Scattered cells with immunoblastic or anaplastic features and Reed–Sternberg-like cells may or may not be present. Mitoses and apoptotic bodies are frequent, and some cases may feature a "starry-sky" pattern. Necrosis is variably seen. Clusters of large lymphoma cells admixed with fibrin can fill the alveoli and give the impression of a pneumonic process, a feature known as "tumoral pneumonia" [6] (Fig. 15.45). In core biopsies, the tumor cells may show artefactual spindle shape and not suggest the diagnosis of lymphoma (Fig. 15.46). Areas of residual MALT lymphoma or "MALT lymphoma with increased large cells" may be observed.

Immunohistochemistry and Other Ancillary Studies

The information presented here refers to DLBCL in general. The lymphoma cells are positive for CD45 and for B-cell markers, namely CD19, CD20, CD79a, PAX5, OCT2, and BOB.1, and are negative for CD15 and for T-cell markers (Figs. 15.47 and 15.48a–c). CD30 is positive in 10–15% of cases (based on information from DLBCL at other sites), and the frequency of CD30 may be higher in anaplastic DLBCL. Today, it is standard practice to determine the cell of origin of a DLBCL using an algorithm or a classifier, among which the one proposed by Hans et al. is widely used [75]. This algorithm takes in consideration the expression of CD10, bcl-6, and MUM1 to either define DLBCL into GCB-like (CD10+, bcl-6+/-, MUM1-) or non-GCB/activated B-cell-like (CD10-, bcl-6+/-, MUM1+) (Fig. 15.49a). The cutoff for all these markers is >30% of lymphoma cells. Non-GCB/ABC-like DLBCL has worse prognosis and a higher frequency of extranodal involvement, and pulmonary DLBCL is likely to belong to this group. In addition, the standard of practice includes assessment of the status of bcl-2 and c-myc by immunohistochemistry (>50% and

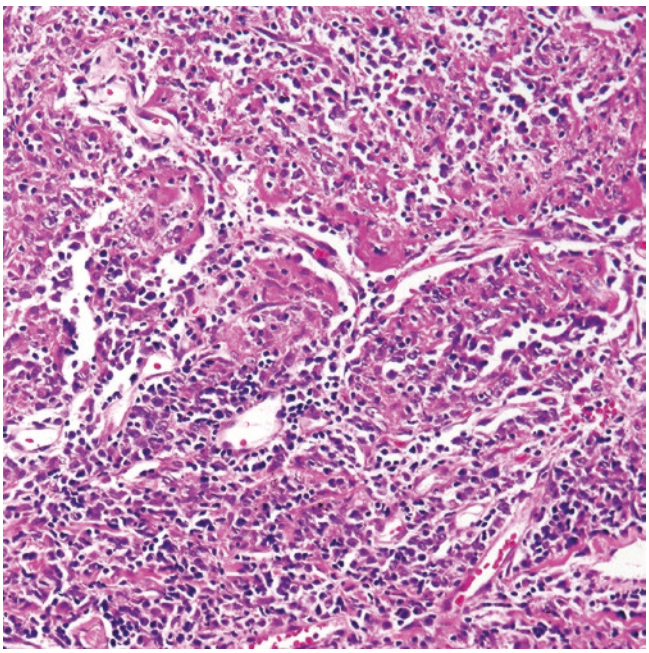

Fig. 15.45 "Tumoral pneumonia" or intraalveolar collections of large lymphoma cells admixed with fibrin mimicking a pneumonic process

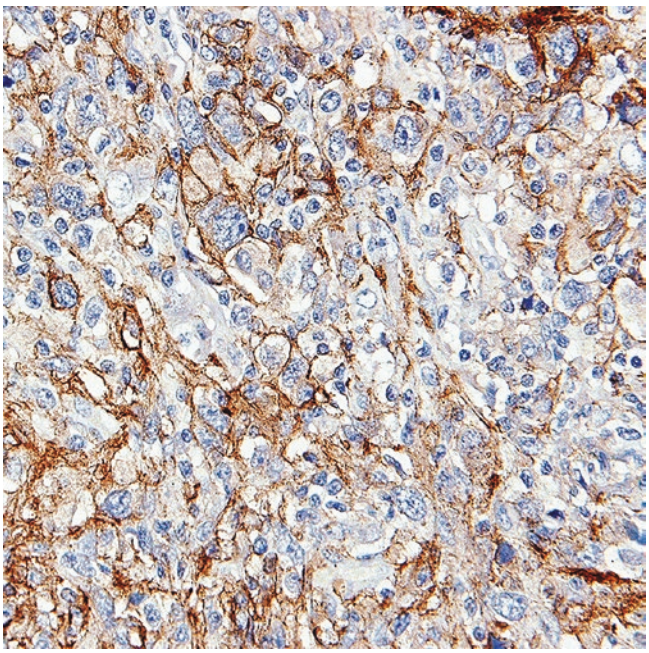

Fig. 15.47 Pulmonary diffuse large B-cell lymphoma, CD20 immunostain

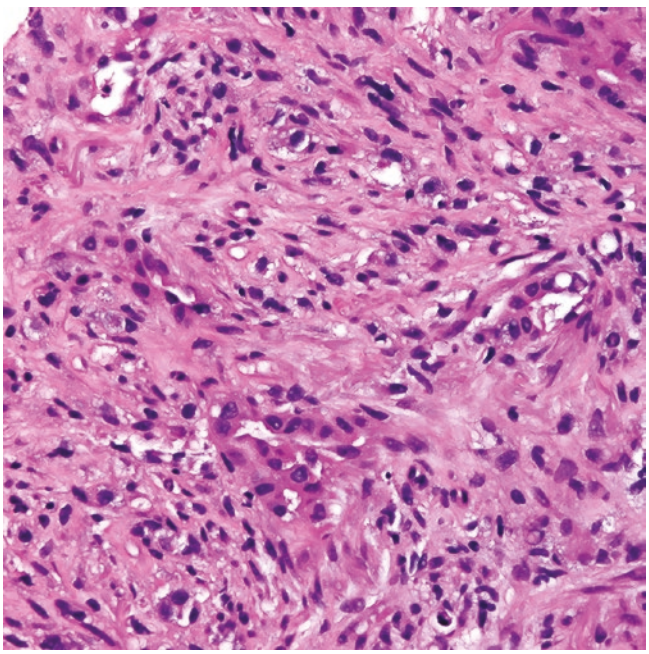

Fig. 15.46 Core biopsy of a pulmonary diffuse large B-cell lymphoma. The lymphoma cells show spindle morphology and resemble a sarcomatoid neoplasm

>40% of tumor cells cutoff, respectively) (Fig. 15.49b–c). DLBCLs that are positive for both markers are referred to as double expressors, and this appears to confer a poor prognosis regardless of the cell of origin. The Ki-67 proliferation index is always elevated (>30%) but usually not higher than 90%. When Ki-67 is >90–95%, it should suggest the possibility of a "high-grade" DLBCL. EBER ISH is negative, and cases that are EBV+ should be classified as EBV+ DLBCL or grade 3 (high grade) lymphomatoid granulomatosis (see corresponding section in this chapter).

Differential Diagnosis

Pulmonary DLBCL needs to be distinguished from a primary mediastinal large B-cell lymphoma (PM-LBCL) extending to the lung, other large cell lymphomas, poorly differentiated lung carcinoma, small cell and large cell carcinoma, and metastatic carcinoma or amelanotic melanoma. Cases with pulmonary DLBCL with spindle morphology need to be distinguished from sarcomatoid carcinoma or primary or metastatic lung sarcoma.

The distinction between pulmonary DLBCL and other large cell lymphomas can be made by a combination of clini-

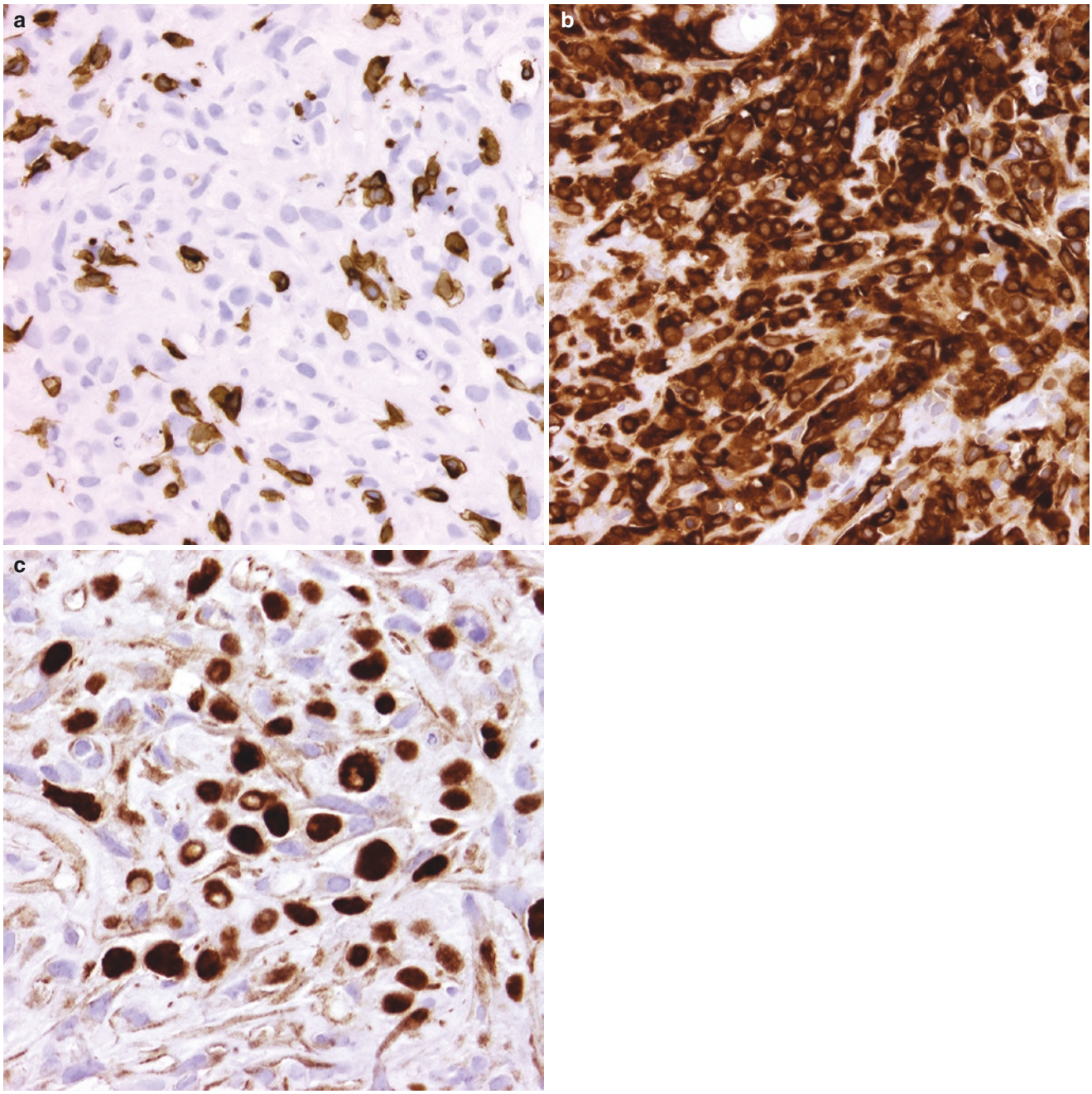

Fig. 15.48 Pulmonary diffuse large B-cell lymphoma with spindle morphology. The lymphoma cells are negative for (**a**) CD3 and positive for (**b**) CD79a and (**c**) PAX5

cal history and the use of ancillary studies. Other large cell lymphomas that resemble pulmonary DLBCL include PM-LBCL extending to the lung, grade 3 (high grade) lymphomatoid granulomatosis, and anaplastic large cell lymphoma. The distinction between PM-LBCL and pulmonary DLBCL may not be possible by histopathologic examination, and sometimes it is only established by the clinical history (young female with an anterior mediastinal mass with lung extension rather than an older man with a solitary lung mass). However, the presence of clear cells, expression of CD23, and a variable expression of CD30 may suggest PM-LBCL over pulmonary DLBCL. Grade 3 (high grade) lymphomatoid granulomatosis is an EBV+ large B-cell lymphoma that presents as multiple lung nodules (see the corresponding section) and not as a single lesion as usually seen in pulmonary DLBCL. This tumor features prominent vasculitis with abundant necrosis, although these features may not be identified in a core needle biopsy. Lymphoid granuloma-

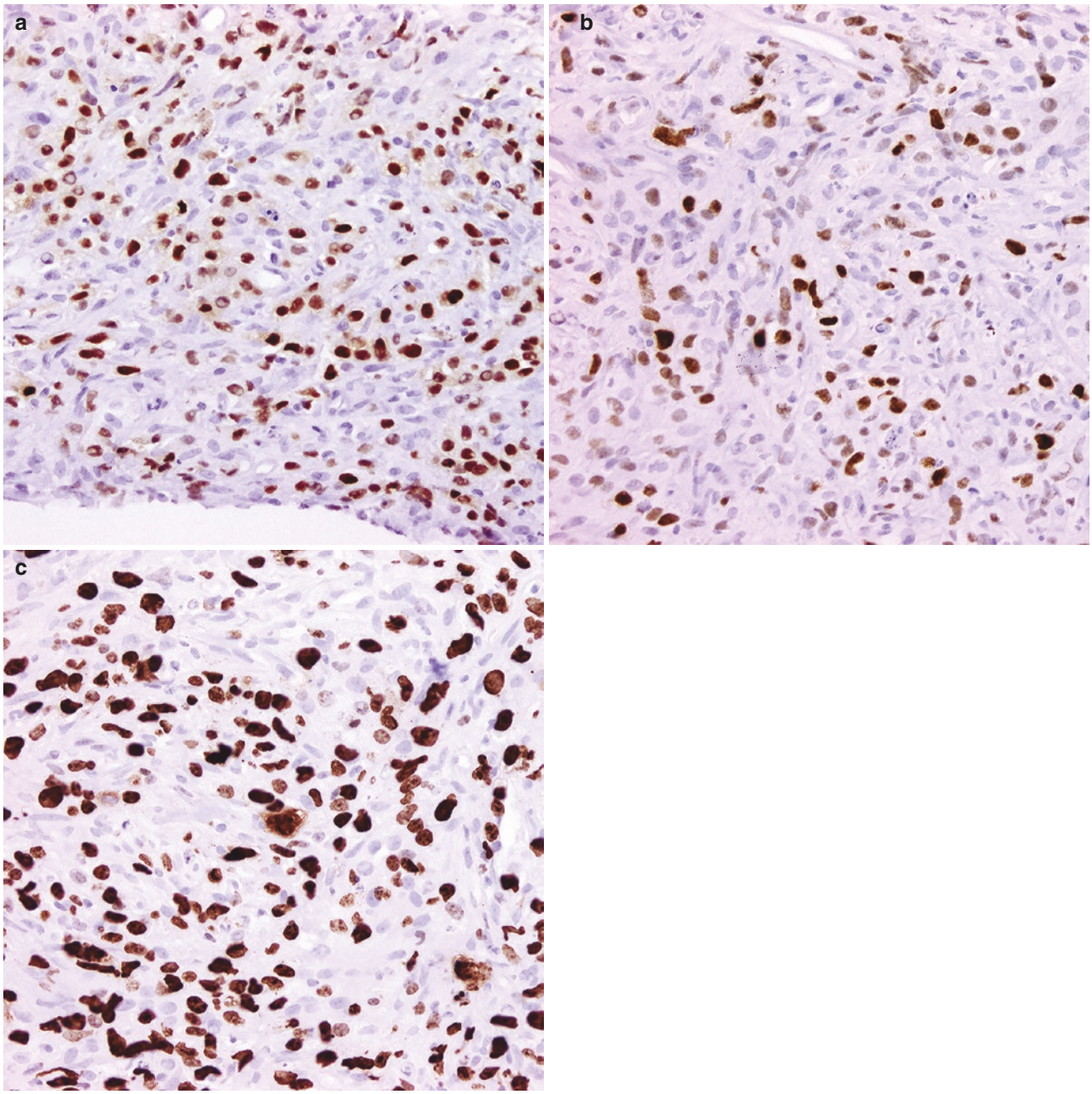

Fig. 15.49 Pulmonary diffuse large B-cell lymphoma with spindle morphology. The lymphoma cells are positive for (**a**) MUM1 and (**b**) c-myc. (**c**) The Ki-67 proliferation index is high (60–70%)

tosis is positive for B-cell markers and EBER, and the latter excludes a diagnosis of conventional pulmonary DLBCL. Anaplastic large cell lymphoma is a T-cell lymphoma with strong and diffuse expression of CD30 with or without expression of ALK and lack of B-cell markers. Pulmonary DLBCL, including cases of the anaplastic variant, are negative for T-cell markers and ALK.

Poorly differentiated carcinomas, metastatic carcinoma, sarcomatoid carcinoma, and small cell and large cell carcinomas are readily distinguished from pulmonary DLBCL by histology because all these neoplasms are positive for cytokeratin and show variable expression of lineage-specific transcription factors (TTF1, etc.), synaptophysin and chromogranin, and are negative for CD45 and all B-cell markers. In a similar fashion, melanoma is positive for melanocytic markers (HMB-45, Melan-A, MART-1) and negative for CD45 and B-cell markers. Expression of CD45 and other B-cell markers in an otherwise malignant spindle cell neo-

plasm in the lung excludes the diagnosis of sarcoma. The differential diagnosis of pulmonary DLBCL is listed in Table 15.10.

Molecular Findings

A full description of all the findings present in DLBCL is outside the scope of this chapter. Pulmonary DLBCL is likely to harbor similar alterations as non-pulmonary cases; however, no studies are available for cases confined to the lung. The most common alteration in DLBCL includes the rearrangement of *bcl6* (~30%), followed by that of *bcl2* (~20%) and *MYC* (~10%). Cases that show *MYC*, *bcl2*, and/or *bcl6* gene rearrangements, also known as double-hit or triple-hit lymphomas, have a very bad prognosis [76], but the frequency of these cases in the lung is uncertain. Detection of *MYC* and *BCL2* rearrangements by FISH (double hit DLBCL) is not interchangeable with double expressor DLBCL. In fact, there is a poor correlation between the FISH findings and immunohistochemical results for these two markers. The novel LymphGen classification stratifies DLBCL into subgroups based on molecular abnormalities identified by depth genomic analysis. Using this classification, GBC-like DLBCLs commonly express *bcl6* and *EZH2* genes and demonstrate alterations in PIK3 signaling, cell migration, and immune cell interactions, whereas non-GCB/ABC-like DLBCLs harbor alterations in chronic B-cell receptor signaling (*MYD88, CD79B*) and activation of the NF-κB signaling [77].

Pulmonary Intravascular Large B-Cell Lymphoma (LBCL)

Introduction

Originally designated systematized endotheliomatosis by Pfleger in 1959 [78] and later known by multiple names such as intravascular reticuloendotheliosis, malignant angioendotheliomatosis, angiotropic large cell lymphoma, and intravascular lymphomatosis, intravascular LBCL—as the disease is known today—is an uncommon subtype of LBCL with unique clinicopathologic features, including the presence of large lymphoma cells within the vascular lumina of multiple organs, hence the name. Lung involvement is usually seen as part of multisystemic disease.

Table 15.10 Differential diagnosis of pulmonary diffuse large B-cell lymphoma

Hematopoietic
Primary mediastinal large B-cell lymphoma with extension to the lung
Syncytial variant of mediastinal classic Hodgkin lymphoma with extension to the lung
Syncytial variant of primary pulmonary classic Hodgkin lymphoma
Anaplastic large cell lymphoma
Lymphomatoid granulomatosis, grade 3
Non-hematopoietic
Poorly differentiated primary lung carcinoma
Small cell carcinoma
Metastatic carcinoma or amelanotic melanoma
Sarcomatoid carcinoma or sarcoma (in cases of diffuse large B-cell lymphoma with spindle morphology)

Clinical Features

There are three clinical presentations of intravascular LBCL, including a cutaneous form, a Western form with predominant skin and brain involvement, and an Asian form with multisystemic involvement and hemophagocytic syndrome [79–81]. The clinical and radiologic presentation is variable and nonspecific. Therefore, clinical diagnosis may be challenging, and a large subset of patients go underrecognized until the diagnosis is established at autopsy. Overall, patients have a poor prognosis despite R-CHOP chemotherapy.

Pathology

Intravascular LBCL cannot be identified grossly. Microscopically, at low magnification, the disease may not be easy to recognize and can be potentially overlooked, particularly in those cases with only a few intravascular lymphoma cells (Fig. 15.50). On the other hand, cases with high tumor burden produce expansion of alveolar capillaries that appear as interstitial widening (Fig. 15.51) and resemble an interstitial pneumonia or interstitial lung disease [82]. At higher magnification, the lymphoma cells are

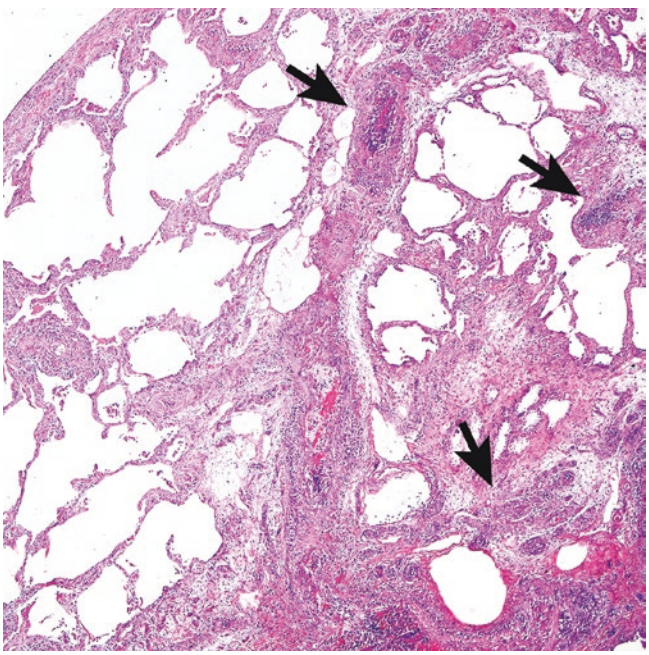

Fig. 15.50 Intravascular large B-cell lymphoma may be completely missed at low magnification. The arrows point to intermediate and small blood vessels filled with lymphoma cells

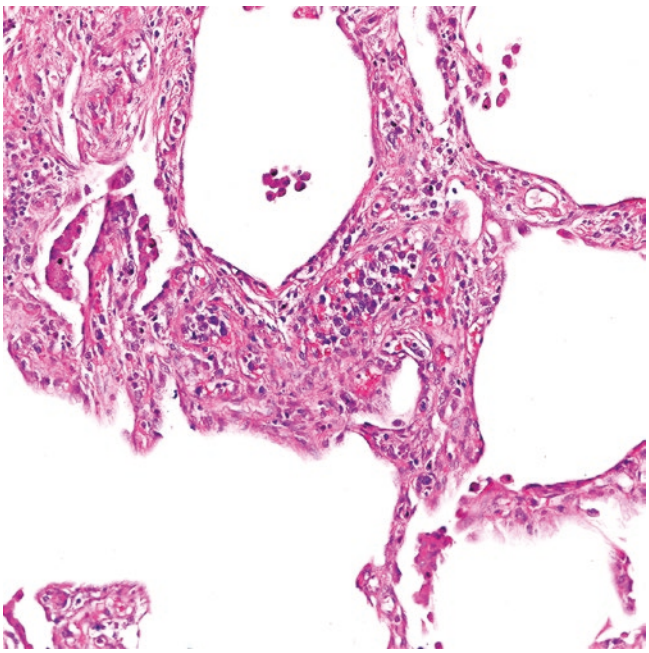

Fig. 15.51 Intravascular large B-cell lymphoma The capillaries are filled with large lymphoma cells

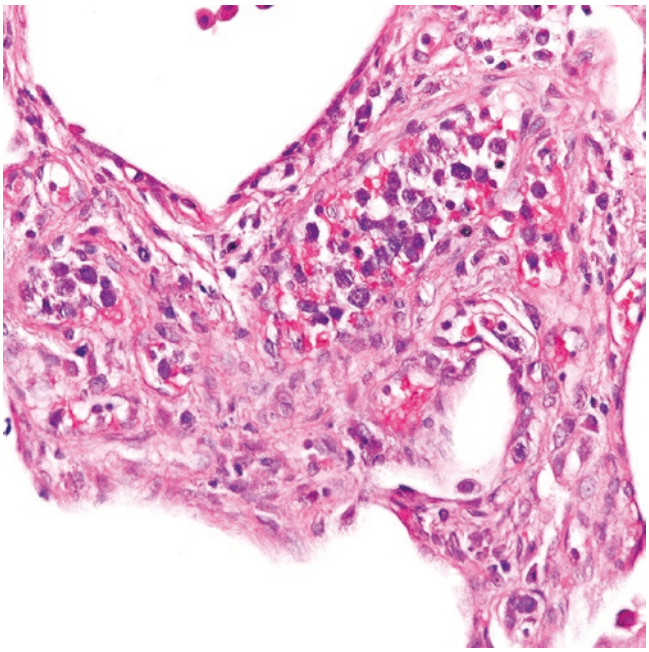

Fig. 15.52 Intravascular large B-cell lymphoma. The capillaries are filled with large lymphoma cells

always found in the lumen of capillaries and small to intermediate-sized blood vessels, and they may or may not be admixed with intravascular fibrin or small thrombi (Fig. 15.52). The morphology of the lymphoma cells is predominantly centroblastic, with oval to round nuclei with fine chromatin, >2 juxtanuclear nucleoli, and scant to moderate amount of basophilic cytoplasm. Occasionally, some larger vessels may contain a few scattered lymphoma cells infiltrating into the vessel wall but not reaching the lung parenchyma. Intravascular LBCL can exhibit four different patterns of involvement with >1 or more of them seen in the same case: a non-cohesive pattern with lymphoma cells floating freely inside the lumen of a blood vessel; a cohesive pattern with aggregates of lymphoma cells filling an entire vascular lumen; a marginated pattern with lymphoma cells attached to vascular endothelium with no associated fibrin or thrombus; and a tumor-associated pattern with intravascular lymphoma cells seen within the vasculature of another tumor but not in blood vessels from adjacent uninvolved tissue [46].

Immunohistochemistry and Other Ancillary Studies

The lymphoma cells are positive for B-cell markers (CD20, PAX5, CD79a), CD45, and bcl-2 and show variable expression of CD5 or CD10 (Fig. 15.53). A subset of cases is double positive for CD5 and CD10. The majority of cases have a non-GCB/activated B-cell-like phenotype (CD10-/bcl-6+/-/MUM1+). Intravascular LBCL is negative for T-cell markers, ALK, and EBER.

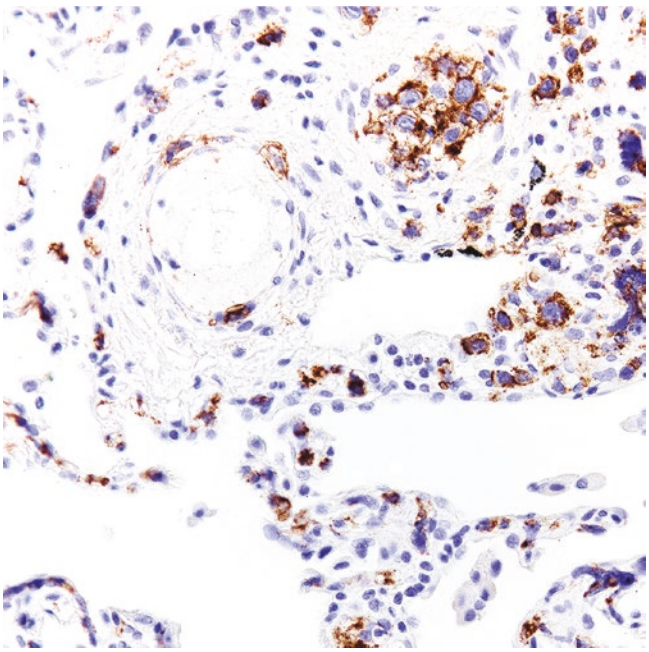

Fig. 15.53 Intravascular large B-cell lymphoma, CD20 immunostain

Differential Diagnosis

Intravascular LBCL with lung involvement should be distinguished from acute leukemia, carcinoma, or melanoma with lymphangitic spread in the lung. A proper set of immunohistochemical markers is helpful in discerning between these diseases. Intravascular LBCL is positive for B-cell markers and negative for cytokeratins, melanoma markers, T-cell

Table 15.11 Differential diagnosis of pulmonary intravascular large B-cell lymphoma

Hematopoietic
Acute myeloid leukemia with lymphangitic spread (hyperleukocytosis)
Non-hematopoietic
Carcinoma, melanoma, or any other solid tumor with lymphangitic spread
At low magnification: deceptively appearing "normal lung" or pattern resembling interstitial pneumonia

markers, CD34, myeloperoxidase, or other myeloid markers, in contrast to the other entities mentioned.

Although intravascular LBCL can mimic interstitial pneumonia at low magnification, the recognition of intravascular tumor cells and not interstitial fibrosis or inflammation at high magnification rules out interstitial lung disease. A CD20 immunostain is extremely valuable in establishing the diagnosis. The differential diagnosis of intravascular LBCL is summarized in Table 15.11.

Molecular Findings

The etiology of intravascular LBCL is not completely understood, but it appears that a lack of homing receptor molecules (CD29/beta-1 integrin and CD54/ICAM-1) in the surface of lymphoma cells impairs their ability to exit into the tissues [83]. Similarly, the interaction between molecules on the surface of lymphoma cells and on endothelial cells promotes retention and proliferation of the tumor cells in the intravascular space, and this may represent another possible pathogenetic mechanism in this subtype of lymphoma [84].

Lymphomatoid Granulomatosis (LYG)

Introduction

In 1972, Liebow and colleagues authored the seminal publication of 40 patients who had a rare pulmonary disease with "lymphoma-like morphology and features that resembled the limited form of Wegener granulomatosis (now granulomatosis with polyangiitis)" and coined the term lymphomatoid granulomatosis (LYG) [85]. The authors hypothesized that this rare entity could occur secondary to EBV infection, and they were correct [85]. However, it was not until 1990–1995 that first Katzenstein and Peiper [86] and then Guinee et al. [87], and Myers et al. [88] independently detected the presence of EBV-infected B-cells in LYG. The current definition of LYG is that of an EBV+ B-cell lymphoproliferative disorder with specific clinical, radiologic, and histopathologic features. Morphologically, this disorder is divided into three grades and each of these reflects a different clinical outcome.

Clinical Features

The disease is rare and usually manifests as a systemic disorder. Lung involvement is very common, present in 80 to 90% of cases. Other organs involved with less frequency include the brain, the kidneys, and the skin. Lymphatic organ and bone marrow involvement is extremely unusual [85]. LYG affects middle-age adults (mean age 46 years) with a male predominance (male to female ratio 2:1) [89, 90]. Immunosuppressed individuals are at higher risk of developing LYG, including those with a genetic or acquired condition, such as Wiskott–Aldrich syndrome, a congenital T-cell deficiency, post-ablation chemotherapy, or HIV infection [91, 92]. Patients who are post-transplant or are taking immunomodulatory drugs and develop a disorder reminiscent of LYG should not be classified as such (see differential diagnosis) [90]. Immunocompetent individuals only rarely develop LYG. Clinical symptoms include systemic B-symptoms and dyspnea, cough, chest pain, and hemoptysis. The symptoms tend to wax and wane over a period of months to years [93, 94].

The prognosis in LYG is variable but overall poor, with a median survival of 2 years [90]. However, patients with pulmonary involvement have a longer survival when compared to those with multiorgan disease or those with brain involvement. Along with the clinical presentation, the histologic grade in LYG is important (see below) since it correlates with the risk of transformation to an EBV+ LBCL (grade 3 LYG) and more aggressive disease with worse prognosis [91]. Treatment depends on the extent of the disease and the histologic grade, and it can range from single-agent rituximab to combined chemotherapy and/or additional immunomodulators [89, 90, 95].

Diagnostic Imaging

On CT, LYG is characterized by well-defined and poorly defined nodules located along bronchovascular structures or interlobular septa [43, 96] (Fig. 15.71). Large masses and vascular occlusion also occur [96]. Other CT features include coarse irregular opacities and small thin-walled cysts [96]. Dee et al. previously described two distinct radiographic patterns of LYG: diffuse reticulonodular pattern, secondary to biopsy-proven granulomatous infiltration without evidence of infarction, and lobular parenchymal masses corresponding to biopsy-proven pulmonary infarcts within lymphomatoid granulomatosis lesions [97]. The halo sign (solid nodule or mass with surrounding ground-glass halo) [98] and reverse halo sign (central ground-glass opacity surrounded by consolidation) [99] have been described with LYG. LYG lesions typically demonstrate marked FDG uptake though centrally necrotic portions will be photopenic [98] (Fig. 15.54a, b).

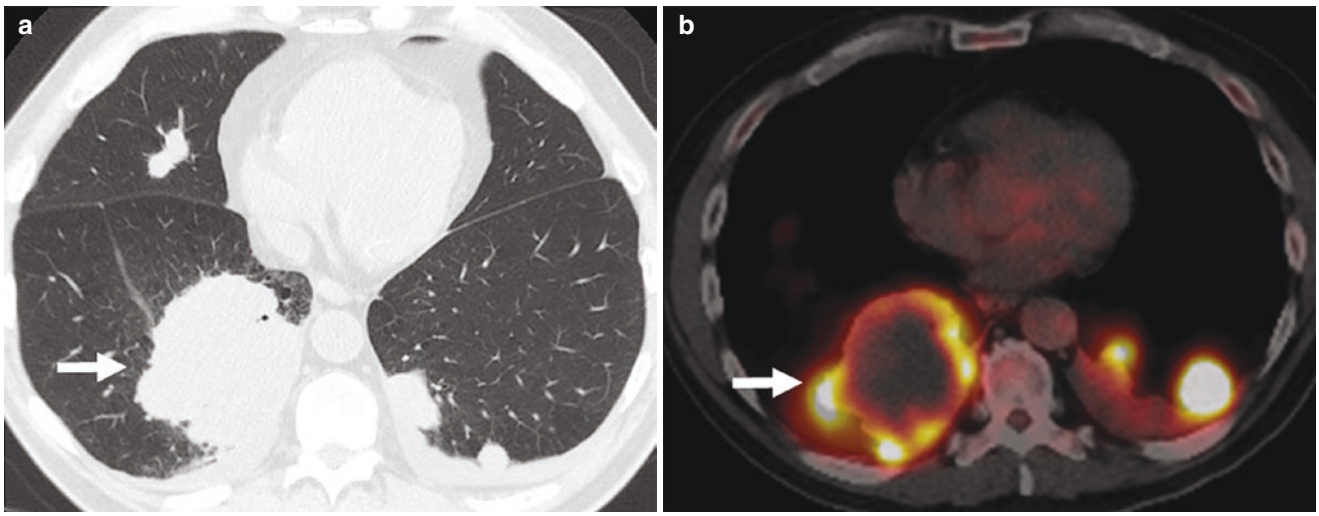

Fig. 15.54 Lymphomatoid granulomatosis. (**a**) CT shows a right lower lobe mass (arrow) and bilateral pulmonary nodules, and (**b**) PET/CT shows that the right lower lobe mass (arrow) and left lower lobe nodules are FDG-avid. Central photopenia in the right lower lobe mass is the result of central necrosis

Pathology

Currently sampling of a lung lesion is usually accomplished via an imaging-guided needle biopsy or a transbronchial biopsy, and the diagnosis is established either in a cytology specimen, a core-needle biopsy, or a transbronchial biopsy. If the diagnosis of pulmonary lymphoproliferative disorder is rendered in any of these specimens, then a wedge resection or a lobectomy is not required. However, a resection may still be done when a biopsy is inconclusive for diagnosis or when the disease manifests as multiple surgically approachable peripheral nodules.

Grossly, LYG has a variable appearance ranging from tan-white to pale yellow firm small nodules (usually <5 cm) to large markedly necrotic lesions with central cavitation with a rim of peripheral viable tissue (usually >5 cm and even >10 cm). Centrally located nodules may erode an adjacent bronchus and produce ulceration of the mucosa. On microscopic examination, the nodules of LYG have a bronchovascular distribution and a sharp demarcation from the adjacent otherwise unremarkable lung (Fig. 15.55). LYG varies from lesions composed of a polymorphic infiltrate of small lymphocytes, macrophages, few plasma cells, and few large atypical lymphoid cells with immunoblastic-like or Reed–Sternberg-like morphology with no or minimal focal necrosis (grade 1–2 lesions) (Figs. 15.56 and 15.57) to nodules containing sheets of large atypical lymphoid cells with extensive necrosis (grade 3 lesions) (Figs. 15.58 and 15.59). In all nodules, there is lymphocytic vasculitis, and the necrosis, if present, is of the coagulative type (eosinophilic) with a lack of neutrophils or karyorrhectic debris (Figs. 15.58 and 15.60). Eosinophils and epithelioid granulomas are not usually seen. As mentioned above, the nodules in LYG wax and wane and histologic evaluation of a regressed nodule shows a paucicellular infiltrate, blood vessels with a recanalized lumen and a fibrotic wall surrounded by alveolar edema, hemorrhage, and fibrosis or infarction [93]. Nodules sampled after therapy show dense fibrosis and necrosis without large atypical lymphoid cells [89].

Immunohistochemistry and Other Ancillary Studies

The large atypical lymphoid cells are of B phenotype, positive for CD45 and B-cell markers (CD20, PAX5, CD79a, OCT2, BOB.1) (Figs. 15.61 and 15.62). These cells are posi-

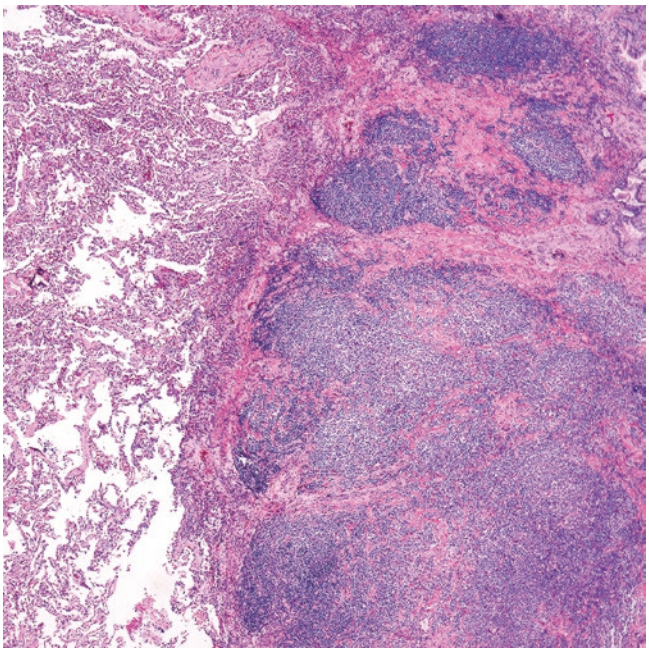

Fig. 15.55 Lymphomatoid granulomatosis (LYG). The nodules of LYG are sharply demarcated from the adjacent and unremarkable lung parenchyma

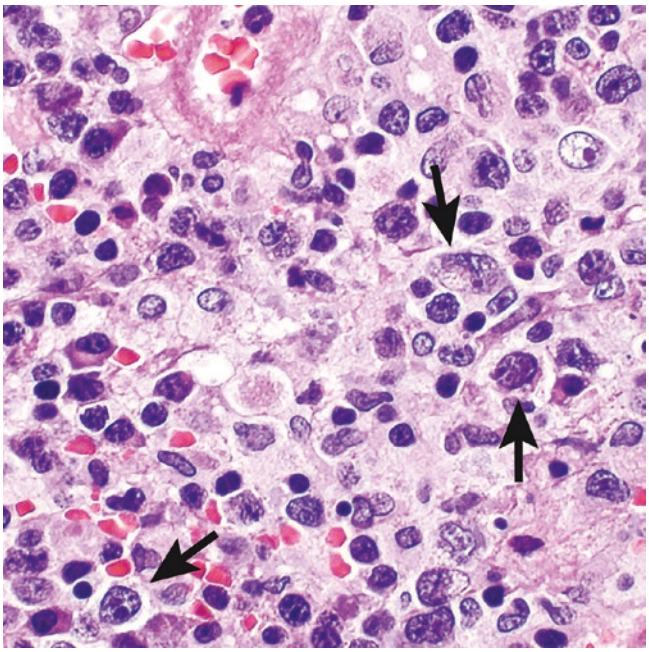

Fig. 15.57 Lymphomatoid granulomatosis, low-grade. A few large atypical lymphoid cells are seen (arrows). The background is composed of macrophages, plasma cells, and small lymphocytes

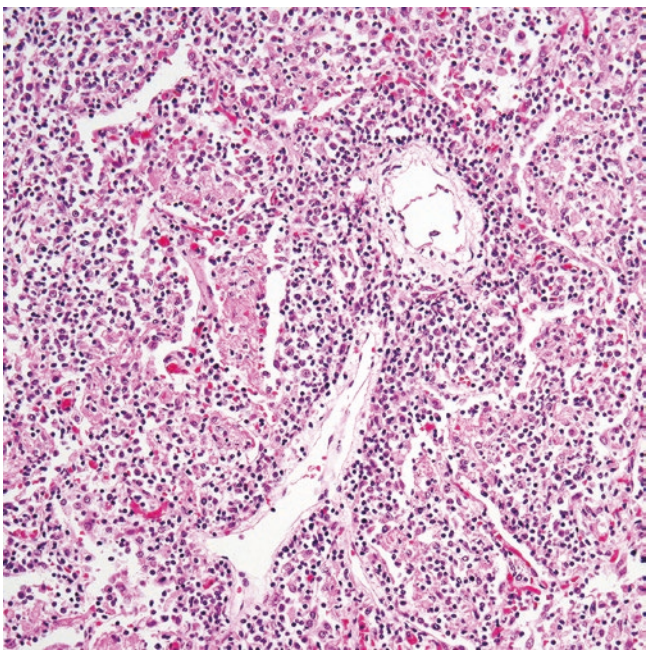

Fig. 15.56 Lymphomatoid granulomatosis, low grade. Lymphocytic vasculitis, scattered large cells, and no significant necrosis

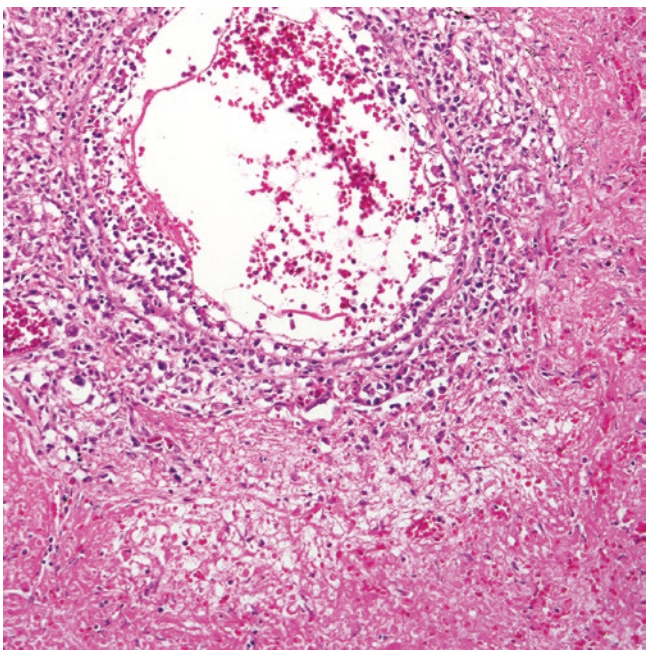

Fig. 15.58 Lymphomatoid granulomatosis, high grade. Lymphocytic vasculitis and extensive necrosis. There are numerous large atypical lymphoid cells around the necrotic vessel wall. No karyorrhectic debris are seen despite the extensive necrosis

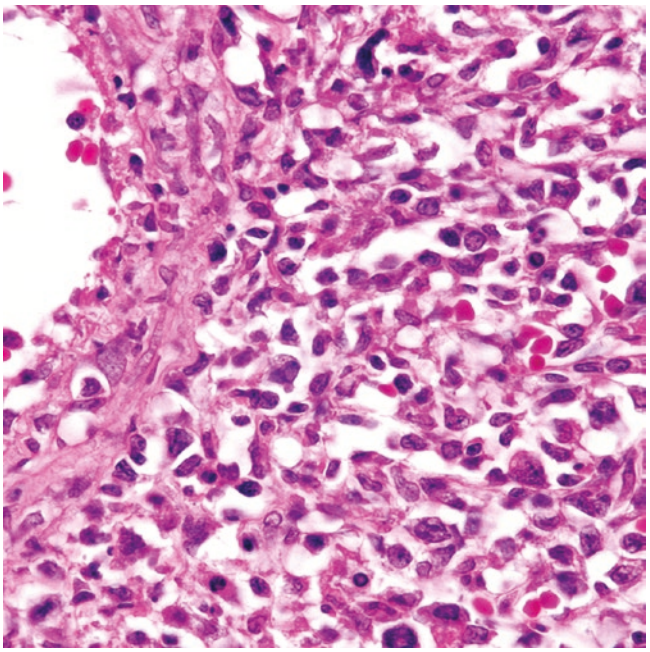

Fig. 15.59 Lymphomatoid granulomatosis, high grade. The wall of this vessel is surrounded by sheets of large atypical lymphoid cells

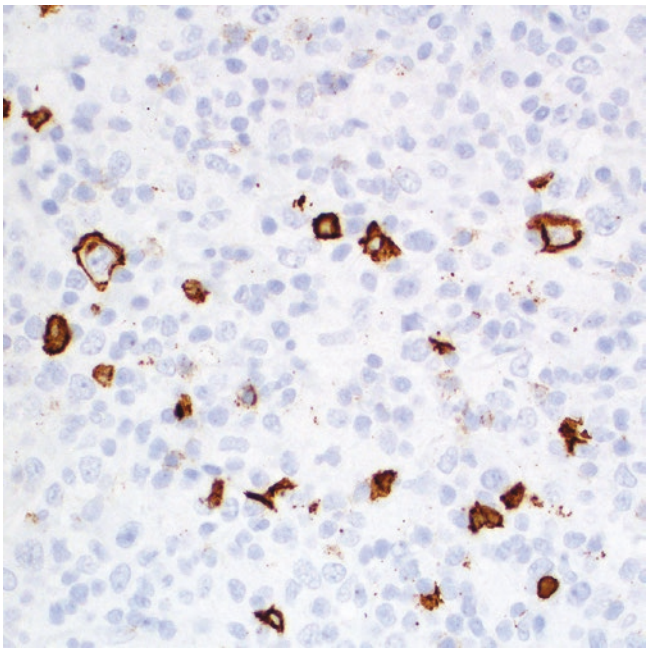

Fig. 15.61 Lymphomatoid granulomatosis, low grade. CD20 immunostain

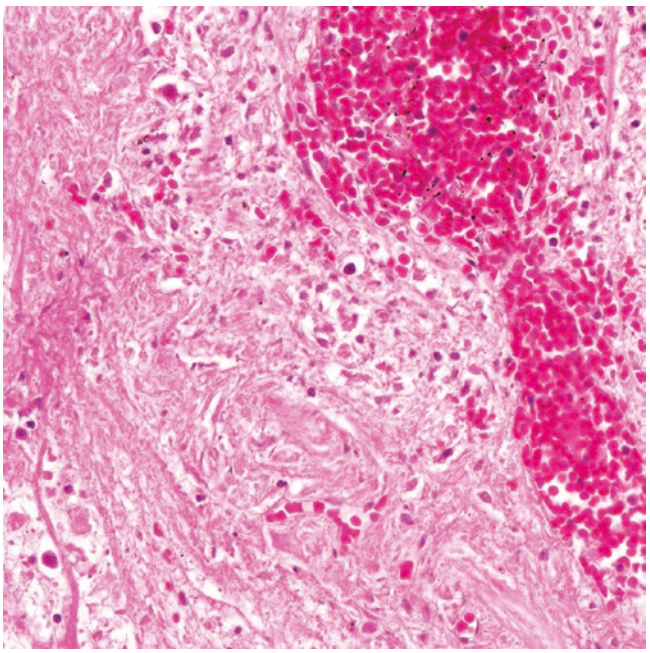

Fig. 15.60 Lymphomatoid granulomatosis, high grade. Area of coagulative (eosinophilic) necrosis devoid of karyorrhectic debris

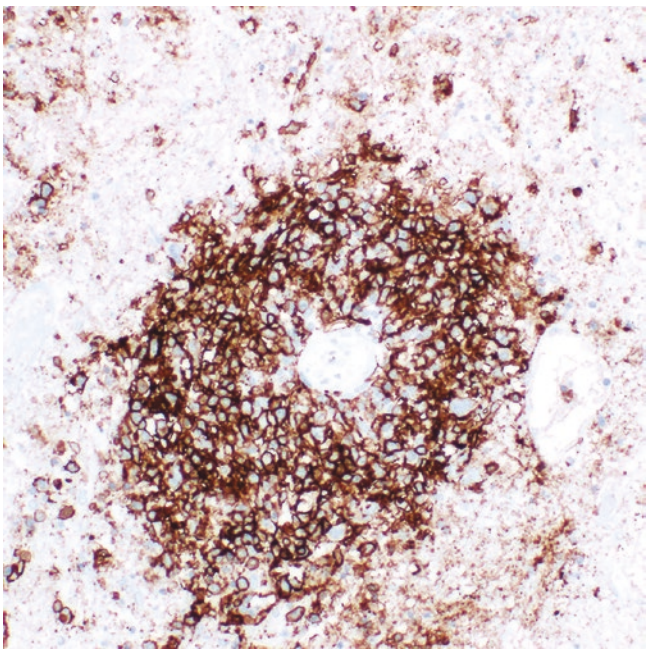

Fig. 15.62 Lymphomatoid granulomatosis, high grade. CD20 immunostain

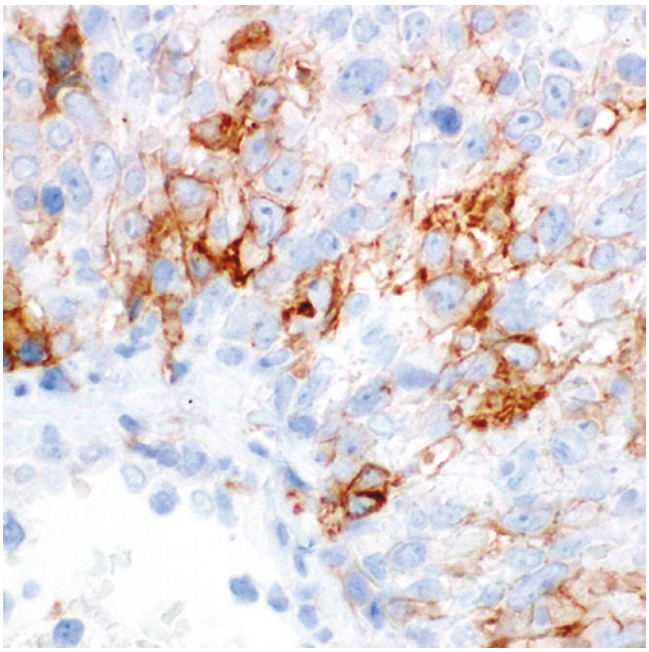

Fig. 15.63 Lymphomatoid granulomatosis, high grade. CD30 immunostain is positive in some large lymphoid cells

tive for CD30 in 30–40% of cases (Fig. 15.63), and CD15 is usually negative [89]. The large cells are also positive for EBER by ISH and for the EBV latent membrane protein-1 (LMP-1) by immunohistochemistry (Fig. 15.64). The large atypical B-cells are negative for T-cell markers and CD56 (Fig. 15.65). The background polymorphic infiltrate consists mostly of T-cells, positive for CD3 with a normal to slightly increased CD4:CD8 ratio and abundant macrophages (CD68+/CD163+) (Figs. 15.66 and 15.67).

Grading System

Currently, the World Health Organization (WHO) recommends grading LYG into three grades based on the amount of EBV+ large atypical cells/10 HPFs [100] since this feature appears to have prognostic relevance. Grade 1 lesions have <5 large atypical EBV+ B-cells/10 HPFs and minimal to no necrosis (Figs. 15.56 and 15.64). Grade 2 lesions contain 5–20 EBV+ B-cells/10 HPFs and variable—but not extensive—necrosis (Fig. 15.64). Grade 3 lesions are composed of sheets of large atypical EBV+ B-cells and extensive necrosis and overlap with EBV+ DLBCL [100] (Figs. 15.58, 15.59 and 15.64). Distinction between LYG grades 1 and 2 is not as relevant as recognizing LYG grade 3 given the significant prognostic impact. Therefore, LYG grades 1 and 2 are designated low-grade LYG whereas grade 3 is designated high-grade LYG. However, this grading system proposed by the WHO is controversial. Katzenstein et al. [90] have pointed out that an EBER ISH-based method for grading LYG is not entirely reliable since the sensitivity of ISH varies from laboratory to laboratory and this may result in an underestimation of the number of EBER+ cells. Similarly, high-grade LYG lesions tend to have extensive necrosis and ISH loses sensitivity in necrotic tissues, which may result in an underestimation of the number of EBER+ cells. Additionally, not all cases of LYG are positive for EBER, which creates confusion as to how to grade these cases. On the other hand, EBER may not only be positive in large B-cells but also in small lymphocytes, which may result in an overestimation of the LYG grading. For all these reasons, Katzenstein et al. [90] have recommended grading LYG by counting the large atypical cells using CD20 immunohistochemistry, which is a method more reliable and reproducible than ISH. Use of CD20 is also excellent for evaluating necrotic tissues since this antigen is well-known to remain present in necrotic tissues for a long period of time (Figs. 15.61 and 15.62). Yet another controversial point of the WHO grading system is related to the heterogeneity of the LYG lesions. For example, it is not uncommon to find nodules of grade 2 or even grade 3 LYG with adjacent grade 1 areas in resection specimens [89]. For this reason, it is also not uncommon to have discrepant results in a core needle biopsy when a lesion is classified as low-grade LYG, but due to sampling issues, the highest grade was not sampled. For a core biopsy showing only low-grade LYG, a comment addressing this issue is recommended, particularly when radiologic imaging shows multiple lung nodules. Given the presence of necrosis, transbronchial biopsies are diagnostic for LYG in only 30% of cases, and in open lung biopsies or lobectomies, extensive sampling of a necrotic LYG lesion is warranted to not miss high-grade areas. Table 15.12 shows a summary of the LYG grading system and its caveats in day-to-day practice.

Differential Diagnosis

LYG should be distinguished from several entities depending on the histologic grade and amount of necrosis. Grade 1 or 2 LYG mimics polymorphic lymphoproliferative disorders, namely CHL, T-cell/histiocyte-rich DLBCL, polymorphic post-transplant lymphoproliferative disorder, extranodal NK/T-cell lymphoma (polymorphic type), and PTCL, NOS. On the other hand, grade 3 LYG resembles DLBCL, ALCL, extranodal NK/T-cell lymphoma, and monomorphic post-transplant lymphoproliferative disorder involving the lung.

Clinical and radiologic correlation is helpful in differentiating between these lymphoproliferative disorders that do not present as multiple migratory lung nodules in an immunosuppressed patient but rather manifest as solitary lung masses or as lung involvement in advanced stages of well-documented lymphoma. The recognition of vasculitis, an angiocentric pattern, and necrosis is helpful since most lymphoproliferative disorders do not exhibit these features with the exception of extranodal NK/T-cell lymphoma, and that only rarely involves the lung. Immunohistochemical stains

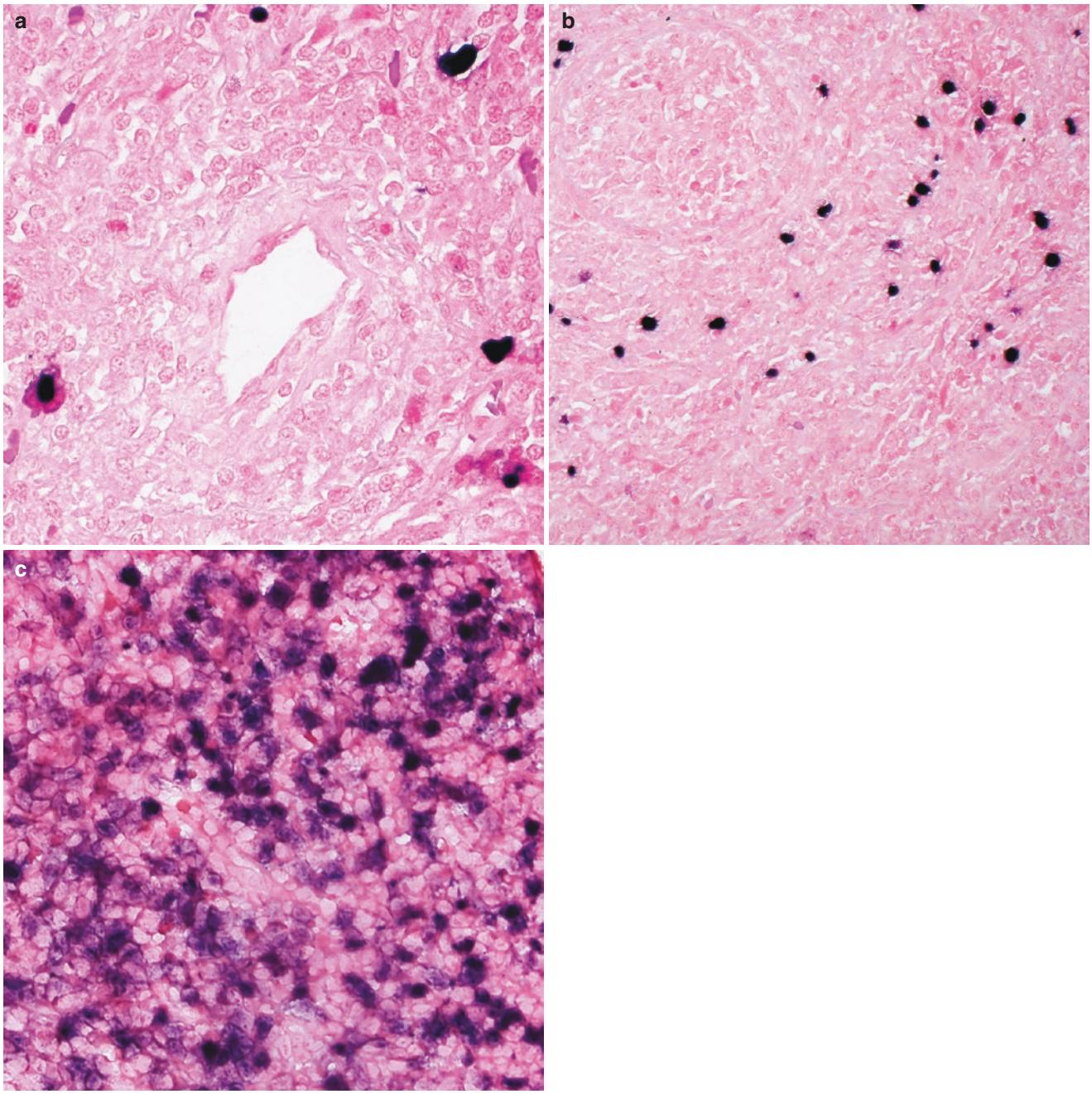

Fig. 15.64 Grading in lymphomatoid granulomatosis (LYG) according to the WHO recommendation using EBER in situ hybridization to count EBER+ cells per high power field. (**a**) Grade 1 LYG. (**b**) Grade 2 LYG. (**c**) Grade 3 LYG. (See text for details)

are needed to distinguish all these lesions. In CHL, the Reed–Sternberg cells are positive for CD30, CD15 (+/-), and PAX5 (weak) and are negative for CD20 and CD45, which contrast with LYG where the large atypical cells are of B phenotype. T-cell/histiocyte-rich DLBCL has a similar immunophenotype to LYG, but the large B-cells are negative for EBER and this lymphoma is commonly seen involving lymph nodes, spleen and bone marrow, sites that are usually spared by LYG. Pulmonary DLBCL is negative for EBER, and when this feature is present, it most likely represents grade 3 LYG and clinical history and imaging are required to further classify the lesion. NK/T-cell lymphoma features vasculitis, variable degrees of necrosis, and is EBER+. However, the necrosis in NK/T-cell lymphoma has abundant karyorrhectic debris—in contrast to the eosinophilic necrosis of LYG—and the EBER+ cells are NK/T-cells positive for CD3, CD8, CD56, and cytotoxic molecules (TIA-1, granzyme, perforin). PTCL, NOS, and ALCL may resemble grade 3 LYG on histology, but these are T-cell lymphomas, and they are negative for EBER.

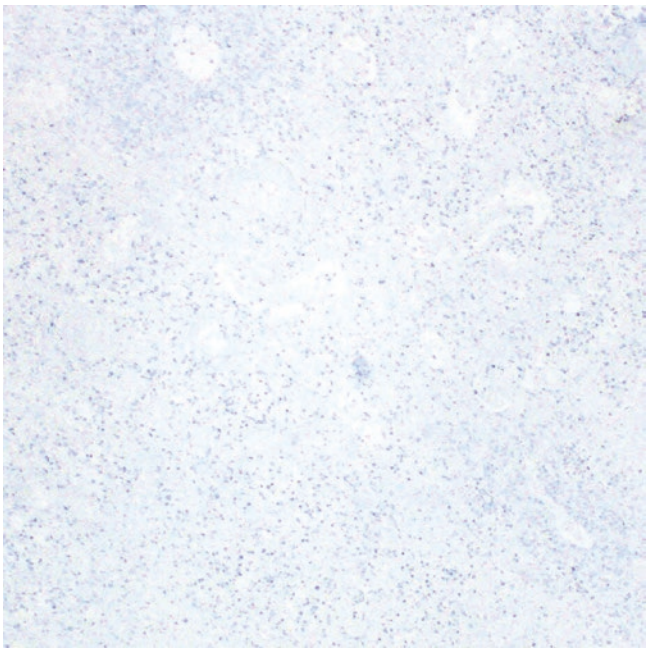

Fig. 15.65 Lymphomatoid granulomatosis, the CD56 immunostain is negative

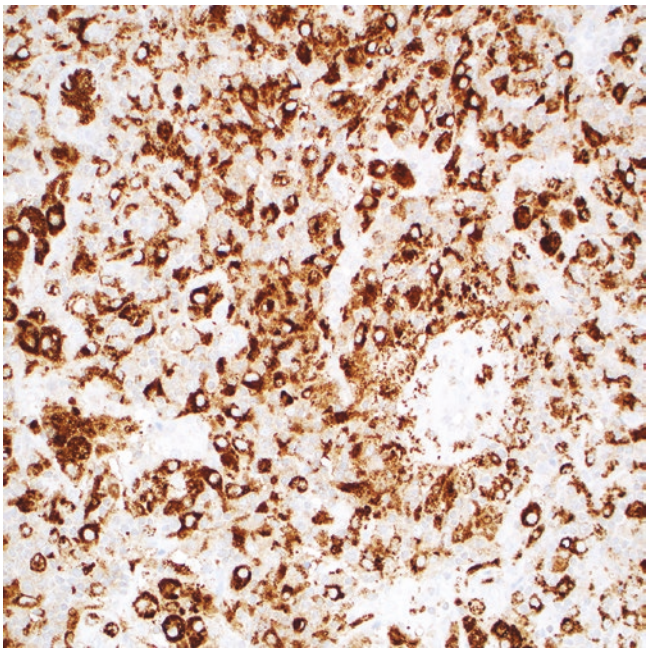

Fig. 15.67 Lymphomatoid granulomatosis, the CD68 immunostain highlights numerous macrophages

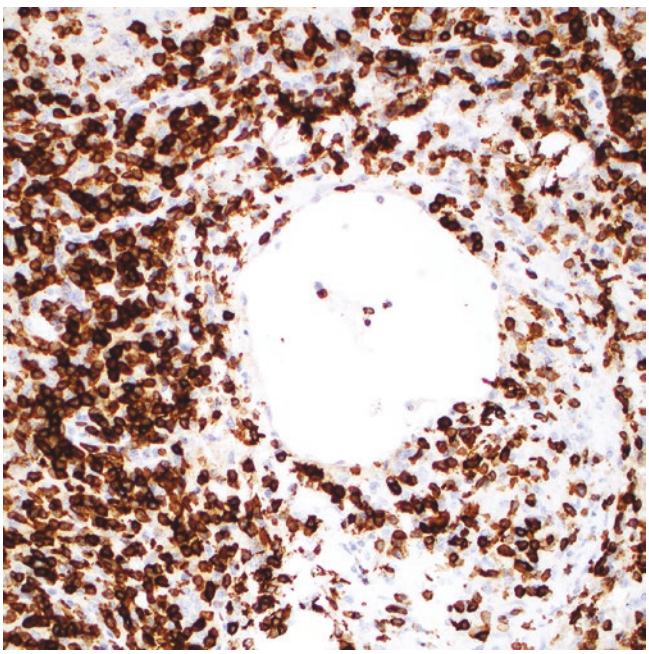

Fig. 15.66 Lymphomatoid granulomatosis, the CD5 immunostain highlights numerous small T-lymphocytes

Table 15.12 Pulmonary LYG grading system (WHO classification)

Grade 1 LYG	<5 large atypical EBV+ B-cells/10 HPFs Focal or no necrosis
Grade 2 LYG	5–20 EBV+ B-cells/10 HPFs Moderate necrosis, but not extensive
Grade 3 LYG	Greater number of large EBV+ B-cells (>50/HPFs) Extensive necrosis
Caveats with the WHO grading system **Underestimation of EBV+ cells:** • Variability of EBER ISH methodology from laboratory to laboratory • Loss of ISH sensitivity in markedly necrotic tissue • Rare cases of LYG are EBER negative **Overestimation of EBV+ cells:** • EBER may also be positive in other lymphoid cells, not only large B-cells **Other:** • Arbitrary numbers for grading LYG. No specification on how to classify cases with 20–50 EBV+ B-cells/10 HPFs • Heterogeneity of LYG lesions (grades 2–3 with areas of grade 1 in the same lesion). Therefore, a core biopsy may show grade 1 LYG, but the highest grade may not have been sampled • Transbronchial biopsies are diagnostic only in 30% of cases, and this percentage may be higher in cases with extensive necrosis	

LYG lymphomatoid granulomatosis, *WHO* World Health Organization, *HPF* high power fields, *EBV* Epstein–Barr virus, *EBER* EBV encoded RNA; *ISH* in situ hybridization

Importantly, a diagnosis of LYG should not be rendered in the post-transplant setting or in patients who are receiving immunomodulatory drugs, namely methotrexate or tumor necrosis factor alpha inhibitors. In these particular scenarios, the diagnosis is most likely either post-transplant lymphoproliferative disorder or iatrogenic immunodeficiency-associated lymphoproliferative disorder [90, 101]. Therefore, it is mandatory to exclude these two conditions before making the diagnosis of LYG.

Extensively necrotic lesions may have a differential diagnosis of pulmonary infarct, a vasculitic process such as granulomatosis with polyangiitis (former Wegener granulomatosis), necrotizing pneumonia (fungal or secondary to *Pseudomonas* or *Klebsiella*), necrotizing sarcoid, or a necrotic metastasis. Correlation with clinical history, imaging, and other laboratory assays is required to confirm or exclude any of these possibilities. Special stains and immunohistochemistry for CD20 may be useful to identify either a microorganism or to evaluate the number and size of B-cells, respectively. A summary of the differential diagnosis of LYG is shown in Table 15.13.

Molecular Findings

Only little information is known about the pathophysiology of LYG besides its association with EBV infection that is of type III latency (EBER+, LMP-1+, EBNA+) [89, 102]. It appears that LYG a low grade lymphoproliferative disorder that later progresses to a clonal process. It has been suggested that in low-grade LYG, the EBV+ B-cells release molecules that attract T-cells and other inflammatory elements to the lung and induce vasculitis. This process may be enhanced by the host-impaired immunologic system that permits the proliferation and thriving of EBV+ B-cells and progression to a lesion such as grade 2 LYG. Eventually, an independent clone of EBV+ B-cells dominates the picture with progression into grade Y LYG/EBV+ DLBCL. This hypothesis is supported by multiple findings. For example, clonal EBV has been detected in grade 3 LYG. Likewise, clonal *IGH* gene rearrangement has been detected in 50% of samples of grade 2 LYG, in 70% of samples of grade 3 LYG, but only in <10% of samples of grade 1 LYG [89]. Although these results may also be directly related to the paucity of EBV+ B-cells in grade 1 cases compared to grade 2 or 3 cases, it also suggests a higher burden of clonal cells with higher grades of LYG. Last, the theory of progression from low-grade to high-grade LYG is also supported by the frequency of progression to EBV+ LBCL. Only about 30% of patients with grade 1 LYG progress to grade 3 LYG, whereas 70–75% of patients with grade 2 LYG progress to grade 3 LYG/EBV+ DLBCL [91].

Table 15.13 Differential diagnosis of pulmonary LYG

Hematopoietic
Grade 1 or 2 LYG
Classic Hodgkin lymphoma
T-cell/histiocyte-rich large B-cell lymphoma
Polymorphic post-transplant lymphoproliferative disorder
Peripheral T-cell lymphoma, not otherwise specified
Extranodal NK/T-cell lymphoma (polymorphic)
Grade 3 LYG/EBV+ large B-cell lymphoma
Diffuse large B-cell lymphoma
Anaplastic large cell lymphoma
Extranodal NK/T-cell lymphoma (mainly with large cells)
Monomorphic post-transplant lymphoproliferative disorder
Non-hematopoietic (especially lesions with extensive necrosis)
Pulmonary infarct
Granulomatosis with polyangiitis (Wegener granulomatosis)
Other vasculitic processes
Necrotizing pneumonia
Necrotizing sarcoid
Necrotic metastasis

LYG lymphomatoid granulomatosis, *EBV* Epstein–Barr virus

Other Small B-cell Lymphomas: Chronic Lymphocytic Leukemia/Small Lymphocytic Lymphoma (CLL/SLL), Mantle Zone Lymphoma, Follicular Lymphoma and Lymphoplasmacytic Lymphoma

Introduction

Small B-cell lymphomas other than MALT lymphoma, namely CLL/SLL, mantle zone lymphoma, follicular lymphoma, and lymphoplasmacytic lymphoma are exceedingly rare as primary lung disease [51, 103–106]. Secondary pulmonary involvement is much more common than primary disease, and this may be detected on imaging when there is high tumor burden. Detection of a new lung mass or multiple lung masses in a patient with a known history of low-grade B-cell lymphoma suggests either large cell transformation, or a different lung condition, namely lung carcinoma, metastasis, lobar pneumonia, sarcoidosis, granulomatous inflammation, etc. Because these tumors are exceedingly rare in the lung, they are only discussed briefly.

Clinical Features

The majority of low-grade B-cell lymphomas affect adults and the elderly. Most patients do not have symptoms and are only symptomatic when there is advanced disease with extensive lung involvement. Clinical symptoms include fever, dry cough, or dyspnea, which may be misdiagnosed as pneumonia.

Pathology

Gross involvement is not obvious, and it may appear as consolidated lung parenchyma and only rarely as a mass. Microscopically, all low-grade B-cell lymphomas are identical to their counterparts at other sites. In the lung, they typically demonstrate lymphangitic or interstitial spread with thickening of alveolar septa (Fig. 15.68). Rarely, CLL/SLL may involve the lung in a bronchiolocentric pattern [12, 107]

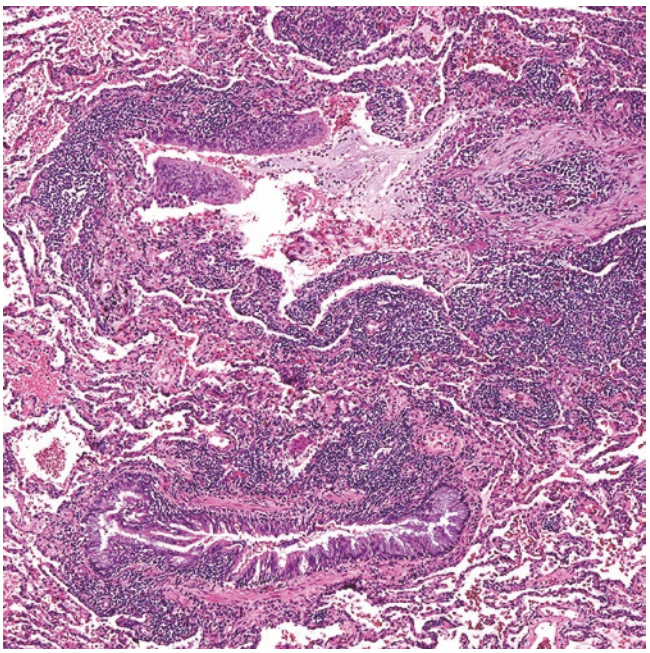

Fig. 15.68 Chronic lymphocytic leukemia/small lymphocytic lymphoma (CLL/SLL) involving lung with bronchovascular distribution. The lobectomy was performed for an adenocarcinoma in a patient with known CLL/SLL

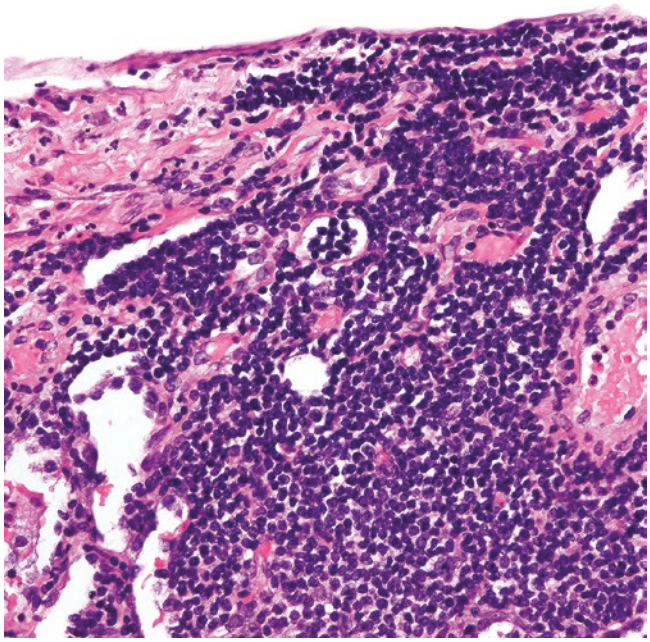

Fig. 15.70 Chronic lymphocytic leukemia/small lymphocytic lymphoma (CLL/SLL) involving the subpleural space. The lobectomy was performed for an adenocarcinoma in a patient with known CLL/SLL

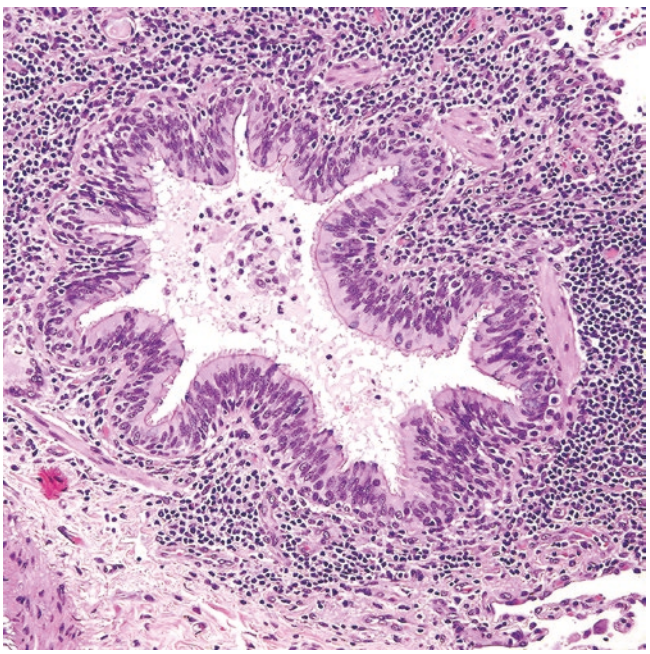

Fig. 15.69 Chronic lymphocytic leukemia/small lymphocytic lymphoma with bronchiolocentric patterns

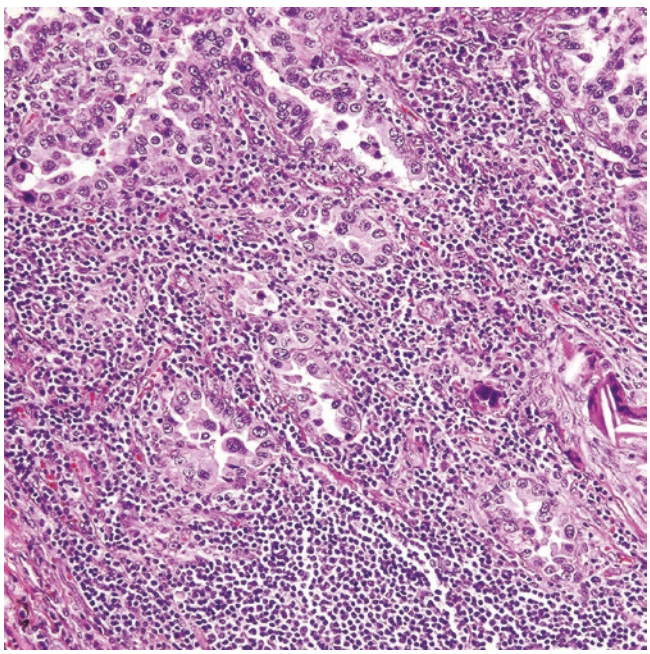

Fig. 15.71 Chronic lymphocytic leukemia/small lymphocytic lymphoma admixed with lung adenocarcinoma

(Fig. 15.69). Visceral pleural involvement may be seen as small aggregates of lymphoma cells right beneath the mesothelial lining or as lymphoid nodules forming pleural polypoid structures (Fig. 15.70). If a lung resection is performed for another reason (carcinoma, metastasis, infection), the lymphoma cells are seen either around or deeply intermingled with the non-lymphomatous process (Fig. 15.71). Bronchovascular bundles and bronchioles apart from the non-hematopoietic process may or may not show aggregates of lymphoma cells.

CLL/SLL cells have a round nucleus, clumped chromatin, and scant cytoplasm. Bronchopulmonary leukemic infiltrates

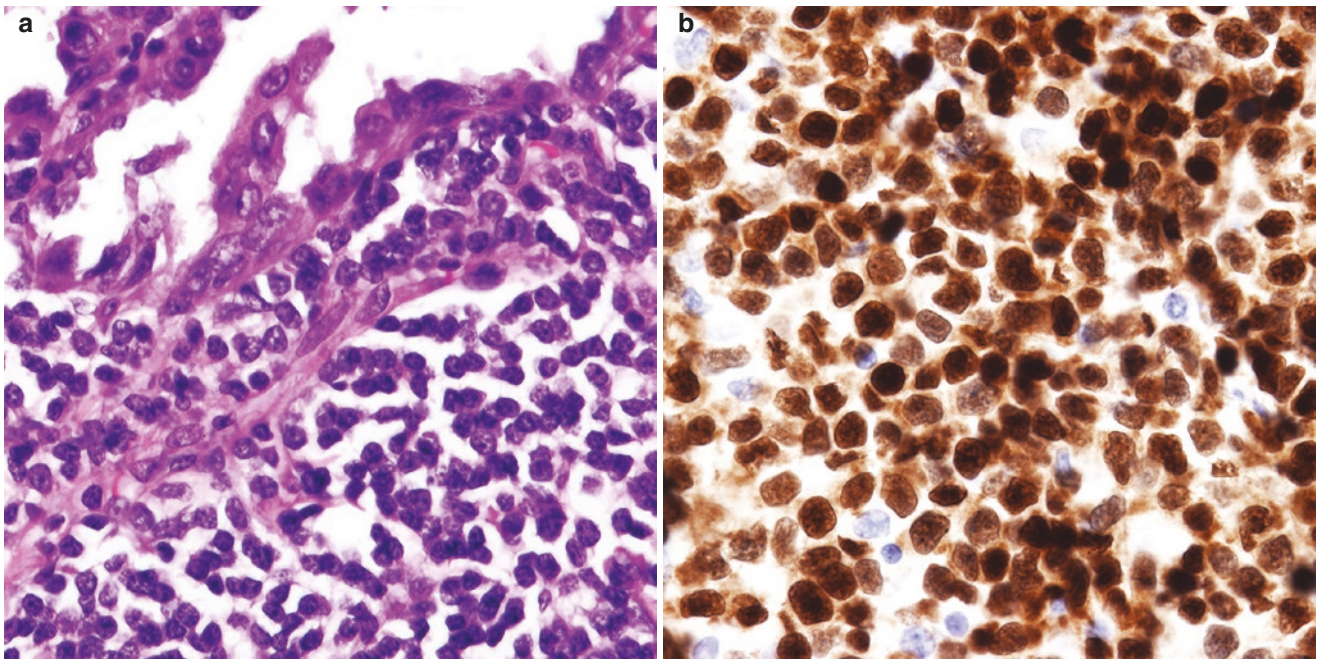

Fig. 15.72 (**a**) Mantle cell lymphoma cells (bottom) adjacent to lung adenocarcinoma (top), (**b**) the lymphoma cells are positive for cyclin D1

are observed in 40% of patients in different types of lung biopsies [108]. Mantle cell lymphoma has cleaved cells with moderately condensed chromatin and inconspicuous nucleolus (Fig. 15.72). Low-grade follicular lymphoma (grades 1–2) consists of neoplastic follicles made of cleaved cells with condensed chromatin or centrocytes and larger cells with fine chromatin and nucleoli or centroblasts (<15/HPF). The neoplastic follicles do not show polarization or tingible-body macrophages and have attenuated mantle zones (Fig. 15.73). If >15 centroblasts/HPF are seen, this suggests high-grade follicular lymphoma (grade 3A when centrocytes are still present and 3B when follicles only contain centroblasts). Pulmonary involvement by follicular lymphoma may occur as multiple bilateral small nodules mimicking sarcoidosis [109]. Lymphoplasmacytic lymphoma is composed of a mixture of small lymphocytes, plasmacytoid lymphocytes, and plasma cells. This lymphoma is probably the least common to involve the lung.

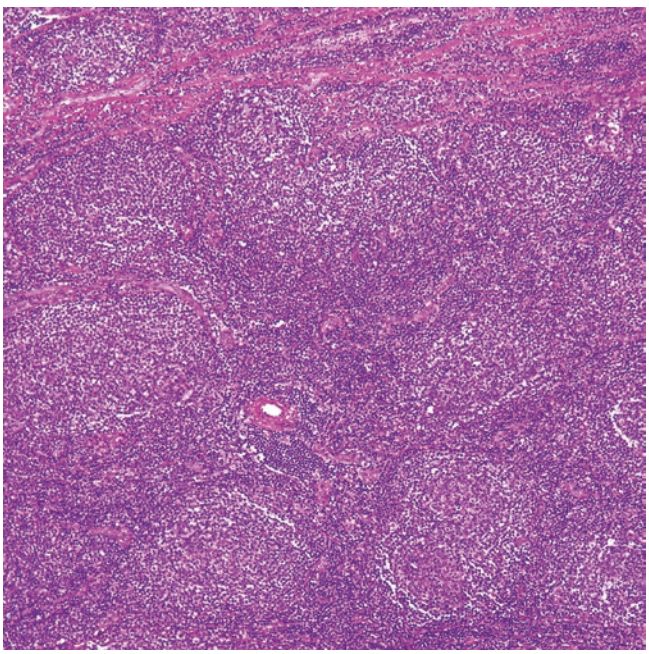

Fig. 15.73 Low-grade follicular lymphoma, composed of back-to-back follicles with no polarization of the germinal centers and attenuated mantle zones. The majority of neoplastic follicles are composed of centrocytes with only a few centroblasts

Immunohistochemistry and Other Ancillary Studies

All of these B-cell lymphomas are positive for CD20, CD22, CD79a, and PAX5. A comprehensive panel of markers to distinguish small B-cell lymphomas includes CD3, CD5, CD10, CD23, CD43, bcl-2, bcl-6, cyclin D1, SOX11, LEF1 (lymphoid enhancer binding factor 1), and LMO2 (LIM domain only 2). Depending on the morphologic features, some—but not all—of these markers may be used to further classify a low-grade B-cell lymphoma. CLL/SLL is positive for CD5, CD23, CD43, and LEF1 and negative for CD10, bcl-6, and cyclin D1 (Fig. 15.74a–d). Mantle cell lymphoma is positive for CD5, CD43, cyclin D1, and SOX11 and negative for CD10, bcl-6, and LEF1. Follicular lymphoma is positive for CD10, bcl-6, variable CD23, and LMO2 and negative for CD5, CD43, and cyclin D1. Lymphoplasmacytic lymphoma is positive for IgM and negative for CD5 and CD10. Importantly, bcl-2 is positive in all these B-cell lym-

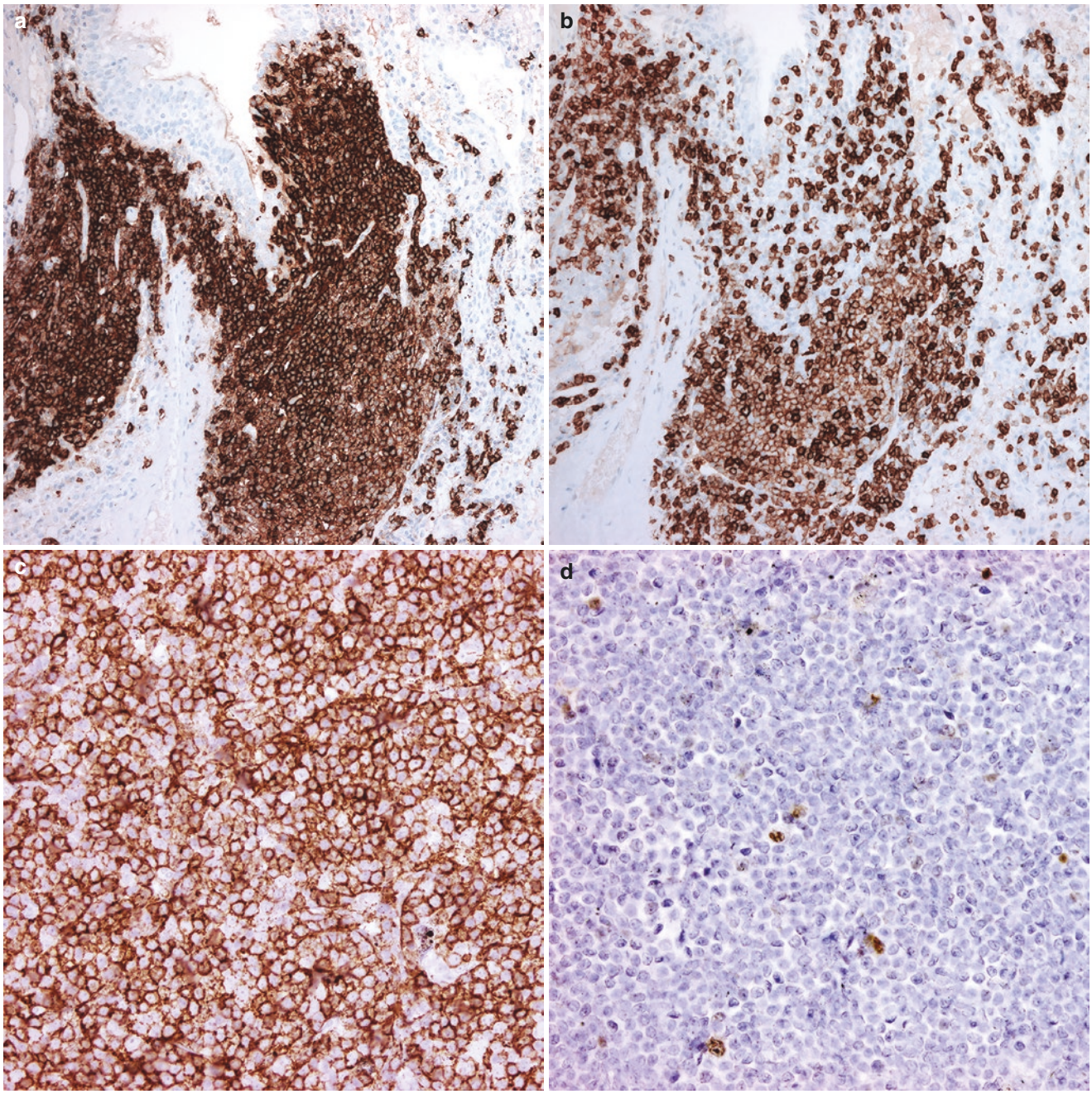

Fig. 15.74 Chronic lymphocytic leukemia/small lymphocytic lymphoma involving the lung. The lymphoma cells are immunoreactive for (**a**) CD20, (**b**) CD5, and (**c**) CD23 and are negative for (**d**) cyclin D1

phomas and expression of this marker does not help to distinguish between these entities; however, bcl-2 is useful to distinguish reactive follicles (bcl-2 negative) from neoplastic follicles in follicular lymphoma (bcl-2+) (Fig. 15.75a, b). The Ki-67 proliferation index in all these lymphomas is low to intermediate (<30%).

Differential Diagnosis

Any pulmonary low-grade B-cell lymphoma should be distinguished from a reactive lymphoid process or pulmonary MALT lymphoma. For additional details, please refer to the section of pulmonary MALT lymphoma.

In reactive lymphoid conditions, lymphocytes do not co-express CD5, CD10, CD43, or bcl-2, and there is no replacement of the architecture by the inflammatory process. Reactive lymphoid follicles, if present, are positive for CD10 and bcl-6 and negative for bcl-2 and show preserved FDC meshworks. Immunohistochemistry, ISH, or flow cytometry shows polytypic B-cells and/or plasma cells.

A prior clinical history of low-grade B-cell lymphoma is extremely helpful to avoid incorrectly interpreting unimpressive lymphoid infiltrates around a lung carcinoma, a pneumonic process, or a metastasis as reactive lymphocytic inflammation. Expression of aberrant markers in the B-cells,

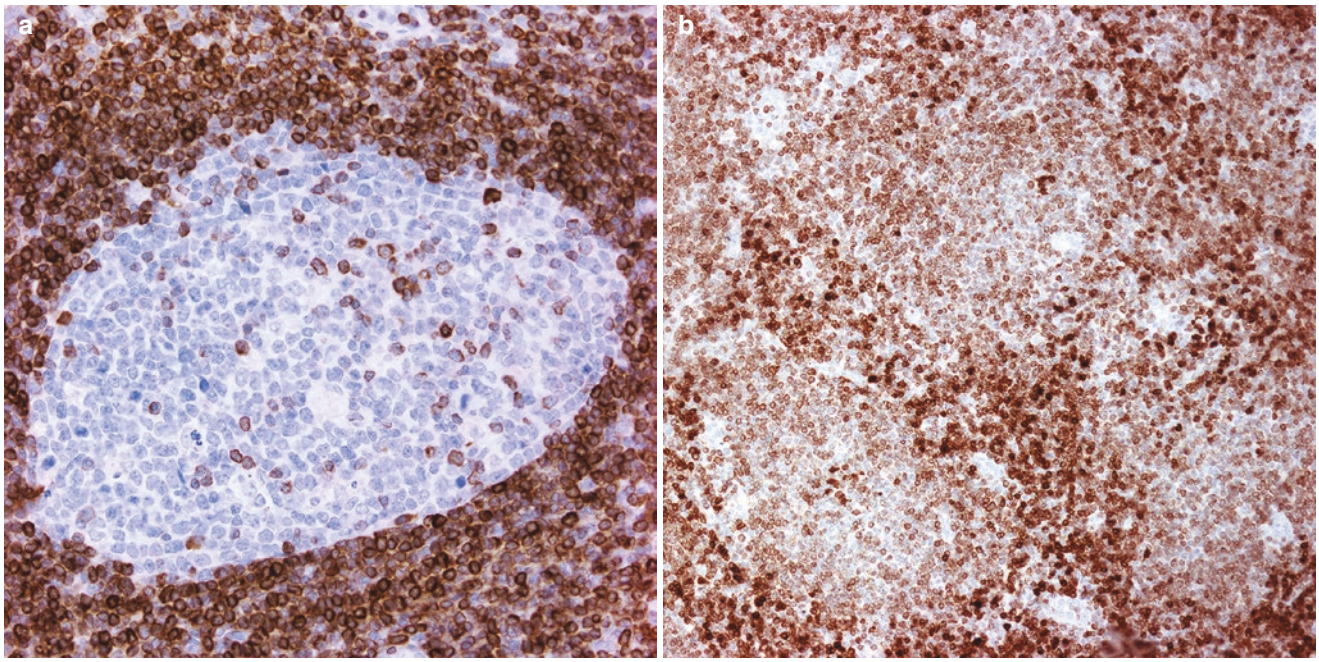

Fig. 15.75 Bcl-2 immunostain is negative in the germinal center of (**a**) a reactive lymphoid follicle and (**b**) positive in neoplastic follicles in follicular lymphoma

such as CD5 (CLL/SLL, mantle cell lymphoma), CD10 and bcl-6 (follicular lymphoma) and co-expression of bcl-2 in B-cells should raise concern for the possibility of concurrent lymphoma. Diffuse expression of cyclin D1 or SOX11 in B-cells supports the diagnosis of mantle cell lymphoma. Follicular lymphoma can mimic follicular hyperplasia, follicular bronchiolitis, or a MALT lymphoma with follicular colonization. Again, a bcl-2 immunostain is helpful in distinguishing between reactive germinal centers (negative for bcl-2) from neoplastic follicles in follicular lymphoma (bcl-2+). Detection of the t(14;18)(*BCL2::IGH*) may be required in difficult cases to confirm the diagnosis of follicular lymphoma. Lymphoplasmacytic lymphoma should be distinguished from chronic lymphoplasmacytic inflammation seen in some autoimmune disorders involving the lung and from MALT lymphoma. A prior history of lymphoplasmacytic lymphoma/Waldeström hypergammaglobulinemia and detection of an IgM paraprotein is extremely helpful to support lymphoplasmacytic lymphoma and excludes the other conditions. Nevertheless, the distinction between lymphoplasmacytic lymphoma and MALT lymphoma may be challenging in some cases since both tumors are negative for CD5 and CD10. In this situation, the clinical presentation and detection of *MYD88* (L265P) mutation are useful to discern between these two lymphomas. *MYD88* (L265P) mutation is common in lymphoplasmacytic lymphoma and infrequent in MALT lymphoma.

Molecular Findings

The specific molecular alterations in each of these lymphomas are outside the scope of this chapter. The reader should consult preferred hematopathology textbooks for additional information.

Extraosseous (Pulmonary) Plasmacytoma

Introduction

Although extraosseous plasmacytoma is relatively common in the upper airways [110], primary pulmonary plasmacytoma is very rare [111]. A subset of primary pulmonary cases may precede plasma cell myeloma for a few months or even years. Secondary lung involvement is more common and usually seen as a multifocal disease in the setting of plasma cell myeloma. This section is focused on primary pulmonary disease.

Clinical Features

Most affected individuals with primary pulmonary plasmacytoma are adults in the 5th to 7th decades of life, whereas those with secondary lung involvement by plasma cell myeloma are in the 6th to 9th decades of life, with some overlap for both at around 50–60 years of age [112]. Clinical symptoms include cough, dyspnea, and hemoptysis. Compression of the airways may produce respiratory distress. About 50% of patients with a primary pulmonary plasmacytoma have an M-protein, in contrast to secondary involvement by plasma cell myeloma where a paraprotein is much more common [111]. A solitary lung lesion may be treated by surgical resection if there is no evidence of disease elsewhere. On the other hand, patients with unresectable disease or plasma cell myeloma are treated with chemoradiation [111, 113–116].

Diagnostic Imaging

Primary pulmonary plasmacytomas most commonly manifest as a solitary nodule or mass with a round to oval shape, homogeneous density, and smooth, well-delineated margins [114, 117] (Fig. 15.76). In a series of five cases reported by Koss et al., tumors ranged from 2.5 to 8 cm in maximum diameter and were either peribronchial or involved a major bronchus; peribronchial and mediastinal lymph nodes were involved in three cases [111]. Less common presentations of primary pulmonary plasmacytomas include multiple nodules, lobar consolidation, and diffuse consolidation [115, 117, 118]. Data on the PET/CT appearance of primary pulmonary plasmacytoma is sparse. In patients with solitary plasmacytoma, whether intraosseous or extraosseous, either PET/CT or whole-body magnetic resonance imaging is recommended to exclude the presence of additional malignant lesions [119].

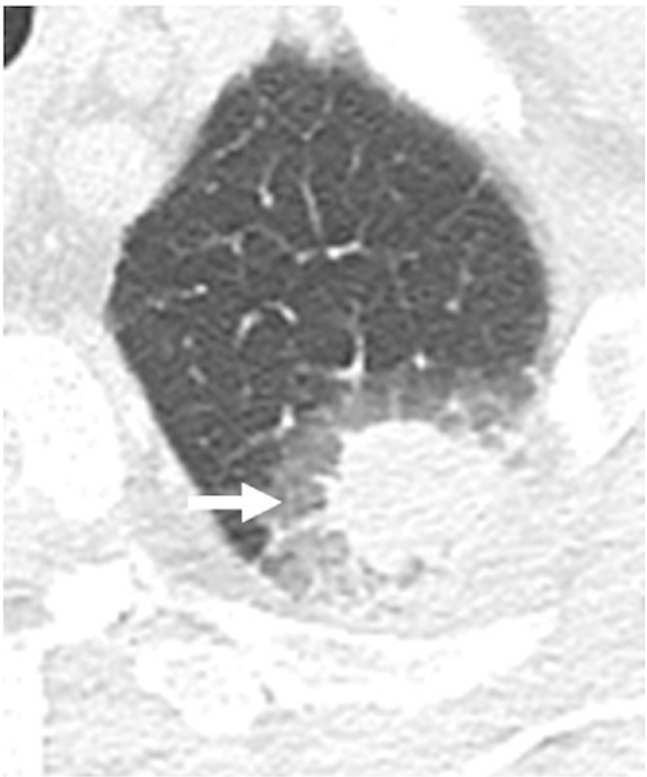

Fig. 15.76 Plasmacytoma. CT shows a left upper lobe nodule with a ground-glass halo. The adjacent ribs are normal

Pathology

Gross descriptions of pulmonary plasmacytoma are not available given its rarity. Microscopically, the tumor is composed of sheets of mature-appearing plasma cells (eccentric round nucleus with cartwheel chromatin, inconspicuous nucleolus, basophilic cytoplasm with a paranuclear hoff/clear Golgi zone) that efface the lung parenchyma (Figs. 15.77 and 15.78). Scattered plasma cells with prominent nucleolus or few pleomorphic forms may or may not be present. Cytoplasmic spherical eosinophilic deposits of immunoglobulin (Russell bodies) or intranuclear eosinophilic immunoglobulin inclusions (Dutcher bodies) are variably seen. Mitoses may be observed, but apoptotic bodies are uncommon unless the tumor exhibits high-grade features. The latter include significant pleomorphic forms or blastic

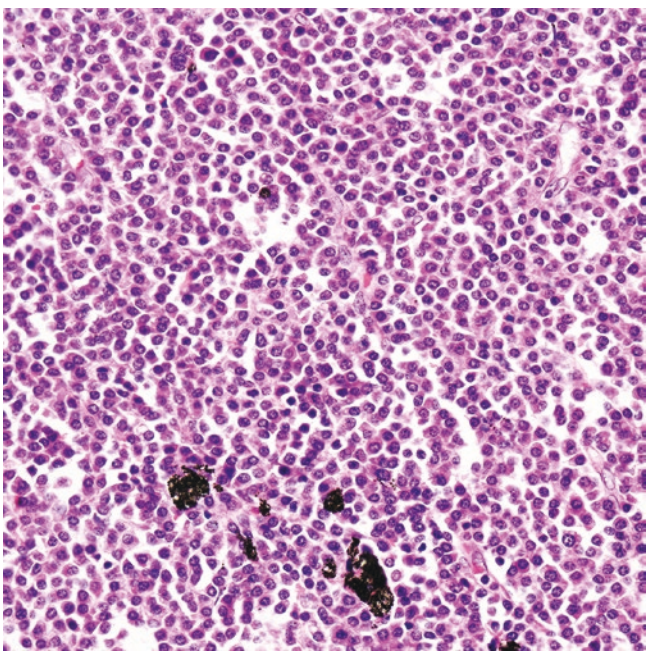

Fig. 15.77 Pulmonary plasmacytoma. Sheets of mature-appearing plasma cells effacing the lung parenchyma. Residual macrophages laden with anthracotic pigment are seen (bottom, center)

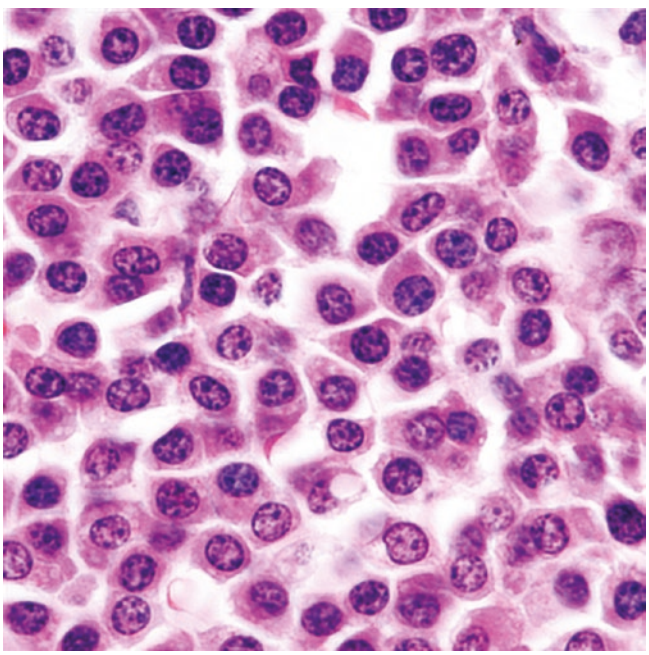

Fig. 15.78 Higher magnification shows sheets of mature-appearing plasma cells

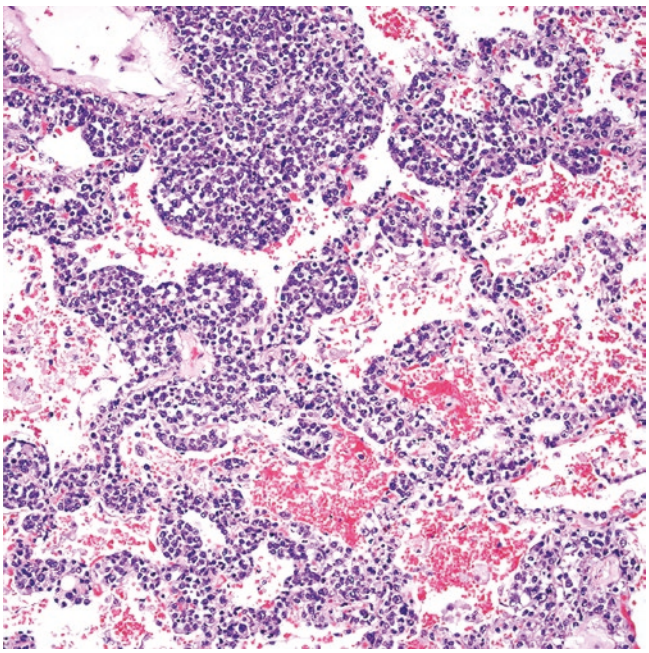

Fig. 15.79 Secondary lung involvement by plasma cell myeloma with interstitial distribution (*Courtesy of Dr. Jeanette Ramos*)

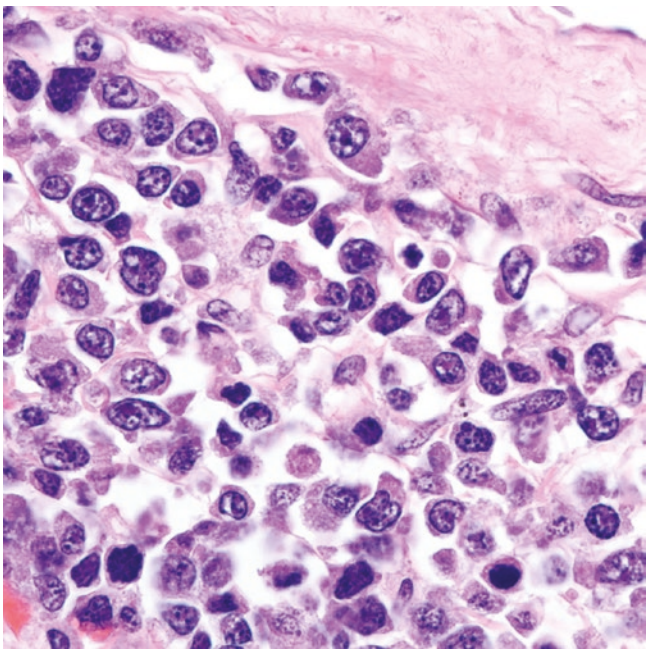

Fig. 15.80 Secondary lung involvement by plasma cell myeloma with interstitial distribution. Higher magnification shows atypical plasma cells with an irregular nucleus and prominent nucleolus (*Courtesy of Dr. Jeanette Ramos*)

morphology. In some instances, plasmacytoma can show a nested or organoid arrangement similar to that of neuroendocrine carcinomas with or without associated chicken-wire vasculature. A sclerotic background stroma may or may not be present, and some cases may be accompanied by amyloid deposits. Secondary involvement by plasma cell myeloma occurs as multifocal infiltrates with ill-defined borders with or without central necrosis. Interstitial infiltrates containing plasma cells may also be seen (Figs. 15.79 and 15.80).

Immunohistochemistry and Other Ancillary Studies

Neoplastic plasma cells are positive for CD138, CD79a, and MUM1, restricted for either kappa or lambda light chain, and frequently show aberrant expression of CD117 and/or CD56, whereas they are weakly positive or negative for CD20, PAX5, and CD45 (Figs. 15.81 and 15.82a, b). The neoplastic plasma cells are negative for T-cell markers, keratins, melanoma markers, or neuroendocrine markers although rare cases of plasmacytoma may show focal expression of T-cell markers as well as focal paranuclear dot expression of keratin (usually CAM5.2). EBER ISH is negative. Flow cytometry is extremely useful for diagnosis. Plasma cells can be assessed for the presence of a monotypic light chain and the expression of bright CD38 and CD138, CD56, and CD117. With this method, diminished expression or loss of CD19, CD45, CD27, and CD81 supports an aberrant plasma cell immunophenotype. In a study of 28 cases of extramedullary plasmacytoma—although most of them not arising in the lung—the majority of cases showed a lack of cyclin D1 labeling, infrequent expression of CD56, and a lower proliferation index when compared with extramedullary plasma cell myeloma [110].

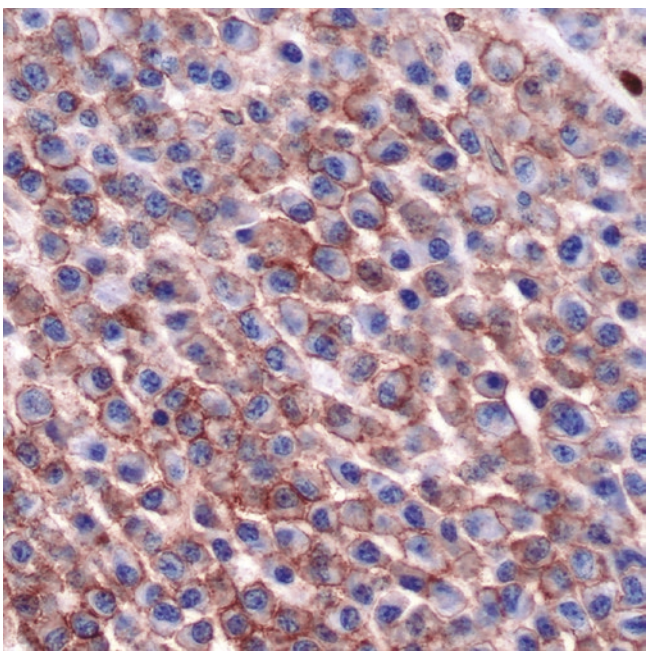

Fig. 15.81 Plasmacytoma, CD138 immunostain

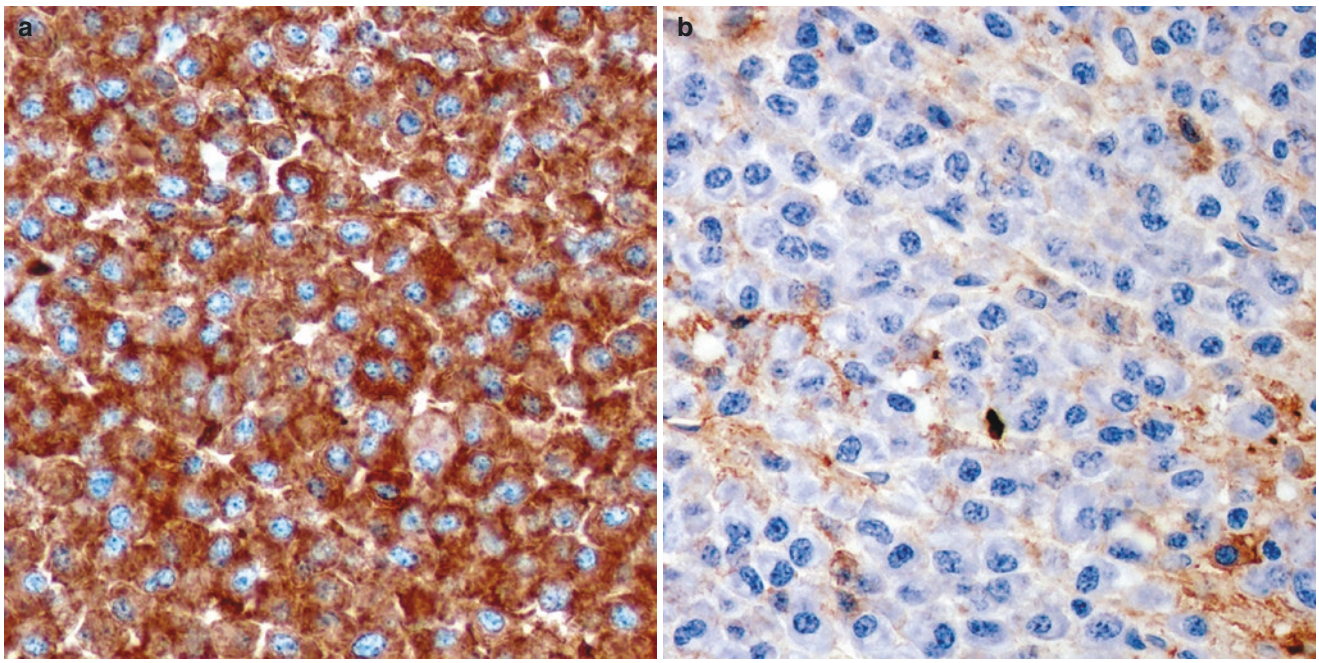

Fig. 15.82 Plasmacytoma. The plasma cells are positive for (**a**) kappa light chain and negative for (**b**) lambda light chain by immunohistochemistry

Differential Diagnosis

Primary pulmonary plasmacytoma should be distinguished from tumefactive reactive conditions rich in plasma cells, namely nonspecific plasmacytic inflammatory infiltrates, IgG4-RLD, plasma cell granuloma/inflammatory pseudotumor, as well as from pulmonary MALT lymphoma with extensive plasmacytic differentiation and lymphoplasmacytic lymphoma involving the lung.

Tumefactive reactive plasmacytic processes are readily distinguished from plasmacytoma by performing immunohistochemistry or ISH studies for kappa and lambda light chains. Nonspecific plasma cell-rich inflammation, IgG4-RLD, and plasma cell granuloma/inflammatory pseudotumor are always polytypic. In addition, plasma cells do not show aberrant expression of CD117 and CD56, or loss of CD19, CD27, or CD81. In IgG4-RLD and in plasma cell granuloma/inflammatory pseudotumor, there is fibrosis with storiform arrangement, increased lymphocytes, and variable presence of obliterative phlebitis, which are not features of a plasma cell neoplasm. IgG and IgG4 are required to confirm the diagnosis. Plasmacytomas are only rarely positive for IgG4.

Pulmonary MALT lymphoma with extensive plasmacytic differentiation and lymphoplasmacytic lymphoma involving the lung usually contain a significant number of lymphocytes, and this feature is not seen in pulmonary plasmacytoma [120]. Immunohistochemistry for CD20, PAX5, and CD45 are positive in MALT lymphoma and lymphoplasmacytic lymphoma and only weakly positive to negative in plasma cell neoplasms. Strong labeling for cyclin D1 is useful to differentiate plasma cell neoplasms with small cell morphology from lymphoplasmacytic lymphoma or MALT lymphoma that are negative for this marker. Plasmacytomas with blastic morphology should be distinguished from plasmablastic lymphoma that is CD20+/-, CD138+, EBER+, immunoblastic DLBCL that is CD20+, PAX5+, CD138-, poorly differentiated carcinoma (either primary or metastatic), neuroendocrine carcinoma, or metastatic melanoma. The latter is easily accomplished by performing stains for cytokeratins, neuroendocrine markers, and/or melanocytic markers that are negative in plasma cell neoplasms. The differential diagnosis of pulmonary plasmacytoma is summarized in Table 15.14.

Table 15.14 Differential diagnosis of pulmonary plasmacytoma

Low-grade (well-differentiated) plasma cell neoplasm
Inflammatory or reactive process with polytypic plasmacytosis
IgG4-related lung disease
Plasma cell granuloma/inflammatory pseudotumor
Marginal zone lymphoma of mucosa-associated lymphoid tissue (MALT lymphoma) with extensive plasmacytic differentiation
Other small B-cell lymphomas with plasmacytic differentiation
Low-grade neuroendocrine carcinoma
Metastatic carcinomas with plasmacytoid morphology
High-grade (poorly differentiated) plasma cell neoplasm
Primary or metastatic poorly differentiated carcinoma, including neuroendocrine carcinoma
Metastatic amelanotic melanoma

Molecular Findings

Pulmonary plasmacytoma most likely exhibits the same molecular alterations as extramedullary plasmacytomas at other sites or as plasma cell myeloma. In a study of 38 extramedullary plasmacytomas, chromosomal gains were the most common cytogenetic abnormality (82%), followed by loss of 13q (40%) [121]. In addition, about 40% of cases showed *IGH* breaks, 16% harbor the t(4;14), but not t(11;14), t(14;16), and t(8;14) or *MALT1*, *bcl6,* or *FOXP1* rearrangements were detected. Based on these findings, this study concluded that extramedullary plasmacytoma and plasma cell myeloma were closely related at the cytogenetic level, with some differences in the distribution of *IGH* translocation partners [121]. However, specific data for primary pulmonary plasmacytoma is lacking.

Pulmonary Non-Hodgkin Lymphomas of T-Cell Origin

Pulmonary Anaplastic Large Cell Lymphoma (ALCL)

Introduction

Before the advent of immunohistochemistry, ALCL was first recognized as histiocytic lymphoma. In 1985, Stein et al. discovered that this tumor was a subtype of T-cell lymphoma that expressed CD30 or Ki-1, hence the term Ki-1 antigen-positive LCL. [122] Later in the mid-1990s, it was discovered that a subset of ALCLs harbor rearrangements of the anaplastic lymphoma kinase-1 (ALK-1), a molecule that has been pivotal in the understanding of tumorigenesis and cancer molecular biology [123–125]. Primary pulmonary ALCL is very rare with only about 25 cases reported to date [126, 127]. Nevertheless, lung involvement can be seen with systemic disease. In this context, ALCL is the most common T-cell lymphoma to involve the lung.

Clinical Features

The mean age at presentation of ALCL involving the lung is ~45 years (combined primary and secondary disease), with sporadic reports in children and HIV-infected individuals [126, 128, 129]. Clinical symptoms include fever, cough, dyspnea, malaise, night sweats, and weight loss. Most patients have been treated by surgical resection and combined chemotherapy with variable outcomes [126, 128]. The presence of ALK and CD30 in this lymphoma has been exploited to develop targeted therapies, namely brentuximab vedotin (antibody against CD30) or crizotinib (ALK-specific inhibitor) [130, 131]. Nevertheless, no studies are available to date to evaluate the efficacy of this therapy in primary pulmonary ALCL.

Diagnostic Imaging

Secondary lung involvement is reported in up to 12% of cases of anaplastic large-cell lymphoma (ALCL), while primary pulmonary ALCL has only been reported in rare cases [128]. Rush et al. in their review of five patients with primary pulmonary ALCL found parenchymal, endobronchial, or intratracheal lesions that ranged from 1.1 to 5 cm in size [128] (Fig. 15.83a, b). Feeney and colleagues found increased FDG uptake [SUVmax range between 3.3 and 37.0] in lymph nodes in 94% of systemic ALCL patients [132]. Similar metabolic activity would be expected in lung lesions.

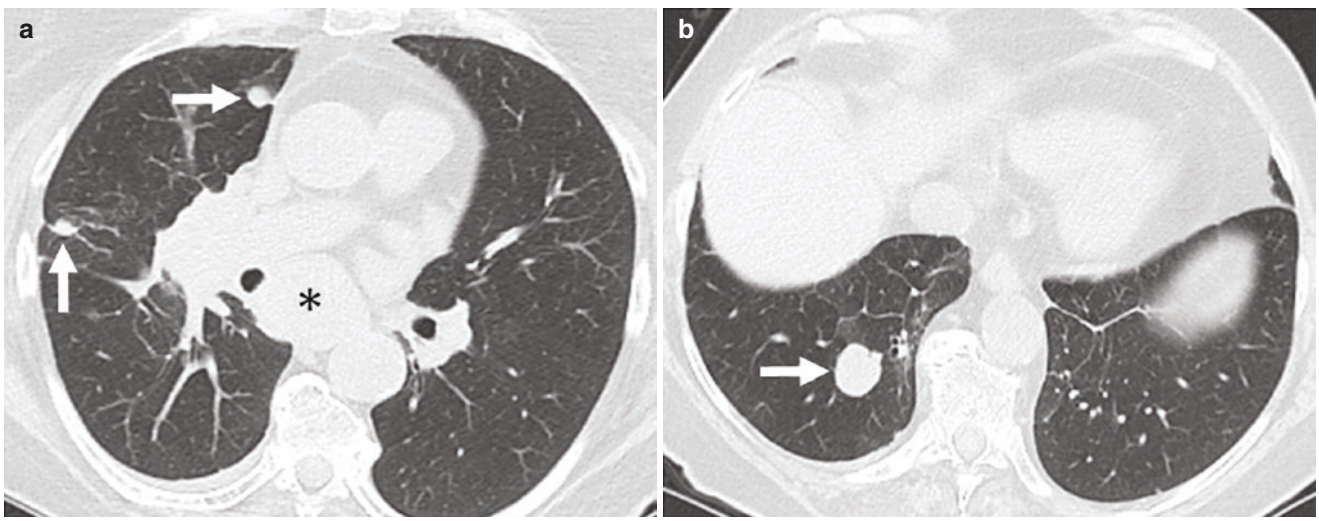

Fig. 15.83 Anaplastic large cell lymphoma. (**a**, **b**) CT show solid right lung nodules (arrows). Note also bulky subcarinal adenopathy (asterisk) in (**a**)

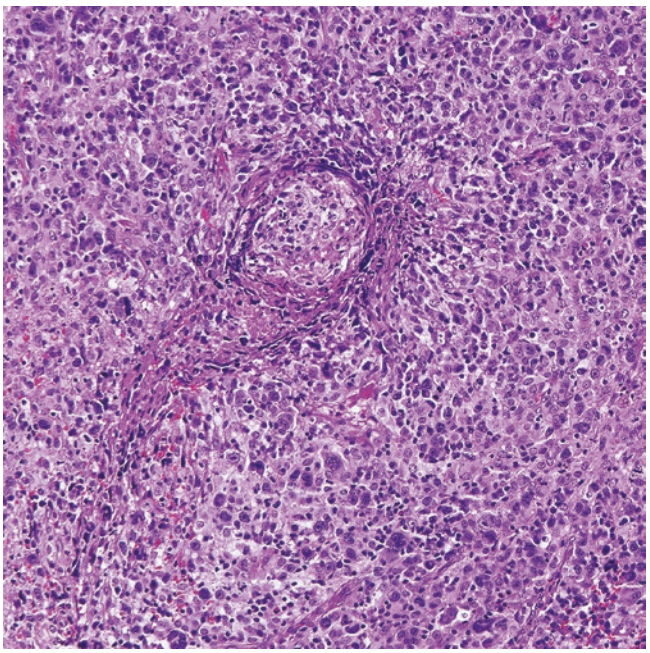

Fig. 15.84 Pulmonary anaplastic large cell lymphoma. Sheets of large pleomorphic lymphoma cells, some with horseshoe-shaped nucleus ("hallmark" cells)

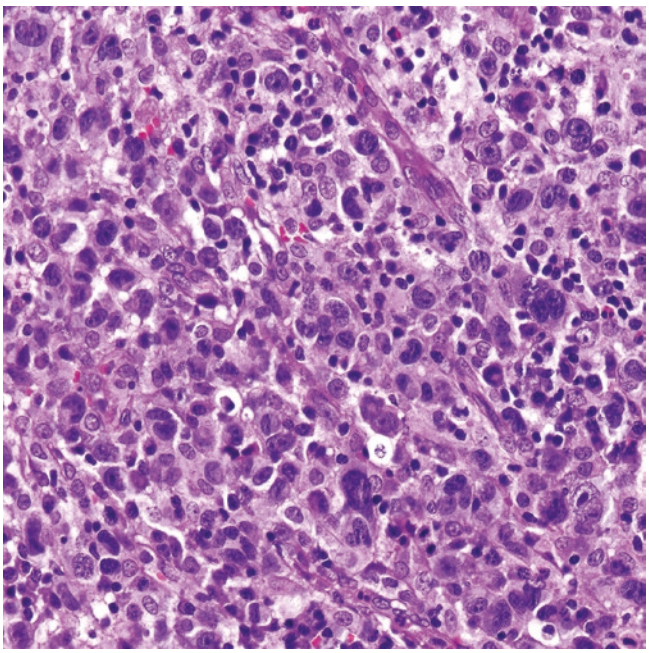

Fig. 15.85 Higher magnification of pulmonary anaplastic large cell lymphoma

Pathology

Grossly, ALCL has been described as a tan-white homogeneous mass with variable necrosis. On microscopic examination, ALCL is composed of sheets of large cells with ample eosinophilic or amphophilic cytoplasm with variable number of cells showing horseshoe-shaped nuclei ("hallmark" cells), ring-like nuclei ("doughnut" cells), Reed–Sternberg-like cells, and pleomorphic and multinucleated forms (Figs. 15.84 and 15.85). Nuclear features also include vesicular chromatin and variable prominent nucleolus. Mitotic figures and areas of necrosis are common. There are several morphologic variants of ALCL, namely a sarcomatoid, a lympho-histiocytic, a neutrophil-rich, an eosinophil-rich, and a small cell variant that may pose diagnostic difficulties if this entity is not considered [133–135]. Pulmonary patterns described in the lung include a nodular, scattered nodular pattern with cyst formation, endobronchial mass with airway obstruction, and intra-alveolar spread of ALCL cells admixed with fibrin identical to the pattern of tumoral pneumonia described for pulmonary DLBCL [127].

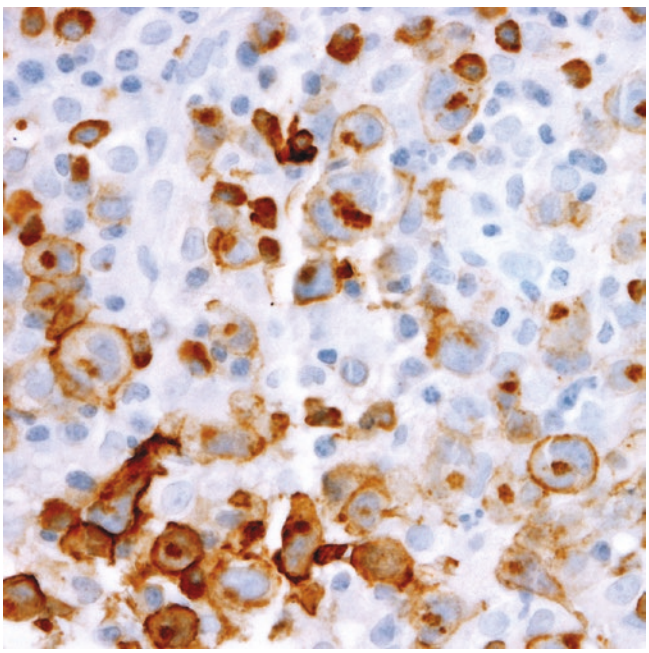

Fig. 15.86 Anaplastic large cell lymphoma, CD30 immunostain with membranous and paranuclear dot (Golgi) labeling

Immunohistochemistry and Other Ancillary Studies

By definition, ALCL is strongly and diffusely positive for CD30, which decorates the neoplastic cells in the membrane and in the Golgi zone (paranuclear dot) (Fig. 15.86). The tumor cells are also commonly positive for CD43 and MUM1. For not well-understood reasons, this T-cell lymphoma shows a paradoxical expression of CD4 and cytotoxic markers (TIA-1, granzyme B, and/or perforin). CD45, CD2, CD3, CD5, CD7, CD8, EMA, and clusterin are variably present (Fig. 15.87). Rare cases of ALCL may show focal expression of keratins [136, 137]. B-cell markers, CD15, and EBV ISH are negative. A subset of ALCLs is positive for ALK, and this is the basis for separating this tumor into

ALK+ or ALK-negative [133]. Normally, the ALK protein is silenced in adult tissues, which makes this immunostain highly sensitive and specific for ALK detection. The subcellular localization of ALK in tumor cells, namely nucleus, nucleus and cytoplasm, diffusely cytoplasmic, and coarse cytoplasmic granules, is an excellent surrogate of the underlying translocation partner with the *ALK* gene (Fig. 15.88a, b) (see Molecular findings).

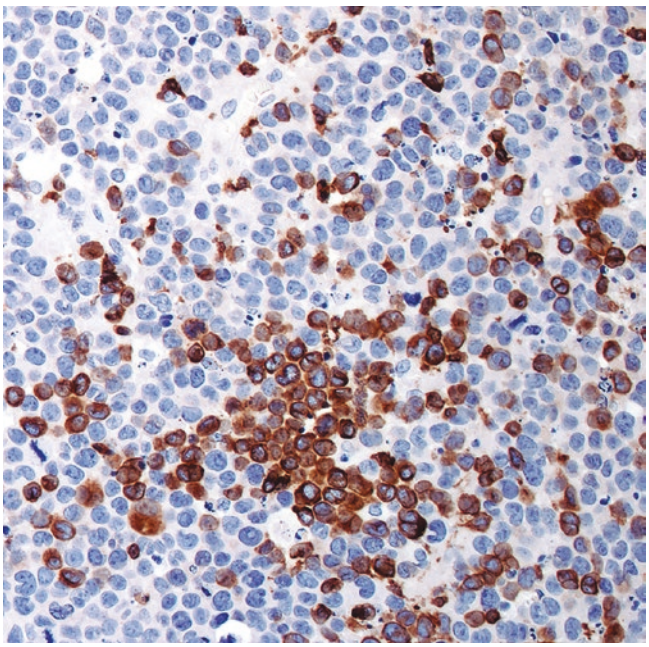

Fig. 15.87 Anaplastic large cell lymphoma. Only a subset of tumor cells is positive for CD3 by immunohistochemistry

Differential Diagnosis

Pulmonary ALCL should be distinguished from hematopoietic and non-hematopoietic tumors involving the lung. Hematopoietic tumors that should be distinguished from ALCL include PTCL, NOS, with large cells, anaplastic DLBCL, and PM-LBCL or mediastinal syncytial variant of nodular sclerosis CHL extending to the lung. A proper panel of immunohistochemical stains is also sufficient to distinguish between these entities. Anaplastic DLBCL and PM-LBCL are positive for B-cell markers which excludes ALCL, and the syncytial variant of nodular sclerosis CHL is positive for PAX5 (weak), CD30, and variable for CD15 and EBER, while negative for T-cell antigens and ALK. PTCL, NOS, with large cells may show an identical morphology to ALCL, and only the expression of CD30 and/or ALK is useful to distinguish between them. A large T-cell lymphoma with focal CD30 should not be classified as ALCL, whereas a case of PTCL, NOS, diffusely positive for CD30 and negative for ALK is difficult to distinguish from ALK-negative ALCL. In this context, prior clinical history of systemic lymphoma, if any, is useful, in addition to performing FISH for *DUSP22* and *TP63* (see molecular findings).

Non-hematopoietic tumors include non-small carcinoma, pleomorphic or undifferentiated carcinoma of the lung, metastatic carcinoma, metastatic melanoma, a germ cell tumor, or a tumor with rhabdoid morphology. Specific morphologic

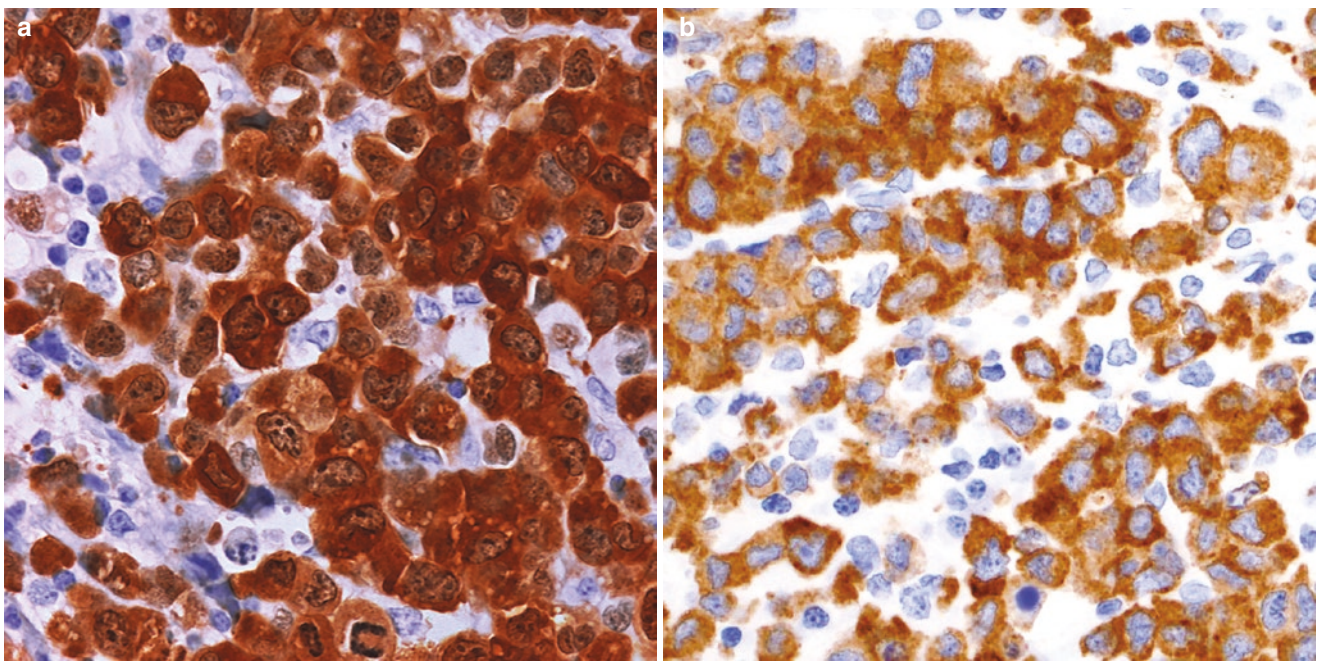

Fig. 15.88 ALK+ anaplastic large cell lymphoma. (**a**) Nuclear and cytoplasmic positivity is a surrogate marker for the presence of t(2;5) (*ALK::NPM*). (**b**) Restricted cytoplasmic labeling is seen in *ALK* rearrangements with multiple other gene partners different from *NPM*

Table 15.15 Differential diagnosis of pulmonary anaplastic large cell lymphoma

Hematopoietic
Large cell peripheral T-cell lymphoma, not otherwise specified
Anaplastic diffuse large B-cell lymphoma
Primary mediastinal large B-cell lymphoma with extension to the lung
Syncytial variant of mediastinal classic Hodgkin lymphoma with extension to the lung
Non-hematopoietic
Non-small cell lung carcinoma
Pleomorphic or undifferentiated carcinoma of the lung
Metastatic carcinoma or amelanotic melanoma
Metastatic germ cell tumor
Tumors with rhabdoid morphology, including INI1/SMARCB1-deficient tumors

variants of ALCL should also be distinguished from non-hematopoietic conditions, namely sarcomatoid carcinoma or sarcoma from the sarcomatoid variant of ALCL, and small cell carcinoma from the small cell variant of ALCL [135]. A proper panel of immunohistochemical stains is sufficient to distinguish between all these entities. ALCL is negative for keratins with rare exceptions, melanoma markers, and germ cell markers (OCT3/4, SALL4). Embryonal carcinoma is strongly positive for CD30, keratin, and germ cell transcription factors and does not express T-cell antigens, ALK, or CD43, which rules out ALCL. Similarly, rhabdoid neoplasms demonstrate loss of INI1 or BRG1 and are negative for CD43 and T-cell markers that are positive in ALCL.

Due to the rarity of ALCL in the lung, this diagnosis may not be suspected, and CD30 and ALK may not be included in the immunohistochemical panel used for diagnosis. Caution should be taken when interpreting EMA or focal keratins in an epithelioid neoplasm as confirmatory of carcinoma since ALCL can be positive for EMA, at least focally for keratins, and weak to negative for CD3 and CD45 [136, 137]. ALK immunohistochemistry is currently used for the detection of ALK-mutated lung cancer. If keratins are not diffusely and strongly positive in an epithelioid and pleomorphic lung neoplasm that is also ALK+ we strongly recommend performing a CD30 immunostain to rule out ALCL [138]. The differential diagnosis of pulmonary ALCL is summarized in Table 15.15.

Molecular Findings

The pathogenesis of ALK+ ALCL is related to the downstream effects of ALK activation. The *ALK* gene is located in 2p23. Multiple *ALK* rearrangements with multiple partners have been described in ALK+ ALCL, and they correlate with the subcellular localization of the ALK protein [133]. The most common translocation partner is *NPM* located in 5q35 with the t(2;5)(p23;q35) resulting in the fusion protein ALK-NPM that can be detected in both nucleus and cytoplasm of the neoplastic cells [123–125, 139] (Fig. 15.88). Other gene partners include *TPM3*, which codifies for tropomyosin 3 located on chromosome 1, resulting in t(1;2) and ALK protein expression restricted to the cytoplasm (Fig. 15.88), and *CLTC*, which codifies for the clathrin heavy chain located on chromosome 17, resulting in t(2;17) and cytoplasmic ALK protein expression with a coarse granular pattern. Multiple other less common gene partners are also known but are outside the scope of this chapter. All these translocations result in ALK activation with downstream activation of multiple signaling pathways, including JAK/STAT and PIK-AKT. As expected, ALK-negative ALCL does not harbor *ALK* translocations. A recent study has shown that ALK-negative ALCL harbors *DUSP22* and *TP63* rearrangements that are found in 30% and 8% of cases, respectively [140]. Cases with *DUSP22* alterations have an intermediate prognosis as compared to ALK+ ALCL, while those with *TP63* alterations have a bad prognosis [140]. Cases that are negative for *ALK, DUSP22,* and *TP63* rearrangements are known as "triple-negative ALCL." T-cell receptor (*TCR)* clonality is positive in 90% of ALCLs; however, clonality can be negative in cases with a "null" phenotype.

Pulmonary Peripheral T-Cell Lymphoma, Not Otherwise Specified (PTCL, NOS)

Introduction

Primary PTCL of the lung is extremely rare, whereas systemic disease is usually diagnosed at an advanced stage. Lung involvement was seen in 8% of 340 PTCL, NOS cases [141]. PTCL, NOS is a diagnosis of exclusion and only made after other specific categories of TCL recognized by the WHO have been ruled out, namely ALCL, angioimmunoblastic T-cell lymphoma, NK/T-cell lymphoma, mycoses fungoides, etc. These specific categories involved the lung even more rarely than PTCL, NOS and are only briefly mentioned in this section for the purpose of differential diagnosis.

Clinical Features

In general, PTCL, NOS is a disease of adults (median age 60 years) [141], and lung involvement occurs in this same age group. Most patients have a known or relatively recent history of PTCL, NOS diagnosed at other sites and the development of respiratory symptoms triggers a pulmonary evaluation. Respiratory symptoms are common but are nonspecific, and in some patients, symptoms can mimic a pneumonic process that does not resolve with antibiotics. The outcome of PTCL, NOS is overall poor despite the use of chemotherapy (CHOP).

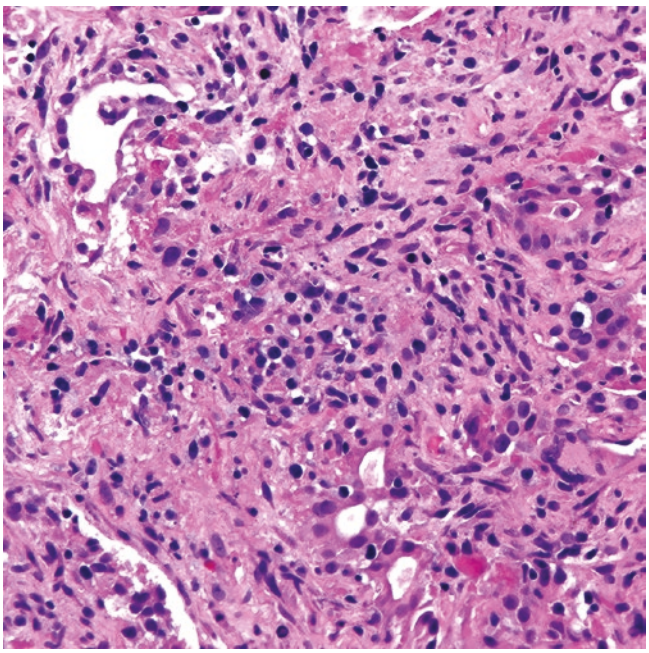

Fig. 15.89 Pulmonary T-cell lymphoma. The lung parenchyma is effaced by small and intermediate atypical lymphoid cells with irregular hyperchromatic nucleus admixed with macrophages and piecemeal necrosis. The patient had a history of systemic T-cell lymphoma

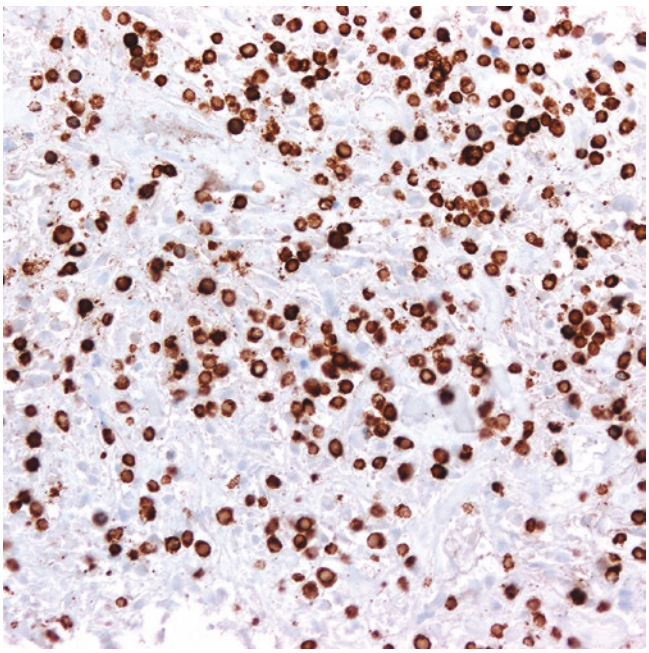

Fig. 15.90 Pulmonary T-cell lymphoma. The lymphoma cells are positive for CD3 by immunohistochemistry

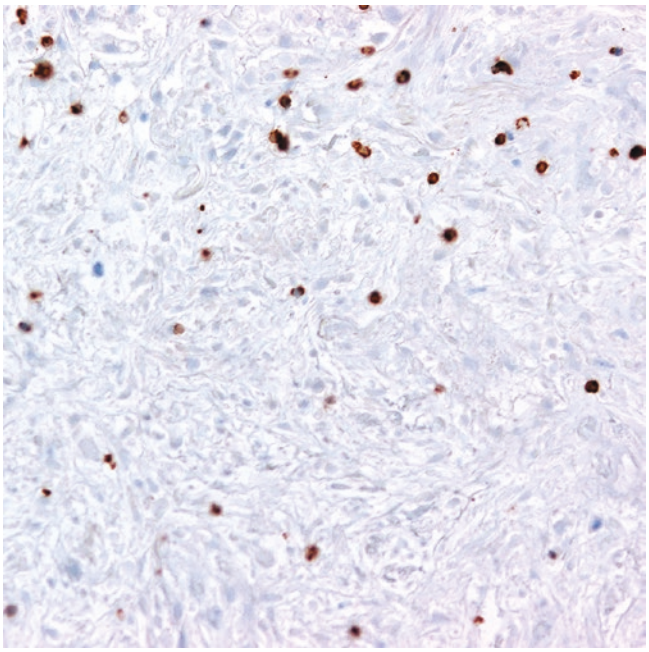

Fig. 15.91 Pulmonary T-cell lymphoma. The CD3+ T-cells are negative for CD7

Pathology

In the lung, PTCL, NOS may be observed as a nodular pattern with replacement of the architecture, or as a diffuse pattern with infiltration of interlobular septa, alveolar walls, and pleura [127]. A perivascular arrangement with or without vasculitis may or may not be seen. Necrosis is also variably seen (Fig. 15.89). The morphology of PTCL, NOS is extremely variable, ranging from monotonous small lymphocytes, polymorphic infiltrates with abundant macrophages, eosinophils, and plasma cells, to cases mimicking CHL or ALCL. The lymphoma cells usually have a convoluted or irregular nucleus with thick nuclear membranes, condensed chromatin, and inconspicuous nucleolus. The cytoplasm may be scant to moderate, clear, or eosinophilic (Fig. 15.89). Cases resembling CHL feature a variable number of Reed–Sternberg-like cells or sheets of pleomorphic or anaplastic cells indistinguishable from ALCL.

Immunohistochemistry and Other Ancillary Studies

PTCL, NOS is positive for T-cell markers (CD2, CD3, CD5, CD7, CD43, and bcl-2) but usually >1 of these markers is aberrantly decreased or completely absent (Figs. 15.90 and 15.91). CD45 may also be decreased and lost in a subset of cells. The majority of cases are CD4+ and CD8-negative, followed by cases that are CD8+ and CD4-negative, and a few cases that are either double negative or double positive for CD4 and CD8. Cases of PTCL, NOS that demonstrate a T follicular helper phenotype (CD4+, CD10+, bcl-6+, CXCL13+, CD57+, and PD-1+) should be classified as such and not included in this category. CD8+ PTCL, NOS, may express >1 of the cytotoxic markers TIA-1, granzyme B, or perforin. CD30 is variably positive, but not strong and diffuse, and may be seen in up to 50% of cases. Antibodies for

the TCR receptor beta (beta F1) and TCR gamma are commercially available and may be useful for diagnosis. All lymphoid cells positive for TCR beta F1 and negative TCR gamma or vice versa support a clonal T-cell process. However, not all pathology laboratories have these antibodies, and these markers may be difficult to interpret in cases with abundant reactive T-cells in the background. PTCL, NOS, is negative for B-cell markers and ALK. PTCL, NOS, typically has very few to rare B-cells in the background. Although most cases are negative for CD56 and EBER ISH, occasional cases may show focal to variable CD56 expression and rare cases may show positivity for EBER.

Flow cytometry immunophenotyping is a sensitive method to detect subtle abnormalities of T-cell markers and to detect small aberrant T-cell populations that may not be readily recognized by morphology [142]. Flow also permits better evaluation of the expression of TCR A/B and TCR G/D, with clonal populations showing positivity for one or the other but not for both receptors.

Differential Diagnosis

PTCL, NOS should be distinguished from chronic reactive inflammatory processes, B-cell lymphomas, CHL, LYG, and other TCLs. PTCL, NOS is a wastebasket category (diagnosis of exclusion) for any TCL that does not fit in a specific category recognized by the WHO, namely ALCL, angioimmunoblastic T-cell lymphoma, NK/T-cell lymphoma, mycoses fungoides, etc.

PTCL, NOS with predominant small cell morphology needs to be distinguished from a chronic lymphoid or lymphohistiocytic inflammatory infiltrate. These processes show a mixture of CD4+ and CD8+ T-cells and no loss or decreased expression of T-cell markers, and they have aggregates of B-cells.

B-cell lymphomas are readily recognized by the expression of B-cell markers (CD20, PAX5, and CD79a) and negative T-cell markers that only highlight background small T-cells. Reactive background T-cells in B-cell lymphomas are also composed of a mixture of CD4+ and CD8+ cells, and they do not show loss of T-cell-related antigens.

PTCL, NOS with polymorphic morphology and scattered Reed–Sternberg-like cells should be distinguished from CHL or LYG. In these cases, the Reed–Sternberg-like cells have a T-cell phenotype similar to that of the atypical smaller lymphocytes; they may be positive for CD30 but are negative for B-cell markers including PAX5. This is not the phenotype seen in CHL (CD15+/−, CD30+, PAX5 dim) and/or LYG (an EBV+ B-cell lymphoproliferative disorder).

PTCL, NOS with large cells with negative or focal CD30 should not be classified as ALCL, whereas a case of PTCL, NOS diffusely positive for CD30 and negative for ALK is difficult to distinguish from ALK-negative ALCL. In this context, prior clinical history of systemic ALCL is useful, as well as the results of FISH for *DUSP22* and *TP63* (see the corresponding section). Cases of PTCL, NOS that demonstrate a T follicular helper phenotype (CD4+, CD10+, bcl-6+, CXCL13+, CD57+, and PD-1+) should be classified as such and not included in this category. A history of a prior nodal or systemic T-cell lymphoma with T follicular helper phenotype may or may not be available. CD8+ PTCL, NOS, may express >1 of the cytotoxic markers TIA-1, granzyme B, or perforin. These cases may also show vasculitis and extensive necrosis. Nevertheless, these cases are negative for CD56 and EBER in contrast to the phenotype seen in NK/T-cell lymphoma (CD56+ and EBER+ in almost all cases) (Fig. 15.92a–c). Mycoses fungoides and Sezary syndrome with lung involvement (so-called visceral mycoses fungoides) may be seen in the late stages of disease, and this confers poor prognosis [143, 144]. In these conditions, a lung infiltrate is suggestive of pneumonia, and a lung biopsy demonstrates infiltration by lymphoma cells with cerebriform nuclear morphology or large cells, if large cell transformation has occurred (Fig. 15.93a–d). A prior history of mycoses fungoides or Sezary syndrome is crucial to further classify the presence of an interstitial or nodular pulmonary lymphoid infiltrate as lymphomatous involvement [144]. Mycoses fungoides and Sezary syndrome are positive for CD2, CD3, CD4, and CD5 with frequent loss of CD7 and are negative for CD8 and EBER. CD30 may be positive in cases of large cell transformation.

Molecular Findings

Molecular studies may be helpful in some cases to identify a clonal *TCR* gene rearrangement. However, interpretation of clonality should be done with caution as some reactive inflammatory processes may be oligoclonal or suggestive of clonality, whereas cases of PTCL, NOS can be negative for *TCR* gene rearrangements. Similar to the cell of origin classification in DLBCL, NOS, recent gene expression profiling data obtained from PTCL, NOS cases have identified two subgroups of this lymphoma characterized by the expression of the transcription factors *GATA3* or *TBX21*, main regulators of the Th2 and Th1 differentiation pathways, respectively [145, 146]. Using an immunohistochemical classifier with these two markers, PTCL, NOS cases can now be categorized as GATA3+ or TBX21+, with the former group showing a more common cytotoxic phenotype, greater genomic complexity, and worse prognosis [145–147]. However, it is uncertain if any of these subgroups may be enriched by cases of pulmonary PTCL, NOS.

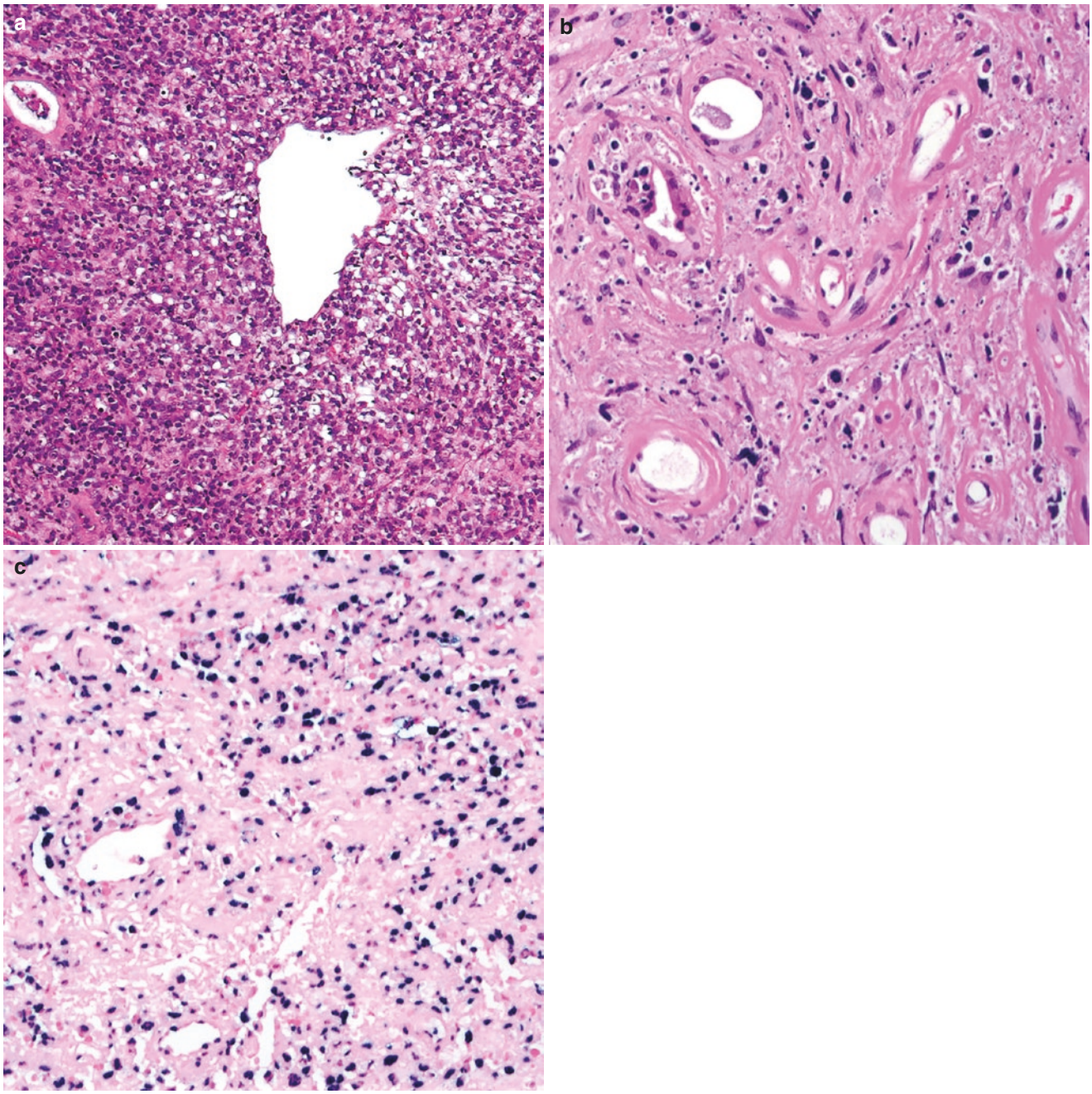

Fig. 15.92 Extranodal NK/T-cell lymphoma. (**a**) Vasculitis and diffuse sheets of lymphoma cells of small and intermediate size. (**b**) Some areas show extensive necrosis and residual glands and blood vessels. (**c**) EBER in situ hybridization is positive in the lymphoma cells

Pulmonary Classic Hodgkin Lymphoma (CHL)

Introduction

Primary pulmonary CHL defined as the presence of confined lung disease at initial presentation with/without minimal hilar lymph node involvement and exclusion of disease at distant sites by clinical, imaging, and pathologic findings is extremely rare, mostly consisting of sporadic case reports [148–155]. However, according to some series, lung involvement is relatively common in extranodal CHL [152]. On the other hand, thoracic involvement is more commonly seen as anterior or middle mediastinal disease with extension into the lung or as extranodal disease in advanced stages. For all these reasons, the exclusion of mediastinal or extrathoracic disease is mandatory before making a diagnosis of primary pulmonary CHL. Please see the chapter on mediastinal lymphoproliferative lesions for additional information on CHL.

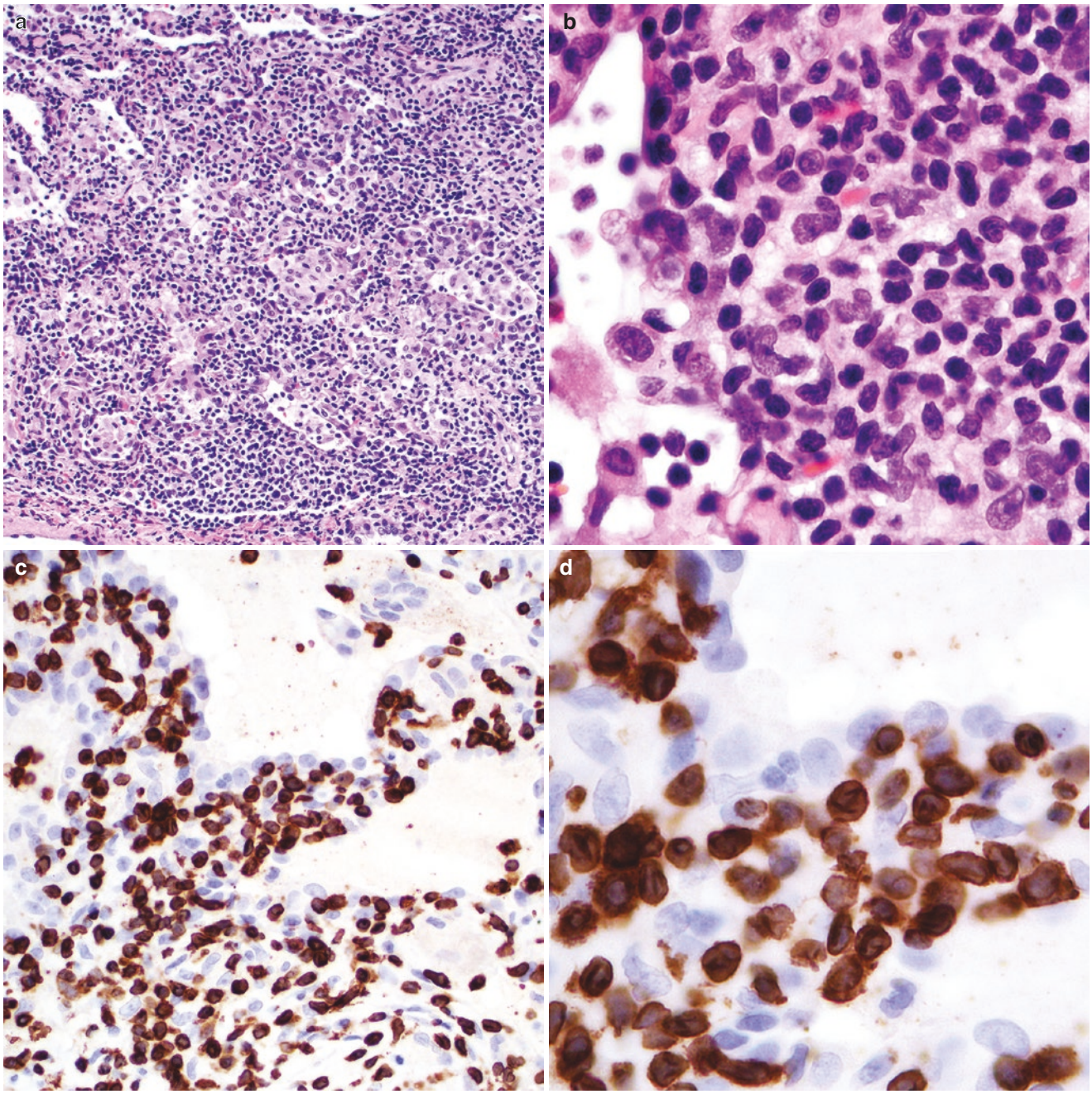

Fig. 15.93 Pulmonary involvement by mycoses fungoides (so-called visceral mycosis fungoides). The patient had a long-standing history of mycosis fungoides in advanced stage and presented with clinical and radiologic features suggestive of pneumonia. (**a**) The alveolar interstitium is distended and filled with numerous atypical lymphoid cells. The alveolar spaces contain abundant macrophages. (**b**) Atypical lymphoid cells with cerebriform nuclei filling the interstitium. (**c** and **d**) Immunohistochemistry for CD3 highlights the lymphoma cells and accentuates the cerebriform nuclear morphology

Clinical Features

Primary pulmonary CHL is more common in women (median age 40 years), which is 1–2 decades later than the first peak seen in mediastinal nodular sclerosis CHL. Lung involvement by CHL can occur in three different clinical contexts: (1) direct extension from the anterior or middle mediastinum, (2) recurrence in the lung in an area just outside the field of prior radiation therapy of mediastinal CHL, or (3) metastatic disease. Clinical symptoms include cough, dyspnea, hemoptysis, and B symptoms. Prognosis is variable, with some studies showing favorable survival [152]. Localized disease occurring in young individuals responds

better to chemotherapy, whereas extensive disease may be accompanied by multiple co-morbidities with a worse outcome.

Diagnostic Imaging

Lung involvement occurs in approximately 10% of Hodgkin's lymphoma (CHL) patients at diagnosis [156]. Parenchymal involvement in CHL is almost always associated with mediastinal and/or hilar lymphadenopathy, and usually there is a contiguous spread of disease from lymph nodes [43] (Figs. 15.94 and 15.95). Isolated parenchymal CHL is extremely rare [43]. In their CT review of 15 patients with CHL of the lung, Lewis et al. found that the most common CT abnormality was a mass or mass-like consolidation, seen in 80%; other manifestations were nodules less than 1 cm (67%), alveolar or interstitial opacities (40%), and peribronchial or perivascular thickening (40%) [157]. HL typically shows high FDG uptake on PET/CT [74] (Fig. 15.96).

Fig. 15.95 Hodgkin's lymphoma. CT shows right-sided peribronchial thickening (dashed oval), contiguous with intrathoracic adenopathy (asterisks)

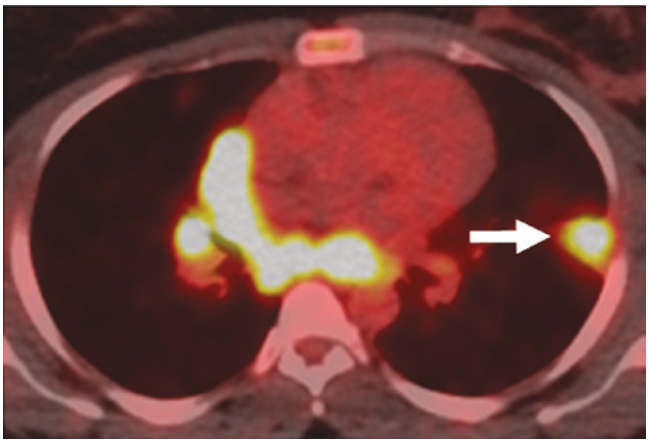

Fig. 15.96 Hodgkin's lymphoma. PET/CT shows an FDG-avid mass in the left lung (arrow) in addition to FDG-avid intrathoracic adenopathy

Pathology

Nowadays sampling of a lung lesion is usually accomplished via an imaging-guided needle biopsy or a transbronchial biopsy, and the diagnosis is established either in a cytology specimen, a core-needle biopsy, or a transbronchial biopsy. If the diagnosis of pulmonary lymphoproliferative disorder is rendered in any of these specimens, then a wedge resection or a lobectomy is not necessary. However, a resection may be still be done when a biopsy is inconclusive for diagnosis.

The most common subtype of CHL involving the lung is nodular sclerosis (70–80% of cases), followed by mixed cellularity (20–30%). However, extranodal CHL tends not to be subclassified. In the lung, CHL spreads in a bronchovascular distribution, in a lymphangitic pattern, or may form a large cavitated mass or multiple solid masses (Fig. 15.97). CHL

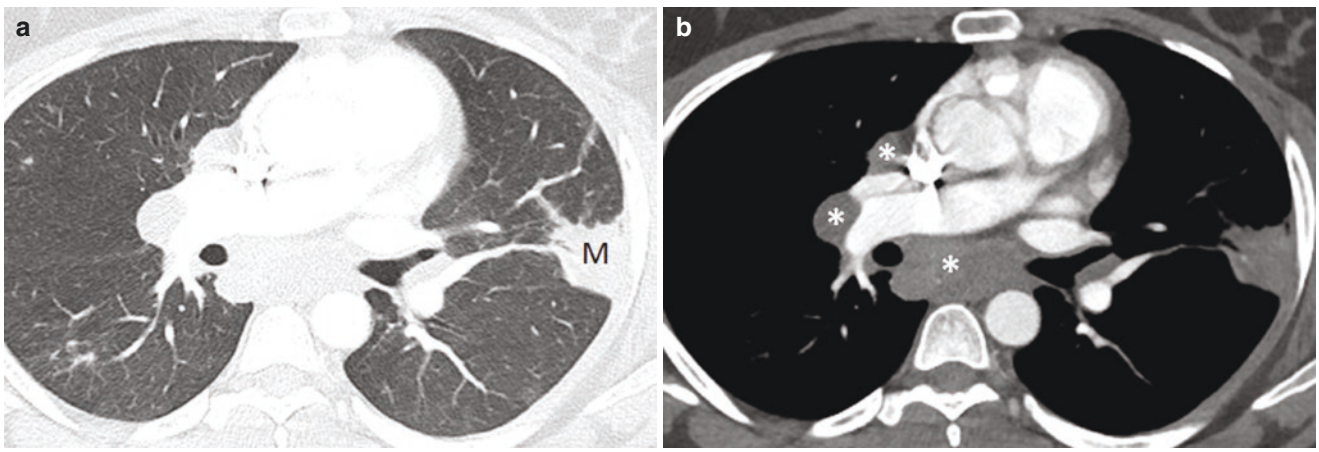

Fig. 15.94 Hodgkin's lymphoma. (**a**) CT (lung windows) shows a mass (M) in the left lung, and (**b**) CT (soft tissue windows) shows intrathoracic adenopathy (asterisks)

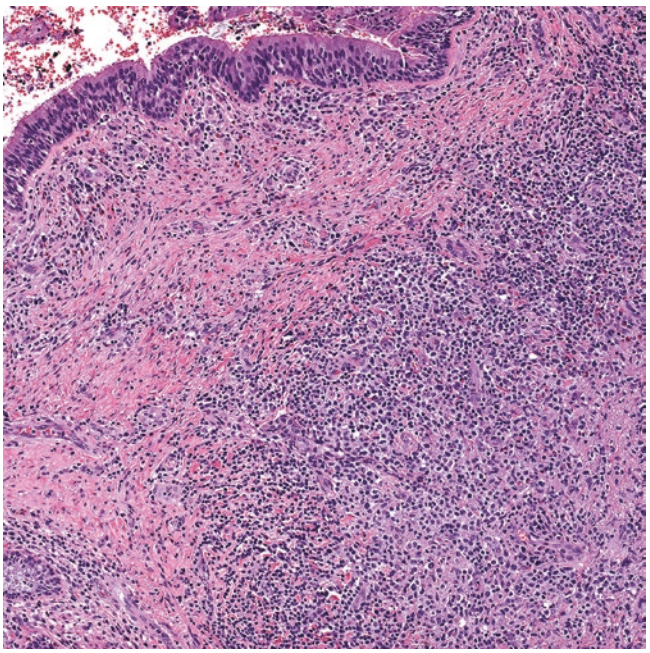

Fig. 15.97 Pulmonary classic Hodgkin lymphoma. The bronchial wall is involved by a polymorphic infiltrate with scattered Reed–Sternberg cells

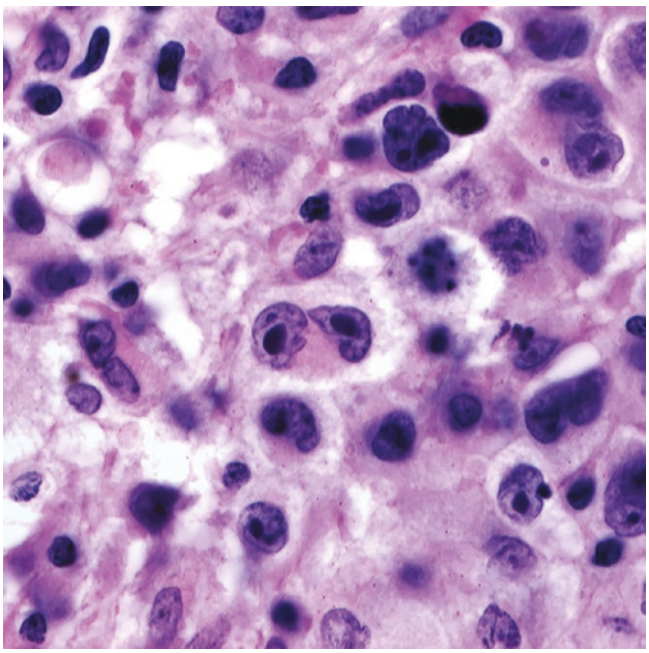

Fig. 15.99 Classic Reed–Sternberg cells with "owl's eye" appearance (center)

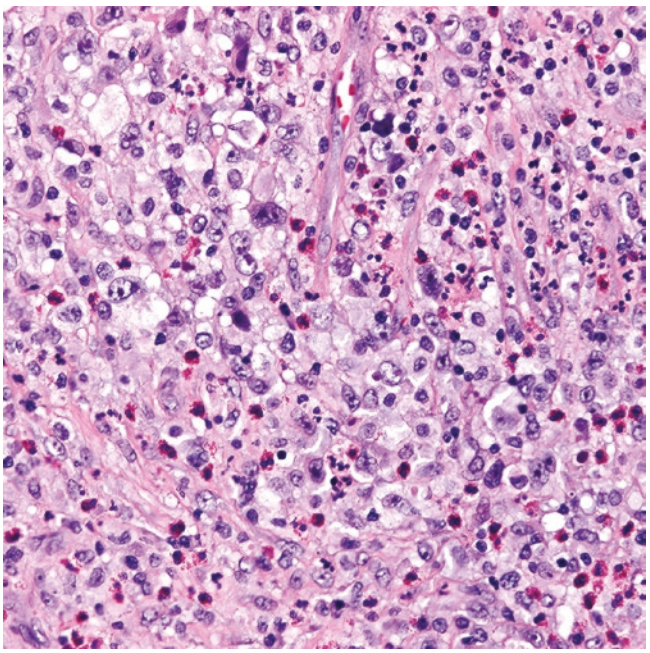

Fig. 15.98 Polymorphic inflammatory infiltrate of neutrophils, eosinophils, macrophages, and small lymphocytes and scattered Reed–Sternberg cells

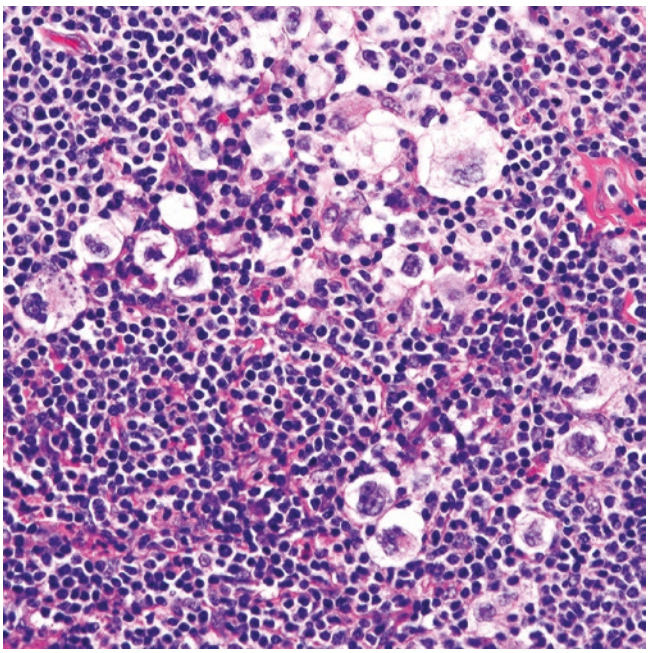

Fig. 15.100 Reed–Sternberg cells with retraction artifact ("lacunar" cells)

extending from the mediastinum shows visceral pleural involvement and penetration into the lung parenchyma. CHL consists of a fibrous background and a mixture of small lymphocytes, eosinophils, neutrophils, plasma cells, and macrophages with a variable number of Reed–Sternberg cells (Fig. 15.98). "Classic" Reed–Sternberg cells are usually binucleated and have large eosinophilic or basophilic nucleoli surrounded by a clear halo imparting these cells an "owl's eye" appearance (Fig. 15.99). The cytoplasm is abundant and eosinophilic to amphophilic. Variants of Reed–Sternberg cells include Hodgkin cells (monolobated), "lacunar" cells, "mummified" cells, and multinucleated cells with nuclei in a wreath-like configuration (Figs. 15.100 and 15.101). Despite "lacunar" cells having been reported more frequently in nodular sclerosis CHL and "classic" Reed–Sternberg cells in

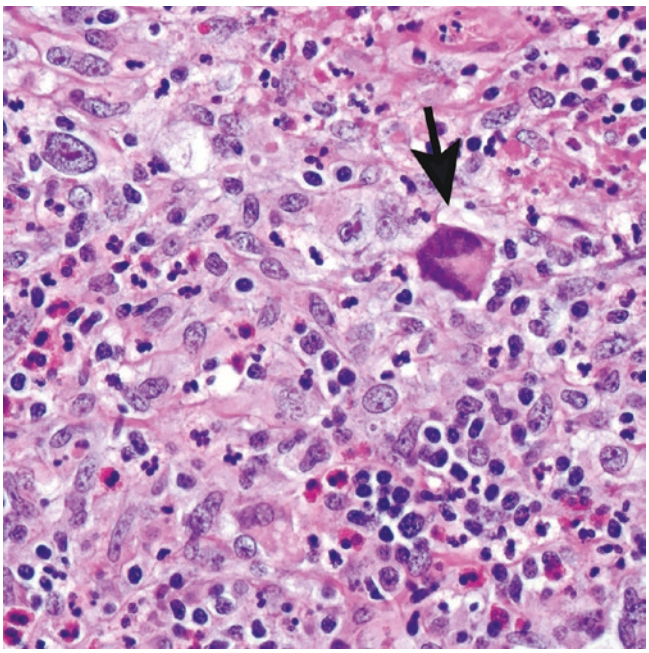

Fig. 15.101 Mummified" cell (arrow) with smudgy chromatin and glassy eosinophilic cytoplasm

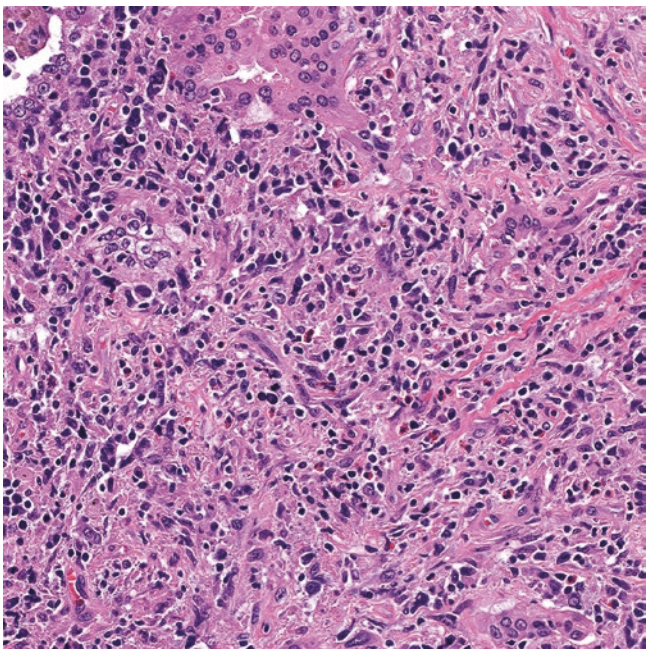

Fig. 15.103 Recurrent pulmonary classic Hodgkin lymphoma. The Reed–Sternberg cells have spindle morphology and resemble a sarcomatoid neoplasm

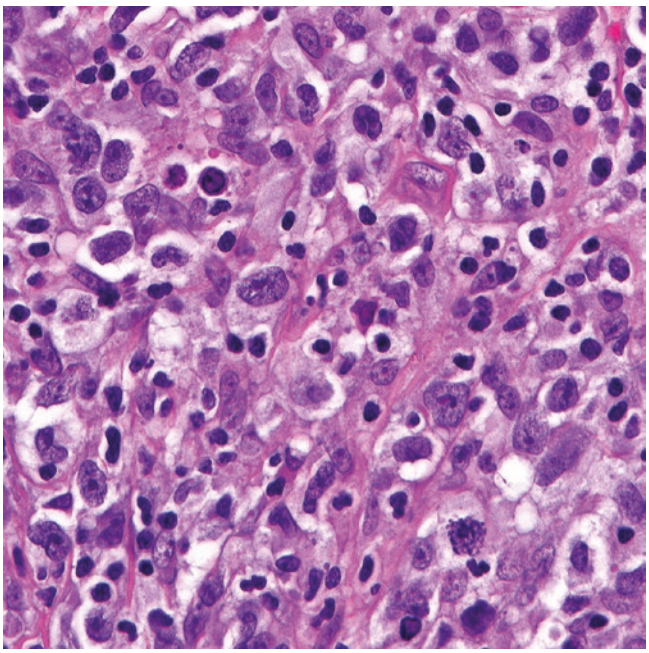

Fig. 15.102 Syncytial variant of nodular sclerosis classic Hodgkin lymphoma. Sheets of Reed–Sternberg cells with only a few scattered small lymphocytes

mixed cellularity CHL, any variant can be seen in any subtype of CHL. When Reed–Sternberg cells form solid sheets that are associated with necrosis or an abscess, it constitutes the syncytial variant of CHL (Fig. 15.102). Necrotizing granulomas and microabscesses may or may not be identified, sometimes prominent enough to obscure the recognition of Reed–Sternberg cells, particularly in cavitated lesions. Cases of recurrent CHL or post-therapy may be composed of sheets of Reed–Sternberg cells with marked pleomorphism and/or spindle morphology (Fig. 15.103).

Immunohistochemistry and Other Ancillary Studies

Reed–Sternberg cells, which are the neoplastic component in CHL, are always strongly positive for CD30, variably positive for CD15 (60–70%), positive for MUM1/IRF4 (>90%), weakly positive for PAX5 when compared to background B-cells, and negative for CD45, CD20 (only seen in 10–20% of cases), bcl-6, BOB.1, OCT2, ALK, CD79a, and T-cell markers [158, 159], (Figs. 15.104, 15.105, 15.106 and 15.107). Only 1–2% of CHL cases may show expression of T-cell markers. CD30 and CD15 decorate Reed–Sternberg cells in a membranous and Golgi (paranuclear dot) pattern, but some cases may show diffuse cytoplasmic labeling (Fig. 15.104). CD15 may be seen only as a cytoplasmic granular pattern (Fig. 15.105). Reed–Sternberg cells are positive for PD-L1 and PD-L2, which justifies treatment with checkpoint inhibitor molecules (see also molecular findings) [160–163]. Nodular sclerosis CHL is only occasionally associated with EBV infection, whereas in mixed cellularity CHL EBV infection is frequent. Therefore, EBER ISH and/or LMP1 immunohistochemistry are more frequently detected in cases of mixed cellularity [164–166]. Expression of EBER and LMP1 in CHL indicates a type II latency infection. The non-neoplastic component in CHL consists mostly of T-cells with an increased CD4 to CD8 ratio. CD3 usually highlights T-cells rimming Reed–Sternberg cells (Fig. 15.108). Macrophages are positive for CD68 and/or CD163. Flow cytometry is not a helpful tool to diagnose CHL.

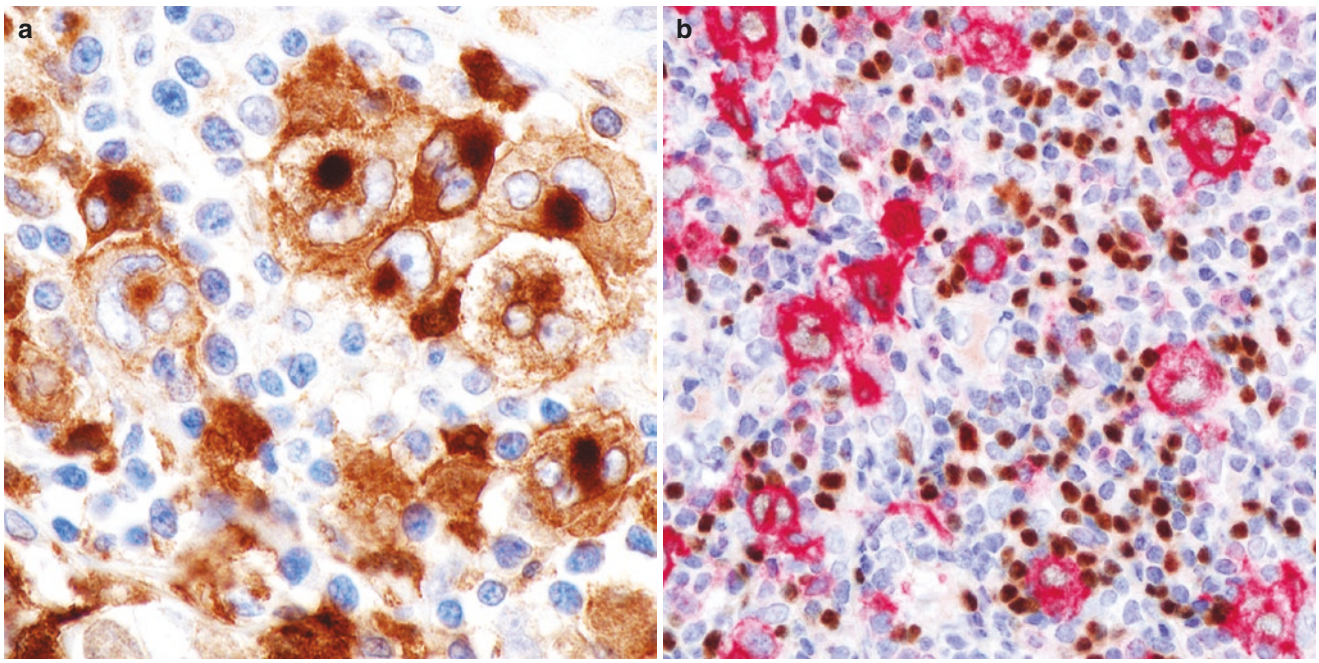

Fig. 15.104 Reed–Sternberg cells are strongly positive for (**a**) CD30 and have a weak expression of (**b**) PAX5 when compared to background B-cells (double labeling: CD30-red, alkaline phosphatase; PAX5-brown, peroxidase)

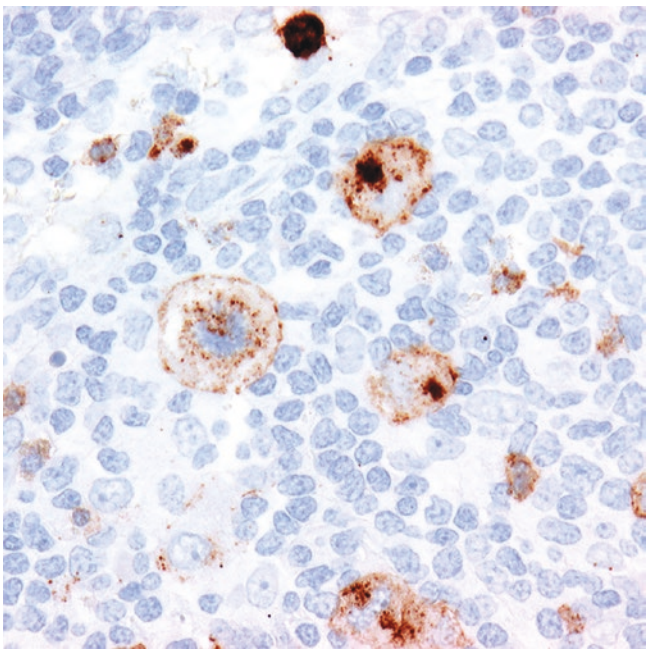

Fig. 15.105 Membranous and granular pattern of CD15 in Reed–Sternberg cells along with paranuclear dot patterns

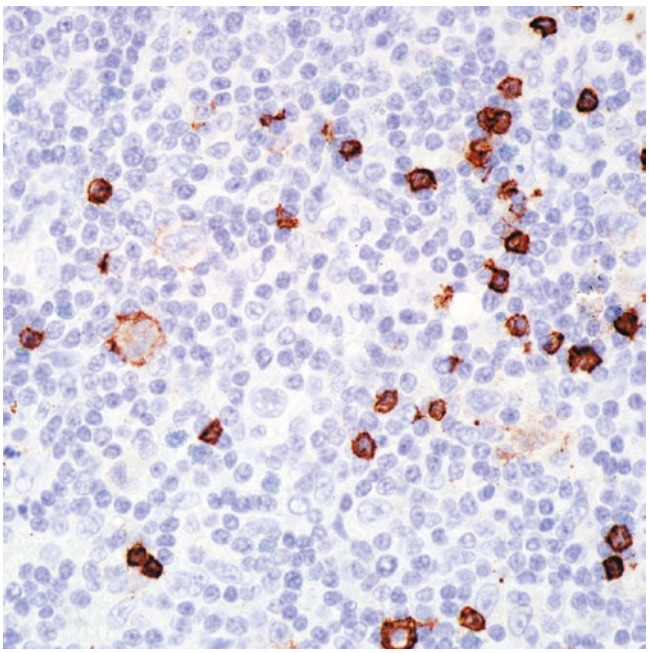

Fig. 15.106 The CD20 immunostain is negative to weakly positive in Reed–Sternberg cells (center and left)

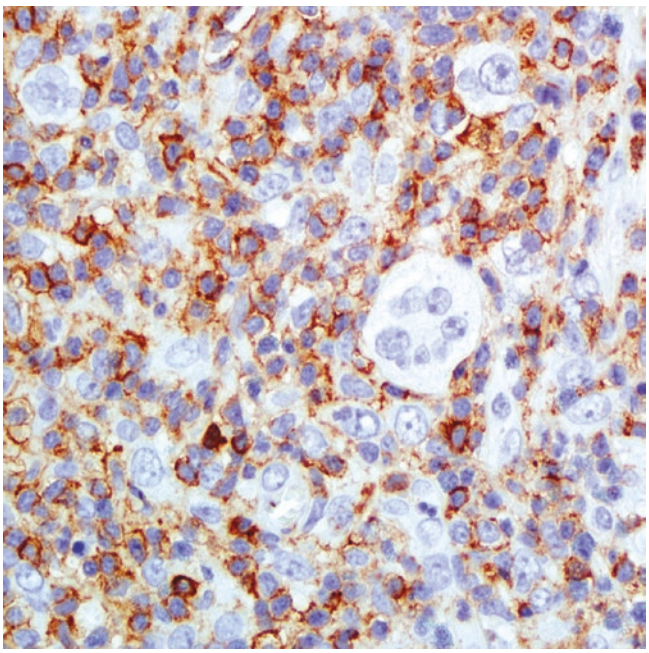

Fig. 15.107 The CD45 immunostain is negative in Reed–Sternberg cells

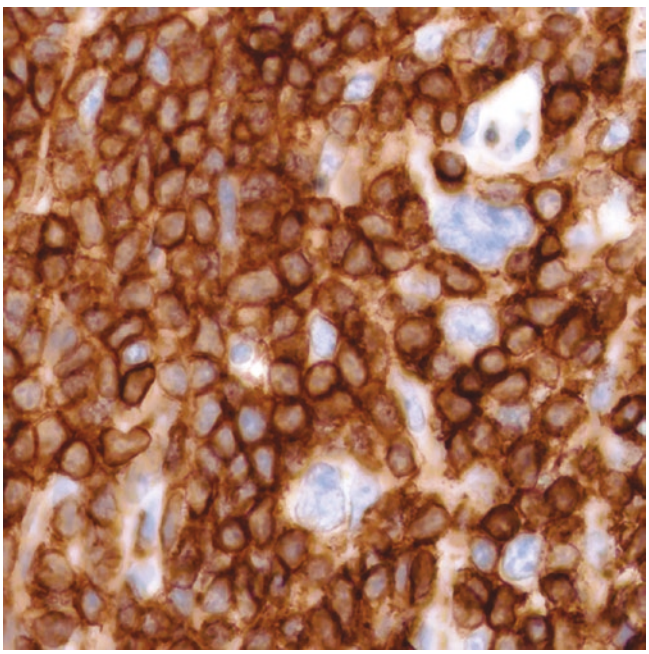

Fig. 15.108 Reed–Sternberg cells are negative for CD3. There are numerous background T-cells including some around Reed–Sternberg cells

Differential Diagnosis

Pulmonary CHL should be distinguished from a reactive granulomatous process, pulmonary Langerhans cell histiocytosis, or LYG (grades 1 and 2), whereas cases of the syncytial variant may resemble grade 3 LYG, pulmonary DLBCL, PM-LBCL with lung involvement, pulmonary ALCL, poorly differentiated primary lung carcinoma, or a lung metastasis. Recurrent CHL with spindle morphology mimics sarcomatoid carcinoma, pleomorphic carcinoma, or sarcoma. A proper panel of immunohistochemical markers is required to differentiate between all these lesions. Reed–Sternberg cells are negative for epithelial or melanoma markers, which rules out carcinoma, sarcomatoid carcinoma, and melanoma.

Table 15.16 Differential diagnosis of pulmonary classic Hodgkin lymphoma

Granulomatous inflammatory process
Neoplastic
Hematopoietic
• Lymphomatoid granulomatosis, grades 1 and 2
• Pulmonary Langerhans cell histiocytosis
If syncytial variant of classic Hodgkin lymphoma:
– Primary mediastinal large B-cell lymphoma with extension to the lung
– Lymphomatoid granulomatosis, grade 3
– Anaplastic large cell lymphoma
Non-hematopoietic
• Poorly differentiated lung carcinoma
• Metastatic carcinoma or amelanotic melanoma
If recurrent disease with spindle cell morphology of Reed–Sternberg cells:
– Sarcomatoid carcinoma
– Sarcoma

LYG can be readily distinguished from pulmonary CHL by the clinical context of a young patient with multiple lung nodules and underlying immunosuppression, as well as by the presence of vasculitis and expression of CD45, CD20, CD79a, PAX5 (strong), and EBER ISH in large cells, even in those cells with Reed–Sternberg-like morphology. Although Reed–Sternberg cells in mixed cellularity CHL are frequently positive for EBER, their immunophenotype differs from that seen in LYG. Likewise, pulmonary DLBCL and PM-LBCL with lung involvement are readily distinguished from the syncytial variant of CHL by the strong expression of B-cell markers in the tumor cells. Pulmonary ALCL is a T-cell lymphoma with strong expression of CD30 and of other T-cell markers, and ALK may be positive or negative. ALCL is negative for PAX5, CD15, CD20, and EBER ISH.

Pulmonary Langerhans cell histiocytosis may resemble a nodule of CHL at low magnification. However, in the former, there are Langerhans cells with reniform to cleaved nucleus, a variable number of eosinophils, and multinucleated cells but no Reed–Sternberg cells. Langerhans cells are positive for CD1a, S100, and langerin/CD207 and negative for CD15, CD30, or PAX5. The differential diagnosis of pulmonary CHL is listed in Table 15.16.

Molecular Findings

The features described here refer to nodal disease, and it is likely that the pathogenesis may be similar to extranodal cases. Reed–Sternberg cells are germinal center/post germinal center B-cells that have undergone somatic hypermuta-

tion with crippled B-cell genes but have escaped the negative selection process [167–169]. These cells have a defective B-cell differentiation program and harbor crippling mutations on immunoglobulin expression genes, which explains the decreased expression of CD20, PAX5, and the transcription factors OCT2 and BOB.1 [167, 170–172]. Reed–Sternberg cells are resistant to apoptosis by multiple different mechanisms, including canonical and noncanonical activation of the NK-κB pathway and activation of the JAK/STAT pathway [173–175]. Activation of NK-κB is used by Reed–Sternberg cells to attract the supportive microenvironment of inflammatory cells and stromal cells characteristic of this lymphoma. EBV infection also induces NK-κB activation with potential oncogenic results [176]. Some genetic abnormalities in CHL overlap with those of PM-LBCL, including mutations of *SOCS1*, a negative regulator in the JAK/STAT pathway [177–180], as well as frequent alterations at 9p24 with overexpression of PD-L1/PD-L2 and JAK2 that result in a suppressive immune response and increased cellular proliferation, respectively [163, 181]. Expression of PD-L1/PD-L2 makes antibody therapies against PD-1 an excellent treatment for CHL. Clinical trials using these blocking agents have shown promising results in refractory/relapsed disease [182, 183]. Last, it appears that the Reed–Sternberg cell morphology may be related to mechanisms of incomplete cytokinesis and cell re-fusion secondary to mutations in midbody/centromere proteins and to cellular endomitosis without division of the cell nucleus [184].

Myeloid Neoplasms: Pulmonary Acute Myeloid Leukemia/Myeloid Sarcoma

Introduction

Extramedullary myeloid sarcoma (a tumor of immature myeloid cells and blasts) is uncommon, in general reported as <10% of all acute myeloid leukemias [156]. Primary lung involvement by acute myeloid leukemia is even rarer [185–187]. The majority of cases reported in the literature include individuals with a diagnosis of acute leukemia in advanced stage [188] or involvement of the lung in the form of a mass or myeloid sarcoma (also known as granulocytic sarcoma or chloroma) [189–196]. Myelomonocytic and monocytic leukemias have a predilection to involve extranodal tissue; however, no particular subtype of acute myeloid leukemia has specific lung tropism.

Clinical Features

According to Wilson and Medeiros, who presented the results of the 2013 Society of Hematopathology/European Association of Hematopathology workshop for extramedullary manifestations of myeloid neoplasms [197], extramedullary acute myeloid leukemia/myeloid sarcoma can be divided into four different subgroups: (1) isolated myeloid sarcoma; (2) myeloid sarcoma and concurrent acute myeloid leukemia; (3) myeloid sarcoma as relapse after chemotherapy or post-transplant therapy; and (4) blast phase/transformation of an underlying myelodysplastic syndrome, myeloproliferative neoplasm, or chronic myelomonocytic leukemia [197]. Patients with significant pulmonary involvement by acute myeloid leukemia are usually at advanced stages and present with respiratory failure in the setting of hyperleukocytosis. Clinically, the symptoms are suspicious of a pneumonic process, pulmonary edema, pulmonary hemorrhage, or transfusion-related acute lung injury [198]. Pulmonary myeloid sarcoma presents as any of the subgroups described above with symptoms related to a mass, including nonproductive or productive cough, dyspnea, hemoptysis, and respiratory distress if the lesion involves an airway. The treatment of myeloid sarcoma includes chemotherapy regimens similar to those used for acute myeloid leukemia. Some patients may have delayed initiation of chemotherapy as a lung infiltrate may be originally thought to be an infectious process until the diagnosis of leukemia is confirmed by morphology.

Diagnostic Imaging

Leukemic pulmonary infiltration, defined as extravascular collections of leukemic cells in the lung parenchyma, has a variety of manifestations including a bronchovascular-lymphangitic pattern (Fig. 15.109) mimicking lymphangitic carcinomatosis; lung nodules (Fig. 15.110); and ground-glass and consolidative opacities where consolidative opacities may predominate in the peribronchovascular regions as a result of infiltration of parenchyma adjacent to perilymphatic tissues in the pulmonary interstitium [199]. Leukemic pulmonary infiltration can occur in all the major leukemias and, at autopsy, is present in 20–40% of patients with leukemia [156].

Imaging in pulmonary leukostasis, which results from the accumulation of leukemic cells in small vessels, may be normal or may resemble interstitial or alveolar edema [156,

Fig. 15.109 Leukemic pulmonary infiltration. CT shows a bronchovascular-lymphangitic pattern mimicking lymphangitic carcinomatosis with thickening of interlobular septa (thin arrow) as well as thickening of the peribronchovascular interstitium (thick arrow)

188]. Proposed mechanisms of edema in leukostasis include increased capillary permeability edema related to the presence of numerous leukemic cells or cardiac failure from coronary artery leukostasis [156]. Leukostasis occurs most commonly in acute myelocytic leukemia (AML) but is also seen the blast phase of chronic myelocytic leukemia (CML).

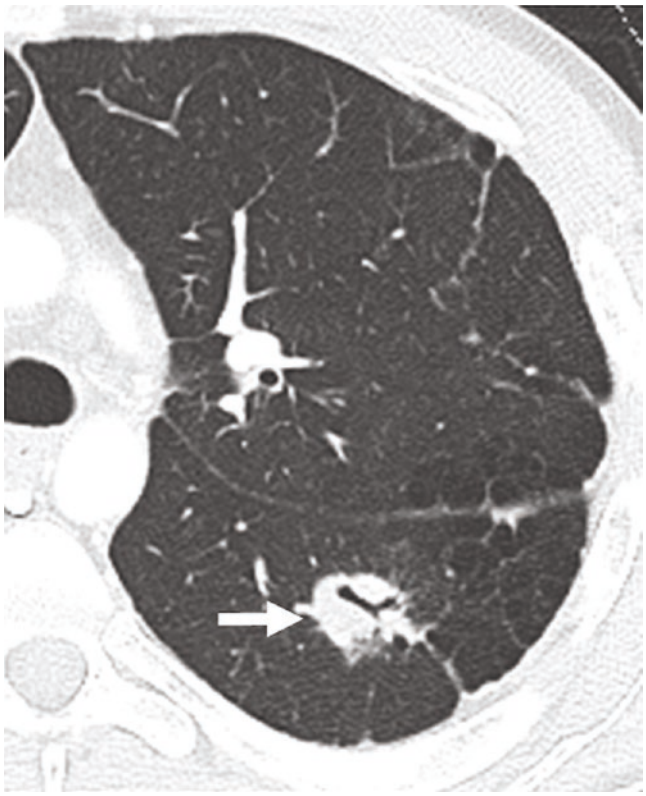

Fig. 15.110 Leukemic pulmonary infiltration. CT shows a left lower lobe nodule (arrow) with air bronchograms

Imaging manifestations of leukemic cell lysis pneumopathy, an acute respiratory distress syndrome that occurs usually within 10–48 h after the start of chemotherapy in patients with high leukocyte counts, are those of acute respiratory distress syndrome and include extensive bilateral airspace consolidation [188]. Leukemic cell lysis pneumopathy is most often seen in patients with acute lymphocytic leukemia [200].

Hyperleukocytic reaction is another type of acute respiratory distress syndrome in which the onset of clinical respiratory symptoms and diffuse lung opacities on imaging parallels a rapid increase in the leukocyte count and the number of blast cells [201]. Hyperleukocytic reaction is more common in AML and in the blast phase of CML [201].

In leukemia, PET/CT is helpful in the detection of Richter transformation in chronic lymphocytic leukemia (CLL), extramedullary involvement in acute leukemia, and myeloid sarcoma [202]. Myeloid sarcoma, a rare presentation of AML, is defined as an extramedullary tumor mass consisting of immature or mature myeloid blast cells [197]. Myeloid sarcoma of the lung is extremely rare and may manifest with discrete or ill-defined nodules or masses or with masslike consolidation [189, 203] (Fig. 15.111a, b). Ueda et al. found that SUVmax ranged from 2.6 to 9.7 in seven patients with myeloid sarcoma though no patients in their study had pulmonary myeloid sarcoma [204].

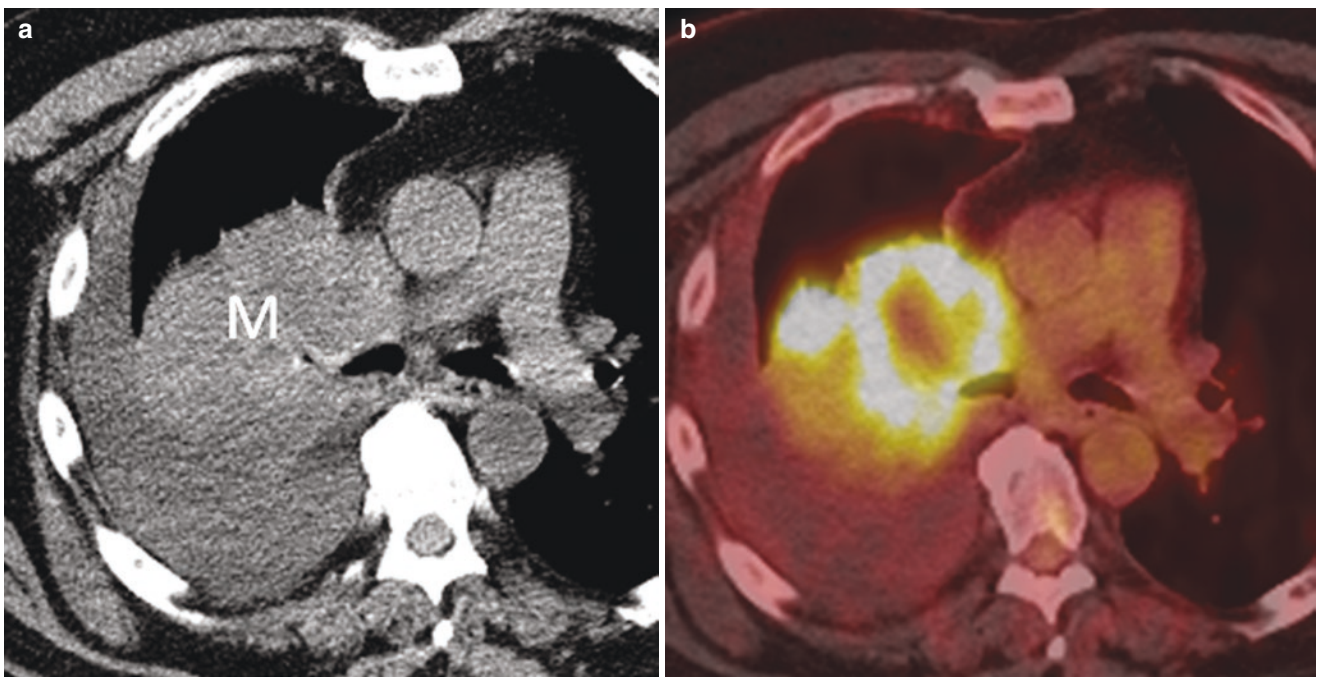

Fig. 15.111 Myeloid sarcoma. (**a**) CT shows a right upper lobe mass (M), (**b**) PET/CT fused axial image shows that the majority of the mass is FDG-avid. Central photopenia is the result of central necrosis

Pathology

Acute myeloid leukemia that involves the lung in the setting of hyperleukocytosis consists of conspicuous infiltrates of blasts of intermediate to large size with oval to cleaved nucleus, fine chromatin, prominent nucleolus, and a moderate amount of granular eosinophilic cytoplasm with a lymphangitic, intravascular, septal, or pleural interstitial pattern of involvement with variable distention of these spaces depending on the burden of disease [188] (Figs. 15.112, 15.113 and 15.114). In contrast, pulmonary myeloid sarcoma consists of a mass or tumefactive lesion made of sheets of immature myeloid cells and blasts (with similar features as described above) that disrupt the lung architecture [185–187, 190–196] (Figs. 15.115 and 15.116). Myeloid sarcoma may contain a variable number of eosinophils, particularly in those cases arising in the setting of a myeloproliferative neoplasm or acute myelomonocytic leukemia with inv [16]. Myeloid sarcomas composed preferentially of left-shifted myeloid cells (promyelocytes, myelocytes, metamyelocytes) include those cases arising in the setting of chronic myeloid leukemia. Abundant mitoses and necrosis are variably seen, and some cases may show a starry-sky pattern. Because the majority of patients with acute myeloid leukemia/myeloid sarcoma are immunosuppressed either by the underlying disease or due to chemotherapy, areas of necrosis and adjacent uninvolved tissue should be evaluated carefully to exclude the presence of a concomitant opportunistic microorganism.

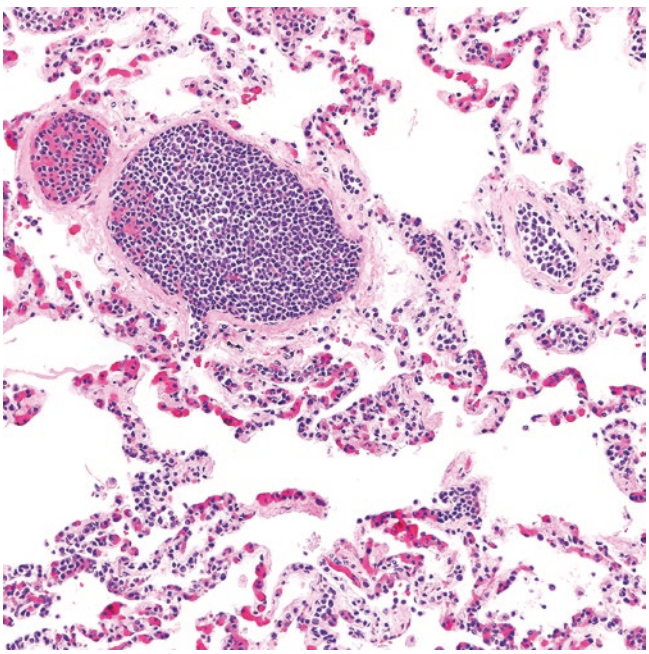

Fig. 15.112 Acute myeloid leukemia involving the lung in a patient with hyperleukocytosis. All blood vessels are filled with blasts. This pattern is also seen in intravascular large B-cell lymphoma

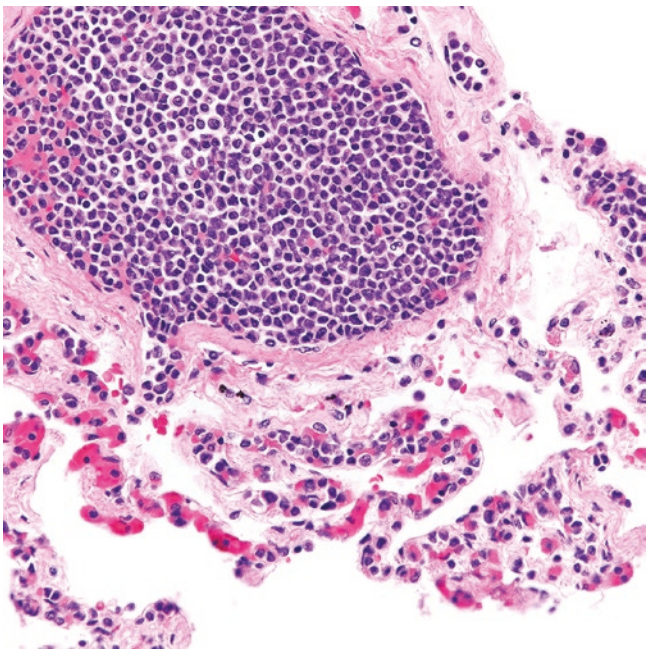

Fig. 15.113 Acute myeloid leukemia involving the lung in a patient with hyperleukocytosis. All blood vessels and capillaries are filled with blasts

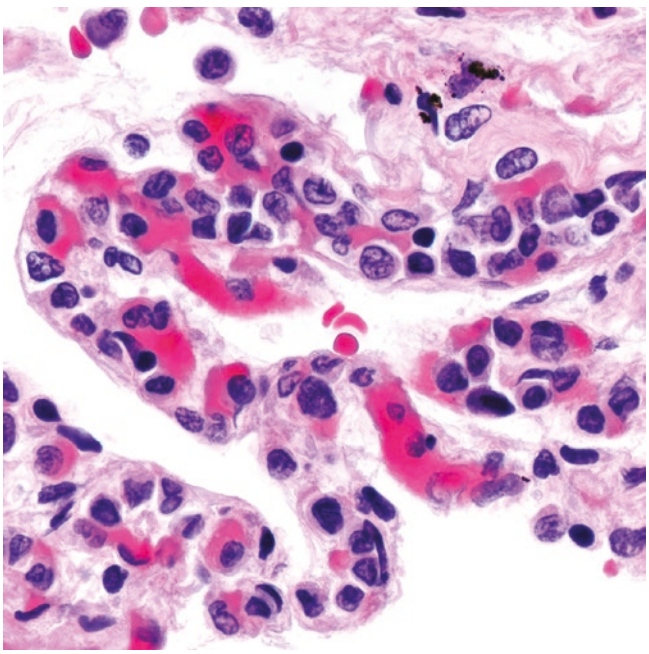

Fig. 15.114 Acute myeloid leukemia involving the lung in a patient with hyperleukocytosis. At higher magnification, the blasts show intermediate to large size with oval to cleaved nucleus, fine chromatin, and scant cytoplasm

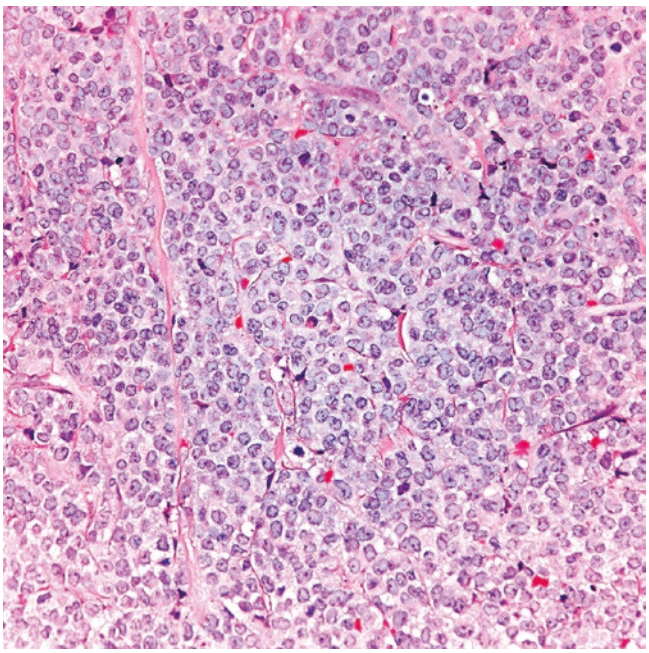

Fig. 15.115 Myeloid sarcoma is composed of sheets of blasts of intermediate to large size with oval to cleaved nucleus, occasional prominent nucleus, vesicular chromatin, and a moderate amount of pale eosinophilic cytoplasm

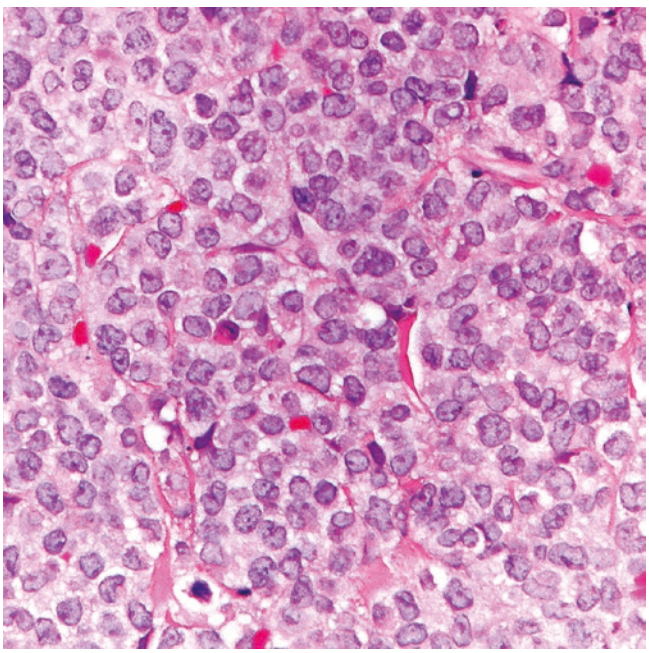

Fig. 15.116 Myeloid sarcoma. Higher magnification showing detail of the blasts with oval to cleaved nucleus, occasional prominent nucleus, vesicular chromatin, and a moderate amount of pale eosinophilic cytoplasm

Immunohistochemistry and Other Ancillary Studies

Myeloblasts are usually positive for CD34, CD33, CD117, CD11c, myeloperoxidase, and lysozyme with variable to weak expression of CD45 (Fig. 15.117). If the leukemic

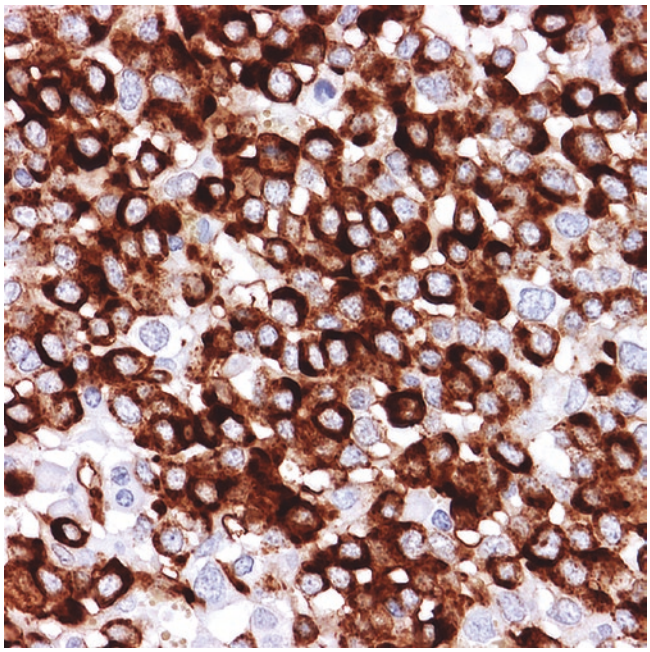

Fig. 15.117 Myeloid sarcoma, the blasts are positive for myeloperoxidase by immunohistochemistry

infiltrate/myeloid sarcoma has monocytic differentiation, the blasts express CD4, CD14, CD33, CD64, and CD68 and they show variable expression of CD117 and are typically negative for CD34 and CD163. Acute myeloid leukemia/myeloid sarcoma is positive for CD43, CD123, and MNDA, and some cases can show expression of CD7, CD56, CD19, and/or PAX5 (the last are seen in cases of acute myeloid leukemia with t(8;21)). TdT is variably expressed and does not translate into a diagnosis of lymphoblastic leukemia. ERG is also positive in immature myeloid cells and acute myeloid leukemia [205]. Thus, expression of ERG in an epithelioid tumor should not always translate into a lesion of vascular origin, particularly in a patient with a history of leukemia. Myeloblasts are negative for CD3 and most of the other T-cell markers and for CD20 and CD79a. If the diagnosis of acute myeloid leukemia is already well-established, a limited panel of markers similar to those of original leukemia can be used to confirm the phenotype in a pulmonary infiltrate or a mass-forming lesion suspicious for myeloid sarcoma. If a leukemia has a particular phenotype, namely megakaryocytic or erythroid origin, additional megakaryocytic markers (CD42b, CD61) or erythroid markers (CD71, glycophorin, hemoglobin A) should be performed.

Flow cytometry is very useful when it is available, but tissue may not always be collected for this test when a lung mass is detected, particularly in cases with no prior history of acute myeloid leukemia. If fresh tissue or unstained slides are prepared, FISH may be used to detect a particular translocation or a rearrangement of specific acute myeloid leukemias subtypes, namely acute myeloid leukemia with t(8;21) (*RUNX1::RUNX1T1*), acute promyelocytic leukemia [t(15;17)(*PML::RARA*)], monocytic sarcoma (*MLL/KMT2A*

rearrangement), or a blast phase in chronic myeloid leukemia [t(9;22)(*BCR::ABL1*)]. Next-generation sequencing may help to reclassify difficult cases of myeloid sarcoma that present as a lung mass with no peripheral blood or bone marrow involvement.

Differential Diagnosis

Acute myeloid leukemia that involves the lung in the setting of hyperleukocytosis should be distinguished from intravascular LBCL. The morphology of intravascular myeloblasts is usually distinct, with more abundant granular cytoplasm and cleaved nucleus, in contrast to the centroblastic or immunoblastic morphology seen in intravascular LBCL. A clinical history of acute myeloid leukemia is extremely informative since pulmonary involvement usually does not go unnoticed as it may occur in patients with intravascular LBCL. Immunohistochemical stains for CD20, PAX5, CD34, CD117, myeloperoxidase, and/or lysozyme are sufficient to confirm the diagnosis. Blastic plasmacytoid dendritic cell neoplasm is positive for CD4, CD56, CD123, and TCL1 and negative for myeloperoxidase and B- and T-cell markers and should also be distinguished from acute myeloid leukemia since the treatment is different.

Pulmonary myeloid sarcoma should be distinguished from LBL, high-grade DLBCL, Burkitt lymphoma, small cell carcinoma, or any small blue round cell tumor primary or metastatic to the lung. Prior clinical history of acute myeloid leukemia is very important to support or exclude the diagnosis. Immunohistochemical stains for CD43, CD45, myeloperoxidase, lysozyme, CD34, and/or CD117 support myeloid sarcoma, whereas the presence of B-cell markers may suggest B-LBL, Burkitt lymphoma or any other B-cell lymphoproliferative disorder. Expression of T-cell markers, CD34, and/or TdT support T-LBL, and keratins and neuroendocrine markers support carcinoma. The differential diagnosis of pulmonary acute myeloid leukemia/myeloid sarcoma is summarized in Table 15.17.

Table 15.17 Differential diagnosis of pulmonary acute myeloid leukemia/myeloid sarcoma

Acute myeloid leukemia as diffuse infiltrates in vascular spaces, secondary to hyperleukocytosis
Hematopoietic
Intravascular large B-cell lymphoma
Leukemic infiltrates of blastic plasmacytoid dendritic cell neoplasm
Non-hematopoietic
Carcinoma or melanoma with lymphangitic spread
Myeloid sarcoma (mass-forming lesion)
Hematopoietic
Lymphoblastic lymphoma
Diffuse large B-cell lymphoma, high-grade
Burkitt lymphoma
Anaplastic large cell lymphoma
Non-hematopoietic
Small cell carcinoma
Small blue round cell tumor (primary or metastatic)

Molecular Findings

Recurrent cytogenetic abnormalities or gene mutations that occur in extramedullary myeloid sarcoma mirror those known to occur in acute myeloid leukemia [197]. A full description of all these abnormalities is out of the scope of this chapter. If a history of a particular acute myeloid leukemia with recurrent cytogenetic abnormalities is available, cytogenetics, FISH, and/or molecular studies could be performed for further evaluation.

Histiocytic Disorders of the Lung

Histiocytic disorders of the lung are rare. Pulmonary Langerhans cell histiocytosis (LCH), Rosai–Dorfman disease, and Erdheim–Chester disease appear to be the most common among these rare diseases. However, two additional conditions, juvenile xanthogranuloma and crystal-storing histiocytosis, have also been described as primary pulmonary histiocytic lesions (see Table 15.18).

Once considered reactive histiocytic proliferations, relatively recent studies have shown that at least a subset of these disorders are clonal and may benefit from targeted therapies. Recurrent molecular alterations that have been identified in histiocytic disorders include gene mutations of molecules involved in the activation of the RAS/RAF/MAPK signaling pathway with resulting overexpression of ERK1.

Pulmonary Langerhans Cell Histiocytosis (LCH)

Introduction

LCH is a subtype of histiocytic disorder that in the second half of the nineteenth century included multiple entities, namely eosinophilic granuloma or Otani's tumor (localized form), Hand–Schüller–Christian disease (multiorgan disease), and Abt–Letterer–Siwe disease (systemic form) [206]. It was not until 1953 that Lichtenstein—and to some extent Otani—hypothesized that these histiocytic proliferations represented different spectrums of the same disease. Lichtenstein coined the term histiocytosis X to point out that this histiocytosis derived from yet unknown cells [206]. Two decades later, Nezelof demonstrated that the cell of origin was a Langerhans cell and then coined the term Langerhans cell histiocytosis [207, 208]. Langerhans cells were described in 1868 by P. Langerhans Jr. using silver impregnations [209]. In 1961, the electron microscopist Birbeck discovered that Langerhans cells contained ultrastructural cytoplasmic membranous bodies that are known today as Birbeck granules [210]. It was not known if LCH represented a reactive or a neoplastic process until 1994 when two independent studies using a HUMARA assay demonstrated that a subset of LCH cases were clonal [211, 212]. Another breakthrough in the field of histiocytoses came in 2010 when the *BRAF* V600E mutation was

Table 15.18 Clinicopathologic features of the most representative histiocytic disorders of the lung

	Pulmonary LCH	Pulmonary RDD	Pulmonary ECD
Age group	Young adults (20–40 years)	Adults (median 40 years)	Adults (40–60 years)
Gender predilection	M = F Older adults F > M	M > F	M > F (3:1)
Clinical symptoms	None to cough, dyspnea, and systemic symptoms; spontaneous pneumothorax, pulmonary HTN	None to dyspnea, cough, chest pain, pleural effusion; occasionally systemic symptoms	Progressive dyspnea, restrictive pattern on pulmonary function tests
Association with cigarette smoking	High (>90%)	No	No
Extrapulmonary disease	Not common in smoking-related pulmonary LCH Yes, in LCH not associated with smoking	All cases, with lymph node, skin, and/or bone involvement	Yes, bilateral and symmetric osteosclerosis of the diaphysis/metaphysis of long bones. Xanthelasmas, pericardial/periaortic and/or retroperitoneal fibrosis, diabetes insipidus, other.
Imaging	Small nodules (<2 cm) in upper and middle lobes, cysts	Single mass or diffuse bilateral lesions	Interlobular septal and subpleural thickening, GGOs
Histopathologic findings	Bronchovascular distribution, nodules at different stages. Early lesions: Langerhans cells, eosinophils, lymphocytes, macrophages, MN giant cells Late lesions: burned-out LCH with fibrosis, cyst formation Usually not subpleural Smoking-related changes	Mass: Large macrophages with emperipolesis, in addition to lymphocytes, and plasma cells. No MN giant cells or eosinophils Interstitial: lymphangitic pattern with bronchiolar, interlobular septa and subpleural distribution and variable fibrosis	Lymphangitic distribution with thickening of pleura, interlobular septa and perivascular interstitium, lesser involvement of peribronchiolar areas. Foamy macrophages with round nucleus, admixed inflammation, and variable fibrosis. MN giant cells of Touton type. No emperipolesis or eosinophils Advanced stages resemble ILD
IHC	Langerhans cells: S100+, CD1a+, langerin+ CD68+/−, CD163−/+	Macrophages: S100+, CD68+, CD163+, CD1a-, langerin-	Macrophages: S100−/+, CD68+, CD163+, CD1a-, langerin-
BRAF V600E (IHC Ab VE-1)	50–70%	Negative (If RDD morphology and BRAF+ diagnosis is ECD)	>50%
Other mutations	*NRAS* (Q61K)(/R) (40%) *MAP2K1* (10–20%) *ARAF, ERBB3, BRAF* fusions (rare)	*MAP2K1, KRAS* (~30%) Hereditary forms (Faisalabad histiocytosis, "H"-syndrome) with *SLC29A3* mutations	*NRAS, KRAS*, and fusions in *PIK3CA* and *ALK* (few cases)
Prognosis	Good with smoking cessation, few patients progress to ILD	Intermediate, promising results with new targeted therapies	Intermediate, promising results with new targeted therapies

LCH Langerhans cell histiocytosis, *RDD* Rosai–Dorfman disease, *ECD* Erdheim–Chester disease, *M* male; *F* female; *HTN* hypertension, *GGOs* ground glass opacities, *MN* multinucleated, *IHC Ab* immunohistochemistry antibody, *ILD* interstitial lung disease

identified in 50–70% of LCH cases by diverse molecular analyses [213, 214]. In 2016, the Histiocyte Society reclassified all histiocytic disorders into several subgroups, each one designated by a letter, with LCH included in group "L" for "Langerhans" [215].

LCH can involve virtually any organ as part of multisystemic disease, including the lung (formerly known as pulmonary LCH granulomatosis). Interestingly, the latter is usually seen as a limited process without affecting other organs. In this context, the development of pulmonary LCH is strongly associated with cigarette smoking, and the disease usually has a good prognosis [216, 217].

Clinical Features

The incidence of LCH is 5 cases/million/year [218]. Pulmonary LCH is even rarer and affects young adults (20–40 years) without a gender predilection, although the disease may be seen more commonly in women at an older age. More than 90% of patients are smokers or ex-smokers [216, 217, 219]. Patients may be asymptomatic, and the disease is discovered incidentally for other reasons. Symptomatic patients present with cough, dyspnea, fever, or systemic symptoms. Complications of pulmonary LCH include the development of spontaneous pneumothorax and/or pulmonary hypertension [220]. Smoking cessation is the most crucial step to improve or stabilize the disease in most patients [217, 221]. The disease may resolve spontaneously or show significant progression with increased morbidity or even death in rare instances [222].

Treatment of progressive pulmonary LCH and in systemic disease is based on cladribine or cytarabine as salvage therapy, whereas treatment with steroids does not appear to confer an additional benefit [223, 224]. The prognosis of pulmonary LCH is good, with about 85% of patients being alive

at 10 years. However, a small subset of patients can progress to end-stage lung disease with significant morbidity [222]. Lung transplantation is reserved for individuals with rapid disease progression despite smoking cessation and chemotherapy; however, the disease may recur in the transplanted lung if the patient resumes smoking [220, 225]**.** Current studies are evaluating the use of vemurafenib (*BRAF* V600E inhibitor) and other inhibitors of the RAS/RAF/MAPK pathway as potential target therapies in this disease [226].

Diagnostic Imaging

Imaging appearance depends upon the stage of the disease. In early stage, HRCT shows upper lung predominant centrilobular nodules with sparing of the lung bases. As the disease progresses, the lung nodules undergo cystic degeneration becoming small round thick-walled cysts. With further disease progression, the lung cysts increase in size and become thin walled, irregular, or bizarre-shaped (Fig. 15.118a, b). HRCT may show different stages of the disease at one time. End-stage disease is characterized by the presence of pulmonary fibrosis. Spontaneous pneumothorax may develop in about 25% of patients due to rupture of sub-pleural cysts [227, 228].

Pathology

Currently, sampling of a lung lesion is usually accomplished via an imaging-guided needle biopsy or a transbronchial biopsy, and the diagnosis is established either in a cytology specimen, a core-needle biopsy, or a transbronchial biopsy. If a diagnosis of pulmonary LCH is rendered in any of these specimens, then a wedge resection or a lobectomy are not performed. However, a resection may still be done when a biopsy is inconclusive for diagnosis or when the disease manifests as multiple surgically approachable peripheral nodules. Langerhans cells can be identified in bronchioalveolar lavages, and this may suggest the diagnosis of pulmonary LCH, but this test has a very low sensitivity and is rarely used for diagnosis [219].

Grossly, pulmonary LCH presents as multiple tan-white small nodules (usually <2 cm) with somewhat ill-defined borders (Fig. 15.119). Cases at the advanced stage may demonstrate prominent cystic changes, especially in the upper and middle lobes and/or changes indistinguishable from end-stage lung disease, namely honeycombing and fibrosis with distortion of the lung parenchyma. On microscopic examination, the nodules of pulmonary LCH have a preferential bronchovascular distribution with a sharp demarcation from the surrounding lung parenchyma (Figs. 15.120 and 15.121). The nodules have variable shapes and compositions depending on the stage of development (Figs. 15.120, 15.121 and 15.122). Early lesions are cellular and composed of collections of Langerhans cells that have an epithelioid morphology with a reniform nucleus—often with grooves—thin nuclear membranes, vesicular chromatin, inconspicuous nucleolus, and abundant eosinophilic and finely granular cytoplasm (Figs. 15.123, 15.124 and 15.125). Occasional multinucleated giant cells may be identified. Increased mitoses and significant atypia are not a feature (Fig. 15.124). The background of these nodules is composed of fibroblasts, small lymphocytes, macrophages, neutrophils, and eosinophils (Figs. 15.123, 15.124 and 15.125). Depending on the size of a nodule, the adjacent airway may or may not be obliterated by the LCH infiltrate. Larger nodules usually disrupt the architecture of an airway and may develop a central

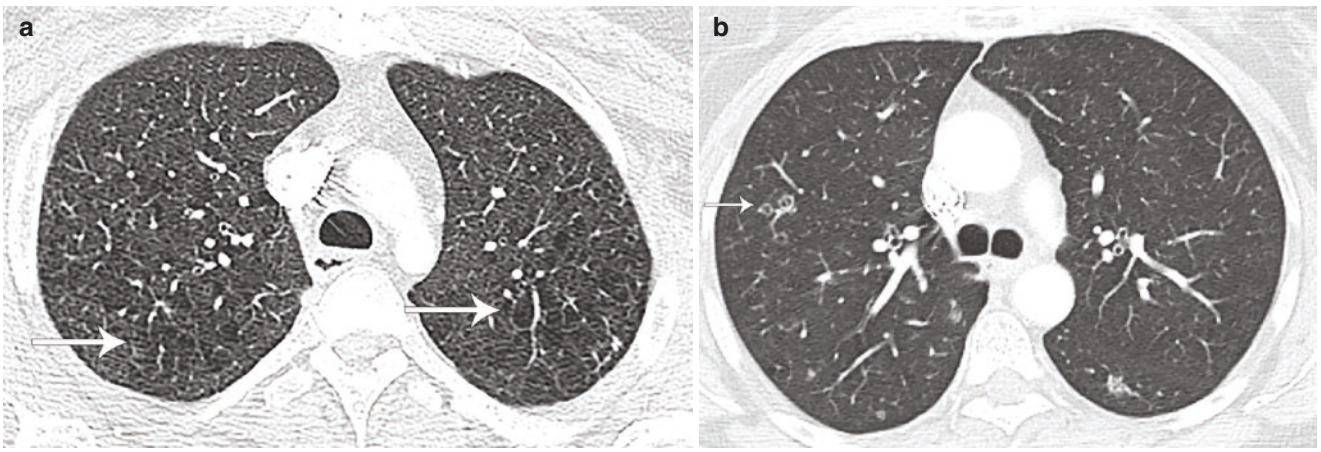

Fig. 15.118 (**a**) Pulmonary Langerhans cell histiocytosis presents as upper lobe predominant, bizarre-shaped, irregular thin walled cysts (arrows), and (**b**) pulmonary Langerhans cell histiocytosis presents as upper lobe centrilobular nodules. Some nodules have undergone cystic degeneration and appear as small round thick-walled cysts (arrow)

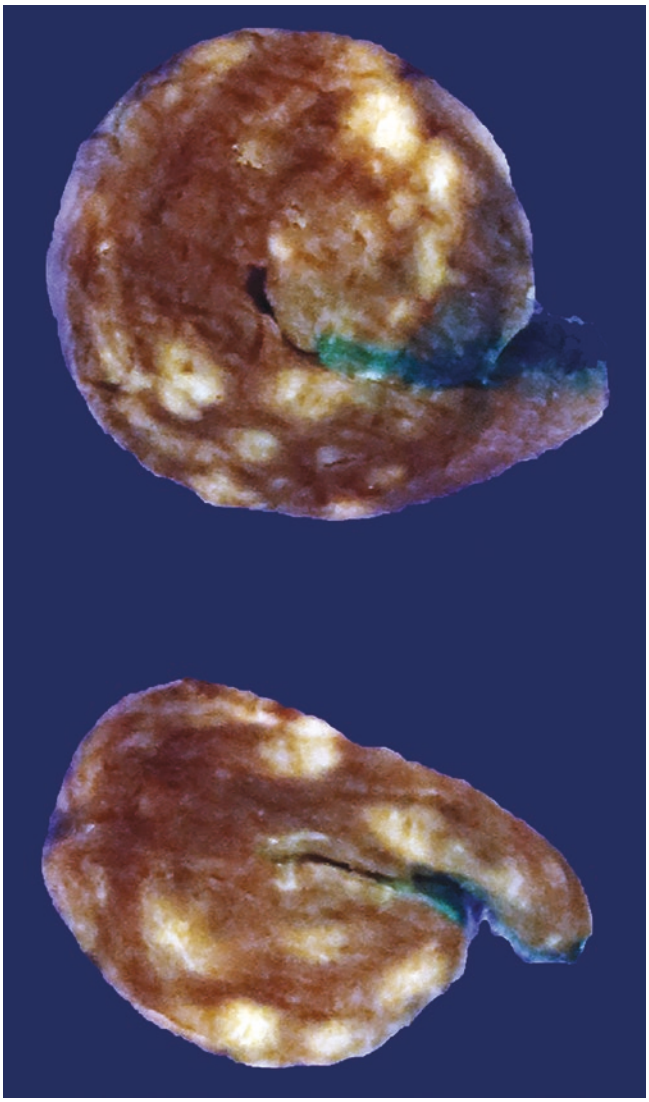

Fig. 15.119 Pulmonary Langerhans cell histiocytosis. The wedge lung resection shows multiple small tan-white to pale-yellow nodules distributed throughout the parenchyma

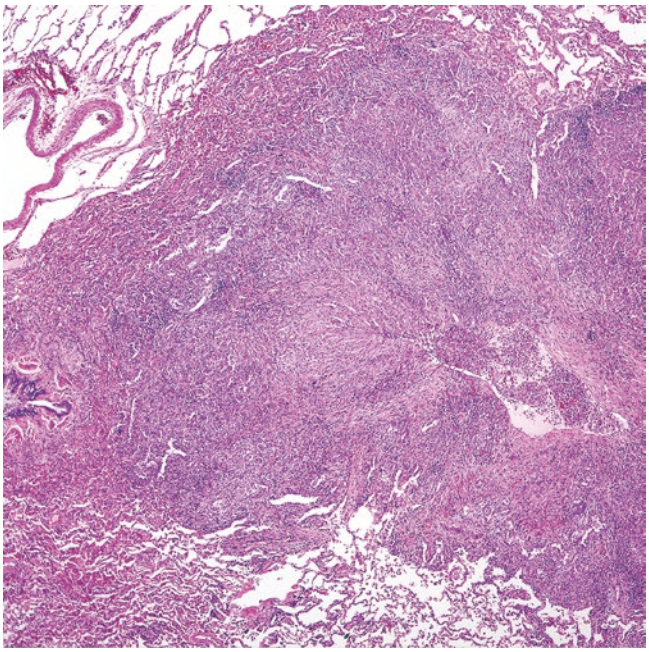

Fig. 15.120 Pulmonary Langerhans cell histiocytosis. Large nodule centered around a distorted bronchovascular bundle. The center of the lesion is necrotic and becoming cystic

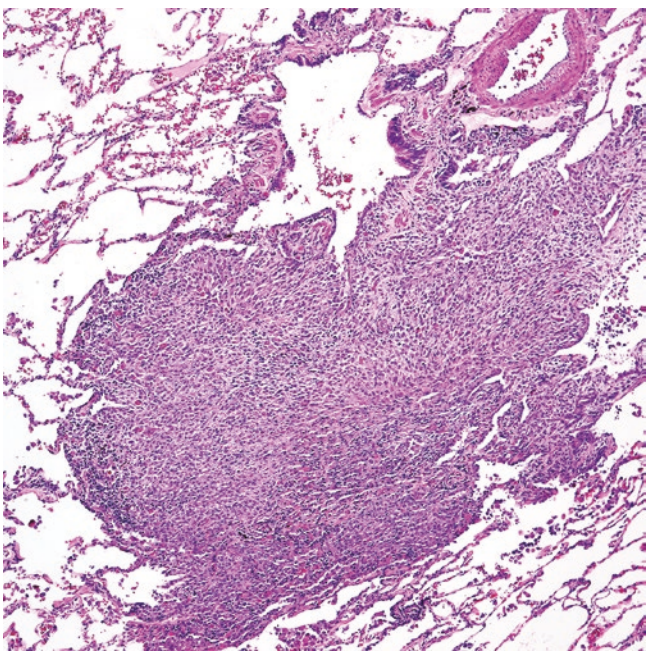

Fig. 15.121 Pulmonary Langerhans cell histiocytosis. Smaller nodule with bronchovascular distribution distorting the airway. The nodule has a sharp demarcation from the adjacent lung and is composed of numerous Langerhans cells, macrophages, small lymphocytes, and eosinophils

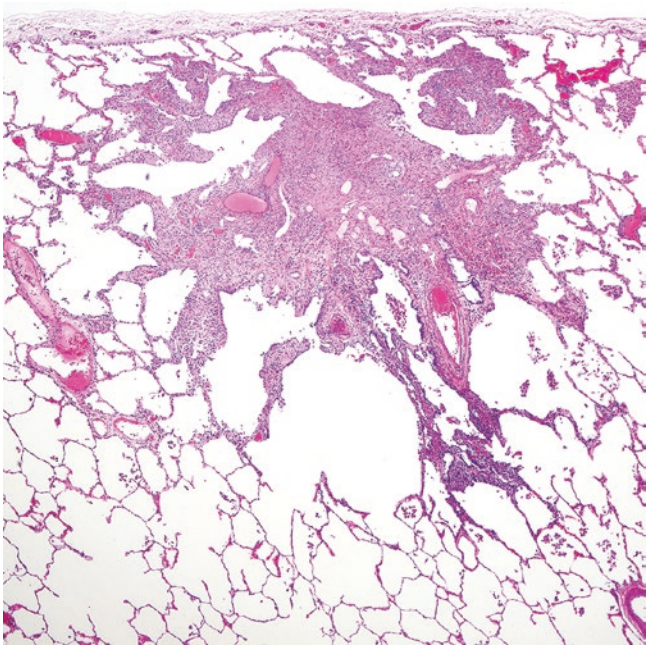

Fig. 15.122 Pulmonary Langerhans cell histiocytosis. Late-stage lesion with stellate shape and central fibrosis. The surrounding airways show traction bronchiectasis and the alveolar spaces show secondary cyst formation

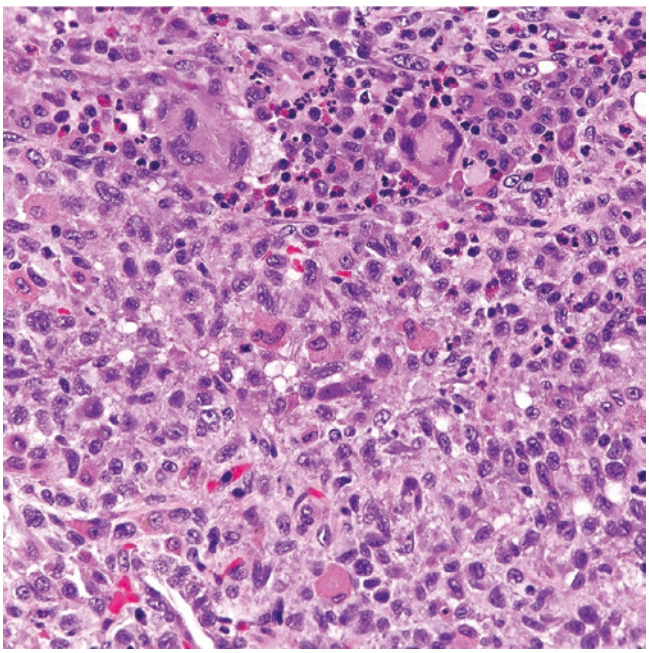

Fig. 15.124 Sheets of Langerhans cells with reniform nuclei, nuclear grooves, and abundant eosinophilic cytoplasm admixed with macrophages, small lymphocytes, eosinophils, and a few multinucleated giant cells (top). A few scattered macrophages with "smoker's pigment" are also present (center)

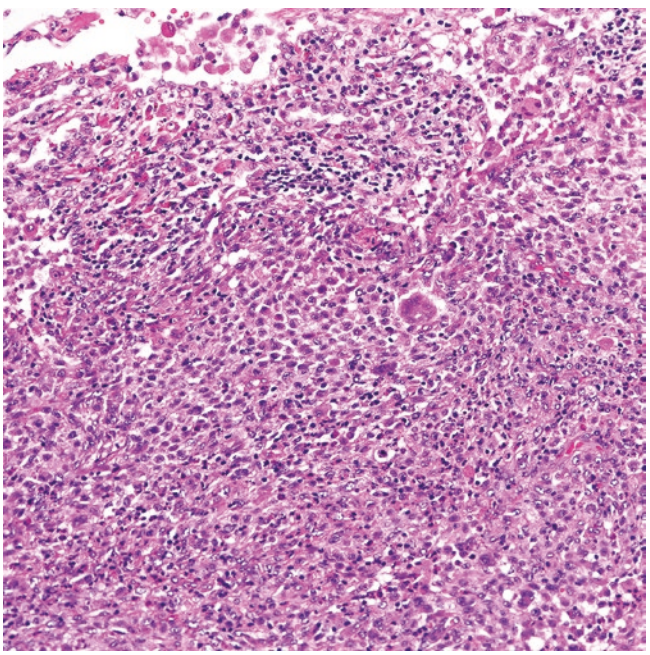

Fig. 15.123 Nodule of pulmonary Langerhans cell histiocytosis composed of numerous Langerhans cells, macrophages, small lymphocytes, and eosinophils. Scattered multinucleated giant cells are also seen

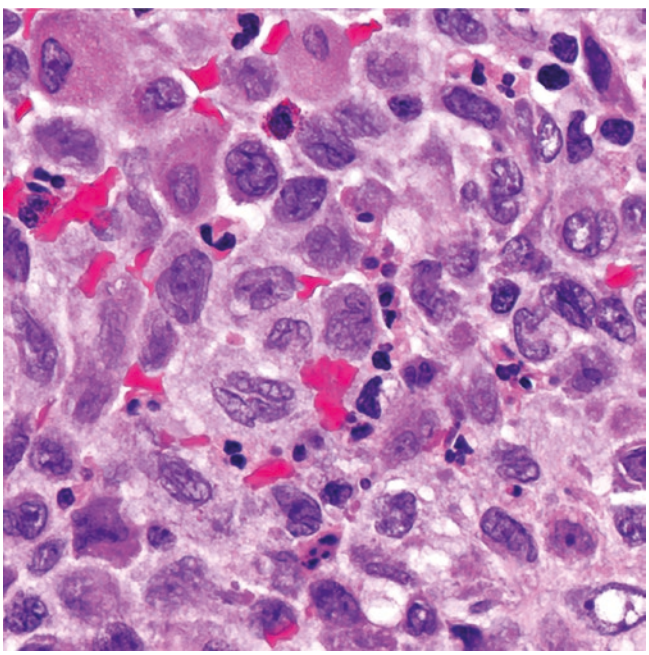

Fig. 15.125 Langerhans cells have reniform to irregular nuclei with nuclear grooves or prominent nuclear indentations and abundant eosinophilic cytoplasm

cavity with the subsequent formation of a cyst (Fig. 15.120). Late lesions, also referred to as "burned-out" LCH, are the hardest to recognize, particularly in a core needle or transbronchial biopsy (Figs. 15.122 and 15.126). They show a stellate shape with finger-like projections to the adjacent lung that show features of mechanical traction (Fig. 15.122). The central portion of a late lesion shows marked fibrosis with a variable number of hemosiderin-laden macrophages and scant to no eosinophils (Fig. 15.126). Langerhans cells are not readily recognized unless they are highlighted by immunohistochemistry. These lesions may or may not be associated with cyst formation. If the specimen is a wedge biopsy or a lobectomy, it is common to identify nodules of LCH at variable stages of development. Additional findings present in the immediate uninvolved lung include respiratory bronchiolitis (abundant intra-alveolar macrophages with so-called "smoker's pigment"), interstitial anthracotic deposits, and emphysematous changes, which are all characteristic of smoking-related lung disease. In some cases, macrophages with "smoker's pigment" may also be present within a nodule of LCH (Fig. 15.124). In progressive disease, the scars become confluent and form larger areas of fibrosis that eventually distort the lung parenchyma with honeycombing and features of end-stage lung disease. Some cases may feature vasculopathy with intimal fibrosis and medial hypertrophy of pulmonary arteries, which correlate with those cases with pulmonary hypertension.

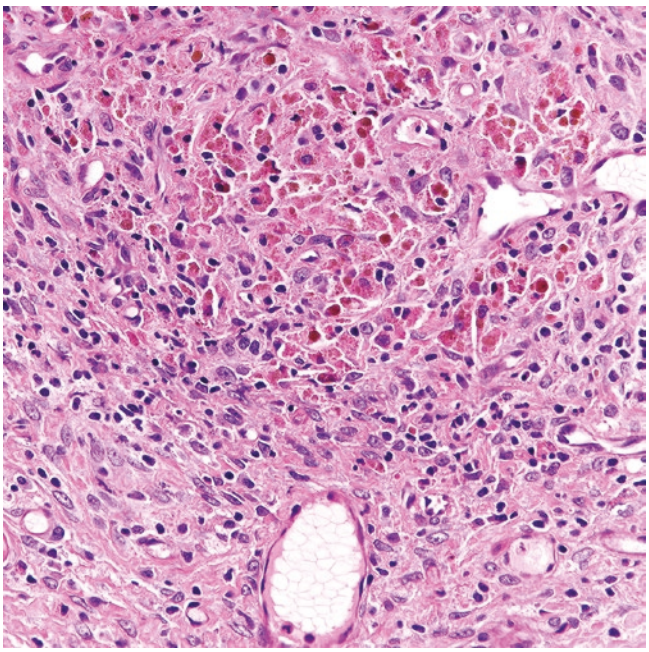

Fig. 15.126 Late-stage lesion of pulmonary Langerhans cell histiocytosis with fibrosis, macrophages with "smoker's pigment," and only a few Langerhans cells

Immunohistochemistry and Other Ancillary Studies

Langerhans cells are positive for S100, CD1a, CD207/langerin, and weak CD4 and may show focal CD68 and CD163 (Figs. 15.127a, b, 15.128a–c and 15.129). The multinucleated giant cells are usually positive for CD68 and CD163 and not for CD1a, suggesting that they are a subtype of macro-

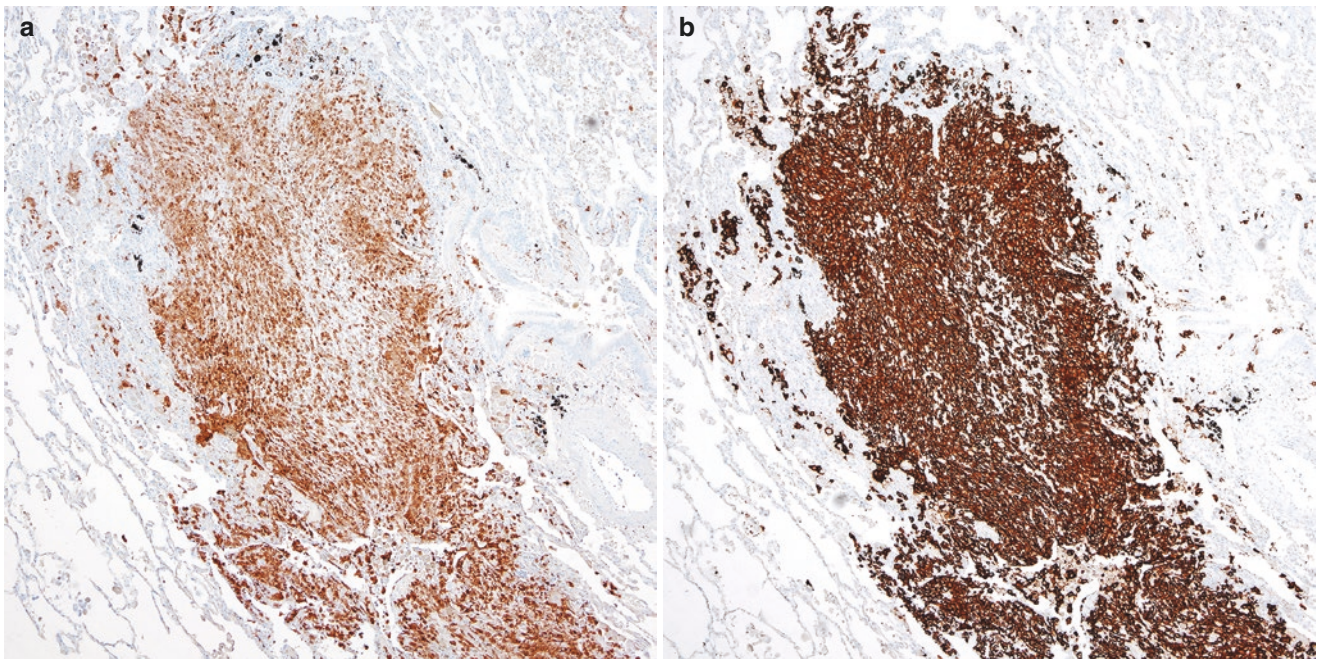

Fig. 15.127 Pulmonary Langerhans cell histiocytosis. Langerhans cells are positive for (**a**) S100 and for (**b**) CD1a

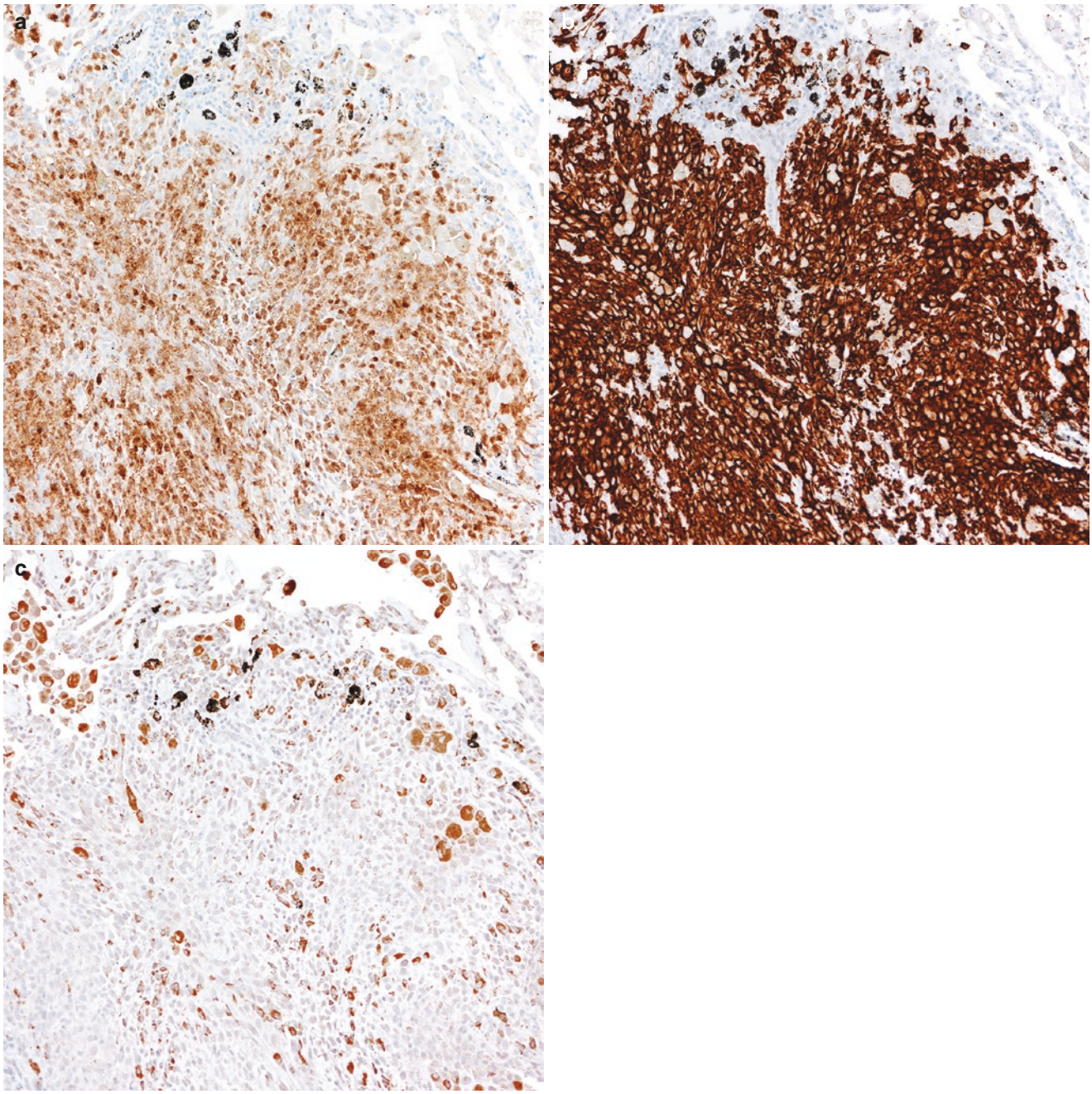

Fig. 15.128 Pulmonary Langerhans cell histiocytosis. Langerhans cells are positive for (**a**) S100 and (**b**) CD1a and negative for (**c**) CD68

phages and not Langerhans cells (Fig. 15.128a–c). LCH is negative for B-cell and T-cell markers, CD15, CD30, FDC markers, keratin, and melanoma markers (SOX10, HMB-45, MART-1). There is a commercially available antibody that detects the mutated BRAF V600E protein (VE-1) that shows cytoplasmic labeling in those cases harboring the mutation [214, 229] (Figs. 15.130 and 15.131). Pathologists should be aware that BRAF VE-1 demonstrates a cross-reaction with dynein proteins present on cilia, and for this reason this immunostain decorates the surface of respiratory epithelium [230] (Fig. 15.130). This feature can create confusion regarding the interpretation of this marker in the context of pulmonary LCH.

Differential Diagnosis

The clinical and pathologic presentation of pulmonary LCH is characteristic, and the diagnosis is usually straightforward, especially when the tissue analyzed consists of a wedge resection or an open-lung biopsy. Nevertheless, the diagnosis may be extremely challenging in a core needle biopsy or

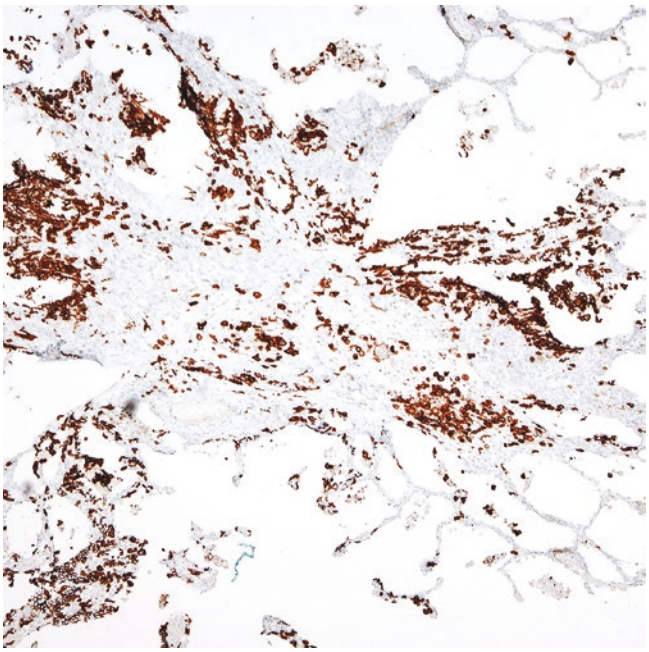

Fig. 15.129 The CD1a immunostain highlights less number of Langerhans cells in late-stage lesions

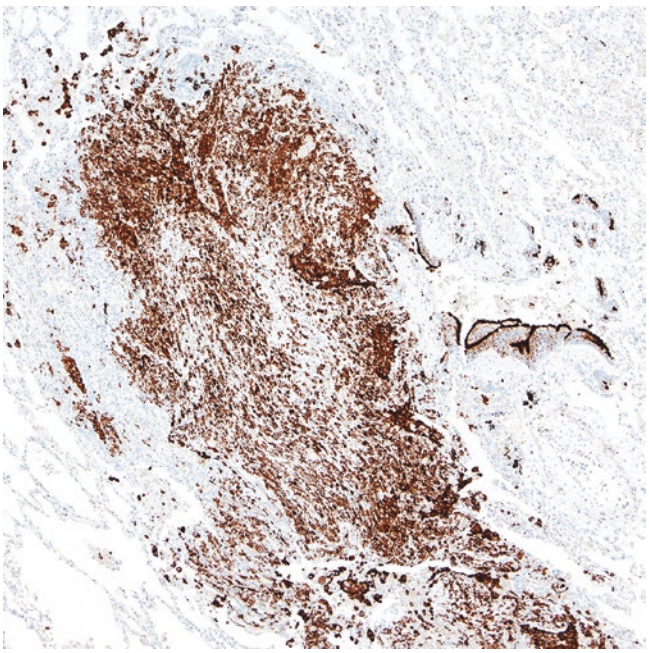

Fig. 15.130 Pulmonary Langerhans cell histiocytosis, positive for BRAF VE1 by immunohistochemistry. The normal respiratory epithelium (right, center) also shows strong immunoreactivity at the ciliated border. This is a cross-reaction of the VE-1 antibody with dynein proteins present on cilia

transbronchial biopsy. The differential diagnosis not only varies depending on the stage of development of an LCH nodule but also on the prominence of smoking-related changes, which may sometimes obscure the LCH infiltrate.

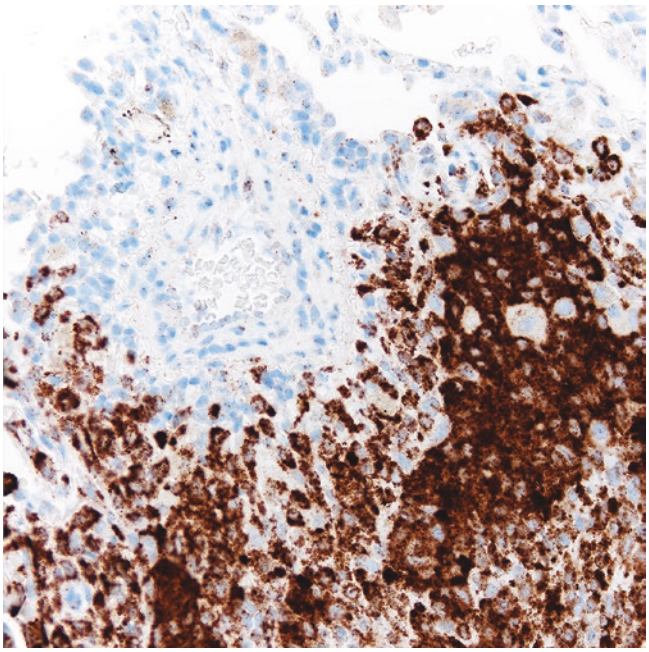

Fig. 15.131 Pulmonary Langerhans cell histiocytosis, positive for BRAF VE1 by immunohistochemistry

Early nodules of LCH may be confused with desquamative interstitial pneumonia, chronic eosinophilic pneumonia, or classic Hodgkin lymphoma involving the lung. Desquamative interstitial pneumonia consists of collections of macrophages filling alveolar spaces rather than interstitial cellular infiltrates containing Langerhans cells. In chronic eosinophilic pneumonia, the alveoli are laden with eosinophils, and these cells are not found in the interstitium or in a nodule with Langerhans cells. Pulmonary classic Hodgkin lymphoma can present as multiple nodules, and some of these may resemble pulmonary LCH given the presence of fibrosis and a polymorphic infiltrate containing macrophages, eosinophils, small lymphocytes, and multinucleated cells. However, *bona fide* Reed–Sternberg cells are not seen in LCH. Immunohistochemistry for CD1a, S100, and langerin/CD207 is helpful in confirming the presence of Langerhans cells, which is not a feature of CHL. In difficult cases, immunostains for CD15, CD30, and PAX5 may be required to exclude the presence of Reed–Sternberg cells.

Large and more cellular nodules of pulmonary LCH should be distinguished from non-Langerhans cell histiocytic disorders, ALCL, primary lung carcinoma, and metastatic carcinoma or melanoma. Pulmonary Rosai–Dorfman disease and Erdheim–Chester disease may resemble pulmonary LCH. In Rosai–Dorfman disease, there are large macrophages featuring emperipolesis, numerous plasma cells, and usually no eosinophils. The macrophages in Rosai–Dorfman disease are positive for S100, CD68, and CD163 and are negative for CD1a, CD207/langerin, and BRAF VE-1. In Erdheim–Chester disease, the histiocytic infiltrate produces

interstitial thickening with a lymphangitic distribution with an expansion of interlobular septa and bronchovascular bundles. There is variable fibrosis and chronic inflammation. The macrophages in Erdheim–Chester disease are positive for CD68, CD163, and variable S100 and are negative for CD1a and CD207/langerin. Consideration should be taken that a large subset of cases of Erdheim–Chester disease are positive for BRAF VE1. An indeterminate dendritic cell tumor is a histiocytic neoplasm that may be morphologically identical to LCH, expresses S100 and CD1a but is negative for langerin/CD207. This rare tumor, however, occurs preferentially in the skin, and lung involvement would be highly unusual.

ALCL and metastatic melanoma and carcinoma may resemble LCH at low power. However, at higher magnification, the neoplastic cells in all these processes have significant atypia and do not show other features of LCH. Moreover, the immunophenotype is completely different: ALCL is positive for >1 T-cell markers, CD30 and/or ALK, whereas melanoma and carcinoma show expression of melanocytic markers and keratins, respectively.

The late stages of pulmonary LCH need to be distinguished from other forms of interstitial lung disease (usually interstitial pneumonia) or other potential conditions that result in end-stage lung disease. Langerhans cells are not increased in any of these conditions. Additionally, clinical history of prior pulmonary LCH and smoking is extremely helpful, if available. Immunohistochemical stains for S100, CD1a, and/or langerin/CD207 may be required in some cases where pulmonary LCH may be suspected. The differential diagnosis of pulmonary LCH is summarized in Table 15.19.

Molecular Alterations

A breakthrough came to the field of histiocytoses in 2010 when the *BRAF* V600E mutation was identified in 50–70% of LCH cases by diverse molecular analyses [213, 214]. After those findings, other studies have identified mutations in multiple other genes codifying for proteins involved in the RAS/RAF/MAPK pathway, including *MAP2K1* (10–20% of cases) and single cases with *ARAF1* and *ERBB3* mutations [231–233]. About 50% of cases of pulmonary LCH also harbor *BRAF* V600E mutation, and about 40% of patients also harbor mutations in (Q61K)(/R) [216, 226, 234]. Alternative mechanisms of BRAF activation (*BRAF* fusions) have also been discovered by whole-exome sequencing [235]. All these findings point to a common mechanism of ERK activation as a major player in LCH pathogenesis and support a clonal origin of the disease at least in the majority of cases [213, 215, 231–233, 236, 237]. The clinical, radiologic, and histopathologic features of pulmonary histiocytic disorders are shown in Table 15.18.

Table 15.19 Differential diagnosis of Langerhans cell histiocytosis

Early/cellular stage
Desquamative interstitial pneumonia
Chronic eosinophilic pneumonia
Non-Langerhans cell histiocytoses: Rosai–Dorfman or Erdheim–Chester disease
Classic Hodgkin lymphoma
Anaplastic large cell lymphoma
Primary lung carcinoma
Metastatic carcinoma or melanoma
Late stage
Interstitial lung disease (usual interstitial pneumonia)
Other causes of end-stage lung disease

Extranodal Pulmonary Rosai–Dorfman Disease (RDD)

Introduction

Sinus histiocytosis with massive lymphadenopathy, or Rosai–Dorfman disease (RDD), is a rare histiocytic disorder with peculiar morphologic features. Although sporadic reports of this disease have been available since the early 1960s, it was not until 1969 when Rosai and Dorfman reported four cases of a self-limited nodal histiocytic disorder that they called massive lymphadenopathy with sinus histiocytosis [238]. During the late 1970s and mid-1980s, Foucar, Rosai and Dorfman collected >100 cases of the disease from around the world, created a registry, and presented a detailed clinicopathologic spectrum of the disease, namely its overall benign behavior and its nodal or extranodal presentation [239–241]. Pulmonary RDD is very rare and is usually part of multiorgan or systemic involvement with sporadic cases of localized tracheal or peribronchial disease [242–246]. Infrequent cases of pulmonary RDD and IgG4-related disease have also been reported [247]. The Histiocyte Society classifies this histiocytic disorder in the group "R" for "Rosai–Dorfman" [215]. Recent studies have shown that a subset of RDD cases is negative for *BRAF* mutations but harbor mutations in *MAPK1* and *KRAS* [248], supporting that at least some cases are clonal.

Clinical Features

Rosai–Dorfman disease involving the lung is very rare, and it may be a manifestation of regional disease or systemic involvement. There is no association between pulmonary RDD and cigarette smoking. The disease can mimic lung cancer, pulmonary LCH, or interstitial lung disease [242–247, 249–253]. In the largest series to date of RDD with lung involvement from France (15 cases), the disease was more common in males, with a median age at diagnosis of 40 years, and the three most common extrapulmonary sites of disease included lymph node, skin, and bone [244]. Some individuals may be asymptomatic while symptomatic patients may present with dyspnea, non-productive cough,

chest pain, pleural effusion, and occasionally systemic symptoms. Common laboratory abnormalities include polyclonal hypergammaglobulinemia and hemolytic anemia [240, 254, 255]. Treatment with corticosteroids and immunomodulatory drugs has variable responses [243, 249] and in some instances, surgical resection may be required when RDD compromises the airways. More recently, there have been promising results with the use of MEK inhibitors [244].

Diagnostic Imaging

Thoracic involvement is reported in 4% of patients with Rosai–Dorfman disease (RDD). Mediastinal and hilar lymphadenopathy and tracheobronchial disease are the most commonly reported thoracic manifestations. Enlarged lymph nodes show homogeneous enhancement on contrast-enhanced CT and calcification is usually absent. Tracheobronchial involvement often results in an intraluminal polypoid mass and less commonly manifests as circumferential wall thickening. Lung parenchymal involvement is less common than airway disease and manifests as a nodule or mass. The lung nodule or mass can have spiculated margins and infiltrate adjacent structures. These lesions are FDG avid on PET/CT and can be difficult to differentiate from primary lung cancer. Biopsy is generally needed to confirm the diagnosis [256, 257] (Fig. 15.132a–c).

Pathology

Grossly, pulmonary RDD has been described as white-yellow masses with relatively well-circumscribed borders. A mass may be located in the lung parenchyma or in the tracheobron-

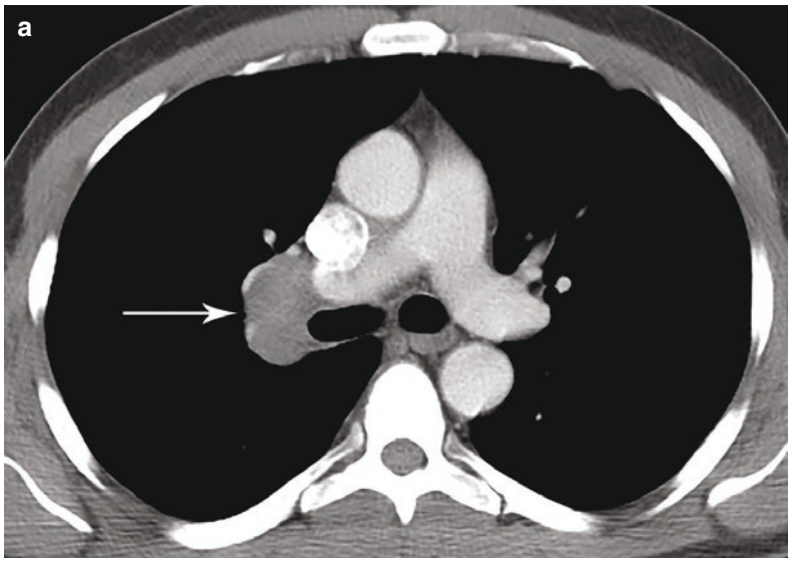

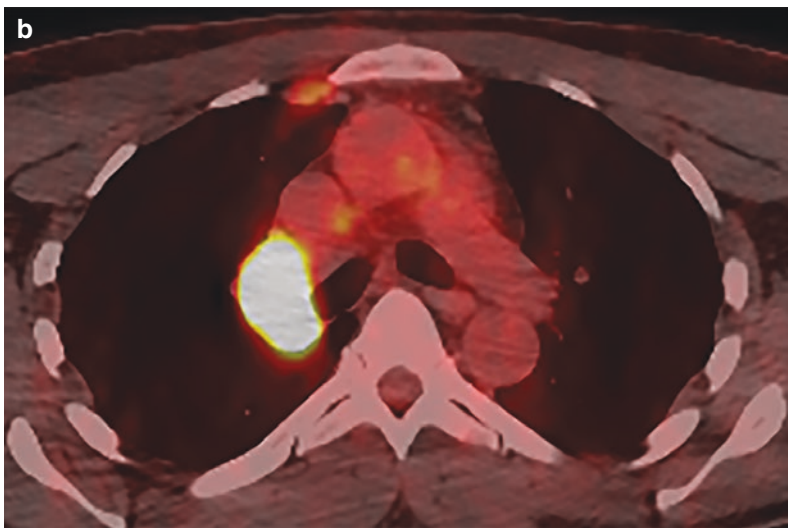

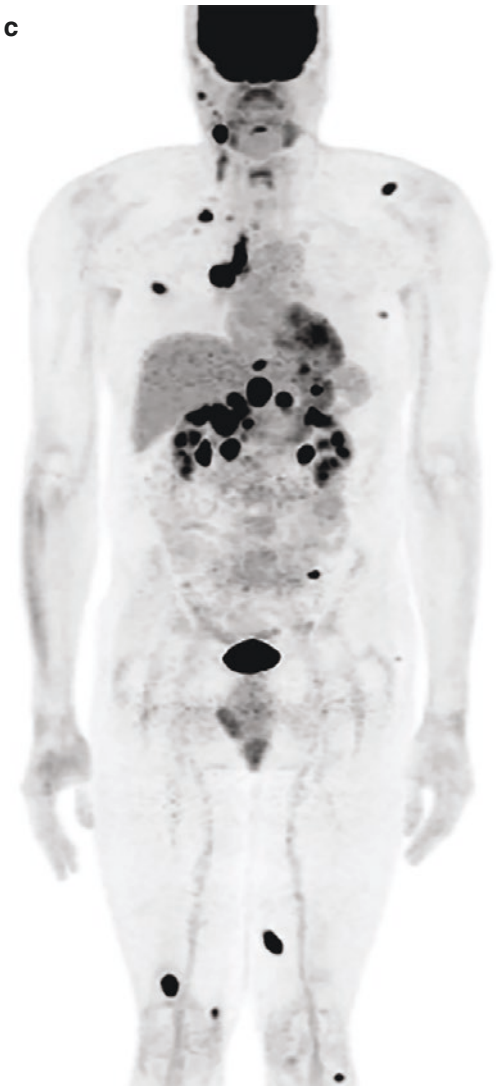

Fig. 15.132 Rosai–Dorfman disease presents with right hilar adenopathy on contrast-enhanced CT (**a**) that is FDG avid on PET/CT (**b**). Whole-body PET (**c**) shows the involvement of lymph nodes in the right cervical, right supraclavicular, right mediastinal, right hilar, and abdominal regions, as well as the bones, muscles, and subcutaneous soft tissues

chial tree. The infiltrate is diffuse with replacement of the architecture. At low power, pulmonary RDD has a "moth-eaten appearance" with variable fibrosis and usually alternating pale and dark areas containing macrophages and abundant lymphocytes and plasma cells (Fig. 15.133), respectively, that give the tissue the resemblance of a lymph node. The macrophages have a central oval nucleus, prominent nucleolus, and voluminous amphophilic cytoplasm filled with a variable number of intact lymphocytes, plasma cells, and/or neutrophils (Fig. 15.134). This feature is known as emperipolesis, a type of transcytosis in which leukocytes have entered the macrophages but remain intact, and it is a pathognomonic finding in this disease [258, 259]. Multinucleated cells, necrosis, hemophagocytosis, or increased eosinophils are infrequent. Areas adjacent of lung parenchyma show alveolar wall thickening, type 2 pneumocyte hyperplasia, and a variable number of foamy intra-alveolar macrophages. Lesions in the tracheobronchial tree partially replace the wall of the airway, and disease located in the hilum demonstrates extension into peribronchial lymph nodes. In cases with an interstitial pattern of spread, the large macrophages and the inflammatory component demonstrate a lymphangitic pattern (bronchiolar, interlobular septa, subpleural) and variable fibrosis.

Immunohistochemistry and Other Ancillary Studies

The macrophages in RDD are weakly positive for CD4 and positive for CD68, CD163, and S100 (Fig. 15.135a, b), and in some cases they may also be positive for CD30 [260], whereas they are negative for CD1a, CD207/langerin, BRAF VE-1, ALK, and any B-cell or T-cell marker. S100, CD68, and CD163 highlight the emperipolesis. Plasma cells are always polytypic. IgG4+ plasma cells may be increased or not, and when they are increased, the possibility of an associated IgG4-related disease should be considered [261–263].

Differential Diagnosis

Pulmonary RDD should be distinguished from infectious/inflammatory processes rich in macrophages, pulmonary LCH, pulmonary Erdheim–Chester disease, pulmonary ALCL, and primary or metastatic tumors to the lung.

Pulmonary infiltration by RDD can mimic an atypical mycobacterial infection, an inflammatory pseudotumor or malakoplakia. AFB and GMS stains should be performed to exclude the presence of microorganisms. Immunohistochemical stains are required to support the presence of S100+, CD68+, and/or CD163+ macrophages to confirm the diagnosis of RDD. In addition, immunohistochemistry for IgG4+ is recommended to exclude the possibility of an associated IgG4-related disease. RDD does not contain Michaelis–Goodman bodies, as seen in malakoplakia.

Although pulmonary LCH may resemble pulmonary RDD clinically and radiologically, in the former the histiocytic component consists mostly of Langerhans cells, multinucleated giant cells, and eosinophils that are not features of

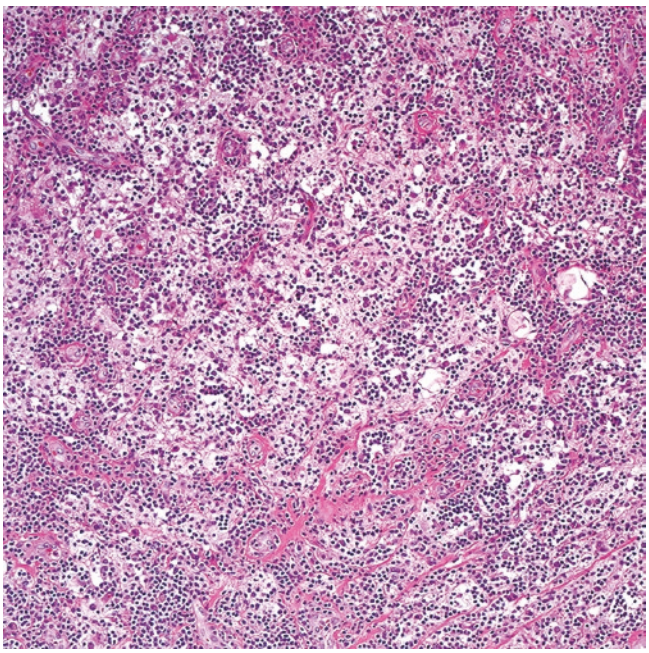

Fig. 15.133 Extranodal Rosai–Dorfman disease. Macrophages with emperipolesis are seen as pale or "moth-eaten" areas alternating with darker areas containing small lymphocytes and plasma cells. There is variable fibrosis in the background

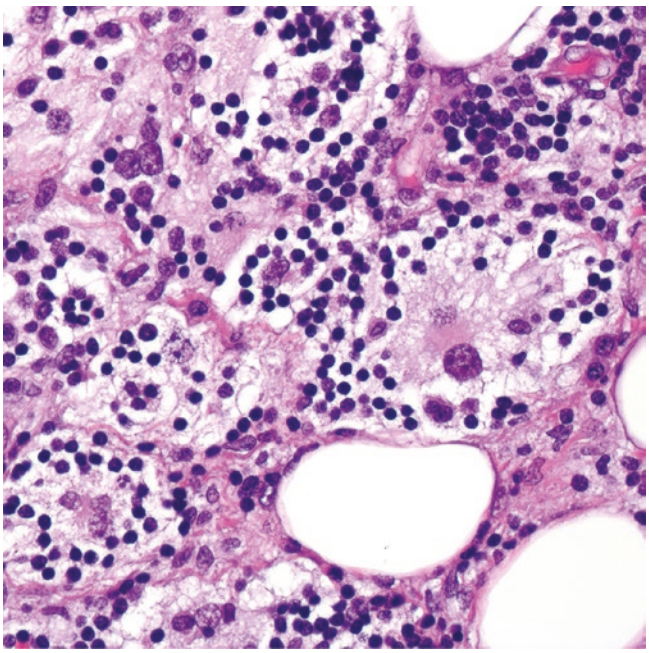

Fig. 15.134 The macrophages in Rosai–Dorfman disease have voluminous cytoplasm and contain a variable number of intracytoplasmic lymphocytes and other leukocytes, a phenomenon called emperipolesis

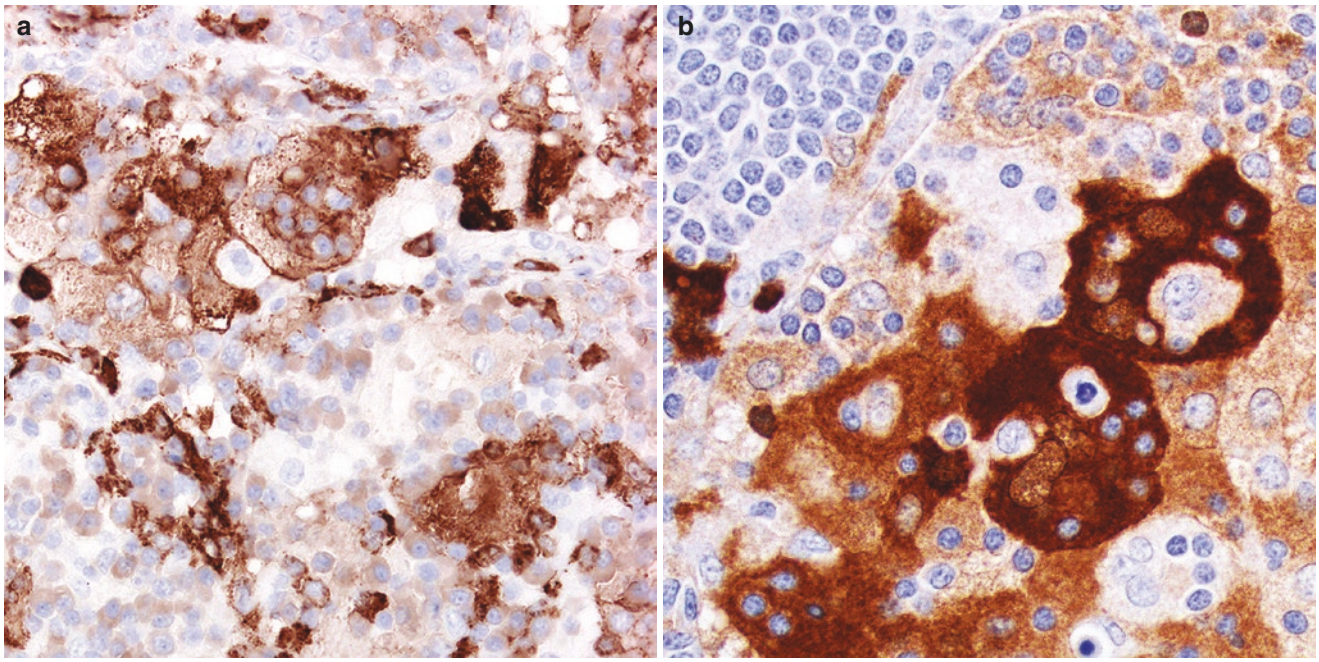

Fig. 15.135 The macrophages in Rosai–Dorfman disease are positive for (**a**) CD68 and (**b**) S100. Both immunostains accentuate intracytoplasmic leukocytes that are negative for these markers

RDD. Emperipolesis is not present in LCH, and by immunohistochemistry, this disease is positive for S100, CD1a, and CD207/langerin with only focal CD68 and CD163, which differs from the findings in RDD. Erdheim–Chester disease is a multiorgan histiocytosis that can affect bone, brain, perirenal and periaortic soft tissues, and the lung [215]. These clinical features are not seen in RDD. Histologically, Erdheim–Chester disease is composed of a bland histiocytic infiltrate with chronic inflammation and variable fibrosis. Some cases harbor a *BRAF* V600E mutation and therefore are positive for the BRAF VE-1 antibody [264]. As mentioned above, BRAF mutations have not been identified in RDD. Pathologists should be aware that some cases of Erdheim–Chester disease may present with identical morphologic features to RDD, and thus, detection of *BRAF* V600E in an otherwise classic case of RDD should raise concern for Erdheim–Chester disease and further evaluation of the patient [265].

Pulmonary ALCL, primary lung cancer, and metastatic melanoma and carcinoma to the lung may resemble RDD at low power. However, at higher magnification, the neoplastic cells in all these processes have significant atypia and do not show emperipolesis or increased plasma cells. Moreover, the immunophenotype is completely different: ALCL is positive for >1 T-cell markers, CD30 and/or ALK, whereas melanoma and carcinoma show expression of melanocytic markers and keratins, respectively. These markers are negative in RDD. Table 15.20 summarizes the differential diagnosis of pulmonary RDD.

Table 15.20 Differential diagnosis of pulmonary Rosai–Dorfman disease

Atypical mycobacterial infection
Pulmonary Langerhans cell histiocytosis
Pulmonary Erdheim–Chester disease
Primary lung cancer, and metastatic melanoma and carcinoma to the lung
Pulmonary malakoplakia

Molecular Findings

RDD may develop secondary to an abnormal macrophage activation response due to immune dysregulation or possibly a viral infection [266–269]. A small subset of cases can occur in association with IgG4-related disease [261–263]. RDD has been reported in identical twins suggesting an underlying genetic component [270]. In addition, the rare hereditary disorders Faisalabad histiocytosis and the "H" syndrome (hyperpigmentation, hypertrichosis, hearing loss, heart anomalies, hepatomegaly, hypogonadism, hyperglycemia, low height, hallux valgus, and hematologic abnormalities) that occur secondary to mutations in the nucleoside transporter SLC29A3 can show histopathologic features reminiscent of RDD [271, 272]. Recent studies have shown that a subset of cases are negative for *BRAF* mutations but instead harbor mutations in *MAPK1*, another molecule of the RAS/RAF/MAPK pathway, as well as mutations in *KRAS* [248], suggesting that a subset of cases is clonal and may benefit from targeted therapies [273, 274].

The clinical, radiologic, and histopathologic features of pulmonary histiocytic disorders are shown in Table 15.18.

Pulmonary Erdheim–Chester Disease (ECD)

Introduction

The eponym "Erdheim–Chester" was coined by Jaffe after reviewing the original description of two cases of a particular lipoid granulomatosis previously reported by Chester in 1930 while he was doing a fellowship with the legendary Austrian pathologist Erdheim [275, 276]. ECD is a rare non-Langerhans cell histiocytosis once considered an orphan disease. Nevertheless, to date ECD is better recognized. The disease is characterized by recurrent genetic alterations in the RAS/RAF/MAPK signaling pathway in about 50% of patients [227, 265]. In one of the largest and most comprehensive studies of 42 patients with ECD, lung involvement was seen only in 6 patients (14%) [265].

Clinical Features

ECD is a rare condition that mostly affects adults 40–60 years of age. The disease has a male-to-female ratio of 3:1. About 95% of patients with ECD have bone involvement as bilateral and symmetric osteosclerosis of the diaphysis/metaphysis of long bones (femur, tibia, humerus) [277]. Other symptoms are widely variable and include xanthelasmas, pericardial fibrosis with restrictive cardiac symptoms, peri-aortic fibrosis, retroperitoneal fibrosis with obstruction of both ureters and development of renal failure, diabetes insipidus due to central nervous system involvement, and exophthalmos [278–280]. Given the rarity of ECD and the unrelated and wide range of clinical symptoms, some individuals may go underdiagnosed for several years, while some others have been diagnosed only after a post-mortem examination. For this reason, consensus criteria for diagnosis of ECD were created in an attempt to better recognize these patients, which include (1) the presence of xanthogranulomatous lesions composed of foamy CD68+/CD1a-negative macrophages often with admixed inflammation and fibrosis and (2) skeletal findings of bilateral and symmetric abnormalities in the diaphyseal and metaphyseal regions of the long bones of the legs [281]. Pulmonary involvement by ECD includes the presence of progressive dyspnea over a period of months or years. Pulmonary function tests demonstrate a restrictive pattern. An unusual presentation of pulmonary ECD from miliary disease to large tumors has been described recently [282]. The traditional therapeutic approach for ECD has been based on immunomodulatory agents, anti-cytokine therapies, and immunosuppressants. However, targeted treatment with BRAF and MEK inhibitors is becoming the first choice in patients with severe disease [283].

Diagnostic Imaging

Erdheim–Chester disease can involve the heart, mediastinum, pleura, and lung parenchyma. Lung involvement can occur in up to two-thirds of patients. The most commonly described pulmonary finding on CT is interlobular septal thickening that can be focal or diffuse. Pulmonary nodules are reported in 20–60% of patients and can be variable in distribution. Ground glass opacities have been described in up to 40% of patients and can exhibit subpleural or peribronchovascular distribution. Other less common imaging manifestations include consolidation or bronchial wall thickening. The most common mediastinal finding with ECD is periaortic soft tissue thickening. Mediastinal fat infiltration and lymphadenopathy are less common manifestations. Pleural involvement may result in unilateral or bilateral pleural effusions that can be associated with focal or diffuse pleural thickening [284] (Fig. 15.136a–c).

Pathology

Given the rarity of this disease, gross pathologic descriptions of pulmonary ECD are not available. Microscopically, ECD consists in a proliferation of histiocytes associated with variable degrees of fibrosis and chronic inflammation composed of small lymphocytes and few plasma cells (Fig. 15.137). The macrophages usually have a small round nucleus with condensed chromatin and may or may not have voluminous or foamy cytoplasm. Macrophages are typically distributed in cords or in a single cell arrangement. Multinucleated giant cells of the Touton type are common. Emperipolesis is unusual, and cellular atypia and well-formed granulomas are not seen. Lung involvement occurs in a lymphangitic distribution associated with thickening of the pleura, interlobular septa, and perivascular interstitium with lesser involvement of peribronchiolar areas [265]. A subset of ECD cases may be accompanied by LCH [229], but these unusual cases have not been reported in the lung. Bronchioalveolar lavages contain abundant foamy macrophages, but this is nonspecific for diagnosis.

Immunohistochemistry and Other Ancillary Studies

The histiocytes in ECD are positive for CD68 and CD163, with variable positivity for other monocytic markers and Factor XIIIa (Fig. 15.138). S100 is focal, and CD1a and langerin/CD207 are negative. BRAF (VE-1) is positive in about 50% of cases.

Differential Diagnosis

Pulmonary ECD should be distinguished from an atypical mycobacterial infection, drug reaction, interstitial lung disease (usual interstitial pneumonia), pulmonary LCH, and pulmonary RDD [265].

AFB and GMS stains should be performed to exclude the presence of microorganisms. In a drug reaction, there are variable amounts of intra-alveolar macrophages in contrast to the pattern of spread and association with fibrosis seen in pulmonary ECD. Clinical and radiologic correlation is also

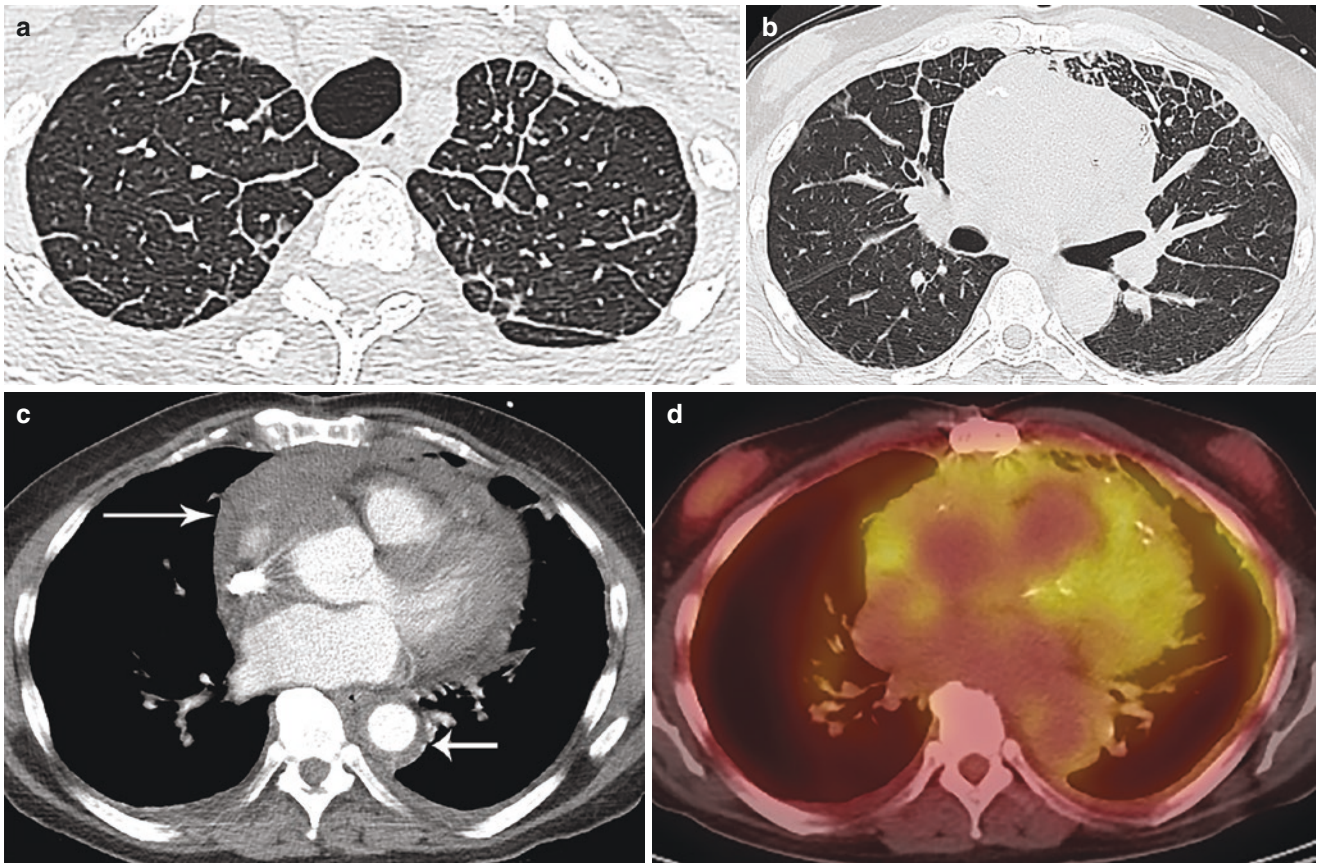

Fig. 15.136 Erdheim–Chester disease presents with interlobular septal thickening in the lungs, more pronounced on the left (**a**, **b**), periaortic soft tissue thickening (short arrow), and involvement of the pericardium (long arrow) and bilateral pleurae on contrast-enhanced CT (**c**). Pericardial thickening and fluid show FDG avidity on PET/CT (**d**)

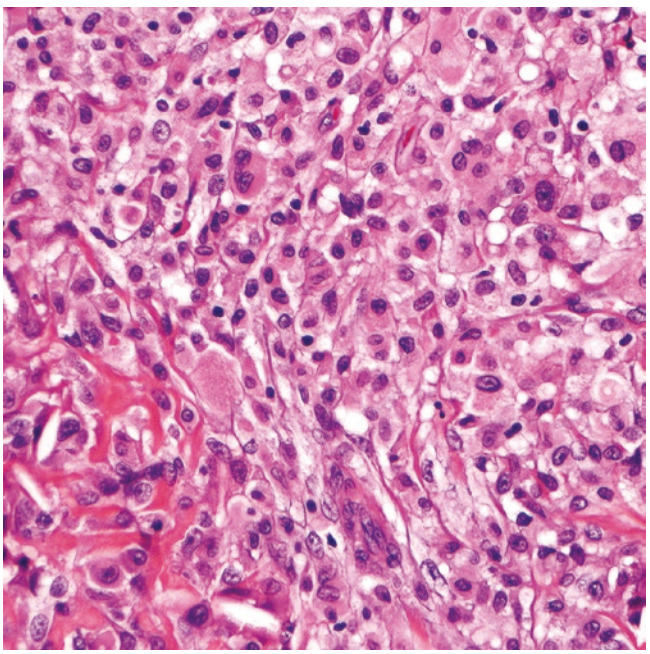

Fig. 15.137 Erdheim–Chester disease. There is an exuberant infiltrate of histiocytes, some with foamy cytoplasm and variable fibrosclerosis

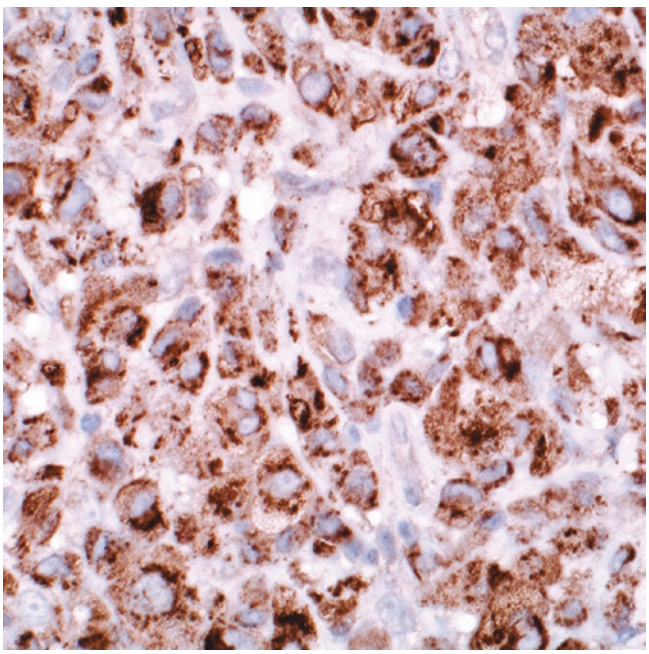

Fig. 15.138 Erdheim–Chester disease. The CD68 immunostain is positive in macrophages

useful to identify features that may favor or not ECD. Despite the presence of subpleural and septal fibrosis in pulmonary ECD, there is no temporal heterogeneity and fibroblastic foci as seen in usual interstitial pneumonia. In addition, the presence of macrophages interspersed among fibrosis supports ECD and not usual interstitial pneumonia.

The overlapping histopathology of pulmonary ECD with pulmonary LCH and RDD makes the diagnosis somewhat challenging. However, a detailed morphologic evaluation along with clinical and radiologic data is usually sufficient to arrive at the correct diagnosis [281]. Pulmonary LCH and RDD may show a similar pattern of distribution as ECD, but the typical cytologic features of LCH (Langerhans cells with cleaved or bean-shaped nuclei with grooves, abundant eosinophils) are not seen in ECD. The interstitial pattern of distribution of RDD in the lung may mimic that of ECD. And although emperipolesis is not a common feature in ECD, the distinction between these entities may primarily rely on clinical and radiologic findings and evaluation of molecular abnormalities. About 50% of cases of ECD harbor a *BRAF* V600E mutation and therefore these cases are positive for the BRAF VE-1 antibody [264], whereas BRAF mutations have not been identified in RDD. Importantly, pathologists should be aware that some cases of ECD may present with identical morphologic features to RDD, and therefore, detection of *BRAF* V600E in an otherwise classic case of RDD should raise concern for ECD and further evaluation of the patient [265, 285].

The differential diagnosis of pulmonary ECD is summarized in Table 15.21.

Molecular Findings

About 50% of ECD cases harbor BRAF V600E mutations [227, 264], and *BRAF* wild-type cases have mutations in *MAP2K1*. Few cases harbor mutations of *NRAS, KRAS*, and fusions in the *PIK3CA* and *ALK* genes [286, 287]. ERK activation appears to represent an important mechanism related to the pathogenesis of ECD, which explains the existence of cases with a concomitant presentation of ECD and LCH. Identification of *BRAF V600E* mutation not only supports the clonal origin of ECD but also has been crucial for the use of BRAF inhibitors as therapeutic targets [227, 264, 278, 283, 288].

The clinical, radiologic, and histopathologic features of pulmonary histiocytic disorders are shown in Table 15.18.

Table 15.21 Differential diagnosis of pulmonary Erdheim–Chester disease

- Atypical mycobacterial infection
- Drug reaction rich in intraalveolar foamy macrophages
- Pulmonary Langerhans cell histiocytosis
- Pulmonary Rosai–Dorfman disease (RDD)
  - If morphology of RDD but BRAF+, this is Erdheim–Chester disease mimicking RDD
- Interstitial lung disease (usual interstitial pneumonia)

Pulmonary Juvenile Xanthogranuloma (PJXG)

Introduction

This is an unusual non-Langerhans cell histiocytosis of unusual occurrence in the lung, with only a few cases reported in the literature [289–292]. Although the origin of this process is not well known, possibilities mentioned in the literature include dendrocytes and plasmacytoid monocytes [290].

Clinical Features

PJXG is more common in children and young adults, and when the lungs are affected, the lesions typically appear as bilateral or unilateral pulmonary nodules. Although single nodules may also occur, they are uncommon. Dermal or other visceral involvement may occur. Due to the rare incidence of this process in the lung, it is difficult to determine clinical outcomes. However, it may be linked to the extent of the disease at the time of diagnosis.

Pathology

The pulmonary nodules appear well circumscribed but not encapsulated, replacing normal lung parenchyma. At high power, the nodules show a histiocytic proliferation composed of small- or medium-size cells with or without nucleoli, which can be associated with an inflammatory reaction composed of lymphocytes and plasma cells. In addition, scattered among the histiocytic proliferation, there are multinucleated giant cells (Fig. 15.139a–c). However, these giant cells may be difficult to find. Nuclear atypia, mitotic activity, necrosis, and/or hemorrhage are not common features in PJXG.

Immunohistochemistry

As in other histiocytic lesions, the cells in PJXG may show positive staining for CD68, factor XIIIa, HLA-DR, LCA (CD-45), CD4, and S-100 protein. However, CD1a, CD3, CD21, CD34, and CD35 are negative.

Differential Diagnosis

The most important differential diagnosis is with other histiocytic lesions that may occur in the lung parenchyma. However, a wider panel of immunohistochemical stains and the presence of multinucleated giant cells among the histiocytic proliferation may lead to a correct interpretation.

Pulmonary Crystal-Storing Histiocytosis

Introduction

This process may or may not be associated with another lymphoproliferative disorder [293, 294]. When it appears in isolation without any lymphoproliferative disorder, the term

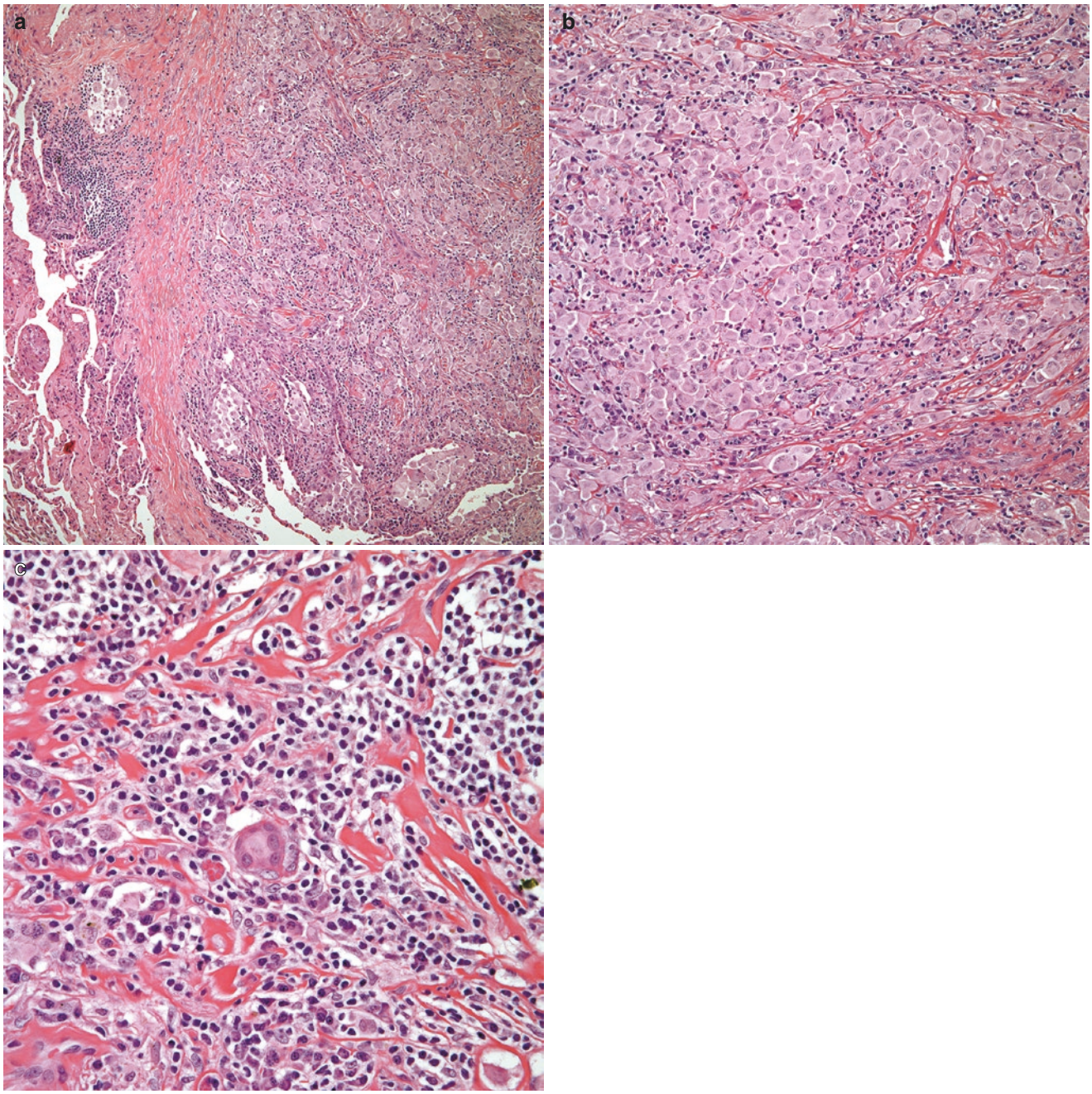

Fig. 15.139 (**a**) Low power view of a PJXG, (**b**) Histiocytic proliferation replacing normal lung parenchyma, (**c**) Scattered multinucleated giant cells

crystal-storing histiocytoma has been suggested. If the process is associated with a lymphoproliferative process, then the nomenclature crystal-storing histiocytosis is suggested. Multiple myeloma is the most common association. The histiocytes appear to store three different components: (1) crystallized immunoglobulins, (2) phagocytosed clofazimine (patients treated for leprosy), and (3) Charcot–Leyden crystals.

The clinical outcome of these patients is given by the underlying conditions that may be associated.

Pathology

At low power view, the alveoli appear to be filled with an eosinophilic material giving the appearance of fibrinous exudate. However, at higher magnification, the eosinophilic material is composed of histocytes with ample cytoplasm and small round nuclei in crystal-storing histiocytosis. The cytoplasm of the cells is filled with crystalloid material (immunoglobulins). In distinction, in cases of crystal-storing histiocytoma, the lung parenchyma is replaced by a histio-

cytic cellular proliferation, which may show elongated cells imitating the appearance of a spindle cell proliferation.

Immunohistochemistry

CD68 shows positive staining in the histiocytic proliferation, while kappa or gamma testing may show monoclonal rearrangement.

References

1. Bienenstock J, Johnston N, Perey DY. Bronchial lymphoid tissue. II. Functional characterisitics. Lab Invest. 1973;28:693–8.
2. Bienenstock J, Johnston N, Perey DY. Bronchial lymphoid tissue. I. Morphologic characteristics. Lab Invest. 1973;28:686–92.
3. Kelemen K, Rimsza LM, Craig FE. Primary Pulmonary B-cell Lymphoma. Semin Diagn Pathol. 2020;37:259–67.
4. Koss MN. Pulmonary lymphoid disorders. Semin Diagn Pathol. 1995;12:158–71.
5. Saltzstein SL. Pulmonary malignant lymphomas and pseudolymphomas: classification, therapy, and prognosis. Cancer. 1963;16:928–55.
6. Koss MN. Malignant and benign lymphoid lesions of the lung. Ann Diagn Pathol. 2004;8:167–87.
7. Kradin RL, Mark EJ. Benign lymphoid disorders of the lung, with a theory regarding their development. Hum Pathol. 1983;14:857–67.
8. Abbondanzo SL, Rush W, Bijwaard KE, Koss MN. Nodular lymphoid hyperplasia of the lung: a clinicopathologic study of 14 cases. Am J Surg Pathol. 2000;24:587–97.
9. Quarello P, Bianchi M, Gambella A, et al. Pulmonary nodular lymphoid hyperplasia in pediatric patients with Hodgkin lymphoma. Pediatr Hematol Oncol. 2020;37:424–30.
10. Guinee DG Jr, Franks TJ, Gerbino AJ, Murakami SS, Acree SC, Koss MN. Pulmonary nodular lymphoid hyperplasia (pulmonary pseudolymphoma): the significance of increased numbers of IgG4-positive plasma cells. Am J Surg Pathol. 2013;37:699–709.
11. Colby TV, Yousem SA. Pulmonary lymphoid neoplasms. Semin Diagn Pathol. 1985;2:183–96.
12. Pina-Oviedo S, Weissferdt A, Kalhor N, Moran CA. Primary pulmonary lymphomas. Adv Anat Pathol. 2015;22:355–75.
13. Yell M, Rosado FG. Pulmonary nodular lymphoid hyperplasia. Arch Pathol Lab Med. 2019;143(9):1149–53.
14. Nicholson AG, Wotherspoon AC, Diss TC, et al. Reactive pulmonary lymphoid disorders. Histopathology. 1995;26:405–12.
15. Gibson M, Hansell DM. Lymphocytic disorders of the chest: pathology and imaging. Clin Radiol. 1998;53:469–80.
16. Liebow AA, Carrington CB. Diffuse pulmonary lymphoreticular infiltrations associated with dysproteinemia. Med Clin North Am. 1973;57:809–43.
17. Travis WD, Fox CH, Devaney KO, et al. Lymphoid pneumonitis in 50 adult patients infected with the human immunodeficiency virus: lymphocytic interstitial pneumonitis versus nonspecific interstitial pneumonitis. Hum Pathol. 1992;23:529–41.
18. Tanaka N, Kim JS, Bates CA, et al. Lung diseases in patients with common variable immunodeficiency: chest radiographic, and computed tomographic findings. J Comput Assist Tomogr. 2006;30:828–38.
19. Bragg DG, Chor PJ, Murray KA, Kjeldsberg CR. Lymphoproliferative disorders of the lung: histopathology, clinical manifestations, and imaging features. AJR Am J Roentgenol. 1994;163:273–81.
20. Kaan PM, Hegele RG, Hayashi S, Hogg JC. Expression of bcl-2 and Epstein-Barr virus LMP1 in lymphocytic interstitial pneumonia. Thorax. 1997;52:12–6.
21. Barbera JA, Hayashi S, Hegele RG, Hogg JC. Detection of Epstein-Barr virus in lymphocytic interstitial pneumonia by in situ hybridization. Am Rev Respir Dis. 1992;145:940–6.
22. Yum HK, Kim ES, Ok KS, Lee HK, Choi SJ. Lymphocytic interstitial pneumonitis associated with Epstein-Barr virus in Systemic Lupus Erythematosus and Sjogren's Syndrome. Complete remission with corticosteriod and cyclophosphamide. Korean J Intern Med. 2002;17:198–203.
23. Swigris JJ, Berry GJ, Raffin TA, Kuschner WG. Lymphoid interstitial pneumonia: a narrative review. Chest. 2002;122:2150–64.
24. Panchabhai TS, Farver C, Highland KB. Lymphocytic Interstitial Pneumonia. Clin Chest Med. 2016;37:463–74.
25. Fishback N, Koss M. Update on lymphoid interstitial pneumonitis. Curr Opin Pulm Med. 1996;2:429–33.
26. Hamano H, Kawa S, Horiuchi A, et al. High serum IgG4 concentrations in patients with sclerosing pancreatitis. N Engl J Med. 2001;344:732–8.
27. Kamisawa T, Funata N, Hayashi Y, et al. A new clinicopathological entity of IgG4-related autoimmune disease. J Gastroenterol. 2003;38:982–4.
28. Kamisawa T, Funata N, Hayashi Y, et al. Close relationship between autoimmune pancreatitis and multifocal fibrosclerosis. Gut. 2003;52:683–7.
29. Bledsoe JR, Della-Torre E, Rovati L, Deshpande V. IgG4-related disease: review of the histopathologic features, differential diagnosis, and therapeutic approach. Apmis. 2018;126:459–76.
30. Zhang XQ, Chen GP, Wu SC, et al. Solely lung-involved IgG4-related disease : a case report and review of the literature. Sarcoidosis Vasc Diffuse Lung Dis. 2016;33:398–406.
31. Yi ES, Sekiguchi H, Peikert T, Ryu JH, Colby TV. Reprint of: Pathologic manifestations of Immunoglobulin(Ig)G4-related lung disease. Semin Diagn Pathol. 2018;35:347–51.
32. Kang J, Park S, Chae EJ, et al. Long-term clinical course and outcomes of immunoglobulin G4-related lung disease. Respir Res. 2020;21:273.
33. Lv X, Gao F, Liu Q, et al. Clinical and pathological characteristics of IgG4-related interstitial lung disease. Exp Ther Med. 2018;15:1465–73.
34. Deshpande V, Zen Y, Chan JK, et al. Consensus statement on the pathology of IgG4-related disease. Mod Pathol. 2012;25:1181–92.
35. Otani K, Inoue D, Itoh T, Zen Y. Transbronchial lung biopsy for the diagnosis of IgG4-related lung disease. Histopathology. 2018;73:49–58.
36. Slim D, Gunawardena H, Calvert JM, Daly RS, Plummeridge MJ, Medford AR. IgG4-related pulmonary disease: the protean impersonator? J R Coll Physicians Edinb. 2018;48:130–3.
37. Ikeda S, Sekine A, Baba T, et al. Abundant immunoglobulin (Ig) G4-positive plasma cells in interstitial pneumonia without extrathoracic lesions of IgG4-related disease: is this finding specific to IgG4-related lung disease? Histopathology. 2017;70:242–52.
38. Nishimura MF, Igawa T, Gion Y, et al. Pulmonary manifestations of plasma cell type idiopathic multicentric castleman disease: a clinicopathological study in comparison with IgG4-related disease. J Pers Med. 2020;10:269.
39. Zhang XY, Gu DM, Guo JJ, Su QQ, Chen YB. Primary Pulmonary Lymphoma: A Retrospective Analysis of 27 Cases in a Single Tertiary Hospital. Am J Med Sci. 2019;357:316–22.
40. Sirajuddin A, Raparia K, Lewis VA, et al. Primary pulmonary lymphoid lesions: radiologic and pathologic findings. Radiographics. 2016;36:53–70.
41. Nicholson AG, Harris NL. Marginal zone B-cell lymphoma of the mucosa-associated lymphoid tissue (MALT) type. In: Travis WD, Brambilla E, Müller-Hermelink HK, Harris CC, editors. WHO classification of tumours, pathology and genetics, tumours of the lung, pleura, thymus and heart. Lyon: IARC Press; 2004. p. 88–90.
42. Berkman N, Breuer R, Kramer MR, Polliack A. Pulmonary involvement in lymphoma. Leuk Lymphoma. 1996;20:229–37.

43. Hare SS, Souza CA, Bain G, et al. The radiological spectrum of pulmonary lymphoproliferative disease. Br J Radiol. 2012;85:848–64.
44. Mentzer SJ, Reilly JJ, Skarin AT, Sugarbaker DJ. Patterns of lung involvement by malignant lymphoma. Surgery. 1993;113:507–14.
45. Isaacson P, Wright DH. Malignant lymphoma of mucosa-associated lymphoid tissue. A distinctive type of B-cell lymphoma. Cancer. 1983;52:1410–6.
46. Sanguedolce F, Zanelli M, Zizzo M, et al. Primary pulmonary B-cell lymphoma: a review and update. Cancers (Basel). 2021;13:415.
47. Khalil MO, Morton LM, Devesa SS, et al. Incidence of marginal zone lymphoma in the United States, 2001–2009 with a focus on primary anatomic site. Br J Haematol. 2014;165:67–77.
48. Borie R, Wislez M, Thabut G, et al. Clinical characteristics and prognostic factors of pulmonary MALT lymphoma. Eur Respir J. 2009;34:1408–16.
49. Zinzani PL, Poletti V, Zompatori M, et al. Bronchus-associated lymphoid tissue lymphomas: an update of a rare extranodal maltoma. Clin Lymphoma Myeloma. 2007;7:566–72.
50. Ahmed S, Kussick SJ, Siddiqui AK, et al. Bronchial-associated lymphoid tissue lymphoma: a clinical study of a rare disease. Eur J Cancer. 2004;40:1320–6.
51. Koss MN, Hochholzer L, Nichols PW, Wehunt WD, Lazarus AA. Primary non-Hodgkin's lymphoma and pseudolymphoma of lung: a study of 161 patients. Hum Pathol. 1983;14:1024–38.
52. Cordier JF, Chailleux E, Lauque D, et al. Primary pulmonary lymphomas. A clinical study of 70 cases in nonimmunocompromised patients. Chest. 1993;103:201–8.
53. He H, Tan F, Xue Q, et al. Clinicopathological characteristics and prognostic factors of primary pulmonary lymphoma. J Thorac Dis. 2021;13:1106–17.
54. Okamura I, Imai H, Mori K, et al. Rituximab monotherapy as a first-line treatment for pulmonary mucosa-associated lymphoid tissue lymphoma. Int J Hematol. 2015;101(1):46–51.
55. Du C, Zhang J, Wei Y, et al. Retrospective analysis of 9 cases of primary pulmonary mucosa-associated lymphoid tissue lymphoma and literature review. Med Sci Monit Basic Res. 2018;24:233–40.
56. Carter BW, Wu CC, Khorashadi L, et al. Multimodality imaging of cardiothoracic lymphoma. Eur J Radiol. 2014;83:1470–82.
57. Bae YA, Lee KS, Han J, et al. Marginal zone B-cell lymphoma of bronchus-associated lymphoid tissue: imaging findings in 21 patients. Chest. 2008;133:433–40.
58. Wislez M, Cadranel J, Antoine M, et al. Lymphoma of pulmonary mucosa-associated lymphoid tissue: CT scan findings and pathological correlations. Eur Respir J. 1999;14:423–9.
59. Maksimovic O, Bethge WA, Pintoffl JP, et al. Marginal zone B-cell non-Hodgkin's lymphoma of mucosa-associated lymphoid tissue type: imaging findings. AJR Am J Roentgenol. 2008;191:921–30.
60. Kurtin PJ, Myers JL, Adlakha H, et al. Pathologic and clinical features of primary pulmonary extranodal marginal zone B-cell lymphoma of MALT type. Am J Surg Pathol. 2001;25:997–1008.
61. Addis BJ, Hyjek E, Isaacson PG. Primary pulmonary lymphoma: a re-appraisal of its histogenesis and its relationship to pseudolymphoma and lymphoid interstitial pneumonia. Histopathology. 1988;13:1–17.
62. Zhang C, Myers JL. Crystal-storing histiocytosis complicating primary pulmonary marginal zone lymphoma of mucosa-associated lymphoid tissue. Arch Pathol Lab Med. 2013;137:1199–204.
63. Johrens K, Shimizu Y, Anagnostopoulos I, et al. T-bet-positive and IRTA1-positive monocytoid B cells differ from marginal zone B cells and epithelial-associated B cells in their antigen profile and topographical distribution. Haematologica. 2005;90:1070–7.
64. Lazzi S, Bellan C, Tiacci E, et al. IRTA1+ monocytoid B cells in reactive lymphadenitis show a unique topographic distribution and immunophenotype and a peculiar usage and mutational pattern of IgVH genes. J Pathol. 2006;209:56–66.
65. Remstein ED, Kurtin PJ, Einerson RR, Paternoster SF, Dewald GW. Primary pulmonary MALT lymphomas show frequent and heterogeneous cytogenetic abnormalities, including aneuploidy and translocations involving API2 and MALT1 and IGH and MALT1. Leukemia. 2004;18:156–60.
66. Farinha P, Gascoyne RD. Molecular pathogenesis of mucosa-associated lymphoid tissue lymphoma. J Clin Oncol. 2005;23:6370–8.
67. Saacson PG. Update on MALT lymphomas. Best Pract Res Clin Haematol. 2005;18:57–I68.
68. Chng WJ, Remstein ED, Fonseca R, et al. Gene expression profiling of pulmonary mucosa-associated lymphoid tissue lymphoma identifies new biologic insights with potential diagnostic and therapeutic applications. Blood. 2009;113:635–45.
69. Wu X, Zhou C, Jin L, Liu H, Liu J, Zhao S. Primary pulmonary lymphoma in children. Orphanet J Rare Dis. 2019;14:35.
70. Bishop MR, Dickinson M, Purtill D, et al. Second-line tisagenlecleucel or standard care in aggressive B-cell lymphoma. N Engl J Med. 2022;386:629–39.
71. Locke FL, Miklos DB, Jacobson CA, et al. Axicabtagene ciloleucel as second-line therapy for large B-cell lymphoma. N Engl J Med. 2022;386:640–54.
72. Inaty H, Artiles C, Yadav R, Garcha P, Mukhopadhyay S, Sahoo D. Diffuse large B-cell lymphoma presenting as diffuse bilateral ground-glass opacities and diagnosed on transbronchial lung biopsy. Ann Am Thorac Soc. 2017;14:605–7.
73. Tokuyasu H, Harada T, Watanabe E, et al. Non-Hodgkin's lymphoma accompanied by pulmonary involvement with diffuse ground-glass opacity on chest CT: a report of 2 cases. Intern Med. 2009;48:105–9.
74. Johnson SA, Kumar A, Matasar MJ, Schoder H, Rademaker J. Imaging for staging and response assessment in lymphoma. Radiology. 2015;276:323–38.
75. Hans CP, Weisenburger DD, Greiner TC, et al. Confirmation of the molecular classification of diffuse large B-cell lymphoma by immunohistochemistry using a tissue microarray. Blood. 2004;103:275–82.
76. Klui PM, Harris NL, Stein H, et al. High-grade B-cell lymphoma. In: Swerdlow SH, Campo E, Harris NL, et al., editors. WHO classification of tumors of the hematopoietic and lymphoid tissues. Lyon: IARC; 2017. p. 335–41.
77. Sehn LH, Salles G. Diffuse large B-cell lymphoma. N Engl J Med. 2021;384:842–58.
78. Pfleger L, Tappeiner J. On the recognition of systematized endotheliomatosis of the cutaneous blood vessels (reticuloendotheliosis?). Hautarzt. 1959;10:359–63.
79. Ferreri AJ, Campo E, Seymour JF, et al. Intravascular lymphoma: clinical presentation, natural history, management and prognostic factors in a series of 38 cases, with special emphasis on the 'cutaneous variant'. Br J Haematol. 2004;127:173–83.
80. Murase T, Yamaguchi M, Suzuki R, et al. Intravascular large B-cell lymphoma (IVLBCL): a clinicopathologic study of 96 cases with special reference to the immunophenotypic heterogeneity of CD5. Blood. 2007;109:478–85.
81. Ponzoni M, Ferreri AJ, Campo E, et al. Definition, diagnosis, and management of intravascular large B-cell lymphoma: proposals and perspectives from an international consensus meeting. J Clin Oncol. 2007;25:3168–73.
82. Matea F, Alowami S, Bonert M, Sur M, Shargall Y, Naqvi AH. Pulmonary intravascular B-cell lymphoma with angiotropism/angioinvasion mimicking interstitial lung disease: a clinical dilemma and potential diagnostic challenge. Case Rep Hematol. 2018;2018:3821392.
83. Ponzoni M, Arrigoni G, Gould VE, et al. Lack of CD 29 (beta1 integrin) and CD 54 (ICAM-1) adhesion molecules in intravascular lymphomatosis. Hum Pathol. 2000;31:220–6.
84. Kanda M, Suzumiya J, Ohshima K, Tamura K, Kikuchi M. Intravascular large cell lymphoma: clinicopathological,

immuno-histochemical and molecular genetic studies. Leuk Lymphoma. 1999;34:569–80.
85. Liebow AA. Lymphomatoid granulomatosis. Calif Med. 1972;116:48–9.
86. Katzenstein AL, Peiper SC. Detection of Epstein-Barr virus genomes in lymphomatoid granulomatosis: analysis of 29 cases by the polymerase chain reaction technique. Mod Pathol. 1990;3:435–41.
87. Guinee D Jr, Jaffe E, Kingma D, et al. Pulmonary lymphomatoid granulomatosis. Evidence for a proliferation of Epstein-Barr virus infected B-lymphocytes with a prominent T-cell component and vasculitis. Am J Surg Pathol. 1994;18:753–64.
88. Myers JL, Kurtin PJ, Katzenstein AL, et al. Lymphomatoid granulomatosis. Evidence of immunophenotypic diversity and relationship to Epstein-Barr virus infection. Am J Surg Pathol. 1995;19:1300–12.
89. Song JY, Pittaluga S, Dunleavy K, et al. Lymphomatoid granulomatosis-A single institute experience: pathologic findings and clinical correlations. Am J Surg Pathol. 2015;39(2):141–56.
90. Katzenstein AL, Doxtader E, Narendra S. Lymphomatoid granulomatosis: insights gained over 4 decades. Am J Surg Pathol. 2010;34:e35–48.
91. Koss MN, Harris NL. Lymphomatoid Granulomatosis. In: Travis WD, Brambilla E, Müller-Hermelink HK, Harris CC, editors. WHO classification of tumours, pathology and genetics, tumours of the lung, pleura, thymus and heart. Lyon: IARC Press; 2004. p. 92–4.
92. Haque AK, Myers JL, Hudnall SD, et al. Pulmonary lymphomatoid granulomatosis in acquired immunodeficiency syndrome: lesions with Epstein-Barr virus infection. Mod Pathol. 1998;11:347–56.
93. Liebow AA, Carrington CR, Friedman PJ. Lymphomatoid granulomatosis. Hum Pathol. 1972;3:457–558.
94. Katzenstein AL, Carrington CB, Liebow AA. Lymphomatoid granulomatosis: a clinicopathologic study of 152 cases. Cancer. 1979;43:360–73.
95. Chavez JC, Sandoval-Sus J, Horna P, et al. Lymphomatoid granulomatosis: a single institution experience and review of the literature. Clin Lymphoma Myeloma Leuk. 2016;16(Suppl):S170–4.
96. Lee JS, Tuder R, Lynch DA. Lymphomatoid granulomatosis: radiologic features and pathologic correlations. AJR Am J Roentgenol. 2000;175:1335–9.
97. Dee PM, Arora NS, Innes DJ Jr. The pulmonary manifestations of lymphomatoid granulomatosis. Radiology. 1982;143:613–8.
98. Chung JH, Wu CC, Gilman MD, Palmer EL, Hasserjian RP, Shepard JA. Lymphomatoid granulomatosis: CT and FDG-PET findings. Korean J Radiol. 2011;12:671–8.
99. Benamore RE, Weisbrod GL, Hwang DM, et al. Reversed halo sign in lymphomatoid granulomatosis. Br J Radiol. 2007;80:e162–6.
100. Pittaluga S, Wilson WH, Jaffe E. Lymphomatoid granulomatosis. In: Swerdlow SH, Campo E, Harris NL, et al., editors. WHO classification of tumors of hematopoietic and lymphoid tissues. Lyon: IARC; 2017. p. 312–4.
101. Kameda H, Okuyama A, Tamaru J, Itoyama S, Iizuka A, Takeuchi T. Lymphomatoid granulomatosis and diffuse alveolar damage associated with methotrexate therapy in a patient with rheumatoid arthritis. Clin Rheumatol. 2007;26:1585–9.
102. Taniere P, Thivolet-Bejui F, Vitrey D, et al. Lymphomatoid granulomatosis--a report on four cases: evidence for B phenotype of the tumoral cells. Eur Respir J. 1998;12:102–6.
103. Begueret H, Vergier B, Parrens M, et al. Primary lung small B-cell lymphoma versus lymphoid hyperplasia: evaluation of diagnostic criteria in 26 cases. Am J Surg Pathol. 2002;26:76–81.
104. Ferraro P, Trastek VF, Adlakha H, Deschamps C, Allen MS, Pairolero PC. Primary non-Hodgkin's lymphoma of the lung. Ann Thorac Surg. 2000;69:993–7.
105. Li G, Hansmann ML, Zwingers T, Lennert K. Primary lymphomas of the lung: morphological, immunohistochemical and clinical features. Histopathology. 1990;16:519–31.
106. Kyrtsonis MC, Angelopoulou MK, Kontopidou FN, et al. Primary lung involvement in Waldenstrom's macroglobulinaemia: report of two cases and review of the literature. Acta Haematol. 2001;105:92–6.
107. Trisolini R, Lazzari Agli L, Poletti V. Bronchiolocentric pulmonary involvement due to chronic lymphocytic leukemia. Haematologica. 2000;85:1097.
108. Agrawal A, Gupta N, Esposito M, Tandon P, Koenig S, Khanijo S. Pathologic Findings in Bronchopulmonary Leukemic Infiltrates in Patients With Chronic Lymphocytic Leukemia. Clin Lymphoma Myeloma Leuk. 2019;19:123–8.
109. Katano T, Hagiwara E, Ikeda S, Ogura T. Pulmonary follicular lymphoma showing diffuse micronodules mimicking sarcoidosis. Intern Med. 2019;58:617–8.
110. Kremer M, Ott G, Nathrath M, et al. Primary extramedullary plasmacytoma and multiple myeloma: phenotypic differences revealed by immunohistochemical analysis. J Pathol. 2005;205:92–101.
111. Koss MN, Hochholzer L, Moran CA, Frizzera G. Pulmonary plasmacytomas: a clinicopathologic and immunohistochemical study of five cases. Ann Diagn Pathol. 1998;2:1–11.
112. Rosado F, Guo L, Fuda F. Hematolymphoid neoplasms with a plasma cell phenotype. Semin Diagn Pathol. 2020;37:268–72.
113. Edelstein E, Gal AA, Mann KP, Miller JI Jr, Mansour KA. Primary solitary endobronchial plasmacytoma. Ann Thorac Surg. 2004;78:1448–9.
114. Kaneko Y, Satoh H, Haraguchi N, Imagawa S, Sekizawa K. Radiologic findings in primary pulmonary plasmacytoma. J Thorac Imaging. 2005;20:53–4.
115. Kim SH, Kim TH, Sohn JW, et al. Primary pulmonary plasmacytoma presenting as multiple lung nodules. Korean J Intern Med. 2012;27:111–3.
116. Niitsu N, Kohri M, Hayama M, et al. Primary pulmonary plasmacytoma involving bilateral lungs and marked hypergammaglobulinemia: differentiation from extranodal marginal zone B-cell lymphoma of mucosa-associated lymphoid tissue. Leuk Res. 2005;29:1361–4.
117. Wise JN, Schaefer RF, Read RC. Primary pulmonary plasmacytoma: a case report. Chest. 2001;120:1405–7.
118. Mohammad Taheri Z, Mohammadi F, Karbasi M, et al. Primary pulmonary plasmacytoma with diffuse alveolar consolidation: a case report. Patholog Res Int. 2010;2010:463465.
119. Caers J, Paiva B, Zamagni E, et al. Diagnosis, treatment, and response assessment in solitary plasmacytoma: updated recommendations from a european expert panel. J Hematol Oncol. 2018;11:10.
120. Suster S, Moran CA. Lymphoid lesions of the lung. In: Suster S, Moran CA, editors. Biopsy interpretation of the lung. 1st ed. Philadelphia: Lippincott Williams & Wilkins; 2013. p. 224–54.
121. Bink K, Haralambieva E, Kremer M, et al. Primary extramedullary plasmacytoma: similarities with and differences from multiple myeloma revealed by interphase cytogenetics. Haematologica. 2008;93:623–6.
122. Stein H, Mason DY, Gerdes J, et al. The expression of the Hodgkin's disease associated antigen Ki-1 in reactive and neoplastic lymphoid tissue: evidence that Reed-Sternberg cells and histiocytic malignancies are derived from activated lymphoid cells. Blood. 1985;66:848–58.
123. Bullrich F, Morris SW, Hummel M, Pileri S, Stein H, Croce CM. Nucleophosmin (NPM) gene rearrangements in Ki-1-positive lymphomas. Cancer Res. 1994;54:2873–7.
124. Morris SW, Kirstein MN, Valentine MB, et al. Fusion of a kinase gene, ALK, to a nucleolar protein gene, NPM, in non-Hodgkin's lymphoma. Science. 1994;263:1281–4.

125. Shiota M, Nakamura S, Ichinohasama R, et al. Anaplastic large cell lymphomas expressing the novel chimeric protein p80NPM/ALK: a distinct clinicopathologic entity. Blood. 1995;86:1954–60.
126. Yang HB, Li J, Shen T. Primary anaplastic large cell lymphoma of the lung. Report of two cases and literature review. Acta Haematol. 2007;118:188–91.
127. Pan Z, Xu ML. T-cell and NK-cell lymphomas in the lung. Semin Diagn Pathol. 2020;37:273–82.
128. Rush WL, Andriko JA, Taubenberger JK, et al. Primary anaplastic large cell lymphoma of the lung: a clinicopathologic study of five patients. Mod Pathol. 2000;13:1285–92.
129. Guerra J, Echevarria-Escudero M, Barrio N, Velez-Rosario R. Primary endobronchial anaplastic large cell lymphoma in a pediatric patient. P R Health Sci J. 2006;25:159–61.
130. Ansell SM. Brentuximab vedotin. Blood. 2014;124:3197–200.
131. Gambacorti Passerini C, Farina F, Stasia A, et al. Crizotinib in advanced, chemoresistant anaplastic lymphoma kinase-positive lymphoma patients. J Natl Cancer Inst. 2014;106:djt378.
132. Feeney J, Horwitz S, Gonen M, Schoder H. Characterization of T-cell lymphomas by FDG PET/CT. AJR Am J Roentgenol. 2010;195:333–40.
133. Xing X, Feldman AL. Anaplastic large cell lymphomas: ALK positive, ALK negative, and primary cutaneous. Adv Anat Pathol. 2015;22:29–49.
134. Wang LJ, Wu HB, Zhang Y, Zhou WL, Wang QS. A rare case of neutrophil-rich, ALK-negative anaplastic large cell lymphoma in the lung mimicking a pulmonary abscess on 18F-FDG PET/CT. Clin Nucl Med. 2019;44:234–7.
135. Yu L, Yan LL, Yang SJ. Sarcomatoid variant of ALK- anaplastic large cell lymphoma involving multiple lymph nodes and both lungs with production of proinflammatory cytokines: report of a case and review of literature. Int J Clin Exp Pathol. 2014;7:4806–16.
136. Nguyen TT, Kreisel FH, Frater JL, Bartlett NL. Anaplastic large-cell lymphoma with aberrant expression of multiple cytokeratins masquerading as metastatic carcinoma of unknown primary. J Clin Oncol. 2013;31:e443–5.
137. Pletneva MA, Smith LB. Anaplastic large cell lymphoma: features presenting diagnostic challenges. Arch Pathol Lab Med. 2014;138:1290–4.
138. Ying J, Guo L, Qiu T, et al. Diagnostic value of a novel fully automated immunochemistry assay for detection of ALK rearrangement in primary lung adenocarcinoma. Ann Oncol. 2013;24:2589–93.
139. Shiota M, Fujimoto J, Takenaga M, et al. Diagnosis of t(2;5)(p23;q35)-associated Ki-1 lymphoma with immunohistochemistry. Blood. 1994;84:3648–52.
140. Parrilla Castellar ER, Jaffe ES, Said JW, et al. ALK-negative anaplastic large cell lymphoma is a genetically heterogeneous disease with widely disparate clinical outcomes. Blood. 2014;124:1473–80.
141. Weisenburger DD, Savage KJ, Harris NL, et al. Peripheral T-cell lymphoma, not otherwise specified: a report of 340 cases from the International Peripheral T-cell Lymphoma Project. Blood. 2011;117:3402–8.
142. Gorczyca W, Weisberger J, Liu Z, et al. An approach to diagnosis of T-cell lymphoproliferative disorders by flow cytometry. Cytometry. 2002;50:177–90.
143. Abel E, Heully F, Arnould P, Dornier R. The pulmonary forms of mycosis fungoides. Rev Med Nancy. 1953;78:117–23.
144. Baser S, Onn A, Lin E, Morice RC, Duvic M. Pulmonary manifestations in patients with cutaneous T-cell lymphomas. Cancer. 2007;109:1550–5.
145. Iqbal J, Wright G, Wang C, et al. Gene expression signatures delineate biological and prognostic subgroups in peripheral T-cell lymphoma. Blood. 2014;123:2915–23.
146. Heavican TB, Bouska A, Yu J, et al. Genetic drivers of oncogenic pathways in molecular subgroups of peripheral T-cell lymphoma. Blood. 2019;133:1664–76.
147. Amador C, Greiner TC, Heavican TB, et al. Reproducing the molecular subclassification of peripheral T-cell lymphoma-NOS by immunohistochemistry. Blood. 2019;134:2159–70.
148. Binesh F, Halvani H, Taghipour S, Navabii H. Primary pulmonary classic Hodgkin's lymphoma. BMJ Case Rep. 2011;2011:bcr0320113955.
149. Chowdhary GS, Mehta R, Tyagi R. Primary pulmonary Hodgkin's lymphoma with pulmonary histoplasmosis. Med J Armed Forces India. 2020;76:462–5.
150. Homma M, Yamochi-Onizuka T, Shiozawa E, et al. Primary pulmonary classical hodgkin lymphoma with two recurrences in the mediastinum : a case report. J Clin Exp Hematop. 2010;50:151–7.
151. Lowenthal BM, Xu X, Subash M, Jih LJ. Hodgkin's lymphoma with unusual pulmonary presentations: Reporting two cases. Indian J Pathol Microbiol. 2017;60:272–4.
152. Ma J, Wang Y, Zhao H, et al. Clinical characteristics of 26 patients with primary extranodal Hodgkin lymphoma. Int J Clin Exp Pathol. 2014;7:5045–50.
153. Oka K, Shinonaga M, Nagayama R, et al. Coexistence of primary pulmonary Hodgkin lymphoma and gastric MALT lymphoma associated with Epstein-Barr virus infection: a case report. Pathol Int. 2010;60:520–3.
154. Schild MH, Wong WW, Valdez R, Leis JF. Primary pulmonary classical Hodgkin lymphoma: a case report. J Surg Oncol. 2014;110:341–4.
155. Sinha A, Patti R, Singh P, Solomon W, Kupfer Y. A diagnostic surprise: primary Hodgkin's lymphoma of the lung. J Investig Med High Impact Case Rep. 2017;5:2324709617734247.
156. Webb WR, Higgins CB. Thoracic imaging : pulmonary and cardiovascular radiology. Philadelphia: Wolters Kluwer; 2017.
157. Lewis ER, Caskey CI, Fishman EK. Lymphoma of the lung: CT findings in 31 patients. AJR Am J Roentgenol. 1991;156:711–4.
158. O'Malley DP, Dogan A, Fedoriw Y, Medeiros LJ, Ok CY, Salama ME. American registry of pathology expert opinions: immunohistochemical evaluation of classic Hodgkin lymphoma. Ann Diagn Pathol. 2019;39:105–10.
159. Carbone A, Gloghini A, Aldinucci D, Gattei V, Dalla-Favera R, Gaidano G. Expression pattern of MUM1/IRF4 in the spectrum of pathology of Hodgkin's disease. Br J Haematol. 2002;117:366–72.
160. Andorsky DJ, Yamada RE, Said J, Pinkus GS, Betting DJ, Timmerman JM. Programmed death ligand 1 is expressed by non-hodgkin lymphomas and inhibits the activity of tumor-associated T cells. Clin Cancer Res. 2011;17:4232–44.
161. Paydas S, Bağır E, Seydaoglu G, Ercolak V, Ergin M. Programmed death-1 (PD-1), programmed death-ligand 1 (PD-L1), and EBV-encoded RNA (EBER) expression in Hodgkin lymphoma. Ann Hematol. 2015;94:1545–52.
162. Tanaka Y, Maeshima AM, Nomoto J, et al. Expression pattern of PD-L1 and PD-L2 in classical Hodgkin lymphoma, primary mediastinal large B-cell lymphoma, and gray zone lymphoma. Eur J Haematol. 2018;100:511–7.
163. Xie W, Medeiros LJ, Li S, Yin CC, Khoury JD, Xu J. PD-1/PD-L1 pathway and its blockade in patients with classic hodgkin lymphoma and non-hodgkin large-cell lymphomas. Curr Hematol Malig Rep. 2020;15:372–81.
164. Pallesen G, Hamilton-Dutoit SJ, Rowe M, et al. Expression of Epstein-Barr virus replicative proteins in AIDS-related non-Hodgkin's lymphoma cells. J Pathol. 1991;165:289–99.

165. Uccini S, Monardo F, Ruco LP, et al. High frequency of Epstein-Barr virus genome in HIV-positive patients with Hodgkin's disease. Lancet. 1989;1:1458.
166. Weiss LM, Movahed LA, Warnke RA, Sklar J. Detection of Epstein-Barr viral genomes in Reed-Sternberg cells of Hodgkin's disease. N Engl J Med. 1989;320:502–6.
167. Re D, Müschen M, Ahmadi T, et al. Oct-2 and Bob-1 deficiency in Hodgkin and reed Sternberg cells. Cancer Res. 2001;61:2080–4.
168. Thomas RK, Re D, Wolf J, Diehl V. Part I: Hodgkin's lymphoma--molecular biology of Hodgkin and Reed-Sternberg cells. Lancet Oncol. 2004;5:11–8.
169. Schwering I, Bräuninger A, Klein U, et al. Loss of the B-lineage-specific gene expression program in Hodgkin and Reed-Sternberg cells of Hodgkin lymphoma. Blood. 2003;101:1505–12.
170. Chan WC. The Reed-Sternberg cell in classical Hodgkin's disease. Hematol Oncol. 2001;19:1–17.
171. Kuppers R, Hansmann ML. The Hodgkin and Reed/Sternberg cell. Int J Biochem Cell Biol. 2005;37:511–7.
172. Stein H, Hummel M. Cellular origin and clonality of classic Hodgkin's lymphoma: immunophenotypic and molecular studies. Semin Hematol. 1999;36:233–41.
173. Hinz M, Lemke P, Anagnostopoulos I, et al. Nuclear factor kappaB-dependent gene expression profiling of Hodgkin's disease tumor cells, pathogenetic significance, and link to constitutive signal transducer and activator of transcription 5a activity. J Exp Med. 2002;196:605–17.
174. Hinz M, Löser P, Mathas S, Krappmann D, Dörken B, Scheidereit C. Constitutive NF-kappaB maintains high expression of a characteristic gene network, including CD40, CD86, and a set of antiapoptotic genes in Hodgkin/Reed-Sternberg cells. Blood. 2001;97:2798–807.
175. Skinnider BF, Elia AJ, Gascoyne RD, et al. Signal transducer and activator of transcription 6 is frequently activated in Hodgkin and Reed-Sternberg cells of Hodgkin lymphoma. Blood. 2002;99:618–26.
176. Farrell K, Jarrett RF. The molecular pathogenesis of Hodgkin lymphoma. Histopathology. 2011;58:15–25.
177. Weniger MA, Melzner I, Menz CK, et al. Mutations of the tumor suppressor gene SOCS-1 in classical Hodgkin lymphoma are frequent and associated with nuclear phospho-STAT5 accumulation. Oncogene. 2006;25:2679–84.
178. Rosenwald A, Wright G, Leroy K, et al. Molecular diagnosis of primary mediastinal B cell lymphoma identifies a clinically favorable subgroup of diffuse large B cell lymphoma related to Hodgkin lymphoma. J Exp Med. 2003;198:851–62.
179. Savage KJ, Monti S, Kutok JL, et al. The molecular signature of mediastinal large B-cell lymphoma differs from that of other diffuse large B-cell lymphomas and shares features with classical Hodgkin lymphoma. Blood. 2003;102:3871–9.
180. Gunawardana J, Chan FC, Telenius A, et al. Recurrent somatic mutations of PTPN1 in primary mediastinal B cell lymphoma and Hodgkin lymphoma. Nat Genet. 2014;46:329–35.
181. Roemer MG, Advani RH, Ligon AH, et al. PD-L1 and PD-L2 Genetic Alterations Define Classical Hodgkin Lymphoma and Predict Outcome. J Clin Oncol. 2016;34:2690–7.
182. Ansell SM. Hodgkin lymphoma: diagnosis and treatment. Mayo Clin Proc. 2015;90:1574–83.
183. Armand P, Shipp MA, Ribrag V, et al. Programmed death-1 blockade with pembrolizumab in patients with classical hodgkin lymphoma after brentuximab vedotin failure. J Clin Oncol. 2016;34:3733–9.
184. Rengstl B, Rieger MA, Newrzela S. On the origin of giant cells in Hodgkin lymphoma. Commun Integr Biol. 2014;7:e28602.
185. Goyal G, Bartley AC, Patnaik MM, Litzow MR, Al-Kali A, Go RS. Clinical features and outcomes of extramedullary myeloid sarcoma in the United States: analysis using a national data set. Blood Cancer J. 2017;7:e592.
186. Movassaghian M, Brunner AM, Blonquist TM, et al. Presentation and outcomes among patients with isolated myeloid sarcoma: a Surveillance, Epidemiology, and End Results database analysis. Leuk Lymphoma. 2015;56:1698–703.
187. Khoury JD, Chen W. Myeloid diseases in the lung and pleura. Semin Diagn Pathol. 2020;37:296–302.
188. Koh TT, Colby TV, Muller NL. Myeloid leukemias and lung involvement. Semin Respir Crit Care Med. 2005;26:514–9.
189. Takasugi JE, Godwin JD, Marglin SI, Petersdorf SH. Intrathoracic granulocytic sarcomas. J Thorac Imaging. 1996;11:223–30.
190. Avraham S, Akria L, Vlodavsky E, Rowe JM. Granulocytic sarcoma with pulmonary involvement. Am J Hematol. 2007;82:222–3.
191. de Paz R, Canales MA, Hernandez-Navarro F. Granulocytic sarcoma (chloroma) of the lung. Br J Haematol. 2003;120:176.
192. Guimaraes MD, Marchiori E, Marom EM, Routbort MJ, Godoy MC. Pulmonary granulocytic sarcoma (chloroma) mimicking an opportunistic infection in a patient with acute myeloid leukemia. Ann Hematol. 2014;93:327–8.
193. Lee DA, Harris CP, Gresik VM, Rao P, Lau CC. Granulocytic sarcoma presenting as pneumonia in a child with t(8;21) acute myelogenous leukemia: diagnosis by fluorescent in situ hybridization. J Pediatr Hematol Oncol. 2004;26:431–4.
194. Stafford CM, Herndier B, Yi ES, Weidner N, Harrell JH 2nd. Granulocytic sarcoma of the tracheobronchial tree: bronchoscopic and pathologic correlation. Respiration. 2004;71:529–32.
195. Wong KF, Chan JK, Chan JC, Lam SY. Acute myeloid leukemia presenting as granulocytic sarcoma of the lung. Am J Hematol. 1993;43:77–8.
196. Hoffman LM, Gore L, Maloney KW. Pulmonary presentation of relapsed acute myeloid leukemia. J Pediatr Hematol Oncol. 2014;36:228–30.
197. Wilson CS, Medeiros LJ. Extramedullary Manifestations of Myeloid Neoplasms. Am J Clin Pathol. 2015;144:219–39.
198. Ido K, Aoyama Y, Nagasaki J, et al. Pulmonary involvement of acute myeloid leukemia mimicking transfusion-related acute lung injury. Intern Med. 2017;56:2493–6.
199. Maile CW, Moore AV, Ulreich S, Putman CE. Chest radiographic-pathologic correlation in adult leukemia patients. Invest Radiol. 1983;18:495–9.
200. Coiffier B, Altman A, Pui CH, Younes A, Cairo MS. Guidelines for the management of pediatric and adult tumor lysis syndrome: an evidence-based review. J Clin Oncol. 2008;26:2767–78.
201. Vernant JP, Brun B, Mannoni P, Dreyfus B. Respiratory distress of hyperleukocytic granulocytic leukemias. Cancer. 1979;44:264–8.
202. Shroff GS, Truong MT, Carter BW, et al. Leukemic Involvement in the Thorax. Radiographics. 2019;39:44–61.
203. Thawani R, Chichra A, Mahajan A, Jadhav L. Granulocytic sarcoma of the lung in acute myeloid leukemia. Indian Pediatr. 2014;51:145–6.
204. Ueda K, Ichikawa M, Takahashi M, Momose T, Ohtomo K, Kurokawa M. FDG-PET is effective in the detection of granulocytic sarcoma in patients with myeloid malignancy. Leuk Res. 2010;34:1239–41.
205. Miettinen M, Wang ZF, Paetau A, et al. ERG transcription factor as an immunohistochemical marker for vascular endothelial tumors and prostatic carcinoma. Am J Surg Pathol. 2011;35:432–41.
206. Coppes-Zantinga A, Egeler RM. The Langerhans cell histiocytosis X files revealed. Br J Haematol. 2002;116:3–9.
207. Breathnach AS, Gross M, Basset F, Nezelof C. Freeze-fracture replication of X-granules in cells of cutaneous lesions of histiocytosis-X. Br J Dermatol. 1973;89:571–85.
208. Nezelof C, Basset F, Rousseau MF. Histiocytosis X histogenetic arguments for a Langerhans cell origin. Biomedicine. 1973;18:365–71.
209. Langerhans P. Ueber die Nerven der Menschlichen Haut. Virchow Arch. 1868;44:325–37.

210. Birbeck MS, Breathnach AS, Everall JD. An electron microscopy study of basal melanocytes and high-level clear cell (Langerhans cells) in vitiligo. J Invest Dermatol. 1961;75:51–64.
211. Willman CL, Busque L, Griffith BB, et al. Langerhans'-cell histiocytosis (histiocytosis X)--a clonal proliferative disease. N Engl J Med. 1994;331:154–60.
212. Yu RC, Chu C, Buluwela L, Chu AC. Clonal proliferation of Langerhans cells in Langerhans cell histiocytosis. Lancet. 1994;343:767–8.
213. Badalian-Very G, Vergilio JA, Degar BA, et al. Recurrent BRAF mutations in Langerhans cell histiocytosis. Blood. 2010;116:1919–23.
214. Capper D, Preusser M, Habel A, et al. Assessment of BRAF V600E mutation status by immunohistochemistry with a mutation-specific monoclonal antibody. Acta Neuropathol. 2011;122:11–9.
215. Emile JF, Abla O, Fraitag S, et al. Revised classification of histiocytoses and neoplasms of the macrophage-dendritic cell lineages. Blood. 2016;127:2672–81.
216. Vassallo R, Harari S, Tazi A. Current understanding and management of pulmonary Langerhans cell histiocytosis. Thorax. 2017;72:937–45.
217. Elia D, Torre O, Cassandro R, Caminati A, Harari S. Pulmonary Langerhans cell histiocytosis: a comprehensive analysis of 40 patients and literature review. Eur J Intern Med. 2015;26:351–6.
218. Nicholson HS, Egeler RM, Nesbit ME. The epidemiology of Langerhans cell histiocytosis. Hematol Oncol Clin North Am. 1998;12:379–84.
219. Tazi A. Adult pulmonary Langerhans' cell histiocytosis. Eur Respir J. 2006;27:1272–85.
220. Dauriat G, Mal H, Thabut G, et al. Lung transplantation for pulmonary Langerhans' cell histiocytosis: a multicenter analysis. Transplantation. 2006;81:746–50.
221. Mogulkoc N, Veral A, Bishop PW, Bayindir U, Pickering CA, Egan JJ. Pulmonary Langerhans' cell histiocytosis: radiologic resolution following smoking cessation. Chest. 1999;115:1452–5.
222. Colby TV, Lombard C. Histiocytosis X in the lung. Hum Pathol. 1983;14:847–56.
223. Donadieu J, Bernard F, van Noesel M, et al. Cladribine and cytarabine in refractory multisystem Langerhans cell histiocytosis: results of an international phase 2 study. Blood. 2015;126:1415–23.
224. Donadieu J, Larabi IA, Tardieu M, et al. Vemurafenib for refractory multisystem langerhans cell histiocytosis in children: an international observational study. J Clin Oncol. 2019;37:2857–65.
225. Etienne B, Bertocchi M, Gamondes JP, et al. Relapsing pulmonary Langerhans cell histiocytosis after lung transplantation. Am J Respir Crit Care Med. 1998;157:288–91.
226. Lorillon G, Tazi A. How I manage pulmonary Langerhans cell histiocytosis. Eur Respir Rev. 2017;26:170070.
227. Ahuja J, Kanne JP, Meyer CA, et al. Histiocytic disorders of the chest: imaging findings. Radiographics. 2015;35:357–70.
228. Castoldi MC, Verrioli A, De Juli E, Vanzulli A. Pulmonary Langerhans cell histiocytosis: the many faces of presentation at initial CT scan. Insights Imaging. 2014;5:483–92.
229. Haroche J, Charlotte F, Arnaud L, et al. High prevalence of BRAF V600E mutations in Erdheim-Chester disease but not in other non-Langerhans cell histiocytoses. Blood. 2012;120:2700–3.
230. Jones RT, Abedalthagafi MS, Brahmandam M, et al. Cross-reactivity of the BRAF VE1 antibody with epitopes in axonemal dyneins leads to staining of cilia. Mod Pathol. 2015;28:596–606.
231. Berres ML, Merad M, Allen CE. Progress in understanding the pathogenesis of Langerhans cell histiocytosis: back to Histiocytosis X? Br J Haematol. 2015;169:3–13.
232. Chakraborty R, Hampton OA, Shen X, et al. Mutually exclusive recurrent somatic mutations in MAP2K1 and BRAF support a central role for ERK activation in LCH pathogenesis. Blood. 2014;124:3007–15.
233. Nelson DS, van Halteren A, Quispel WT, et al. MAP2K1 and MAP3K1 mutations in Langerhans cell histiocytosis. Genes Chromosomes Cancer. 2015;54:361–8.
234. Mourah S, How-Kit A, Meignin V, et al. Recurrent NRAS mutations in pulmonary Langerhans cell histiocytosis. Eur Respir J. 2016;47:1785–96.
235. Chakraborty R, Burke TM, Hampton OA, et al. Alternative genetic mechanisms of BRAF activation in Langerhans cell histiocytosis. Blood. 2016;128:2533–7.
236. Egeler RM, Katewa S, Leenen PJ, et al. Langerhans cell histiocytosis is a neoplasm and consequently its recurrence is a relapse: In memory of Bob Arceci. Pediatr Blood Cancer. 2016;63:1704–12.
237. Alayed K, Medeiros LJ, Patel KP, et al. BRAF and MAP2K1 mutations in Langerhans cell histiocytosis: a study of 50 cases. Hum Pathol. 2016;52:61–7.
238. Rosai J, Dorfman RF. Sinus histiocytosis with massive lymphadenopathy. A newly recognized benign clinicopathological entity. Arch Pathol. 1969;87:63–70.
239. Foucar E, Rosai J, Dorfman RF. Sinus histiocytosis with massive lymphadenopathy. Arch Otolaryngol. 1978;104:687–93.
240. Foucar E, Rosai J, Dorfman RF. Sinus histiocytosis with massive lymphadenopathy. An analysis of 14 deaths occurring in a patient registry. Cancer. 1984;54:1834–40.
241. Foucar E, Rosai J, Dorfman RF, Eyman JM. Immunologic abnormalities and their significance in sinus histiocytosis with massive lymphadenopathy. Am J Clin Pathol. 1984;82:515–25.
242. Al-Maghrabi H, Elmahrouk A, Feteih M, Jamjoom A, Al-Maghrabi J. Rosai-Dorfman disease with pulmonary involvement mimicking bronchogenic carcinoma. J Cardiothorac Surg. 2020;15:37.
243. Boissière L, Patey M, Toubas O, et al. Tracheobronchial involvement of rosai-dorfman disease: case report and review of the literature. Medicine (Baltimore). 2016;95:e2821.
244. Moyon Q, Boussouar S, Maksud P, et al. Lung involvement in destombes-rosai-dorfman disease: clinical and radiological features and response to the MEK inhibitor cobimetinib. Chest. 2020;157:323–33.
245. Santosham R, Santosham R, Jacob SS, Phadke AU, Ponduru T. Rosai-Dorfman disease of the trachea: an extremely rare benign tumor. Asian Cardiovasc Thorac Ann. 2019;27:132–4.
246. Uzunhan Y, Chabrol A, Kambouchner M, Martinod E. Bronchial involvement in rosai dorfman disease. Ann Thorac Surg. 2018;105:e33.
247. de Jong WK, Kluin PM, Groen HM. Overlapping immunoglobulin G4-related disease and Rosai-Dorfman disease mimicking lung cancer. Eur Respir Rev. 2012;21:365–7.
248. Garces S, Medeiros LJ, Patel KP, et al. Mutually exclusive recurrent KRAS and MAP2K1 mutations in Rosai-Dorfman disease. Mod Pathol. 2017;30(10):1367–77.
249. Al Umairi R, Blunt D, Hana W, Cheung M, Oikonomou A. Rosai-dorfman disease: rare pulmonary involvement mimicking pulmonary langerhans cell histiocytosis and review of the literature. Case Rep Radiol. 2018;2018:2952084.
250. Gallego CT, Bueno J, Cruces E, Stelow EB, Mancheño N, Flors L. Pulmonary histiocytosis: beyond Langerhans cell histiocytosis related to smoking. Radiologia. 2019;61:215–24.
251. Goupil de Bouillé J, de Muret A, Diot E, et al. Pulmonary manifestations revealing Rosai-Dorfman disease. Sarcoidosis Vasc Diffuse Lung Dis. 2015;32:275–7.
252. Hasegawa M, Sakai F, Okabayashi A, et al. Rosai-dorfman disease of the lung overlapping with IgG4-related disease: the difficulty in its differential diagnosis. Intern Med. 2017;56:937–41.
253. Ji H, Zhang B, Tian D, Wu S, Wang X, Zhu Y. Rosai-Dorfman disease of the lung. Respir Care. 2012;57:1679–81.

254. Costa AL, Silva NO, Motta MP, Athanazio RA, Athanazio DA, Athanazio PR. Soft tissue Rosai-Dorfman disease of the posterior mediastinum. J Bras Pneumol. 2009;35:717–20.
255. Cunha BA, Durie N, Selbs E, Pherez F. Fever of unknown origin (FUO) due to Rosai-Dorfman disease with mediastinal adenopathy mimicking lymphoma: diagnostic importance of elevated serum ferritin levels and polyclonal gammopathy. Heart Lung. 2009;38:83–8.
256. Mar WA, Yu JH, Knuttinen MG, et al. Rosai-dorfman disease: manifestations outside of the head and neck. AJR Am J Roentgenol. 2017;208:721–32.
257. Cartin-Ceba R, Golbin JM, Yi ES, Prakash UB, Vassallo R. Intrathoracic manifestations of Rosai-Dorfman disease. Respir Med. 2010;104:1344–9.
258. Overholtzer M, Brugge JS. The cell biology of cell-in-cell structures. Nat Rev Mol Cell Biol. 2008;9:796–809.
259. Rastogi V, Sharma R, Misra SR, Yadav L, Sharma V. Emperipolesis—a review. J Clin Diagn Res. 2014;8:ZM01-2.
260. Bonetti F, Chilosi M, Menestrina F, et al. Immunohistological analysis of Rosai-Dorfman histiocytosis. A disease of S-100 + CD1-histiocytes. Virchows Arch A Pathol Anat Histopathol. 1987;411:129–35.
261. Liu L, Perry AM, Cao W, et al. Relationship between Rosai-Dorfman disease and IgG4-related disease: study of 32 cases. Am J Clin Pathol. 2013;140:395–402.
262. Zhang X, Hyjek E, Vardiman J. A subset of Rosai-Dorfman disease exhibits features of IgG4-related disease. Am J Clin Pathol. 2013;139:622–32.
263. Menon MP, Evbuomwan MO, Rosai J, Jaffe ES, Pittaluga S. A subset of Rosai-Dorfman disease cases show increased IgG4-positive plasma cells: another red herring or a true association with IgG4-related disease? Histopathology. 2014;64:455–9.
264. Emile JF, Charlotte F, Amoura Z, Haroche J. BRAF mutations in Erdheim-Chester disease. J Clin Oncol. 2013;31:398.
265. Ozkaya N, Rosenblum MK, Durham BH, et al. The histopathology of Erdheim-Chester disease: a comprehensive review of a molecularly characterized cohort. Mod Pathol. 2018;31:581–97.
266. Levine PH, Jahan N, Murari P, Manak M, Jaffe ES. Detection of human herpesvirus 6 in tissues involved by sinus histiocytosis with massive lymphadenopathy (Rosai-Dorfman disease). J Infect Dis. 1992;166:291–5.
267. Mehraein Y, Wagner M, Remberger K, et al. Parvovirus B19 detected in Rosai-Dorfman disease in nodal and extranodal manifestations. J Clin Pathol. 2006;59:1320–6.
268. Ortonne N, Fillet AM, Kosuge H, Bagot M, Frances C, Wechsler J. Cutaneous Destombes-Rosai-Dorfman disease: absence of detection of HHV-6 and HHV-8 in skin. J Cutan Pathol. 2002;29:113–8.
269. Tsang WY, Yip TT, Chan JK. The Rosai-Dorfman disease histiocytes are not infected by Epstein-Barr virus. Histopathology. 1994;25:88–90.
270. Marsh WL Jr, McCarrick JP, Harlan DM. Sinus histiocytosis with massive lymphadenopathy. Occurrence in identical twins with retroperitoneal disease. Arch Pathol Lab Med. 1988;112:298–301.
271. Morgan NV, Morris MR, Cangul H, et al. Mutations in SLC29A3, encoding an equilibrative nucleoside transporter ENT3, cause a familial histiocytosis syndrome (Faisalabad histiocytosis) and familial Rosai-Dorfman disease. PLoS Genet. 2010;6:e1000833.
272. Rossbach HC, Dalence C, Wynn T, Tebbi C. Faisalabad histiocytosis mimics Rosai-Dorfman disease: brothers with lymphadenopathy, intrauterine fractures, short stature, and sensorineural deafness. Pediatr Blood Cancer. 2006;47:629–32.
273. Matter MS, Bihl M, Juskevicius D, Tzankov A. Is Rosai-Dorfman disease a reactve process? Detection of a MAP2K1 L115V mutation in a case of Rosai-Dorfman disease. Virchows Arch. 2017;471(4):545–7.
274. Jacobsen E, Shanmugam V, Jagannathan J. Rosai-Dorfman disease with activating KRAS mutation—Response to Cobimetinib. N Engl J Med. 2017;377:2398–9.
275. Chester W. Uber lipoidgranulomatose. Virchows Arch Pathol Anat. 1930;279:561–602.
276. Jaffe HL. Gaucher's disease and certain other inborn metabolic disorders: lipid (cholesterol) granulomatosis. In: Jaffe HL, editor. Metabolic, degenerative and inflammatory diseases of bones and joints. Philadelphia: Lea & Febiger; 1972. p. 535–41.
277. Zaveri J, La Q, Yarmish G, Neuman J. More than just Langerhans cell histiocytosis: a radiologic review of histiocytic disorders. Radiographics. 2014;34:2008–24.
278. Haroche J, Cohen-Aubart F, Charlotte F, et al. The histiocytosis Erdheim-Chester disease is an inflammatory myeloid neoplasm. Expert Rev Clin Immunol. 2015;11:1033–42.
279. Haroche J, Amoura Z, Dion E, et al. Cardiovascular involvement, an overlooked feature of Erdheim-Chester disease: report of 6 new cases and a literature review. Medicine (Baltimore). 2004;83:371–92.
280. Mazor RD, Manevich-Mazor M, Kesler A, et al. Clinical considerations and key issues in the management of patients with Erdheim-Chester Disease: a seven case series. BMC Med. 2014;12:221.
281. Diamond EL, Dagna L, Hyman DM, et al. Consensus guidelines for the diagnosis and clinical management of Erdheim-Chester disease. Blood. 2014;124:483–92.
282. Shiihara J, Ohta H, Ikeda S, Baba T, Okudera K, Ogura T. Erdheim-Chester disease progression from miliary pulmonary nodules to large tumours. Respirol Case Rep. 2019;7:e00475.
283. Pegoraro F, Papo M, Maniscalco V, Charlotte F, Haroche J, Vaglio A. Erdheim-Chester disease: a rapidly evolving disease model. Leukemia. 2020;34:2840–57.
284. Das JP, Xie L, Riedl CC, Hayes SA, Ginsberg MS, Halpenny DF. Cardiothoracic manifestations of Erdheim-Chester disease. Br J Radiol. 2019;92:20190473.
285. Zanelli M, Smith M, Mengoli MC, et al. Erdheim-Chester disease: description of two illustrative cases involving the lung. Histopathology. 2018;73:167–72.
286. Emile JF, Diamond EL, Hélias-Rodzewicz Z, et al. Recurrent RAS and PIK3CA mutations in Erdheim-Chester disease. Blood. 2014;124:3016–9.
287. Diamond EL, Durham BH, Haroche J, et al. Diverse and targetable kinase alterations drive histiocytic neoplasms. Cancer Discov. 2016;6:154–65.
288. Haroche J, Cohen-Aubart F, Emile JF, et al. Dramatic efficacy of vemurafenib in both multisystemic and refractory Erdheim-Chester disease and Langerhans cell histiocytosis harboring the BRAF V600E mutation. Blood. 2013;121:1495–500.
289. Bakir B, Unuvar E, Terzibasioglu E, Guven K. Atypical kung involvement in a patient with systemic juvenile xanthogranuloma. Pediatr Radiol. 2007;37:325–7.
290. Krauss MD, Haley JC, Ruiz R, Essary L, Moran CA, Fletcher CD. Juvenile xanthogranuloma: an immunophenotypic study with reappraisal of histogenesis. Am J Dermatopathol. 2001;23:104–11.
291. Kourilsky S, Pieron R, Renault P, Parrot R, Demay C. Isolated round intrapulmonary mass in a young person: xantogranuloma. J Fr Med Chir Thorac. 1965;19:307–19.
292. Diard R, Cadier L, Billaud C, Trojani M. Neonatal juvenile xantogranulomatosis with pulmonary extrapelural and hepatic involvement. One case report. Ann Radiol (Paris). 1982;25:113–8.
293. Ionescu DN, Pierson DM, Qing G, Li M, Colby TV, Leslie KO. Pulmonary crystal storing histiocytoma. Arch pathol Lab Med. 2005;129:1159–63.
294. Prassad ML, Charney DA, Sarlin J, Keller SM. Pulmonary immunocytoma with massive crystal storing histiocytosis: a case report with review of the literature. Am J Surg pathol. 1998;22:1148–53.